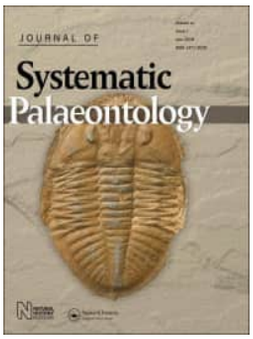

Journal of Systematic Palaeontology

ISSN: (Print) (Online) Journal homepage: www.tandfonline.com/journals/tjsp20

Revision of Romanian sauropod dinosaurs reveals high titanosaur diversity and body-size disparity on the latest Cretaceous Haţeg Island, with implications for titanosaurian biogeography

Verónica Díez Díaz, Philip D. Mannion, Zoltán Csiki-Sava & Paul Upchurch

To cite this article: Verónica Díez Díaz, Philip D. Mannion, Zoltán Csiki-Sava & Paul Upchurch (2025) Revision of Romanian sauropod dinosaurs reveals high titanosaur diversity and body-size disparity on the latest Cretaceous Haţeg Island, with implications for titanosaurian biogeography, Journal of Systematic Palaeontology, 23:1, 2441516, DOI: 10.1080/14772019.2024.2441516

To link to this article: https://doi.org/10.1080/14772019.2024.2441516

Journal of Systematic Palaeontology, 2025
Vol. 23, No. 1, 2441516
http://dx.doi.org/10.1080/14772019.2024.2441516

Revision of Romanian sauropod dinosaurs reveals high titanosaur diversity and body-size disparity on the latest Cretaceous Haţeg Island, with implications for titanosaurian biogeography

Verónica Díez Díaz[a]*, Philip D. Mannion[b], Zoltán Csiki-Sava[c] and Paul Upchurch[b]

[a]*Museum für Naturkunde, Leibniz-Institut für Evolutions- und Biodiversitätsforschung, Invalidenstraße 43, 10115 Berlin, Germany;* [b]*Department of Earth Sciences, University College London, Gower Street, London, WC1E 6BT, UK;* [c]*Laboratory of Paleontology, Faculty of Geology and Geophysics, University of Bucharest, 010041 Bucharest, Romania*

(Received 23 May 2024; accepted 14 November 2024)

The Haţeg Basin and surrounding areas in Transylvania, western Romania, have been a hotspot for research on vertebrate faunas of the Late Cretaceous European Archipelago. One of the historically earliest titanosaurian sauropod dinosaurs to be discovered, the 'dwarfed' species *Magyarosaurus dacus* comes from lower Maastrichtian deposits in this basin; however, this species has been neglected, with no modern treatment of its anatomy, taxonomy or phylogenetic affinities. Via detailed anatomical study of historical and undescribed remains, combined with archival data, we identify shared autapomorphies that link multiple partial skeletons. Our analysis of hundreds of specimens (including >20 monospecific assemblages) enables the stabilization of the type species *Magyarosaurus dacus*. We propose the presence of three additional, but only partly contemporaneous taxa – *Paludititan nalatzensis*, *Petrustitan* ('*Magyarosaurus*') *hungaricus* n. gen. and *Uriash kadici* n. gen. n. sp. (the latter being amongst the largest known sauropods of the Late Cretaceous European Archipelago). We present a new phylogenetic analysis (152 taxa scored for 570 characters), with implications for broader titanosaurian evolutionary relationships and biogeography: *Magyarosaurus* is recovered either as a member or a close relative of Saltasauridae; *Paludititan* has affinities with Lognkosauria, along with the contemporaneous *Lohuecotitan*; *Petrustitan* is most closely related to South American early diverging eutitanosaurian taxa; and *Uriash* also shares affinities with Gondwanan taxa. Our findings strengthen the hypothesis that latest Cretaceous European titanosaurs belonged to Gondwanan lineages that invaded the former area during the Barremian–Albian. We interpret the presence of body-size disparity as either evidence that large-bodied taxa were ecologically excluded from body-size reduction by competition with small-bodied titanosaurs, or that dwarfing occurred stratigraphically earlier among several lineages and the small-bodied titanosaurs on Haţeg Island are the descendants of existing dwarfed ancestors. Finally, we find no indication of a body size-related titanosaurian turnover in the uppermost Cretaceous of the Transylvanian area.

Keywords: Cretaceous; Titanosauria; Haţeg Basin; Romania; island dwarfism; palaeobiogeography

Introduction

Titanosaurian sauropod dinosaurs include the largest animals to ever walk on land, with gigantic species that exceeded 60 tonnes (Benton et al., 2014; Bonaparte & Coria, 1993; Carballido et al., 2017; Sander et al., 2011). By the late Early Cretaceous, titanosaurs had achieved a near-global distribution (Gallina et al., 2021; Gorscak & O'Connor, 2016; Mannion, Upchurch, Jin, et al., 2019), with their remains known from every landmass in the Late Cretaceous (Cerda et al., 2011; Curry Rogers, 2005; Hocknull et al., 2009; Upchurch et al., 2004). Despite a rich and global fossil record, titanosaurian evolutionary relationships are poorly known (Carballido et al., 2022; Curry Rogers, 2005; Gorscak et al., 2023; Mannion, Upchurch, Schwarz, et al., 2019), limiting our understanding of this diverse clade of megaherbivores (the only group of sauropods to survive into the latest Cretaceous; Salgado et al., 1997). In particular, European titanosaurs have largely been neglected in phylogenetic analyses (Mannion, Upchurch, Schwarz, et al., 2019). This neglect mainly stems from the historical predominance of Gondwanan species, as well as the scarcity and incompleteness of Laurasian remains, especially from Europe (Le Loeuff, 1993; Mannion, Upchurch, Schwarz, et al., 2019; Wilson & Upchurch, 2003). However, this has begun to change through a combination of reassessments of existing taxa and specimens (Díez Díaz et al., 2011, 2015; Díez Díaz, Pereda-Suberbiola, et al., 2012, 2013a, 2013b; Díez Díaz, Tortosa, et al., 2013), as well as the discovery of new remains, including articulated, partial skeletons (Csiki,

*Corresponding author. Email: diezdiaz.veronica@gmail.com

Published online 20 Feb 2025

Codrea, et al., 2010; Díez Díaz, Garcia, et al., 2012; Díez Díaz et al., 2014, 2016, 2018, 2021; Garcia et al., 2010; Le Loeuff et al., 2013; Vila et al., 2022). As such, the latest Cretaceous (late Campanian–Maastrichtian) European sauropod fossil record, in particular, is starting to reveal a rich evolutionary history, with increasingly recognized importance for biogeographical scenarios (e.g. Holwerda et al., 2018; Mannion, Upchurch, Schwarz, et al., 2019; Sallam et al., 2018; Vila et al., 2022) and growing incorporation into phylogenetic analyses (Díez Díaz et al., 2018, 2021; Gorscak et al., 2023; Gorscak & O'Connor, 2019; Sallam et al., 2018; Vila et al., 2022).

Despite these developments, one of the historically earliest titanosaurs to be discovered from Europe, *Magyarosaurus dacus*, from the uppermost Cretaceous (Maastrichtian) beds of Haţeg Basin in Transylvania, western Romania (Fig. 1A), remains neglected, with no modern treatment of its anatomy, taxonomy or phylogenetic affinities. This is despite the referral of numerous remains to this taxon, representing most parts of the skeleton (e.g. Huene, 1932), including cranial elements (Weishampel et al., 1991) (Fig. 2). First described as a species of *Titanosaurus* (*T. dacus*) by Nopcsa (1915), this taxon was subsequently placed in its own genus, *Magyarosaurus*, by Huene (1932), who erected two additional species (*M. transsylvanicus* and ?*M. hungaricus*). Subsequent to Huene's (1932) taxonomic revision, with some notable exceptions (see below), most titanosaur remains recovered from the Maastrichtian of the Transylvanian area were simply referred to *Magyarosaurus* (or *Titanosaurus*) *dacus*, usually without supporting evidence (e.g. Codrea et al., 2010; Jianu et al., 1997; Jianu & Weishampel, 1999; Mamulea, 1953a; Vremir, 2010; Vremir et al., 2015). This practice resulted in the view that a monospecific (at most monogeneric) titanosaur taxon was present in the Transylvanian area of Romania during the latest Cretaceous (e.g. McIntosh, 1990; Upchurch et al., 2004). The diminutive size of these fossil remains has also interested researchers since the initial discovery of the Transylvanian titanosaurs (e.g. Grellet-Tinner et al., 2012; Jianu & Weishampel, 1999; Nopcsa, 1915; Stein et al., 2010; Weishampel et al., 2010), particularly given the gigantic nature of most members of the group (Bonaparte & Coria, 1993; Carballido et al., 2017; Lacovara et al., 2014). The consensus is that this represents an instance of island dwarfism during heightened Late Cretaceous sea levels, when Europe formed an archipelago (e.g. Csiki-Sava et al., 2015; Nopcsa, 1923b; Stein et al., 2010; Weishampel et al., 1991, 2010).

The taxonomy of *Magyarosaurus* is problematic. Firstly, there is a great deal of uncertainty regarding the historical association of specimens, making it unclear whether it represents a chimaera. Secondly, although most authors have considered only *M. dacus* to be valid (e.g. Le Loeuff, 1993; Upchurch et al., 2004), it is unclear whether the other two named species are synonyms or represent greater diversity. Thirdly, an additional taxon – *Paludititan nalatzensis* – was recognized in 2010 (Csiki, Codrea, et al., 2010), demonstrating the presence of at least a second approximately contemporaneous Romanian titanosaur. This emphasizes the danger that past referrals of fragmentary and non-overlapping specimens to *Magyarosaurus* might have created a chimaeric taxon. Finally, osteohistological research targeting the Romanian titanosaurs has also hinted at the presence of at least one other, large-sized taxon in the faunal assemblage besides the small-bodied *M. dacus* and *Paludititan* (Stein et al., 2010). As such, it remains unclear what actually comprises *Magyarosaurus*, limiting its utility in evolutionary and palaeobiogeographical studies of Titanosauria.

In this study, we provide a comprehensive revision of *Magyarosaurus*. We combine detailed anatomical study of historical and undescribed remains, coming mainly from the Haţeg Basin, with archival data to identify shared autapomorphies that link multiple partial skeletons. This forms the basis for a revision of the systematics of *M. dacus*, ?*M. hungaricus* and *M. transsylvanicus*, and an evaluation of their phylogenetic and biogeographical affinities with respect to *Paludititan* and other titanosaurs from Europe and elsewhere.

Institutional abbreviations

LPB (FGGUB), Laboratory of Palaeontology, Faculty of Geology and Geophysics, University of Bucharest, Romania; **MCDRD,** Muzeul Civilizatiei Dacice si Romane (Museum of Dacian and Roman Civilisation), Deva, Romania**; NHMUK,** Natural History Museum, London, UK; **SZTFH**, Collection of the Supervisory Authority for Regulatory Affairs (formerly the Geological Institute of Hungary [MAFI], Budapest, Hungary); **UBB,** Babeș-Bolyai University, Cluj-Napoca, Romania.

Axial anatomical abbreviations

ACDL, anterior centrodiapophyseal lamina; **ACPL,** anterior centroparapophyseal lamina; **CDF,** centrodiapophyseal fossa; **CPOL,** centropostygapophyseal lamina; **D,** diapophysis; **lSPRL,** lateral spinoprezygapophyseal lamina; **mSPRL,** medial spinoprezygapophyseal lamina; **NC,** neural canal; **PA,** parapophysis; **PACDF,** parapocentrodiapophyseal fossa; **PCDL,** posterior

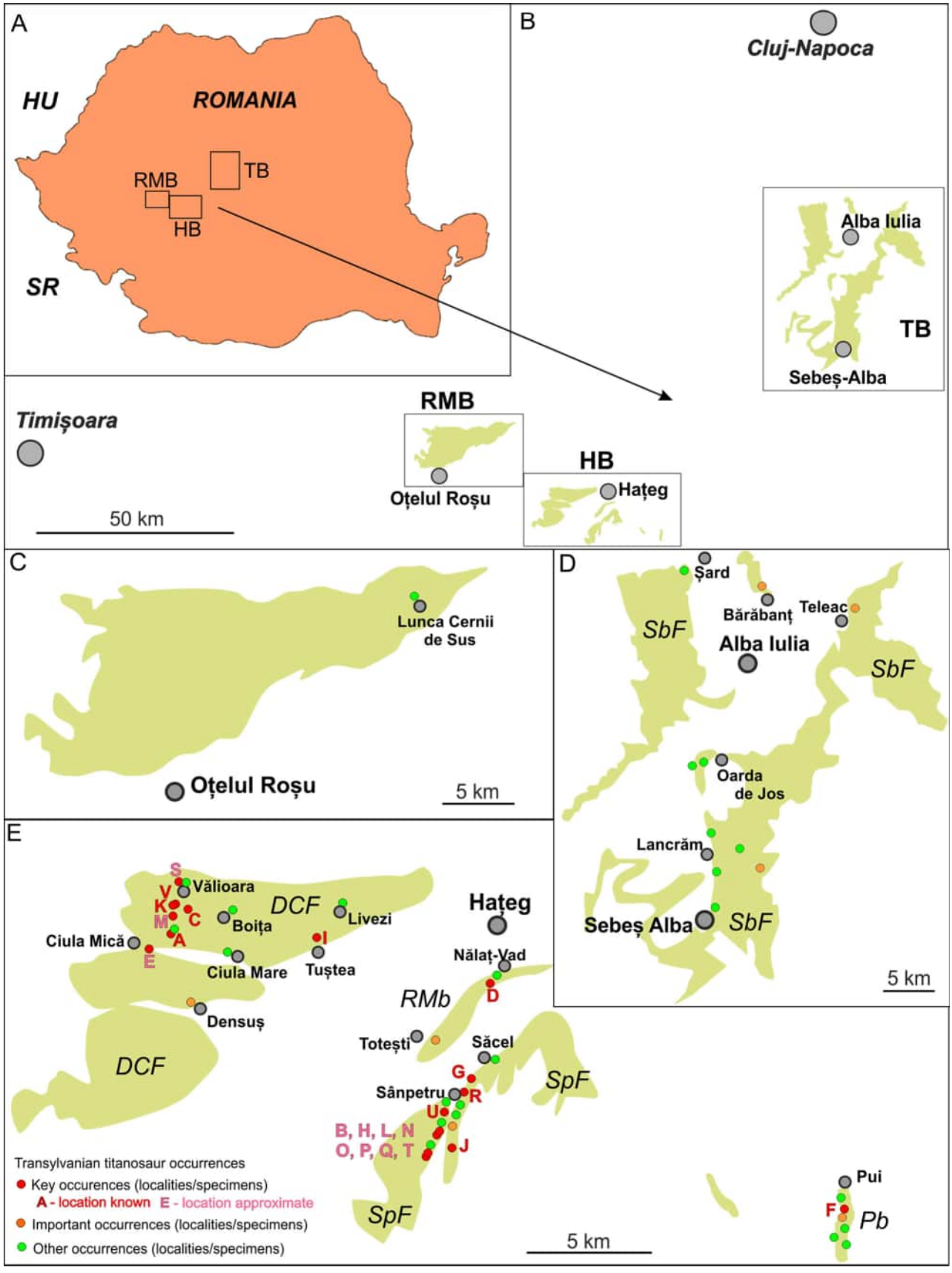
A
HU
ROMANIA
SR
RMB
TB
HB
B
Cluj-Napoca
Alba Iulia
TB
Sebeș-Alba
RMB
HB
Timișoara
Oțelul Roșu
Hațeg
50 km
C
Lunca Cernii de Sus
Oțelul Roșu
5 km
D
Șard
Bărăbanț
Teleac
SbF
Alba Iulia
SbF
Oarda de Jos
Lancrăm
Sebeș Alba
SbF
5 km
E
S
V
K
M
C
A
Vălioara
Boița
DCF
Livezi
Ciula Mică
E
I
Ciula Mare
Tuștea
Densuș
DCF
Hațeg
Nălaț-Vad
D
RMb
Totești
Săcel
G
Sânpetru
R
U
B, H, L, N
O, P, Q, T
J
SpF
SpF
Pui
F
Pb
5 km
Transylvanian titanosaur occurrences
Key occurences (localities/specimens)
A - location known E - location approximate
Important occurrences (localities/specimens)
Other occurrences (localities/specimens)

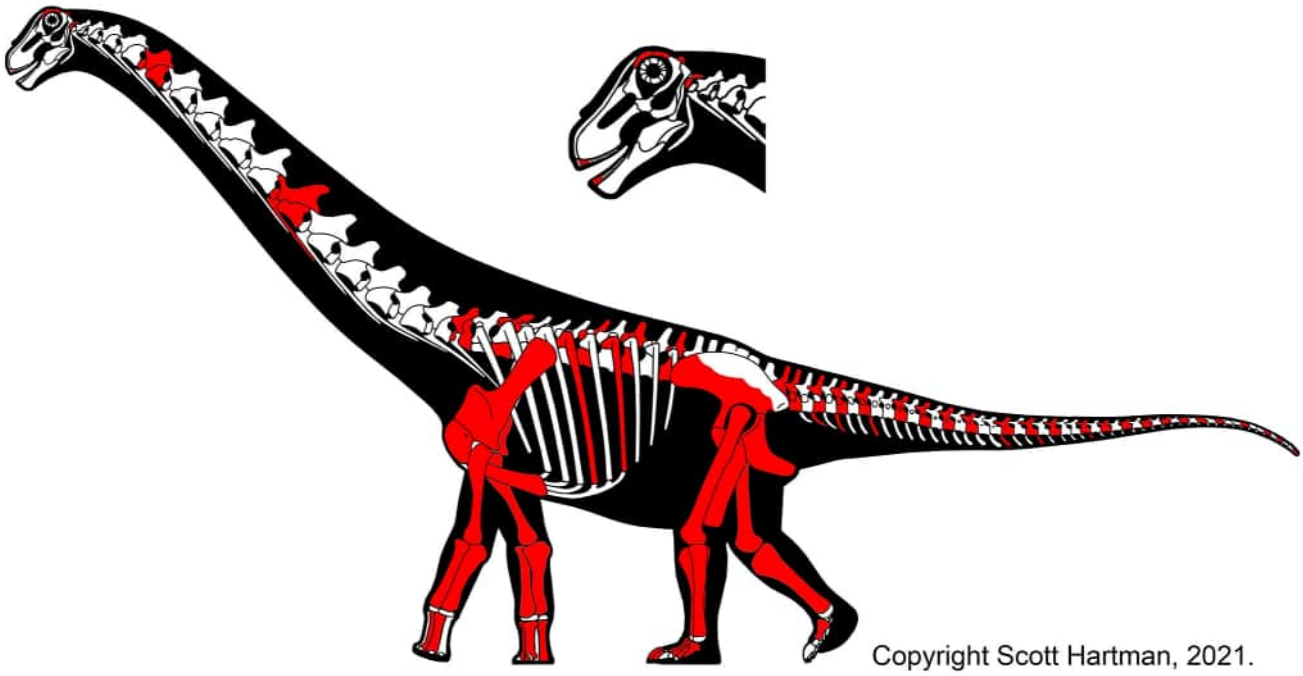

Figure 2. Record of documented anatomy based on all Transylvanian titanosaur remains described in this work, summarized in one individual. Not to scale. Skeletal drawing after Scott Hartman, used with permission.

centrodiapophyseal lamina; **PCPL,** posterior centroparapophyseal lamina; **PO,** postzygapophysis; **POCDF,** posterior centrodiapophyseal fossa; **PODL,** postzygodiapophyseal lamina; **PPDL,** paradiapophyseal lamina; **PRCDF,** prezygocentrodiapophsyeal fossa; **PRDL,** prezygodiapophyseal lamina; **PRE,** prezygapophysis; **PRSL,** prespinal lamina; **SDF,** spinodiapophyseal fossa; **SPDL,** spinodiapophsyeal lamina; **SPOF,** spinopostzygapophyseal fossa; **SPOL,** spinopostzygapophyseal lamina; **SPRF,** spinoprezygapophyseal fossa; **TPOL,** interpostzygapophyseal lamina.

Other abbreviations

aEI (*sensu* Chure et al., 2010), average elongation index, which scales the non-condylar centrum length divided by the mean average of the mediolateral width and dorsoventral height of the non-condylar centrum articular surface; **DWI** (*sensu* Poropat et al., 2016), distal width index, defined as the ratio of the mediolateral width of the distal end to the total proximodistal length of the limb bone; **ECC** (*sensu* Wilson & Carrano, 1999), eccentricity index, calculated as the mid-shaft mediolateral width divided by the anteroposterior diameter of long bones; **Hafd** (*sensu* Upchurch et al., 2015), humeral anconeal fossa depth divided by the anteroposterior width of the distal end; **PWI** (*sensu* González Riga, 2003), proximal width index, the ratio of the mediolateral width of the proximal end to the total proximodistal length of the limb bone; **RI** (*sensu* Wilson & Upchurch, 2003), robustness index, the ratio of the mean average of the mediolateral widths of the proximal and distal ends, as well as the minimum mediolateral diameter of the shaft, to the total proximodistal length of the limb bone.

Geological setting

Uppermost Cretaceous fossiliferous continental beds are distributed patchily across several sedimentary basins in western Romania; the most productive and concentrated localities are in the Haţeg Basin and the south-western

Figure 1. Distribution of titanosaur fossil occurrences in Romania. **A,** position of the major areas with fossiliferous uppermost Cretaceous continental deposits (labelled boxes); and **B,** areal distribution of the uppermost Cretaceous continental beds from these major areas, highlighted in light green (HB – Haţeg Basin, RMB – Rusca Montană Basin, TB – south-western Transylvanian Basin). C–E, main titanosaur-bearing fossiliferous localities in **C,** Rusca Montană Basin; **D,** south-western Transylvanian Basin (SbF – Sebeș Formation); and **E,** Haţeg Basin (DCF – Densuș-Ciula Formation, Pb – 'Pui beds', RMb – 'Râul Mare beds', SpF – Sînpentru Formation). For details on key occurrences (coded A to V in Fig. 1E) see text ('Key localities and skeletal associations' section).

part of the neighbouring and larger Transylvanian Basin (Codrea et al., 2010; Csiki-Sava et al., 2016; Nopcsa, 1905; Vremir et al., 2015) (Fig. 1). Spatially more restricted and relatively fossil-poor deposits are also known from the Rusca Montană Basin (Fig. 1), as well as from the western and north-western marginal areas of the Transylvanian Basin (e.g. Codrea et al., 2010, 2012; Codrea & Godefroit, 2008; Csiki-Sava et al., 2016). These deposits were laid down at the feet of mountain chains uplifted by latest Cretaceous orogenic events that shaped the nappe structure of the inner Carpathian area (e.g. Willingshofer et al., 2001). They are dominated by fluvial (coarser channel and finer-grained floodplain) siliciclastic sediments, associated in the more western areas (central-western Haţeg Basin, Rusca Montană Basin) with volcanoclastic material, volcanic tuffs, and minor lava flows, as well as coal bed intercalations (Csiki-Sava et al., 2016). Deposition took place within the confines of a subtropical island ('Haţeg Island' or Transylvanian Landmass), part of the Late Cretaceous European Archipelago that fringed the northern margin of the Mesozoic Neotethys-Alpine Tethys oceanic realm (e.g. Benton et al., 2010; Csiki-Sava et al., 2015). Such a palaeogeographical position, as well as the presence of a dominantly semi-arid climate (e.g. Therrien, 2005), is supported by palaeomagnetic studies that place Haţeg Island at an approximate palaeolatitude of 29° N (Panaiotu & Panaiotu, 2010). The age of these continental beds is loosely constrained to the Maastrichtian by their position atop biostratigraphically dated Campanian marine beds (Melinte-Dobrinescu, 2010; Ţabără et al., 2022; Vremir et al., 2014), corroborated by magnetostratigraphy (Panaiotu & Panaiotu, 2010), palynostratigraphy (Antonescu et al., 1983; Botfalvai et al., 2021; van Itterbeeck et al., 2005), and a few radiometric ages (Bojar et al., 2011). Locally, the transitional-to-continental beds also include part of the uppermost Campanian, marking the onset of terminal Cretaceous continental deposition well before 72 Ma (Bălc et al., 2024; Vremir et al., 2014).

Several approximately synchronous lithostratigraphical units have been defined within the continental uppermost Cretaceous of Transylvania (for a recent review see Csiki-Sava et al., 2016), although direct correlation between these is largely tentative because of their patchy spatial exposure and lack (even locally) of extensive marker beds. In the Haţeg Basin, these units include: the Sînpetru Formation (Maastrichtian) in the central part of the basin; the partly volcanoclastic Densuș-Ciula Formation (Maastrichtian) in its north-western marginal areas (Grigorescu, 1992); and as yet not formally defined sedimentary successions in the west-central ('Râul Mare Beds'; probably 'middle' to upper Maastrichtian) and eastern-central ('Pui Beds', upper part of lower to lower part of upper Maastrichtian) areas of the depression. Fossils, including vertebrate remains, are common throughout these units (Csiki-Sava et al., 2016; Grigorescu, 1983; Nopcsa, 1915). In the Transylvanian Basin, the major fossil-bearing unit is the Sebeș Formation (uppermost Campanian–upper Maastrichtian; (Vremir, 2010; Vremir et al., 2015); = Șard Formation (Codrea et al., 2010), distributed in its south-western part, whereas the Maastrichtian–Paleocene Jibou Formation (Codrea et al., 2010) that outcrops in its western-north-western areas has yielded only rare latest Cretaceous fossils (Codrea & Godefroit, 2008). Finally, the uppermost Cretaceous (Maastrichtian) continental beds of the Rusca Montană Basin have yet to receive a formal lithostratigraphical designation; these have only recently yielded vertebrate fossils (Codrea et al., 2012; Csiki-Sava et al., 2016; Vasile & Csiki, 2011).

For more than a century (e.g. Nopcsa, 1897), a rich continental assemblage has been recovered from these Transylvanian uppermost Cretaceous deposits. Plants are represented by diverse palynological assemblages (e.g. Antonescu et al., 1983; Botfalvai et al., 2021; Csiki et al., 2008; Ţabără et al., 2022; Ţabără & Csiki-Sava, 2024; van Itterbeeck et al., 2005), mesofloral elements (seeds, fructifications; May Lindfors et al., 2010), as well as macroplant remains (e.g. Popa et al., 2014, 2016). Invertebrates are less well studied, but ostracods (Silye et al., 2014), gastropods (Páll-Gergely et al., 2023; Pană et al., 2002), and insects (Augustin et al., 2019; Csiki, 2006; Vremir, 2009) have all been reported. Vertebrates make up the best-known component of the local palaeoecosystem, and these include diverse taxa of fish, anurans, albanerpetontids, turtles, lizards, snakes, crocodyliforms, pterosaurs, non-avian dinosaurs (various theropods, titanosaur sauropods, rhabdodontid and hadrosauroid ornithopods, nodosaurid ankylosaurs), birds, and multituberculate mammals (e.g. Benton et al., 2010; Csiki-Sava et al., 2015, 2016; Nopcsa, 1923a; Weishampel et al., 2010).

Among the dinosaurs, titanosaur sauropods represent one of the most commonly occurring groups (e.g. Csiki, Grigorescu, et al., 2010, fig. 3; Grigorescu, 1983). Titanosaur remains are widespread, having been discovered in most major vertebrate localities in the Haţeg, south-western Transylvanian, and Rusca Montană basins, as both associated and isolated skeletal elements (e.g. Botfalvai et al., 2021; Codrea et al., 2010, 2012; Csiki, Codrea, et al., 2010; Grigorescu, 1983; Huene, 1932; Nopcsa, 1915; Vremir, 2010; Vremir et al., 2015). Caudal vertebrae, pectoral girdle, and appendicular elements represent the most commonly occurring titanosaur

skeletal remains recovered, whereas presacral vertebrae, elements of the pelvic girdle, and skull remains are uncommon to very rare (Fig. 2; see below and Supplemental Material). Contrary to their wide geographical distribution in Romania, their stratigraphical distribution seems to be more skewed, with the few latest Campanian–earliest Maastrichtian vertebrate-bearing localities apparently lacking titanosaur remains (e.g. Bălc et al., 2024; Vremir et al., 2014).

History of titanosaur discoveries and research in Transylvania

Specimen discoveries

Despite their common presence in the continental uppermost Cretaceous of Romania, and the relatively large number of studies devoted to them in the past, the taxonomy, systematics and phylogenetic affinities of the Transylvanian titanosaurs remain problematic. Confusion and disagreement have arisen mainly because of the often isolated and fragmentary nature of their remains, as well as the quasi-absence of reliable locality and association data for the material that was discovered and excavated before 1990.

The first reports to mention the presence of latest Cretaceous vertebrate remains in the Hațeg Basin were by Halaváts (1897) and Nopcsa (1897). Although neither of these publications specifically recorded the presence of sauropod remains in the area, inspection of the SZTFH collections and registry records in Budapest shows that the first sauropod remains currently on record were discovered in 1896 in the Sibișel Valley, south of Sânpetru (stratotype area of the Sînpetru Formation; Grigorescu, 1992, figs 1, 3). These specimens, represented by two caudal vertebrae inventoried as SZTFH Ob.1945 and Ob.1947 (Fig. 3), were collected by Gyula Halaváts, a geologist of the Hungarian Royal Geological Survey, who was mapping in the central-eastern parts of the Hațeg Basin (Halaváts, 1897). The Halaváts specimens remained unidentified until 1904, when they were officially accessioned in the SZTFH collections (L. Makádi, pers. comm. February 2019). The first explicit mention of sauropod remains in the Hațeg Basin was by Ferenc (= Franz) Nopcsa (1902a). Slightly later, Nopcsa (1904, 1905) noted the presence of as many as three different sauropod taxa in the Hațeg faunal assemblage, including *Titanosaurus*, which he identified based on its caudal vertebral morphology (and to which he also referred a humerus, an ischium, and two femora), and two indeterminate taxa whose presence was suggested by distinctive and divergent vertebral and humeral morphologies. However, none of these sauropod specimens were described or figured, and no information was offered in support of these taxonomic identifications, except for a personal communication from the French geologist and palaeontologist Charles Deperét, who noted the similarity of some Transylvanian caudal vertebrae to those of titanosaurs. The presence of titanosaurs in the uppermost Cretaceous

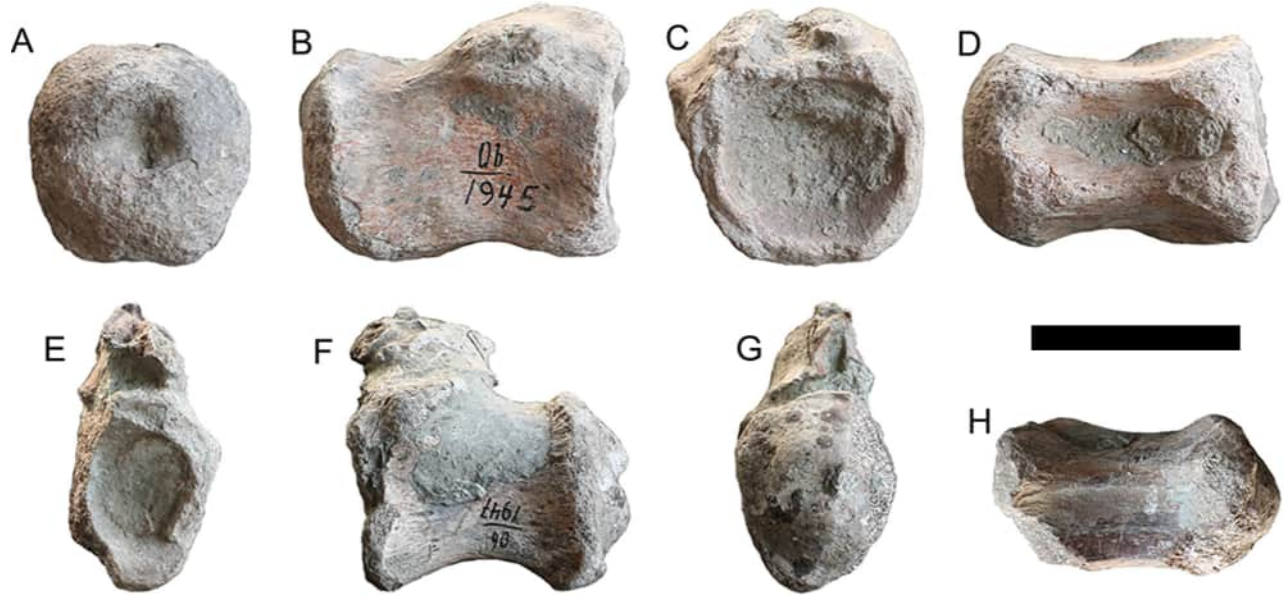

Figure 3. First Late Cretaceous vertebrate remains reported in the Hațeg Basin (Halaváts, 1897; Nopcsa, 1897), two titanosaur anterior caudal vertebrae: SZTFH Ob.1945 in **A,** posterior; **B,** right lateral; **C,** anterior; and **D,** ventral views. SZTFH Ob.1947 1945 in **E,** anterior; **F,** left lateral; **G,** posterior; and **H,** ventral views. Scale bar equals 50 mm.

continental beds of the Transylvanian region was thus first identified by Nopcsa based mainly on his personal collection from Sânpetru, excavated along the Sibișel Valley (Hațeg Basin), and which was subsequently purchased by the NHMUK (London) in 1906.

The aforementioned titanosaur specimens from the Hațeg Basin were by no means the first ones discovered in the wider Transylvanian region. In his geological overview of south-western Transylvania, including the Hațeg Basin, Nopcsa (1905) also mentioned the previous discovery of sauropod remains (a humerus and femur) from Râpa Roșie, north-east of Sebeș, in the south-western Transylvanian Basin (Fig. 1D), that had been misidentified as large mammal bones by Koch (1894). To these, Nopcsa added a large-sized sauropod ulna he had recovered from the same locality. Together with a very incomplete and poorly preserved large limb bone from Bărăbanț (also south-western Transylvanian Basin; Fig. 1D), discovered in 1860 but only recognized as a possible sauropod tibia more than a century later (Codrea & Mărginean, 2007), these fossils from Râpa Roșie represent not only the first sauropod remains, but also the first dinosaur remains discovered from the entire Transylvanian area. Unfortunately, the Râpa Roșie specimens appear to be lost now, and the Bărăbanț specimen is very poorly preserved; thus, the precise nature and affinities of these early sauropod discoveries from Transylvania remain unknown.

Another important early collection of vertebrate (including titanosaur) fossils was amassed by Ottokár Kadić, a geologist of the Hungarian Royal Geological Survey. He was assigned to map in the north-western Hațeg Basin, where he discovered dinosaur bones around Vălioara (Fig. 1E) in 1909 (Kadić, 1911). In subsequent years, he returned to this area to conduct several successful excavation campaigns, the results of which today form the core of the SZTFH collection of latest Cretaceous continental vertebrates in Budapest (Botfalvai et al., 2021; Kadić, 1916). Together, the NHMUK material collected by Nopcsa at Sânpetru and the SZTFH collection of Kadić from Vălioara allowed Nopcsa (1915) to write his first synthesis on the composition and palaeobiology of the Transylvanian dinosaur fauna, a study that also includes the first description and taxonomic identification of a sauropod from this fauna. Despite his previous comments concerning the presence of several sauropod taxa in the Hațeg Basin, and his earlier interpretation that titanosaur-like vertebrae belonged instead to the hadrosauroid *Telmatosaurus* (Nopcsa, 1910), Nopcsa (1915) recognized the presence of a single taxon of titanosaur sauropod as a new species of the (now obsolete; Wilson & Upchurch, 2003) genus *Titanosaurus*, namely *T. dacus*. He briefly characterized this new species and figured a few of the referred skeletal elements from the SZTFH collection (Nopcsa, 1915, pl. III, figs 4, 5, 8), represented by isolated middle and posterior caudal vertebrae from Vălioara, and an ungual (now lost, but presumably also from Vălioara). Later, in his second synthesis of the Transylvanian vertebrate fauna, Nopcsa (1923a) commented further on the anatomy of *T. dacus*, as well as on the evolutionary and palaeobiogeographical implications of its presence in uppermost Cretaceous rocks of eastern Europe.

Nopcsa had planned to describe this material himself as part of his 'Dinosaurierreste aus Siebenbürgen … ' series of monographs, according to letters to Friedrich Huene in 1926–1927 (translated in Weishampel & Kerscher, 2013), but these plans never came to fruition. Thus, unlike the significantly larger amount of work (and number of publications) he devoted to the study of ornithischians and turtles of this fauna (e.g. Nopcsa, 1900, 1902a, 1923b, 1929), these two short contributions (i.e. Nopcsa, 1915, 1923a) represent the extent of Nopcsa's published research efforts towards the study of the Transylvanian sauropod material. In order to compensate for this shortcoming (partly caused by health problems; see Weishampel & Jianu, 2011; Weishampel & Kerscher, 2013), Nopcsa invited Huene to study and describe the Transylvanian titanosaur material, sending him his notes, drawings, and even shipping several specimens from the Budapest collection to Tübingen, south-west Germany, where Huene was based. This study was first envisaged as a collaboration between the two workers (Weishampel & Jianu, 2011, p. 203), but Nopcsa subsequently entrusted it entirely to Huene (Weishampel & Kerscher, 2013), and thus Huene included an extensive chapter on the Transylvanian titanosaurs in his monograph on saurischian dinosaurs (Huene, 1932).

Huene's detailed survey of the Transylvanian sauropod material available at that time (i.e. the entirety of the London and Budapest sauropod collections), supported by his previous work on South American titanosaurs and overall sauropod diversity (e.g. Huene, 1929), led him to refer this material without exception to Titanosauria. Furthermore, he recognized morphological differences between the Transylvanian titanosaur material and the holotype of *Titanosaurus* (*T. indicus*) from the uppermost Cretaceous of India (Lydekker, 1877), which led him to erect a new genus, *Magyarosaurus*, for the Hațeg titanosaur remains. In order to account for perceived morphological, proportional, and dimensional differences within the studied material, Huene also erected two further species within *Magyarosaurus*, recognizing the small-to-medium sized *M. dacus* and *M.*

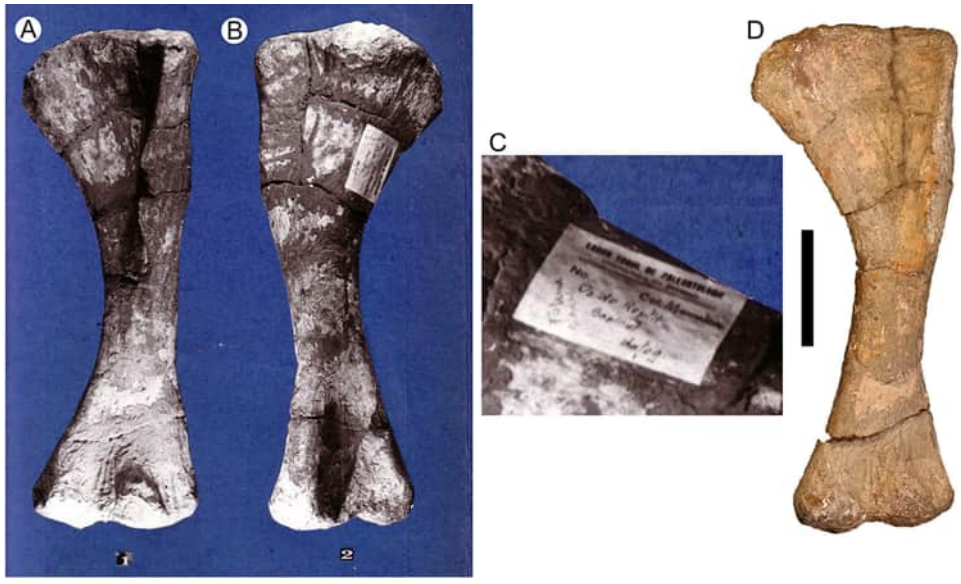

Figure 4. Left humerus LPB (FGGUB) R.1047 from Individual E, collected by M. A. Mamulea (indicated in the paper label attached to it). **A,** anterior view; and **B,** posterior view, from Ungureanu (1979). **C,** paper label, from Ungureanu (1979). **D,** anterior view. Scale bar equals 100 mm.

transsylvanicus, and the larger ?*M. hungaricus*, while assigning other remains as either *Magyarosaurus* sp. or as indeterminate titanosaurs.

Following the Nopcsa and Kadić excavations and the survey of Huene, there was a significant reduction in the pace of the collection and study of Transylvanian titanosaurs that extended until the last decades of the twentieth century. Nevertheless, even though subsequent collecting efforts were serendipitous and not systematic, important titanosaur specimens were discovered in the Hațeg region by prospecting geologists and university staff carrying out fieldwork between 1932 and 1977. Foremost of these are the fossils excavated by field geologist Mihai Alfred Mamulea in the neighbourhood of Ciula Mică (Fig. 1E). Although at first he only reported the discovery of unspecified dinosaur bones in bluish-reddish sandstones (Mamulea, 1953a), he specified that he had recovered from Ciula Mică 'a few nicely preserved fossil remains belonging to *T. dacus* NOPCSA' in a second, more detailed geological report dealing with the central part of Hațeg Basin (Mamulea, 1953b, p. 250, in Romanian in the original). According to personal information retrieved from faculty staff members at the FGGUB (T. Neagu, D. Grigorescu, pers. comm., 2004), Mamulea donated specimens he collected in the Hațeg area to the LPB (FGGUB) collection after retiring. Some of these specimens were figured in an unpublished BSc thesis (Ungureanu, 1979), including one well-preserved titanosaur humerus (LPB [FGGUB] R.1047) displaying a paper label attached which indicates that it was collected by Mamulea (Fig. 4); unfortunately, this label was removed and probably lost during subsequent preparation and consolidation of the specimen. Based on this circumstantial evidence, as well as preservational similarities and commensurate size, a series of titanosaur skeletal elements were identified in the LPB (FGGUB) collections that correspond to the fossils excavated by Mamulea. Furthermore, the absence of overlapping skeletal elements within this assemblage (see 'Key localities and skeletal associations' and 'Systematic palaeontology' sections) and their commensurate size suggest that these specimens were not only excavated together from the same locality, but they most probably represent parts of one incomplete skeleton that includes associated and relatively well-preserved dorsal and caudal vertebrae (some of them still in articulation), as well as limb elements. As such, this individual ('Individual E': see 'Key localities and skeletal associations' section) represents one of the few cases of historical titanosaur discoveries from Transylvania where skeletal association can be reasonably assumed, with important consequences for our understanding of the anatomy and systematics of *Magyarosaurus*.

Before 1980, further isolated titanosaur remains – besides the 'Mamulea specimen' – were also recovered from Sânpetru and Pui (Fig. 1E). Several titanosaur fossils from Sânpetru (caudal vertebrae and limb bones) were excavated from a fossiliferous pocket by Nicolae Mészáros and H. Krauss in 1966. These specimens, together with isolated titanosaur bones found by Mészáros and Téglás in 1979, are now registered in the

Figure 5. Titanosaur middle caudal vertebra LPB (FGGUB) R.1062 from Sânpetru previously referred to *Titanosaurus* cf. *indicus* in **A,** right lateral; **B,** ventral views; **C,** anterior; **D,** left lateral; **E,** posterior; **F,** ventral; and **G,** dorsal views. A and B are taken from Dincă et al. (1972). NHMUK R.40867 (holotype of *Titanosaurus indicus* from India) in **H,** anterior; **I,** left lateral; **J,** posterior; **K,** ventral; and **L,** dorsal views, for comparison. Scale bars equal 50 mm.

UBB collections (Jianu et al., 1997). All of these sauropod remains, mostly fragmentary and rather poorly preserved, were later referred, without further detail or argumentation, to *M. dacus* (Jianu et al., 1997). Dincă et al. (1972) reported the discovery of an isolated caudal vertebra from Sânpetru (LPB [FGGUB] R.1062; Fig. 5A–G), and tentatively referred it to *Titanosaurus* cf. *indicus*. These authors suggested *in passim* – and without supporting evidence – that '*T*'. *dacus* might be synonymous with *T. indicus* (see the Supplemental Material). At Pui, dinosaur remains were collected by Mamulea (1953b) and Stilla (1985); of these, a few isolated titanosaur specimens donated by Alexandru Stilla (scapula fragment, LPB [FGGUB] R.1153, and humerus shaft, LPB [FGGUB] R.0555) are now curated in the collections of the FGGUB.

Despite the occasional discovery of mainly isolated and some more complete titanosaur specimens, such as those noted above, it was only with the renewal of palaeontologically focused exploration and excavation efforts after 1977 that more significant collections of latest Cretaceous continental vertebrates were amassed (see Grigorescu [2010] for a review). These post-1977 efforts led to the assembly of important collections at the University of Bucharest (LPB [FGGUB]), the Babeș-Bolyai University in Cluj-Napoca (UBB), and the Muzeul Civilizației Dacice și Romane in Deva, Hunedoara County (MCDRD). Significantly, details on locality and skeletal association were recorded for many of these more recent titanosaur discoveries, a source of information that is largely lacking for older collections and whose absence has led to the confusion and

misinterpretation that has plagued the taxonomy of Transylvanian titanosaurs. Starting in 1979, systematic excavation campaigns focused primarily on the Hațeg Basin, but also targeted the south-western Transylvanian and Rusca Montană basins. These efforts were initiated through collaboration between the FGGUB (coordinated by Dan Grigorescu, more recently also including ZCs-S) and the MCDRD (first conducted by Ion Groza, then by Coralia-Maria Jianu). From the mid-1990s, these prospecting and excavation activities were joined by the UBB (coordinated by Vlad Codrea), the Transylvanian Museum Society (Mátyás Vremir), and the Ioan Raica Museum, in Sebeș-Alba (Radu Totoianu), and were often made in collaboration with colleagues from abroad. This work resulted in the discovery and excavation of a large number of vertebrate localities that have yielded a considerable amount of titanosaur material either in isolation or mixed with other vertebrates. These titanosaur specimens occasionally include associated skeletal remains (e.g. Botfalvai et al., 2021; Csiki-Sava et al., 2012; Groza, 1983; van Itterbeeck et al., 2004), and even partial skeletons (Csiki, Codrea, et al., 2010). Because of these new discoveries, the areal coverage of known titanosaur localities expanded to include sites in the Hațeg Basin such as Pui (e.g. Codrea & Solomon, 2012; Grigorescu et al., 1985; Știucă, 1983; van Itterbeeck et al., 2004), Nălaț-Vad (Csiki, Codrea, et al., 2010; 2016; Smith et al., 2002), Livezi (Grigorescu & Csiki, 2008), Tuștea (Csiki-Sava et al., 2012), and Boița (Csiki-Sava et al., 2018), in addition to further occurrences around Sânpetru (Csiki, Grigorescu, et al., 2010; Groza, 1983; Știucă et al., 1982), Vălioara and Ciula Mică (Botfalvai et al., 2021). Outside of the Hațeg Basin, in the south-western Transylvanian Basin, the Râpa Roșie locality continued to yield titanosaur remains (e.g. Grigorescu, 1987, misidentified as ankylosaur elements; Codrea et al., 2008; Csiki & Vremir, 2011; Jianu et al., 1997), and new titanosaur localities (Șard, Oarda de Jos, Lancrăm, Sebeș-Glod, Teleac, MI6) were also identified (e.g. Codrea et al., 2010; Vremir, 2010; Vremir et al., 2015). Finally, rare titanosaur fossils were also discovered in the Rusca Montană Basin (Codrea et al., 2012).

Recent decades have brought about some outstanding titanosaur discoveries from the Transylvanian area. These include the excavation and identification of a well-preserved and fairly complete braincase at Pui (Știucă, 1983; Weishampel et al., 1991), the only currently known cranial material of a Transylvanian titanosaur, as well as isolated teeth (Botfalvai et al., 2021; Grigorescu et al., 1985; Ősi et al., 2017a). The La Cărare locality from Sânpetru has yielded the only known titanosaur osteoderm from Romania, associated with caudal vertebrae and limb bones, showing that at least some Transylvanian titanosaurs were armoured (Csiki, 1999). Although at the time of their first identification, megaloolithid eggs from the Hațeg Basin were preliminarily attributed to titanosaurs (Grigorescu et al., 1990), most of these are now considered to belong to hadrosauroid dinosaurs (e.g. Grigorescu, 2010). Nevertheless, Grellet-Tinner et al. (2012) suggested that certain megaloolithid eggs from Totești-Baraj (Fig. 1E) were laid by titanosaurs, thus further expanding the list of sauropod fossil localities. However, these titanosaur remains will not be covered in this work, especially given that their taxonomic affinities are practically impossible to establish because of the lack of clear association with postcrania.

Taxonomic and phylogenetic work

The persistence of substantial systematic uncertainties that surround Transylvanian titanosaurs is perhaps surprising given the large volume of contributions that have addressed this topic in the past. After the identification of the titanosaur species *T. dacus* by Nopcsa (1915) and its referral, together with two other new species (*M. transsylvanicus*, ?*M. hungaricus*), to the newly erected genus *Magyarosaurus* by Huene (1932), the issue of the taxonomic identity of the Transylvanian sauropod material entered a long period of neglect, followed by dissenting opinions. Steel (1970) and McIntosh (1990) recognized all three previously formalized taxa as valid species, but these authors assigned them to *Titanosaurus* and *Magyarosaurus*, respectively. Despite this, McIntosh (1990) noted that these species could barely be diagnosed by autapomorphies, although he recognized that it was conceivable that more than one taxon was present within the known fossil material. After first-hand study of the London and Budapest collections of Transylvanian titanosaurs, Le Loeuff (1993) suggested that the three species separated by Huene within *Magyarosaurus* could not be differentially diagnosed, and that they were in fact synonymous, falling under the name *M. dacus* (see also Csiki, 1999; Le Loeuff, 2005a). Le Loeuff (1993) stated that the first titanosaur specimens described by Nopcsa (1915), while naming *T. dacus*, correspond to two articulated dorsal vertebrae (NHMUK R.4896). Le Loeuff accordingly designated these vertebrae as the lectotype of the species (a designation also accepted, as 'type', by Jianu & Weishampel, 1999). However, this is incorrect, as we explain below in the 'Systematic palaeontology' section. Synonymy of the three *Magyarosaurus* species was also accepted in the reviews of Wilson and Upchurch (2003), Upchurch et al. (2004), and Curry Rogers (2005).

The contrasting viewpoint that there was a higher diversity of titanosaurs on the Transylvanian landmass was re-stated by Csiki and Grigorescu (2004). More specifically, the occurrence of large-sized titanosaur specimens with a distinctive morphology was noted by Csiki and Grigorescu (2006), Csiki et al. (2007), and Csiki and Vremir (2011). These authors preliminarily interpreted these large specimens as potentially representing taxa distinct from Nopcsa's and Huene's small-sized *M. dacus*, but possibly attributable to Huene's larger ?*M. hungaricus*. The presence of a larger titanosaur taxon was also supported by the osteohistological study of Stein et al. (2010). More recently, the existence of a higher taxic diversity was firmly established with the description of a second small-bodied titanosaur genus, *Paludititan nalatzensis*, from the Transylvanian area (Csiki, Codrea, et al., 2010), and was also hinted at in a preliminary overview of the Transylvanian titanosaur material by Csiki et al. (2011). This high diversity hypothesis was also supported by Mocho et al. (2023), based on their interpretation of four distinct caudal vertebral morphotypes.

An unusual outlier in the history of Transylvanian titanosaur taxonomy is the proposed presence of *Titanosaurus* cf. *indicus* in the Hațeg Basin, as suggested by Dincă et al. (1972). However, our recent relocation of this specimen (Fig. 5A–G) in the collections of the LPB (FGGUB) demonstrates that it cannot be referred to *Titanosaurus indicus*, and thus the proposed presence of this taxon in the Transylvanian area cannot be supported (see 'Additional titanosaur remains' section in the Supplemental Material).

Magyarosaurus, considered to be a 'titanosaurid' by McIntosh (1990), a non-saltasaurid lithostrotian by Upchurch et al. (2004), and a saltasaurid by Le Loeuff (2005a), has only been included previously in one phylogenetic data matrix (Curry Rogers, 2005), where it was recovered as a lithostrotian titanosaur of uncertain placement (see also Mannion & Upchurch, 2011). In light of the more recently recognized diversity of Transylvanian titanosaurs, it is likely that the operational taxonomic unit (OTU) used as *Magyarosaurus* by Curry Rogers (2005) represents a 'chimera' based on skeletal elements derived from more than one taxon. More recently, *Paludititan* has been included in several phylogenetic analyses, in which it was also recovered as a lithostrotian titanosaur, although its position varied between studies (Csiki, Codrea, et al., 2010; Díez Díaz et al., 2018, 2021; Gorscak & O'Connor, 2016, 2019; Navarro et al., 2022; Sallam et al., 2018; Vila et al., 2022).

In summary, the taxonomic status of the Transylvanian titanosaurs is far from resolved, as emphasized by several authors (e.g. Csiki, 1999; Le Loeuff, 1993; Upchurch et al., 2004; Weishampel et al., 1991), but it appears that they formed a more diverse assemblage than often acknowledged in the past. In light of these taxonomic uncertainties, the phylogenetic affinities of these titanosaurs also remain unclear.

Key localities and skeletal associations

In this section, we draw together multiple lines of evidence (including field notes, museum labels, registry notes, published data, and specimen preservation) to establish a set of titanosaur individuals, or in some cases assemblages from a given locality, in order to provide the basis for recognizing diagnosable specimens and justifiable taxonomic referrals. We do not attempt to identify every specimen that has ever been referred to *Magyarosaurus*: instead, we focus on key name-bearing historic specimens and 'Rosetta Stone' specimens that are crucial in terms of their potential diagnostic characters and/or overlapping anatomy that enable comparisons and referrals.

Background

The complicated and ultimately poorly understood taxonomic framework concerning the Transylvanian latest Cretaceous titanosaurs stems from several different sources. One factor pertains to preservational biases, such as the predominance of disarticulated and often isolated specimens, and the severe underrepresentation or even absence of certain body parts (especially the skull and the pelvic girdle; Fig. 2). Disarticulated, isolated, and/or fragmentary specimens, that were discovered in different and sometimes distant localities, are often difficult to compare meaningfully, let alone refer with certainty to the same taxon. Despite this, aggregation of non-associated and anatomically non-overlapping specimens into named taxa (primarily *Magyarosaurus dacus*) has been the dominant taxonomic practice since the original discovery of this fauna (see above). A second confounding factor is the lack of detail in the available field documentation concerning the discovery and excavation of many specimens. This is particularly true for the historical, pre-1978 collections, which include key material such as the remains from Sânpetru discovered by Nopcsa (now registered in the NHMUK collections), and those from Vălioara excavated by Kadić (now part of the SZTFH collections): these two collections represent the foundation of the original taxonomic opinions proposed by Nopcsa (1915) and Huene (1932). Documentation for most of these early specimens simply mentions Sânpetru or Vălioara as their place of origin,

without reference to a particular location in the surroundings of these villages. Although general information (approximate location, lithology, and/or palaeontological content) for particular excavation sites is recorded in some early publications (e.g. Kadić, 1916; Nopcsa, 1902a, 1902b, 1914), it tends to lack explicit details on both the precise identity of the titanosaur specimens that were excavated from these sites and the potential skeletal association of these specimens. Other sources of provenance information (i.e. field notes, geographical and quarry maps, photographs, collection registry entries, or labels accompanying the specimens) are equally rare, albeit with some notable exceptions (see below). Even more frustratingly, it appears that the omission of the existing excavation or registry details was common during this period, as most saliently demonstrated by Nopcsa's failure to convey information on skeletal association for the titanosaur material he sent to Huene for study in Tübingen (see below). In short, most of the original information concerning the provenance and field association of the historical titanosaur specimens should be considered lost and nearly impossible to reconstruct. The situation is somewhat improved for the titanosaur material collected after 1977, for which more precise locality and/or field association data are available (e.g. Csiki, Codrea, et al., 2010; Csiki-Sava et al., 2012; Groza, 1983), or at least such information can be retrieved from personal or orally transmitted accounts of their discoveries, unpublished field notes, and/or museum collection records (see below).

In this section, we review localities that have yielded historically important (e.g. type specimens) and/or associated skeletal material, in order to document the main sources of information that are instrumental in our revision of the systematics of the latest Cretaceous Transylvanian titanosaurs. Here, we gather, collate, and synthesize all available data for the different key titanosaur localities and individuals (Fig. 1E) to provide support for our inferences of association and provenance. This is especially important given that we are dealing with material collected over a period of more than a century by researchers of different backgrounds and aims, and covering a relatively large geographical area. A necessary part of this process is to identify and clarify confusions and misinterpretations promulgated by previous publications. For ease of discussion, we designate each key set of associated specimens as 'individuals' (considered to represent one incomplete skeleton), or as 'assemblages' when there is element duplication or other reasons for questioning the presence of just one individual (though in some cases these assemblages appear to largely comprise a single individual with just a small number of extraneous elements from others). These individuals and assemblages are labelled A, B, C, etc. We also present a graphical overview of the skeletal parts represented for the most important key individuals to aid comparisons and highlight overlapping skeletal parts among them.

Kadić locality I (= *Magyarosaurus dacus* type locality), Ciula Mică – Assemblage A

When erecting the new taxon *Titanosaurus dacus*, Nopcsa (1915, pl. III) figured only three specimens (two procoelous caudal vertebrae and an ungual; Fig. 6). All of these specimens belong to the Kadić collection that was assembled in the neighbourhood of Vălioara village (Kadić, 1916) and is housed in the SZTFH. Of the three specimens figured by Nopcsa, and referred explicitly to *T. dacus*, the ungual (Nopcsa, 1915, pl. III, fig. 8; SZTFH Ob.3098; Fig. 6M, N) is now lost. The other two referred specimens represent an incomplete distal anterior caudal vertebra (Nopcsa, 1915, pl. III, fig. 4; SZTFH Ob.3091; Fig. 6A–F) and a posterior caudal centrum (Nopcsa, 1915: pl. III, fig. 5; SZTFH Ob.4215; Fig. 6G–L). Only in the case of the latter specimen does the plate caption make a direct reference to the species epithet (i.e. *dacus*), although Nopcsa's intention to refer the other two figured specimens to the same species can be reasonably inferred for two reasons. First, he recognized only one titanosaur species, to which he referred all the sauropod material collected throughout the Haţeg Basin. Second, in the overview list of the figured material that precedes the plates and their captions, the distal anterior caudal (SZTFH Ob.3091) is also listed explicitly as *T. dacus*. In addition to these three specimens, Nopcsa (1915, pl. III, figs 6, 7) referred two platycoelous posterior caudal vertebrae to an indeterminate species of *Megalosaurus*, a theropod dinosaur, but these are clearly referable to a titanosauriform sauropod based on first-hand inspection (SZTFH Ob.3105 *in partim*; Fig. 7).

In his review of the Transylvanian titanosaurs, Huene (1932, p. 263) emphasized that he regarded SZTFH Ob.3091 as the specimen that typifies *Magyarosaurus* ('*Titanosaurus*') *dacus* ("*Diesen Wirbel nehme ich als den Typus der Art*"). Given that Nopcsa (1915) did not formally designate a type for *T. dacus*, we follow Huene (1932) in regarding SZTFH Ob.3091 as the lectotype for the species (see also Csiki, Codrea, et al., 2010). This decision is also appropriate because SZTFH Ob.3091 is the most complete and diagnostic element of the three originally figured specimens.

Huene (1932) mistakenly mentioned that SZTFH Ob.3091 came from Sânpetru, but the type locality for this taxon must be located somewhere in the vicinity of Vălioara, the locus of Kadić's collecting efforts.

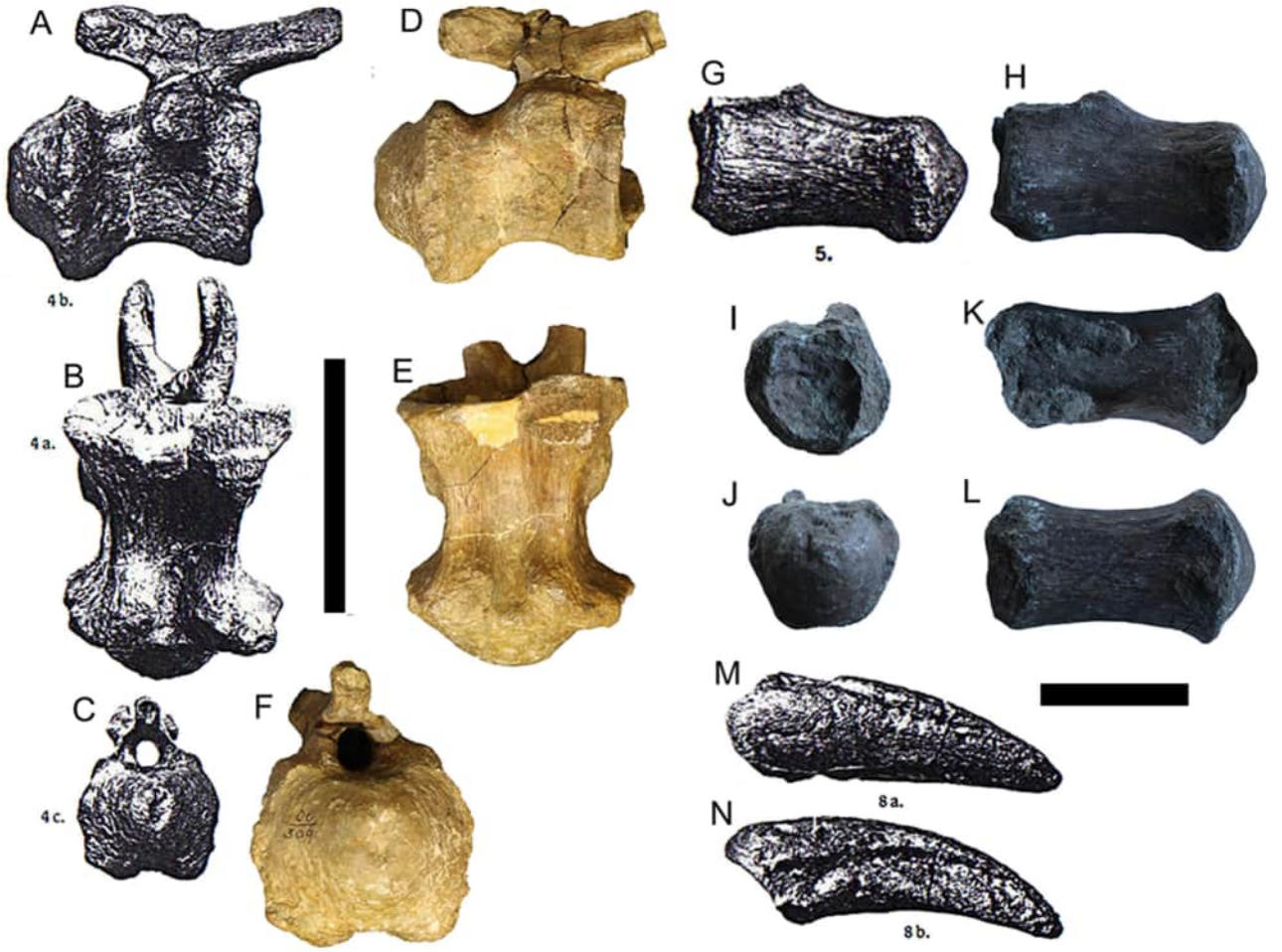

Figure 6. Titanosaur remains used to erect *Titanosaurus dacus* by Nopcsa (1915). Anterior caudal vertebra SZTFH Ob.3091 in **A,** right lateral; **B,** ventral; **C,** posterior; **D,** right lateral; **E,** ventral; and **F,** posterior views. Posterior caudal centrum SZTFH Ob.4215 in **G,** left lateral; **H,** left lateral; **I,** anterior; **K,** dorsal; **J,** posterior; and **L,** ventral views. Ungual SZTFH Ob.3098 (now lost) in **M,** medial; and **N,** lateral views. A–C, G, M and N are taken from Nopcsa (1915). Scale bars equal 100 mm for A–F, and 50 mm for G–N.

However, for a long time, the precise position of the locality yielding SZTFH Ob.3091 remained unknown because the only known account of the discovery and excavation of these specimens was Kadić's (1916) brief and very general activity report. Recently, the hand-coloured map Kadić used in the field was found in the archive of the SZTFH. This map marks the locations of his excavation sites in the neighbourhood of Vălioara, and has allowed their re-identification. Using a combination of approaches, including field mapping around the original fossil-bearing sites, sedimentological and taphonomic investigations, and rare earth element (REE) geochemistry, coupled with the brief details on the sites presented in Kadić (1916), Botfalvai et al. (2021) were able to confidently identify the locality that yielded SZTFH Ob.3091 as Locality I of Kadić (1916). This locality occurs in the terminal part of the Pârâul Vârtopilor ravine, a left-side tributary of the Răchitova Valley, south-west of Vălioara and near Ciula Mică (Fig. 1E). Based on data from Csiki-Sava et al. (2016) and Botfalvai et al. (2021), this locality can be placed in the lowermost part of the 'middle member' of the Densuș-Ciula Formation, and, as such, is most probably of earliest Maastrichtian age (Fig. 8).

Other lines of evidence corroborate and extend the above conclusions. Kadić (1916, p. 575) wrote with respect to his Locality I: "… the matrix yielding the bones was a red-coloured, sericite-rich mudstone rich in carbonate concretions. The bones we found here are thus reddish in colour, with a perfect preservation state-…" (translated from Hungarian by ZCs-S). Based on the taphonomic conditions, state of preservation, and the REE spectra of the specimens in the SZTFH collections, Botfalvai et al. (2021) suggested that the locality

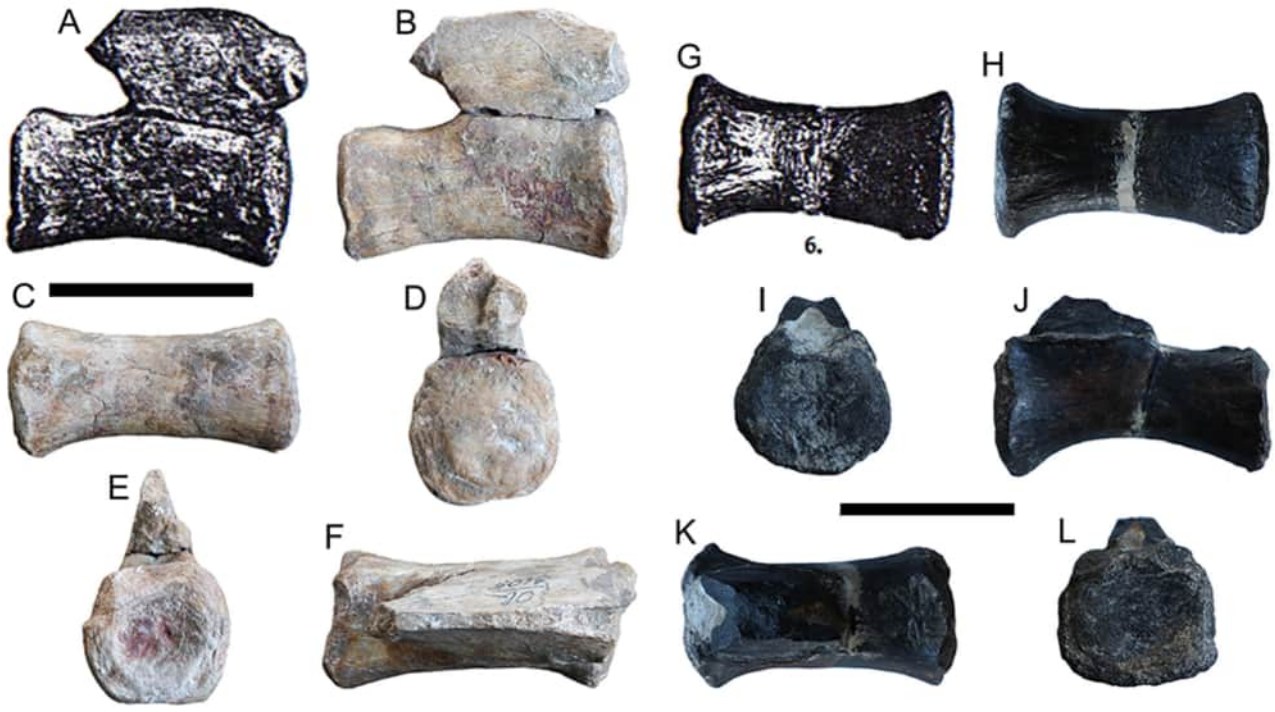

Figure 7. Titanosaur posterior caudal vertebrae SZTFH Ob.3105 referred to *Megalosaurus* sp. by Nopcsa (1915). First specimen in **A,** right lateral; **B,** right lateral; **C,** ventral; **D,** posterior; **E,** anterior; and **F,** dorsal views. Second specimen in **G,** ventral; **H,** ventral; **I,** anterior; **J,** left lateral; **K,** dorsal; and **L,** posterior views. A and G are taken from Nopcsa (1915). Scale bars equal 50 mm.

yielding SZTFH Ob.3091 also produced two other titanosaur specimens from those they sampled geochemically: SZTFH Ob.3088, a left femur, and SZTFH Ob.3089, a left humerus. The similar preservation style and red-speckled yellowish-cream colour of the three elements imply that they probably share a common taphonomic history, and their commensurate size and the spatially restricted nature of the excavations (called 'nests' by Kadić, suggesting the presence of relatively small lenticular bonebeds [Csiki, Grigorescu, et al., 2010]) support the idea that they belong to the same taxon or even the same individual.

There is another set of titanosaur remains in the SZTFH collections, not included in the set sampled for geochemistry by Botfalvai et al. (2021), that shares with the specimens discussed above the same characteristics in terms of preservation style, colour and size. This set includes: SZTFH Ob.3100 (left ulna), SZTFH Ob.3101 (left radius), SZTFH Ob. 3096 (metacarpal), SZTFH Ob.3086 (two left fibulae), SZTFH Ob.3102 (left fibula), and one of the posterior caudal vertebrae included under SZTFH Ob.3105, corresponding to the specimen that Nopcsa (1915, pl. III, fig. 7) referred to *Megalosaurus* sp. (see Fig. 7A–F). The similar preservation style of these specimens with that of SZTFH Ob.3088, 3089 and 3091 strongly indicates that they were excavated from the same locality as SZTFH Ob.3091 (i.e. Locality I of Kadić, 1916), and – as suggested by their largely commensurate size – that several of them might belong to the same individual as the lectotypic anterior caudal vertebra. That some of these bones are commensurate in size with the first, geochemically sampled set, is independently supported by osteohistology: Stein et al. (2010) sampled the humerus (SZTFH Ob.3089) and the two fibulae accessioned under SZTFH Ob.3086, and concluded that all these remains exhibit the same stage of (advanced) ontogenetic development (Histological Ontogenetic Stage [HOS] 14). The presence of three left fibulae, representing the only subset of anatomically overlapping remains, clearly attests to the presence of at least three individuals. However, their largely matching size and morphology (see the 'Systematic palaeontology' section) is consistent with the assessment that these probably represent individuals of approximately the same size that belong to the same titanosaur species. In short, taking all of the archival, morphological, taphonomic, osteohistological and geochemical evidence together, we regard it as highly probable that this entire set of titanosaur remains came from a single spatiotemporally restricted fossil site, and that most of the listed specimens belong to a single disarticulated skeleton. In the following discussions, we designate this set of elements, to which many (maybe even most) of the titanosaur remains from

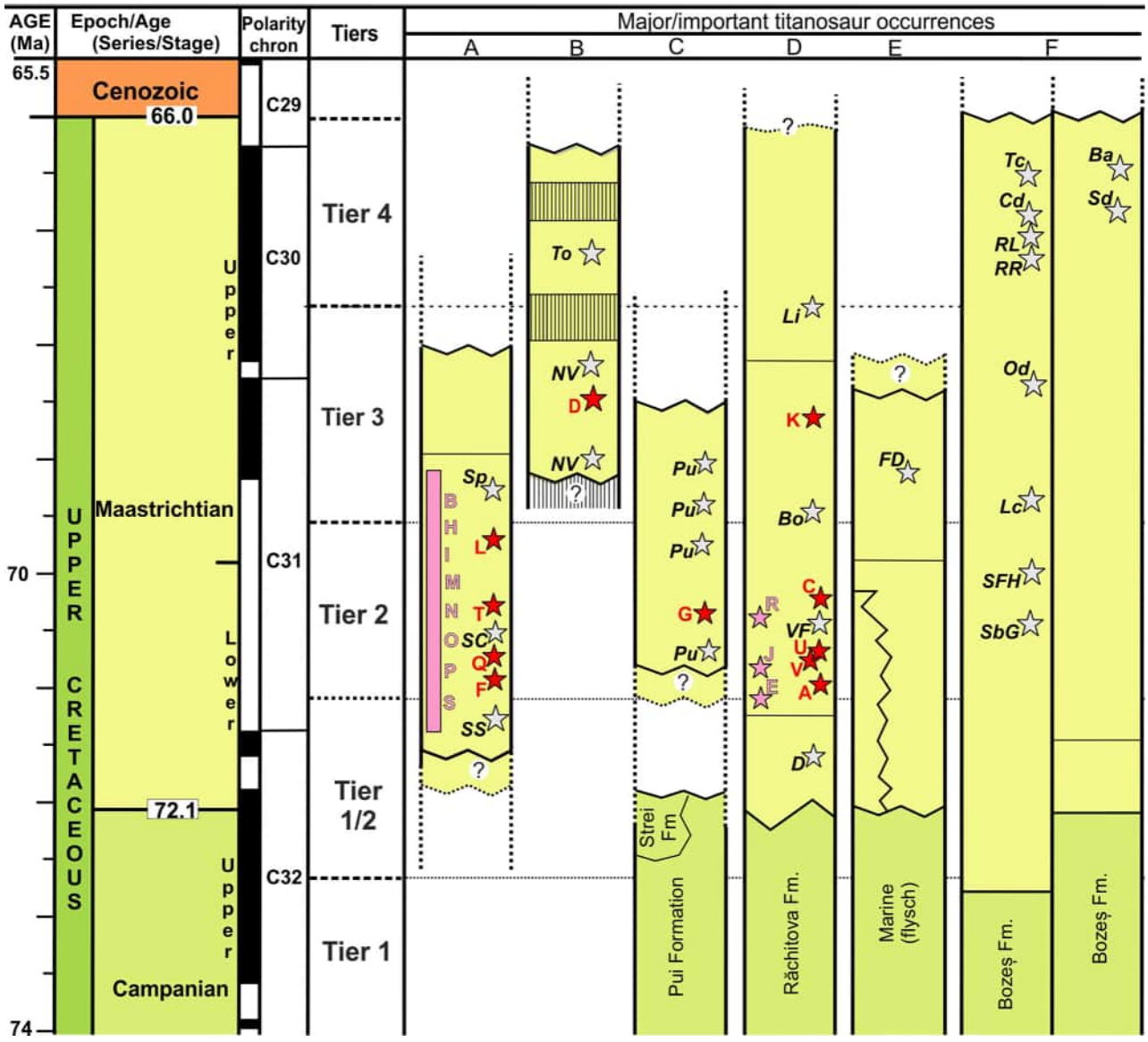

Figure 8. Synthetic stratigraphical distribution of key titanosaur individuals/assemblages (coded A to V; red stars – stratigraphical location well constrained, pale red stars – stratigraphical position approximate; see text and Fig. 1E for more details), and other significant titanosaur occurrences (grey stars). **Abbreviations for stratigraphical columns: A–D**, Hațeg Basin; **A**, Sînpetru Formation, Sibișel Valley section; **B**, 'Râul Mare Beds'; **C**, 'Pui Beds'; **D**, Densuș-Ciula Formation; **E**, Rusca Montană Basin; **F, G**, south-western Transylvanian Basin; **F**, left side of Mureș Valley; **G**, right side of Mureș Valley. **Abbreviations for titanosaur localities, other than key individuals/assemblages: Ba**, Bărăbanț; **Bo**, Boița; **Cd**, Ciugud; **D**, Densuș; **FD**, Fărcădeana; **Li**, Livezi; **Lc**, Lancrăm; **NV**, Nălaț-Vad, several sites; **Od**, Oarda de Jos; **Pu**, Pui, Bărbat River, several sites; **RR**, Sebeș, Râpa Roșie; **RL**, Râpa Lancrămului; **SbG**, Sebeș-Glod; **SC**, Sânpetru, Cărare; **Sd**, Șard; **SFH**, Secaș, Fetilor Hill; **Sp**, Sânpetru, several sites; **SS**, Sânpetru, Scoabă; **Tc**, Teleac; **To**, Totești; **VF**, Vălioara, Fântânele 1. Updated from Csiki-Sava et al. (2016, fig. 14) and Botfalvai et al. (2021, fig. 12).

Locality I of Kadić belong to, as 'Assemblage A' (Fig. 9).

As a final historical note, it is worth pointing out that some of the Assemblage A specimens were examined first-hand by Huene during his study of Transylvanian titanosaurs. These were sent to him at Nopcsa's personal instructions, as documented by handwritten notes present in the SZTFH registry book (Fig. 10). Of these, one of the fibulae registered as Ob.3086 was referred by Huene (1932) to *M. dacus*, together with the lectotypic caudal vertebra (Ob.3091), whereas two other fibulae (the second specimen registered under Ob.3086, and Ob.3102), together with the ulna (Ob.3100), were attributed to the second species of the genus erected by him,

M. transsylvanicus. It seems that Huene was unaware that: (1) all these specimens most probably came from the same fossiliferous site, and that some were possibly from the same individual; and (2) further titanosaur remains existed in the SZTFH collections, and that some of these originated from the same Kadić Locality I as the lectotype and thus potentially also belonged to *M. dacus*. The selective way Nopcsa sent specimens from Budapest to Tübingen is difficult to explain (see also below), but it almost certainly affected Huene's opinions concerning the taxonomy and anatomy of the Transylvanian titanosaurs.

The *'Magyarosaurus' hungaricus* type locality, Sânpetru – Individual B

Among the material excavated by Nopcsa before 1906 in the Sibișel Valley, south of Sânpetru (Fig. 1E), and subsequently purchased by the NHMUK, there is an associated and relatively large left tibia and fibula registered under the same accession number, NHMUK R.3853. The fibula was described by Huene (1932, p. 269, pl. 47, fig. 1) as the holotype (and only specimen) of his new species ?*Magyarosaurus hungaricus*, which he differentiated from *M. dacus* and *M. transsylvanicus* primarily based on the larger size and distinctive morphology of the fibula. Furthermore, Huene (1932, p. 274, pl. 48, fig. 3) suggested that the tibia bearing the same specimen number as the holotype fibula could also belong to the same species, based on its size, although he referred to this tibia as *Magyarosaurus* sp. in the text. First-hand examination of the fibula and tibia confirms that they are commensurate in size, have a similar preservation style, and share an unusual interlocking mechanism at their distal ends (see the 'Systematic palaeontology' section). These observations support Huene's assessment of potential conspecificity of the two specimens. Furthermore, in our view, these features also strongly suggest that these two specimens belonged not only to the same species, but were excavated from the same locality, and represent associated distal hind limb elements of the same individual. Such an association would also be consistent with these elements being registered under the same NHMUK specimen number at the time of their purchase in 1906. We therefore designate this material as Individual B (Fig. 11).

Unfortunately, almost nothing is known about the locations, stratigraphy or fossil content of the fossiliferous sites excavated by Nopcsa in the Sibișel Valley, and field details are unavailable for most. This includes the locality that yielded NHMUK R.3853, so it can only be constrained as belonging to the type section of the Sînpetru Formation near Sânpetru (Fig. 1E), and is thus most probably of early to early late Maastrichtian age (Csiki-Sava et al., 2016) (Fig. 8).

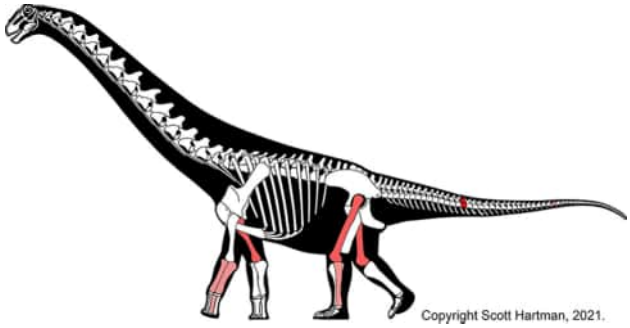

Figure 9. Fossil remains belonging to Assemblage A, Kadić locality I, the *Magyarosaurus dacus* type locality, Ciula Mică. Not to scale. Skeletal drawing after Scott Hartman, used with permission.

Kadić Locality VI (Pârâul Budurone), Vălioara – Individual C

Kadić (1916, pp. 575–576) reported his Locality VI as a 'nest' (Csiki, Grigorescu, et al., 2010) found in "fine-grained bluish loose sandstones from where we have excavated thick limb-bone fragments and exquisitely

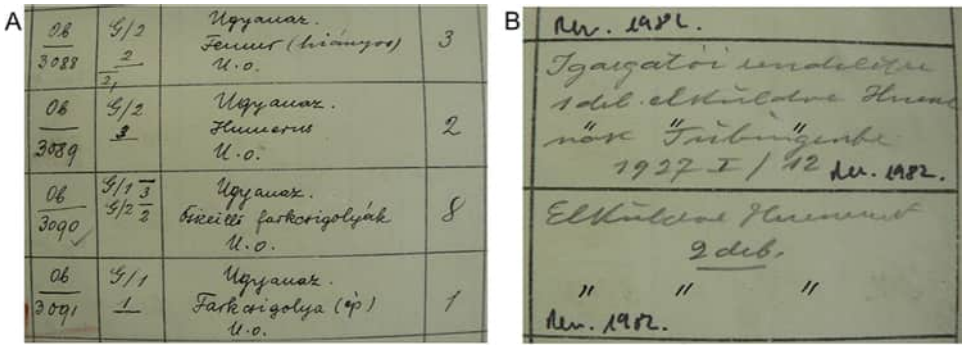

Figure 10. Handwritten notes in the registry book of the SZTFH. **A**, indication that SZTFH Ob.3090 comprises eight 'matching (= associated) caudal vertebrae' ('összeillő farokcsigolyák' in Hungarian). **B**, indication that caudal vertebrae SZTFH Ob.3090D and G were sent to Huene in Tübingen ('Elküldve Huenenek, 2 drb.' in Hungarian).

preserved large vertebrae. The colour of the bones is here, too, black" (translated from Hungarian by ZCs-S). As already noted by Csiki and Grigorescu (2006; see also Csiki et al., 2011), and subsequently by Botfalvai et al. (2021), the only set of bones in the SZTFH collections that matches this description is represented by a series of large titanosaur remains comprising several caudal centra (SZTFH Ob.3090), an incomplete right humerus (SZTFH Ob.3104), fragmentary left and right femora (SZTFH Ob.3103), and a metatarsal (SZTFH Ob.3095). These specimens are all much larger than most of the titanosaur remains from Transylvania, and share a consistent preservation style with one another, including their black colour with a shiny, smooth periosteum (except where it is originally fibrous in aspect).

Furthermore, handwritten notes in the registry book of the SZTFH state that SZTFH Ob.3090 comprises eight "matching [= associated] caudal vertebrae" ("*összeillő farokcsigolyák*" in Hungarian in original; Fig. 10A), whereas SZTFH Ob.3103 consists of the "right and left femur from a gigantic individual" ("*Jobb és bal combcsont óriás példánytól*" in Hungarian in original; Fig. 12A), with SZTFH Ob.3104 representing the "humerus of the same (gigantic) individual" ("*Humerus ugyanattól a példtól*" in Hungarian in original; Fig. 12A). These notes were added when the specimens were registered in 1914, i.e. approximately when they were collected, and clearly indicate that this set of specimens was identified as originating from the same skeleton. The series of eight associated (and possibly articulated) caudal vertebrae was initially included under the specimen number SZTFH Ob.3090. However, when one of us (ZCs-S) first visited the SZTFH collections in 2003, only four of these vertebrae could be located. Besides the specimen numbers, the four remaining vertebrae are also marked with poorly preserved letters written in ink: B, D, G and H. Based on the morphology of the individual elements (see description in the 'Systematic palaeontology' section), the vertebrae marked with B and D occupied more anterior positions in the tail than vertebrae G and H, and B appears to be somewhat more anterior in position than D. Taken together, these observations suggest that the original eight vertebrae were lettered sequentially according to their position in the tail, with A, C, E and F now missing. In 1927, two of these vertebrae (D and G) were sent to Huene in Tübingen: a handwritten note in the SZTFH register (Fig. 10B – second line) reads "Sent to Huene, 2 pieces" ("*Elküldve Huenenek, 2 drb.*" in Hungarian in original), following up a similar note (Fig. 10B – first line) for SZTFH Ob.3089 dated 12 January 1927 which states that "By

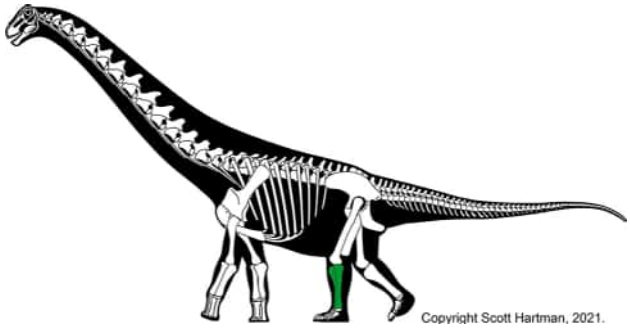

Figure 11. Fossil remains belonging to Individual B, the *Petrustitan* ('*Magyarosaurus*') *hungaricus* n. gen. type locality, Sânpetru. Skeletal drawing after Scott Hartman, used with permission.

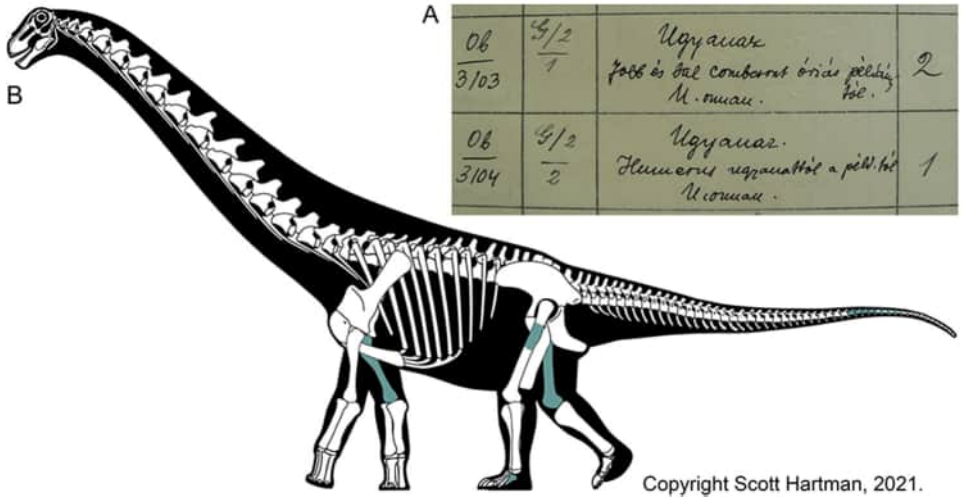

Figure 12. **A,** handwritten notes in the registry book of the SZTFH on the titanosaurian remains referred to Individual C. **B,** fossil remains referred to Individual **C,** the *Uriash kadici* n. gen. n. sp. type locality, Kadić Locality VI (Pârâul Budurone), Vălioara. Skeletal drawing after Scott Hartman, used with permission.

instruction of the Director [i.e. Nopcsa at that time], 1 piece sent to Huene to Tübingen" ("*Igazgatói rendeletre 1 drb. elküldve Huenenek Tübingenbe*", in Hungarian in original). Huene figured and briefly described these two vertebrae (Huene, 1932, p. 271–272, 274, pl. 47, figs 4, 5), referring at least one of them tentatively to ?*Magyarosaurus hungaricus*. However, it appears that Huene was not aware that these two vertebrae belong to a more complete vertebral series, nor that there were appendicular elements also referable to this individual.

The right humerus (SZTFH Ob.3104) has a complicated curatorial history. After being registered as a humerus belonging to the same individual as the femora SZTFH Ob.3103 (Fig. 12A), SZTFH Ob.3104 is mentioned as lost in the SZTFH registry book in 1938. In 2003, however, one of us (ZCs-S) located a small fragment of the humeral midshaft that still bore the original specimen number, in the same drawer as the SZTFH Ob.3103 femora. A much larger portion of this humerus, including the region of the deltopectoral crest, had been re-registered as v.13491 in the second half of the twentieth century. When examined in 2003, the latter element was found to be of commensurate size, as well as having a matching breakage surface and an identical preservation style, with the smaller fragment still bearing the original specimen number (SZTFH Ob.3104). The two large and black-coloured humeral fragments thus definitively belong to the same element, and were reconstructed as such in 2003. Le Loeuff, (2005a, fig. 1A) figured this specimen already reconstructed, missing only a small fragment of the proximolateral end (which was also relocated and restored in 2004), although he still referred to it using the new registry number borne by the larger fragment (v.13491) and not the original specimen number (Ob.3014). However, as with Huene (1932), Le Loeuff (2005a) was apparently not aware that this humerus belongs to a large titanosaur individual that is represented by further skeletal elements (most probably because he used the new registry number). Botfalvai et al. (2021) geochemically sampled three specimens from this set of bones (two caudal vertebrae from SZTFH Ob.3090, and the right femur, SZTFH Ob.3103). Their analysis showed a remarkable similarity between the three elements in their REE spectra, lending further support to the idea that they originated from the same fossiliferous site.

Combining the above evidence, most of which comes from notes and observations recorded around the time of their discovery, it is highly probable that the set of large black titanosaur bones documented above represent elements of a single partial skeleton, herein identified as Individual C (Fig. 12B). These specimens were excavated from Locality VI of Kadić (1916), which was recently reidentified by Botfalvai et al. (2021) in a ravine joining the left side of Vălioara Valley, just south-west of Vălioara village (Fig. 1E). Based on its geographical position, the site can be placed in the lower part of the 'middle member' of the Densuș-Ciula Formation, although stratigraphically somewhat higher than Locality I discussed above (Fig. 8). Csiki-Sava et al. (2016) and Botfalvai et al. (2021) suggested that the age of the locality is early Maastrichtian.

The remains belonging to Individual C have been evaluated in several previous studies (e.g. Le Loeuff, 2005a; Stein et al., 2010; see 'Dwarfism' section), although mostly without noting either their skeletal association or site of origin. As noted above, two elements of the caudal vertebral series SZTFH Ob.3090 were sent to Huene in Tübingen by Nopcsa. Huene (1932, pp. 271–274, pl. 47, figs. 4, 5) identified these vertebrae as *Magyarosaurus* sp., although he noted that they might belong to ?*M. hungaricus* (a referral also emphasized in the corresponding plate captions). The associated nature of Individual C was first recognized and discussed by Csiki and Grigorescu (2006). Following Huene's arguments and accepting his view of one large titanosaur taxon present in the Transylvanian area, these authors maintained the referral of these remains to ?*M. hungaricus*.

Locality NV10, Nălaț-Vad (= *Paludititan nalatzensis* type locality) – Individual D

Unlike the historical titanosaur specimens from Sânpetru and Vălioara discussed above, the partial skeleton UBB NVM 1 has well-documented provenance and skeletal association data, and was established by Csiki, Codrea, et al. (2010) as the holotype of the second titanosaur genus described from the Transylvanian area – *Paludititan nalatzensis*. It preserves parts of the dorsal and caudal vertebral series, as well as most of the pelvis, together with a large number of rib fragments, several chevrons, a small fragment of the femur, and two pedal unguals (see the 'Systematic palaeontology' section). It was excavated in 2002 during a joint Romanian–Belgian field season. One of the current authors (ZCs-S) was actively involved in the excavation process, and recorded the position of the different skeletal elements recovered. Numerous aspects support the interpretation of one single disarticulated partial titanosaur skeleton at this locality, which we designate as Individual D (Fig. 13). These include: the progress of the excavation itself; the resultant quarry map showing the different skeletal parts in their disarticulated, but quasi-*in vivo* position (see Csiki, Codrea, et al., 2010, fig. 1B); the presence of *in situ* skeletal articulation in the case of the pelvic girdle and a series of caudal

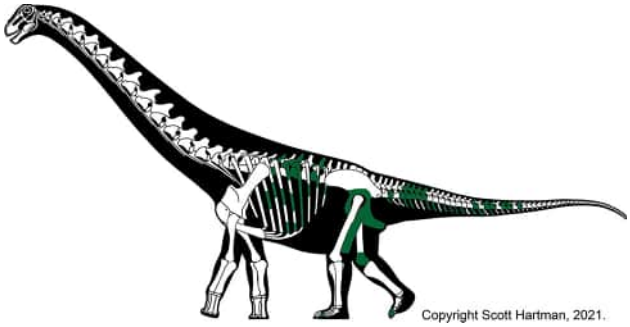

Figure 13. Fossil remains belonging to Individual D, the *Paludititan nalatzensis* type locality, locality NV10, Nălaț-Vad. Skeletal drawing after Scott Hartman, used with permission.

vertebrae; the commensurate size and non-duplicated nature of the elements; and the consistent preservation style.

Besides specimen association data, there are also high-resolution geographical and stratigraphical data available for Locality NV 10 (Nălaț-Vad) and thus for Individual D. This locality belongs to the 'Râul Mare Beds', a not yet formally defined lithostratigraphical unit that either represents the uppermost part of the Sînpetru Formation (being slightly younger than most of the type section located along the Sibișel Valley), or is a distinct unit (see review in Csiki-Sava et al., 2016). The relatively extensive outcrop at Nălaț-Vad, lying in the lower part of the Râul Mare Beds, was mapped carefully in 2001–2002 (see Smith et al., 2002; van Itterbeeck et al., 2004), and the position of the site yielding UBB NVM 1 is also recorded with precision, in the upper part of the locally outcropping section (Fig. 1E). Furthermore, preliminary palynostratigraphical (van Itterbeeck et al., 2005) and magnetostratigraphical (Panaiotu et al., 2011) data are also available for the Nălaț-Vad succession, suggesting that the age of Locality NV 10 falls most probably around the early/late Maastrichtian boundary or in the earliest late Maastrichtian (Fig. 8). Based on the overall distribution pattern of the vertebrate fossil record of the Hațeg Basin (e.g. Csiki-Sava et al., 2016; Therrien et al., 2009), Locality NV 10 is most probably somewhat stratigraphically younger in age than the ?*Magyarosaurus hungaricus* type locality, and definitely younger than localities I and VI of Kadić, which makes Individual D stratigraphically younger than Individuals/Assemblages A, B and C (Fig. 8).

Mamulea locality, Ciula Mică – Individual E

As already noted, after Nopcsa ceased his collecting activity at Sânpetru in the 1920s, Mamulea was the first to report the discovery of dinosaur remains from the uppermost Cretaceous of the Hațeg Basin (Mamulea, 1953a, p. 250). No further details were given concerning this discovery; however, in another report, Mamulea, (1953b) added that the dinosaur remains he had discovered at Ciula Mică were found in purplish sandstones within the coarse, red, conglomeratic continental succession that, in his view, overlay a lower, dominantly greyish 'fluvio-lacustrine' succession. Because he considered that this upper red unit (which he reported to be otherwise palaeontologically barren) represented the Paleocene, contrary to previous opinions expressed by Nopcsa (1905), Schafarzik (1909, 1910), Kadić (1916), and Laufer (1925), Mamulea (1953b) also regarded the dinosaur bones he found there as being reworked. However, subsequent work in the Ciula Mică-Vălioara area, from which these remains were collected, firmly established that the red siliciclastic deposits are indeed fossiliferous and are from the lower part of the 'middle member' of the uppermost Cretaceous Densuș-Ciula Formation (e.g. Antonescu et al., 1983; Bojar et al., 2011; Botfalvai et al., 2021; Csiki-Sava et al., 2016; Grigorescu, 1992). Thus, the titanosaur remains reported by Mamulea must have originated from these lowermost Maastrichtian deposits (Csiki-Sava et al., 2016) (Fig. 8). More precise pinpointing of the geographical location of this site is not currently possible, beyond it being in the vicinity of Ciula Mică (Fig. 1E).

The titanosaur remains discovered by Mamulea at Ciula Mică, and reported without any other details, description, or illustrations, were re-identified in the collections of the FGGUB. These consist of a set of postcranial remains that include incomplete dorsal and caudal vertebrae, a chevron, the left humerus and radius, several incomplete metacarpals, the left femur together with corresponding proximal tibia-fibula, and the right femur (see complete list of elements in the 'Systematic palaeontology' section).

The listed elements are commensurate in size, and there is no duplication within the set. Their preservation style is consistent, pointing to a common taphonomic history, and all display a greyish-green-spotted yellowish-reddish colour, suggesting that they come from a somewhat reductive, variegated and relatively fine-grained sediment (probably a fine sandstone). At least some of the specimens are virtually complete and well preserved (e.g. Fig. 4; see also the 'Systematic palaeontology' section), and others preserve their original, *in vivo* skeletal articulation (i.e. dorsal centra, caudal centra, and proximal tibia-fibula). These features argue strongly against potential reworking or long-distance transport being involved in the formation of the taphocoenosis corresponding to the set, and thus an allochthonous origin, as advocated by Mamulea (1953b), can be safely discarded. Finally, Stein et al. (2010) sampled

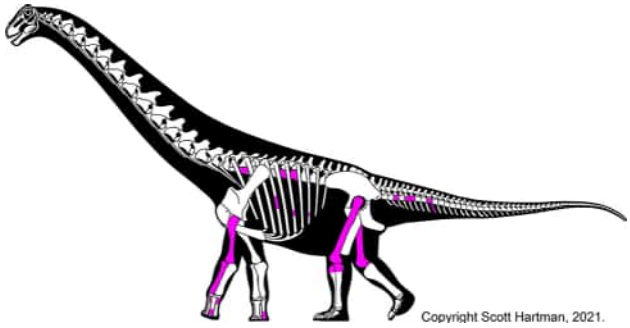

Figure 14. Fossil remains belonging to Individual E, referred here to *Magyarosaurus dacus*, Mamulea locality, Ciula Mică. Skeletal drawing after Scott Hartman, used with permission.

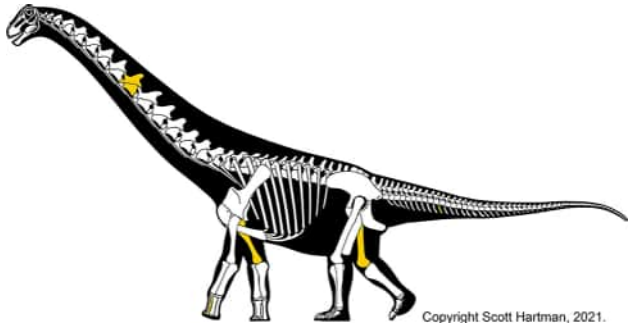

Figure 15. Fossil remains belonging to Assemblage F, referred here to *Magyarosaurus dacus*, MD locality, Pui. Skeletal drawing after Scott Hartman, used with permission.

the histology of two specimens from this set (the left humerus LPB [FGGUB] R.1047, and the left femur R.1046), and found that their HOS values were very similar (13 and 14, respectively; see the 'Dwarfism' section). Although circumstantial, this result is consistent with these two elements belonging to a single individual.

Based on all of this information, the set of titanosaur elements from the FGGUB collections listed above can be regarded as originating from one fossiliferous site, and almost certainly represents the associated remains of a single partial skeleton. We identify this as Individual E (also termed the 'Mamulea specimen'; Fig. 14).

MD locality, Pui – Assemblage F

This locality was discovered in 2015, when a partial titanosaur cervical vertebra (LPB [FGGUB] R.2505) was found and excavated. Subsequent prospecting in 2016 yielded several other titanosaur remains, including a well-preserved humerus (LPB [FGGUB] R.2506), a metacarpal (LPB [FGGUB] R.2509), two femora (one complete – LPB [FGGUB] R.2507; one partly complete – R.2508), and a chevron (LPB [FGGUB] R.2510). At that time, no other vertebrate remains had been found at this site, although in 2019 it also yielded remains referable to ornithischian dinosaurs. All the titanosaur specimens were recovered from a small area and from the same fossiliferous level, in a dominantly red-coloured, fine to medium-grained silty sandstone, with local greenish and sandier intercalations (ZCs-S pers. obs.). Most of these remains are approximately commensurate in size, and they share a similar whitish-reddish yellow colour and preservation style, suggesting that they probably originate from one disarticulated partial skeleton. One exception is represented by the less complete femur: in addition to being less well preserved, it is slightly larger than the other femur and comes from the same side, indicating that a second, slightly larger titanosaur individual is also represented at the MD site. Nevertheless, this larger specimen is morphologically similar to the other femur, and most probably they belong to the same species. Thus, although we consider it probable that all of these specimens, apart from the larger femur, belong to the same individual, we conservatively designate the titanosaur remains from the MD locality as Assemblage F (Fig. 15).

The MD locality is situated in the lower part of the uppermost Cretaceous continental succession cropping out along the Bărbat River (Fig. 1E), a succession considered to be either part of the Sînpetru Formation (e.g. Grigorescu, 1992; Mamulea, 1953a), or a different, but approximately time-correlative, unit (Csiki-Sava et al., 2016; Therrien, 2005). A palynological sample collected from the middle part of the succession, from a stratigraphically higher level than that hosting site MD, was dated as close to the early/late Maastrichtian boundary (van Itterbeeck et al., 2005); as such, the MD locality (and thus, Assemblage F) should be considered to be of early Maastrichtian age (Fig. 8).

Râpa Mocioconilor locality, Sânpetru – Individual G

Renewed fossil vertebrate collecting in the Hațeg Basin in the late 1970s led to the discovery of several important vertebrate accumulations ('fossiliferous pockets' or small-sized lenticular macrovertebrate bonebeds; Csiki, Grigorescu, et al., 2010) along the Sibișel Valley, near Sânpetru (e.g. Grigorescu, 1983; Groza, 1983). One of these accumulations is represented by the Râpa Mocioconilor (= Mocioconilor ravine) site, situated on the right side of the valley, between the villages of Sânpetru and Săcel, and excavated by teams of the Muzeul Civilizației Dacice și Romane, Deva, between 1979 and 1982. The location of this site is provided in Groza (1983, fig. 1; see also Csiki, Grigorescu, et al.,

2010, fig. 1C), and, according to its stratigraphical position, it should be placed in the lower part of the dominantly reddish-brown informal lower subunit of the Sînpetru Formation type section, which crops out along the Sibișel Valley (Grigorescu, 1992; Therrien et al., 2009) (Fig. 1E). This constrains its age most probably to the early, or, at most, earliest late, Maastrichtian (Csiki-Sava et al., 2016) (Fig. 8).

According to the brief, preliminary account of the excavations by Groza (1983, p. 52, pl. 2, figs 1–6), this site yielded several specimens in 1980; these included six titanosaur posterior caudal vertebrae (MCDRD 255, 266, 267, 268, 269 [one of these six vertebrae could not be located in the collections]), four of which were found in articulation. Groza (1983) referred these specimens to *T. dacus*. He also reported the recovery of an associated pair of limb elements from the same site, collected in 1979. These elements (MCDRD 149 and 150) were identified as a tibia and fibula of the rhabdodontid ornithopod *Zalmoxes robustus* (referred to as *Rhabdodon priscum* by Groza, 1983, pp. 53–54, pl. 4, figs 4, 5). However, examination of the published illustrations and first-hand study of MCDRD 149 and 150 demonstrates their sauropod affinities, and that they represent a matching pair of radius and ulna instead.

Although not recognized as such by Groza (1983) at the time of his report's publication, further titanosaur remains were also discovered at the Râpa Mocioconilor locality in the same excavations, including a metacarpal, a partial ilium, and a fibula (see the complete list of specimens in the 'Systematic palaeontology' section). These fossils match the previously listed elements well in terms of their relative size and preservation style. Moreover, I. Groza identified these bones as being found together with the specimens discussed in his report (personal communication in the early 1990s to C.-M. Jianu, at that time curator of the palaeontology collections of the MCDRD, and through her to one of the authors [ZCs-S]), and were doubtlessly considered by him to be associated with the latter. Based on these data, we regard these elements from the MCDRD collections originating from the Râpa Mocioconilor site as being conspecific, and most probably parts of the same partial skeleton, which we designate as Individual G (Fig. 16).

Green Four locality, Sânpetru – Individual H

In the NHMUK collections there is a set of skeletal elements (inventoried under NHMUK R.4891) that is accompanied by a handwritten label from the time of its registration; this states that it contains "associated bones of *Titanosaurus*, Szentpéterfalva (all bones of this individual marked 'green 4')" (Fig. 17A). This represents

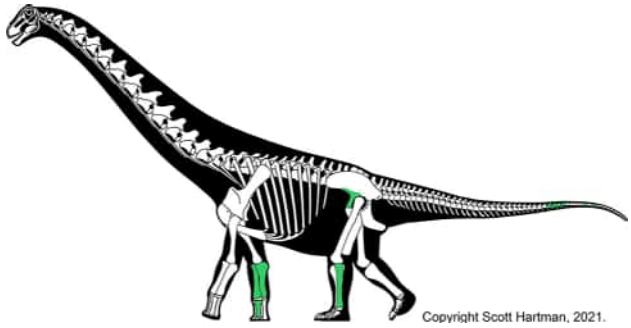

Figure 16. Fossil remains belonging to Individual G, referred here to *Petrustitan hungaricus* n. gen., Râpa Mocioconilor locality, Sânpetru. Skeletal drawing after Scott Hartman, used with permission.

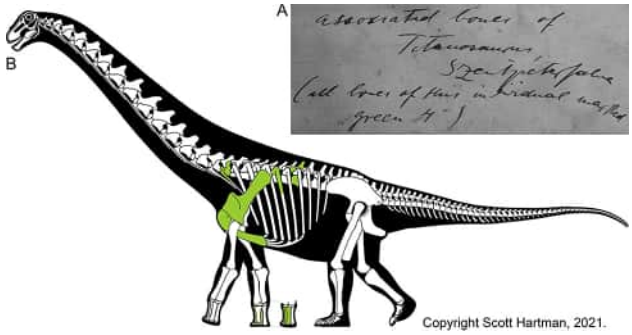

Figure 17. A, handwritten label from the NHMUK collections, indicating that it contains 'associated bones of *Titanosaurus*, Szentpéterfalva (elements under NHMUK R.4891, all bones of this individual marked "green 4")'. **B,** fossil remains belonging to Individual H, Lithostrotia *incertae sedis*, Green Four locality, Sânpetru. Skeletal drawing after Scott Hartman, used with permission.

the best and most detailed record of an original skeletal association among the sauropod material excavated by Nopcsa at Sânpetru. This is also corroborated by notes in the Nopcsa repository in the NHMUK archives, dated 1923, that lists the Transylvanian specimens Nopcsa offered for purchase to the museum. These notes record the "associated remains of one individual of *Titanosaurus*, ribs, vertebrae, parts of pelvis, including ilium, ?scapulae, 3 metacarpals, found in contact […], Szentpéterfalva". As in the case of most of the other assemblages discussed above, elements of this set (including dorsal vertebrae, ribs, sternal plate, scapula, coracoid, and three articulated metacarpals) are commensurate in size, lack duplicated elements, and show a similar preservation style, including the presence of a light grey, fine-grained sandy-silty matrix that is still adhered to some of the specimens. Based on these lines of evidence, the remains registered under NHMUK R.4891 can be considered as originating from one single

partial skeleton, identified here as Individual H (or the 'green 4' individual; Fig. 17B).

Unfortunately, little is known about the provenance of this material, except that it was excavated from the Sînpetru Formation, outcropping in the Sânpetru area (Fig. 1E). Because no more precise locality data are available, its age can be constrained only as Maastrichtian, following the review by Csiki-Sava et al. (2016) (Fig. 8).

Several of the elements belonging to Individual H were described and figured by Huene (1932). It is striking, however, that he decided to split up this material, referring the articulated metacarpus to *Magyarosaurus transsylvanicus* (Huene, 1932, pp. 268–269, pl. 46, fig. 10). By contrast, he regarded the dorsal ribs and pectoral girdle elements as belonging to an indeterminate titanosaur (Huene, 1932, pp. 270–272), although he explicitly emphasized that they probably originated from one and the same large individual: "The left 2nd dorsal rib … obviously of the same individual" and "… the piece carries the same number as the first two large dorsal ribs of the same site, it is probably found together with them and perhaps belongs to the same individual" ("*Die linke 2. Dorsalrippe … offenbar des gleichen Individuums*" and "… *das Stück die gleiche Nummer trägt wie die beiden ersten großen Dorsalrippen gleichen Fundort, ist es wahrscheinlich mit ihnen zusammen gefunden und gehört vielleicht zum gleichen Individuum*" in German in the original). Given his usage of the name ?*Magyarosaurus hungaricus* for the large-sized taxon (and thus, any large-sized titanosaur remains) from Transylvania, Huene (1932, p. 274) suggested that the dorsal ribs and the pectoral girdle elements could conceivably belong to this species: "It is also probably that these remains belong to the same species as the left fibula R.3853 …, which would be *Magyarosaurus hungaricus*" ("*Es dürfte auch wahrscheinlich sein, daß diese Reste zur gleiche Art gehören wie die linke Fibula R.3853 …, das wäre Magyarosaurus hungaricus*" in German in the original). This taxonomic opinion was reiterated in the plate captions of the respective figures (Huene, 1932, pl. 47, figs 9–11). Huene's (1932) decision to consider the remains accessioned under NHMUK R.4891 as belonging to more than one species is surprising, especially given that the evidence of association was available to him, and that he apparently studied these materials first-hand.

Tuștea titanosaur, Tuștea-Oltoane nesting site – Individual I

The Tuștea-Oltoane dinosaur nesting site is the first of its kind to be discovered in the uppermost Cretaceous of the Transylvanian area (e.g. Grigorescu et al., 1990, 2010) (Fig. 1E). It has yielded eggs and nests assigned to Megaloolithidae, an ootaxon that is usually considered to have been laid by titanosaurs (e.g. Horner, 2000; Sander, 2008; Vila et al., 2010), as supported by the discovery of embryonic remains associated with such eggs in Argentina (Chiappe et al., 1998, 2001). Accordingly, the eggs from Tuștea were also referred initially to *Magyarosaurus* (Grigorescu et al., 1990). However, they were subsequently found to be associated with hatchling remains of hadrosauroids (Grigorescu et al., 1994), and have therefore been considered to belong to this group instead (Botfalvai et al., 2017; Grigorescu, 2010, 2017; Grigorescu et al., 1994, 2010). Further support for this interpretation came from the total absence of sauropod remains from this site, despite years of careful excavations, a pattern that strikingly departs from the widespread and abundant occurrences of titanosaur remains in the Hațeg Basin (Csiki, Grigorescu, et al., 2010). However, this situation changed in 2008, when caudal vertebrae, chevrons, and an almost complete sacrum with a co-ossified partial ilium of a titanosaur were discovered at this locality (Csiki-Sava et al., 2012). All these elements were found at approximately the same stratigraphical level within the site, and were closely associated. The tight clustering of these remains, combined with the absence of other titanosaur specimens from elsewhere within the nesting site, suggests that they probably represent elements from one individual, herein identified as Individual I (Fig. 18). Such a conclusion is also consistent with the matching size and similar overall preservation of the specimens (Botfalvai et al., 2017). This locality is situated in the middle–upper part of the 'middle member' of the Densuș-Ciula Formation (Fig. 1E), and thus the stratigraphical age of Individual I is probably 'middle' (late early to early late) Maastrichtian (Csiki-Sava et al., 2016) (Fig. 8).

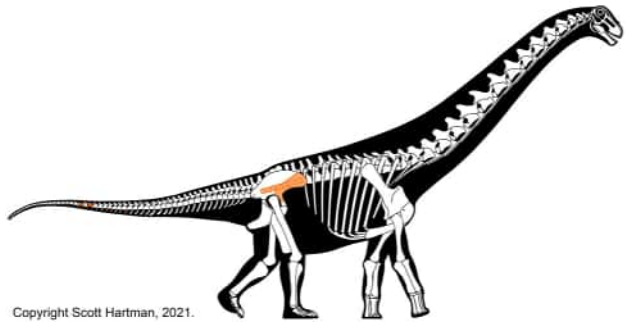

Figure 18. Fossil remains referred to Individual I, Lithostrotia *incertae sedis*, Tuștea titanosaur, Tuștea-Oltoane nesting site. Skeletal drawing (reversed) after Scott Hartman, used with permission.

The Groapă titanosaur assemblage, Sânpetru – Assemblage J

The Groapă locality is one of the major sites excavated in the Sibișel Valley after 1977 (Csiki, 2005; Csiki, Grigorescu, et al., 2010; Groza, 1983, fig. 1C). Researchers from both the FGGUB and MCDRD have worked at this site intermittently over the years, but unfortunately there is no record of the exact position of the skeletal elements recovered from here, except for the period between 1992 and 1994, when more systematic excavations took place. Since 1995, when the quarry was considered largely depleted and was abandoned, it has been revisited occasionally to uncover fossils that were still eroding out, but this activity has had little success. Accordingly, taphonomic information such as position in the site, orientation, and skeletal association, is scant or completely absent for most of the specimens excavated from here. Even the complete list of specimens originating from the Groapă locality is difficult to reconstruct, because in many instances these were labelled under different locality names in the two participating institutions, when they were labelled at all. Nevertheless, it is clear that the locality was relatively richly fossiliferous and that more than 50% of the identifiable macrovertebrate remains discovered here belong to titanosaurs (Csiki, 2005; Csiki, Grigorescu, et al., 2010). Based on the number of overlapping skeletal elements and variation in size, at least seven titanosaur individuals are represented at this site. These specimens appear to share a common taphonomic history, although there is some variation; for example, most of the titanosaur fossils are isolated and often fragmentary, whereas a few remains are articulated, including several series of dorsal and (mainly) caudal vertebrae, as well as an articulated tibia-fibula and associated partial pes. The duplicated skeletal elements (humeri, femora, fibulae) do not appear to represent distinct morphotypes, and do not differ widely in overall size, suggesting that all these individuals probably represent the same taxon and a similar ontogenetic stage. The latter received support from the osteohistological study of Stein et al. (2010), who demonstrated that, despite their relatively small size, all elements sampled from this site show an advanced HOS (12–14) and thus were attributed to *M. dacus*. Given that it is not possible to assign the recovered elements to distinct individuals, we designate the Groapă locality titanosaur remains as Assemblage J (Fig. 19).

The Groapă locality is probably situated in the middle part of the informal lower subunit of the Sînpetru Formation type section (Fig. 1E; see also Csiki, Grigorescu, et al., 2010, fig. 1C); as such, Assemblage J is most probably early to 'middle' Maastrichtian in age

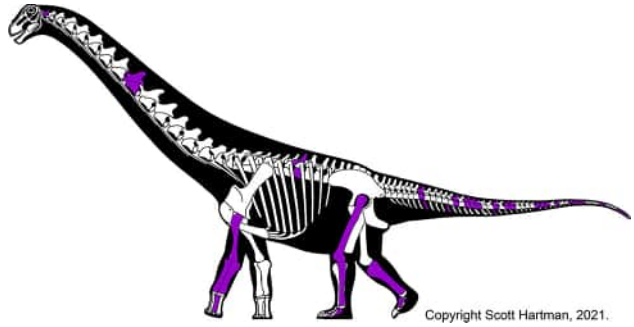

Figure 19. Fossil remains referred to Assemblage J, Lithostrotia *incertae sedis*, Groapă titanosaur assemblage, Sânpetru. Skeletal drawing after Scott Hartman, used with permission.

(Csiki-Sava et al., 2016). This also means that Assemblage J is stratigraphically somewhat younger than Individual G from the Râpa Mocioconilor site (Fig. 8).

Unfortunately, although several titanosaur specimens from the Groapă Quarry are fairly complete, their overall state of preservation is often poor. Both pre-burial and post-burial fracturing is common, and the periosteum of the bones is often missing entirely, exposing the cancellous inner bone texture. These observations are indicative of a relatively long sub-aerial exposure period in their taphonomic history, during which, weathering and environmental agents that promote disarticulation, dispersal, breakage and splintering were active. Furthermore, most of the titanosaur remains are preserved in a very hard, silica-cemented, fine, silty grey matrix that covers the bones in a concretionary manner and invades their incomplete and porous epiphyses. These factors make preparation very difficult and time-consuming to the extent of being almost prohibitive. Because of these unfortunate circumstances, the morphology of Assemblage J is less well known and documented than its skeletal representation would suggest.

Other less inclusive and/or less reliably supported skeletal associations. In addition to the localities and skeletal associations discussed above, there are several other instances where skeletal association of a number of titanosaur fossils from Transylvania can be ascertained with some degree of confidence. In many of these cases, however, skeletal association is restricted mainly to one region of the body, thus providing a more limited basis for comparison with the existing nominal taxa. In other cases, inferences of skeletal association rely on circumstantial evidence to a much greater degree. Arguments to support these associations are sometimes based on excavation records and/or registry or other written information, but more commonly rest on similar taphonomic features and commensurate size. Below, we

discuss such assemblages, and briefly review the data supporting their potential skeletal association (for a more detailed description of these remains see the Supplemental Material).

Pârâul Neagului titanosaur, Vălioara – Assemblage K

As noted below (see Individual N), a left humerus accessioned under NHMUK R.4882 is part of a set of "four imperfect limb bones" presented by Lady Woodward in 1923 to the NHMUK, and was supposedly collected from Sânpetru (Nopcsa archive list 22e, dated May 1923). However, it seems unlikely that this humerus came from the same locality as the other three specimens. Firstly, the humerus shows a clearly different preservation style compared to the other three specimens, suggesting that they probably came from different localities. Secondly, one of the identifying features of the humerus is a small quadrangular paper sticker glued to it, with the number "26" written in ink. As far as we are aware, there are only two other specimens from the entire Transylvanian titanosaur collection in the NHMUK that show this particular type of labelling: a partial left femur, NHMUK R.11126 (bearing "28"), and a large scapular blade (NHMUK R.11144, bearing "13"). No collecting data are available for NHMUK R.11126, but the scapular blade is registered as being part of the Nopcsa collection purchased through Count Szapary in 1924. Moreover, besides the small sticker, the scapula also has a larger paper label attached to it that identifies its place of origin as Valiora (= Vălioara), and more specifically as the "Pareu Niagului, right-side branch, second collecting point" ("*Pareu Niagului jobb oldali mellékág, 2^{ik} gyüjtőpont.*", in Hungarian in original), which corresponds perfectly with the details of one of the main excavation sites (II) of Kadić in the Vălioara area (Kadić, 1916). It is the only titanosaur material from the entire NHMUK collection that is known to come from this locality, and also one of only a few for which such written confirmation of its provenance is available. It is also worth noting that a large sample of vertebrate remains, showing the same type of preservation and dark brown to black colour, as well as the same type of small quadrangular paper labels with numerals written in ink, exists in the collections of the SZTFH. The provenance of the latter collection can be definitively identified as the Kadić excavations from Vălioara.

Based on the above observations, it seems reasonable to assume that the three NHMUK elements with these quadrangular paper labels also originated from the fossiliferous localities excavated by Kadić along the Pârâul Neagului (= Pareu Niagului; Kadić, 1916), near Vălioara, which, according to that report, produced dominantly dark, blackish remains. Moreover, based on their commensurate size, similar preservation style, and dark colour, the humerus (NHMUK R.4882) and the femur (NHMUK R.11126) could potentially have come from the same locality, and possibly even from the same individual (herein designated as Assemblage K). Although their exact provenance remains unknown, these specimens were most probably recovered from the continental successions cropping out along the Pârâul Neagului ravine (Fig. 1E), from the lower part of the 'middle member' of the Densuș-Ciula Formation, of early Maastrichtian age (Botfalvai et al., 2021; Csiki-Sava et al., 2016) (Fig. 8).

NHMUK R.3849, Sânpetru – Individual L

Several titanosaur specimens are registered under NHMUK R.3489 and are part of the Hațeg vertebrate collection purchased from Nopcsa in 1906. Unfortunately, as far as we are aware, no details are available concerning the reasons for this grouping of specimens. They include several caudal vertebrae, as well as more or less complete elements of the right forelimb (humerus, ulna, radius) and hind limb (femur and tibia). The humerus was described and figured by Huene (1932, p. 265, pl. 45, fig. 5), who referred it to *M. dacus*. All of the limb elements accessioned as NHMUK R.3489 are of commensurate size and have a similar preservation state (i.e. colour and preservation style of the specimens, as well as colour and grain-size of the matrix still adhering to the elements), which might indicate that these specimens were excavated from the same locality and might belong to the same individual, herein designated as Individual L.

As in the other cases of material excavated by Nopcsa at Sânpetru, there are no precise locality data associated with Individual L. Consequently, its provenance can only be identified as the Sînpetru Formation stratotype section along the Sibișel Valley (Fig. 1E) (see also, e.g. Individuals B and O, both from Sânpetru).

Dark Red titanosaur, Vălioara – Assemblage M

Huene (1932, pp. 265–266, pl. 45, fig. 6) described a dark-red-coloured, partial right ulna from Vălioara, which is part of the Kadić collection. He referred this specimen to *Magyarosaurus dacus* on the basis of its robustness. Based on the corresponding figure, this specimen (for which no other identification was given) can be identified as SZTFH Ob.3099. Although incomplete, it is a well-preserved element that shows a distinct

bowing of the shaft. Huene (1932) noticed this bowing and interpreted it as a genuine feature of the ulna; however, close inspection of the specimen demonstrates that it is most probably the result of post-mortem taphonomic deformation. Recognition of the taphonomic nature of this feature has notable consequences because Huene (1932) regarded the bowing as a key morphological difference between the otherwise similar ulnae of the species *M. dacus* and *M. transsylvanicus*. Later in the same monograph, Huene (1932) paired the ulna with a fibula of Assemblage A (SZTFH Ob.3086a), when attributing them to *M. dacus*. Meanwhile, Huene (1932, p. 268, pl. 46, fig. 9) referred a well-preserved right humerus to *M. transsylvanicus*, indicating that it had a similar size and shape as the one he referred to *M. dacus* (NHMUK R. 3849), but being more gracile, together with an ulna and a second fibula from Assemblage A (see above). Although no other identification data is given for this humerus, either, except that it comes from Vălioara, it can be clearly identified as specimen SZTFH v.13492, belonging to the Kadić collection. However, overall, the ulna SZTFH Ob.3099 that Huene referred to *M. dacus* displays preservational characteristics (including colour) similar to those of the right humerus SZTFH v.13492 of *M. transsylvanicus*, suggesting a potentially common taphonomic history. Furthermore, given that no other specimen from the Kadić collection shows the same combination of preservation state and dark-red–purple colour with the ulna SZTFH Ob.3099 and the humerus SZTFH v.13492, it is conceivable that they indeed originated from the same site, but one which is distinct from those yielding Assemblage A, or individuals C and K, all of which are characterized by differing sets of preservational features. Nevertheless, these specimens most probably did not come from the same individual, given that the ulna is only slightly shorter than the humerus, and are thus designated here as Assemblage M. The humerus SZTFH v.13492 was subsequently figured by Jianu and Weishampel (1999, figs 5, 6) and by Le Loeuff (2005a, fig. 1b), with both of these studies referring it to *M. dacus*.

Unfortunately, the limited information available regarding the provenance of the specimens in the Kadić collection means that it is not currently possible to re-identify the locality that yielded the humerus and ulna. As noted above, it seems highly probable that they did not originate from the main collecting sites excavated by Kadić (1916) near Vălioara, because they fit neither of the briefly described sets of preservational and taphonomic attributes that characterize these sites. Nevertheless, all of the fossils from the Kadić collection originate either from the neighbourhood of Vălioara or, in far fewer cases, that of nearby Boița, situated east of Vălioara (Fig. 1E). Uppermost Cretaceous continental sediments crop out near both villages, belonging to the lower part of the 'middle member' of the Densuș-Ciula Formation. Given this setting, the stratigraphical age of Assemblage M is likely to be early Maastrichtian (Csiki-Sava et al., 2016) (Fig. 8).

NHMUK R.4882, Sânpetru – Individual N

NHMUK R.4882 comprises four titanosaur limb elements. According to the NHMUK registry, they were collected from Sânpetru and then donated by Lady A. S. Woodward in 1923. This information is also confirmed by a list (no. 22e, dated May 1923) preserved in the Nopcsa archive of the NHMUK, that enumerates several fossils presented by Lady Woodward, and which mentions "four imperfect limb bones" under number R.4882. Three of the four specimens (right ulna, femur and tibia) are commensurate in size and show a similar preservation style, suggesting that they might have originated from the same locality, and possibly from the same individual. By contrast, the fourth specimen, a left humerus, is notably different in preservation, and it appears unlikely that it came from the same locality as the other three specimens (see above, Pârâul Neagului titanosaur, Vălioara – Assemblage K). As such, the ulna, femur, and tibia are tentatively considered to represent a single titanosaur individual, designated herein as Individual N.

As with other historical Sânpetru collections, the precise locality data are not known for Individual N. It can only be constrained as probably coming from the stratotype Sînpetru Formation along the Sibișel Valley (Fig. 1E) (see e.g. Individuals B and O, also from Sânpetru).

NHMUK unnumbered (VIII H 916) – Individual O

Among the incompletely prepared specimens housed in the NHMUK collections that were purchased from Nopcsa in 1923, there is an unregistered left tibia and fibula that both have "VIII H 916" written in ink on their surfaces. This type of coded identification was used by Nopcsa to mark specimens he considered to represent parts of one individual; for example, in his letter to the NHMUK dated 16 July 1920, preserved in the Nopcsa repository in the NHMUK archives, he listed several specimens of turtles, dinosaurs and crocodyliforms represented by associated material, offered to the NHMUK for purchase, and in which such individuals are identified as "A VIII 1916" (*Kallokibotion*), "B VIII 916" (*Zalmoxes*), etc. Assessment of skeletal

associations in these cases was most probably based on his own (otherwise specifically unrecorded) observations made during excavation of the specimens. The unnumbered NHMUK tibia and fibula display a similar preservation style to one another and preserve the same type of sedimentary matrix (a light-coloured, greenish-grey siltstone). They are commensurate in size, and, most importantly, have the same unusual distal articulation as that already noted in Individual B. Based on all these observations, this tibia-fibula pair is considered as probably originating from one locality and representing the same individual, designated here as Individual O.

As in the case of the other vertebrate remains that Nopcsa excavated at Sânpetru, there is no precise locality data associated with Individual O. As such, its origin can only be identified as the Sînpetru Formation stratotype section along the Sibișel Valley (Fig. 1E), and loosely constrained as early to early late Maastrichtian in age (Csiki-Sava et al., 2016) (Fig. 8).

NHMUK R.3852, Sânpetru – Individual P

Two associated partial pubes are registered under NHMUK R.3852. These are of comparable size, represent the left and right sides, and have a very similar preservation style and morphology. This suggests that they probably belong to the same individual, which we herein designate as Individual P. The right pubis was briefly described and figured by Huene (1932, p. 273, pl. 48, fig. 1), with him seemingly being unaware of its counterpart. Huene (1932) tentatively assigned this element to the large-sized Transylvanian titanosaur taxon he identified as ?*M. hungaricus*. The provenance of Individual P can only be identified as Sânpetru (Fig. 1E), and it most probably originates from the stratotype Sînpetru Formation (see Individuals B and O, both also from Sânpetru).

NHMUK R.4892, Sânpetru – Individual Q

NHMUK R.4892 includes an associated pair of scapulocoracoids, from Sânpetru, that most probably belong to the same individual (herein designated as Individual Q), based on their identical size, morphology and preservation style. These specimens were acquired from Nopcsa by the NHMUK in 1923. As with other historical Sânpetru collections, the location and stratigraphical age of this individual can only be loosely constrained as the early to early late Maastrichtian stratotype section of the Sînpetru Formation (Csiki-Sava et al., 2016) (Figs 1E, 8).

La Humă titanosaur, Sânpetru – Individual R

One of the first fossiliferous localities identified at Sânpetru, after the re-initiation of palaeontological explorations in the last few decades of the twentieth century, is the La Humă (După Râu) site (Csiki, Grigorescu, et al., 2010, fig. 1C). This is a 'fossiliferous pocket' that was excavated mainly in 1979 (Grigorescu, 1983; Știucă et al., 1982). It has yielded numerous vertebrate remains, including an incomplete left scapula (LPB [FGGUB] R.0003) and coracoid (LPB [FGGUB] R.0024) of a titanosaur. The two specimens are commensurate in size and have a very similar preservation style, suggesting that they could represent elements from the same individual (herein designated Individual R). A large titanosaur posterior caudal vertebra (LPB [FGGUB] R.0017) was also recovered from the same locality, but it is less clear whether it belongs to Individual R. The only titanosaur skeletal element previously figured from this site (the scapula) was referred to *T. dacus* by Știucă et al. (1982, pl. I, figs 3, 4).

Although age constraints are poor on the right-side succession of the Sibișel Valley, the La Humă site is located in the lower part of the informal lower subunit of the stratotype Sînpetru Formation (Fig. 1E). Accordingly, the age of the site is most probably early Maastrichtian (Csiki-Sava et al., 2016) (Fig. 8).

Vălioara purple titanosaur – Individual S

Two titanosaur skeletal elements registered in the FGGUB collections, an incomplete right scapula (LPB [FGGUB] R.1038) and an almost complete right coracoid (LPB [FGGUB] R.1051), possess a very similar style of preservation. This includes the dark reddish-purple hue of the bones, the absence of the periosteum exposing the underlying porous bone texture, and a dark grey, fine silty matrix adhering to both bones, as well as filling some of the pores. Based on these taphonomic characteristics, these two elements can clearly be differentiated from most other titanosaur bones in the FGGUB collections. Coupled with their commensurate size, it is possible that they came from the same site, and potentially even from the same individual (herein designated as Individual S). Locality data is only recorded for the coracoid, and this is imprecisely identified as coming from Vălioara, in the north-western part of the Hațeg Basin (Fig. 1E). Both elements were probably collected between 1978 and 1989, but no other information is available concerning their provenance. Based on the known distribution of the uppermost Cretaceous continental beds of the Hațeg Basin, these elements were probably recovered from the lower part of the 'middle member' of the Densuș-Ciula Formation,

and, as such, are early Maastrichtian in age (Csiki-Sava et al., 2016) (Fig. 8).

NHMUK R.4880, Sânpetru – Individual T

According to the list of specimens presented by Lady Woodward to the NHMUK in 1923 (list 22e, dated May 1923, from the NHMUK Nopcsa Archive), NHMUK R.4880 includes a set of "associated caudal vertebrae" belonging to "*Titanosaurus*". Indeed, there are several titanosaur caudal vertebrae registered under this number in the NHMUK collections, but based on their taphonomic features some of these might not have even come from the same site, let alone the same individual. However, among those specimens registered under NHMUK R.4880 there is a set of three procoelous anterior–middle caudal vertebrae that can be arranged into a continuous series, and share a similar preservation style, suggesting that these indeed might have been originally associated. This set is designated as Individual T.

As in the case of the other specimens presented to the NHMUK by Lady Woodward, no more detailed provenance data are associated with these specimens, except that they came from Sânpetru (i.e. from the stratotype section of the Sînpetru Formation; Fig. 1E) (see also Individuals B and O from Sânpetru).

LPB (FGGUB) R.1358, Sânpetru – Individual U

Specimen LPB (FGGUB) R.1358 consists of six partial titanosaurian posterior caudal vertebrae discovered in 1994. This material was recovered from a discontinuous series of outcrops along the left side of the Sibișel Valley, south of Sânpetru, identified as 'Maluri' by the local inhabitants (see Groza, 1983). The vertebrae were discovered in semi-articulation, lying parallel with the bedding plane, within a mottled, grey-greenish and brownish fine silty sandstone. No other vertebrate remains were identified in their proximity. Their degree of articulation, good state of preservation, and position within the fossiliferous level suggest that these vertebrae were not transported. These observations are consistent with this material coming from one skeleton (see Csiki, Grigorescu, et al., 2010), and thus are regarded as the associated remains of one individual, herein designated as Individual U.

The locality yielding Individual U (Fig. 1E) is located slightly upstream (i.e. up-section) of a large fossiliferous outcrop ('Scoabă'; see Csiki-Sava et al., 2016) in which the deposits were magnetostratigraphically dated as early Maastrichtian (Panaiotu & Panaiotu, 2010). Based on the position of the site from which Individual U was discovered, it also belongs to the lower part of the informal lower subunit of the Sînpetru Formation, and is thus most probably early Maastrichtian in age (Csiki-Sava et al., 2016) (Fig. 8).

K2 titanosaur, Vălioara – Individual V

In an attempt to relocate the original collecting sites of Kadić (1916), Botfalvai et al. (2021) identified several new localities yielding titanosaur remains. Of these, the most notable discovery consists of 10 caudal vertebrae (LPB [FGGUB] R.2715), three of which are preserved in articulation, and one chevron. The vertebrae, recovered from Botfalvai et al.'s (2021) locality K2 from the Pârâul Neagului ravine west of Vălioara village (Fig. 1E), can be arranged into a discontinuous series along the tail. The specimens were excavated from the same bed, came from a small area (less than 1 m^2), and are taphonomically similar, which suggest that they most probably represent elements of the same tail; this conclusion is also supported by the report of other associated/partially articulated dinosaur skeletons present in the same locality (Magyar et al., 2024). Thus, only one individual is likely to be represented by this material, herein designated as Individual V. Deposits exposed along the Pârâul Neagului ravine belong to the lower part of the 'middle member' of the Densuș-Ciula Formation, and, as such, are of early Maastrichtian age (Fig. 8). Moreover, this locality is only very slightly younger than locality I of Kadić (1916), which yielded the type material of *M. dacus* (see above). The titanosaur material from K2 is not yet completely prepared, and is still under study; however, the preliminary report of Botfalvai et al. (2021) suggested that it presents features known solely in the titanosaur *Paludititan* (otherwise represented only by Individual D). The detailed interpretation of this specimen will have to await its full preparation and description.

Methods

This section summarizes all methods used in this study, with the exception of those pertaining to the phylogenetic analyses. The latter is presented in a separate section within the Results given that the Romanian titanosaur OTUs in our phylogenetic data set depend on the results of our descriptions, comparisons and taxonomic decisions set out below. All measurements are detailed in Supplemental Material Table S1.

Anatomical descriptions

We use 'Romerian' terms (Wilson, 2006) for anatomical structures (e.g. 'centrum', not 'corpus') and their

orientation (e.g. 'anterior', not 'cranial'). The landmark-based terminology for vertebral laminae (Wilson, 1999) and fossae (Wilson et al., 2011) is also employed. Serial variation in caudal vertebrae has been determined using the criteria outlined by Mannion et al. (2013), wherein: (1) anterior caudal vertebrae possess ribs, even reduced ones; (2) middle caudal vertebrae lack ribs, but have distinct neural spines and postzygapophyses; (3) posterior caudal vertebrae lack ribs, as well as distinct neural spines and postzygapophyses; and (4) distal caudal vertebrae lack ribs and neural arches. To facilitate its description, the scapulocoracoid is described with the long axis of the scapular blade oriented horizontally. Similarly, metacarpals are described with their internal (palmar) surfaces facing ventrally, as if they were held horizontally, as a standard orientation for description (Mannion & Otero, 2012; Poropat, Upchurch, et al., 2015), although in life they would have been held in a vertical position, forming a 'U'-shaped manus.

Estimation of body size and mass

For body size and mass estimates, we use the equations proposed by Seebacher (2001) [M(kg) = 214.44L(m)×1.46] for calculating size, and Packard et al. (2009) [M(g) = 3.352PerH + F2.125] and Benson et al. (2018) [M(kg) = (10(2.749 × log(PerH + F)–1.104))/1000] for mass calculations for quadrupeds, in which M = body mass, PerH + F = sum of the perimeters of the humerus and femur in mm, and L = body length. The latter equation is based on the scaling equations provided by Campione and Evans (2012) and Campione et al. (2014).

Systematic palaeontology

Sauropoda Marsh, 1878
Titanosauriformes Salgado, Coria & Calvo, 1997
Titanosauria Bonaparte & Coria, 1993
Lithostrotia Upchurch, Barrett & Dodson, 2004
Eutitanosauria Sanz, Powell, Le Loeuff, Martínez & Pereda Suberbiola, 1999
Magyarosaurus Huene, 1932
Magyarosaurus dacus Nopcsa, 1915
1915 ***Titanosaurus dacus*** Nopcsa: 14–15
1915 ***Megalosaurus*** Nopcsa, *partim*: 15
(Figs. 20–34)

Lectotype. Anterior caudal vertebra (SZTFH Ob.3091, Assemblage A).

Paralectotype (Assemblage A). posterior caudal centrum (previously referred to *Megalosaurus*, SZTFH Ob.3105), left humerus (SZTFH Ob.3089), left ulna (SZTFH Ob.3100), left radius (SZTFH Ob.3101), metacarpal (SZTFH Ob.3096), left femur (SZTFH Ob.3088), three left fibulae (SZTFH Ob.3086 [two with the same specimen number], SZTFH Ob. 3102).

Referred specimens. Individual E. three dorsal vertebrae (LPB [FGGUB] R.1061 [two in articulation], R.1063), three fragmentary dorsal ribs (LPB [FGGUB] R.1861, R.1863, R.1865), four incomplete caudal vertebrae (LPB [FGGUB] R.1069, R.1070 [two in articulation], R.1071), one chevron (LPB [FGGUB] R.0076), left humerus (LPB [FGGUB] R.1047), two fragments of the left radius (LPB [FGGUB] R.1049 + R.1060), five metacarpal fragments (LPB [FGGUB] R.0074, R.0077, R.1053, R.1862, R.1864), left (LPB [FGGUB] R.1046) and right (LPB [FGGUB] R.1992) femora, proximal end of left tibia and fibula (LPB [FGGUB] R.2299).

Assemblage F. fragmentary cervical vertebra (LPB [FGGUB] R.2505), chevron (LPB [FGGUB] R.2510), right humerus (LPB [FGGUB] R.2506), metacarpal (LPB [FGGUB] R.2509), right femur (LPB [FGGUB] R.2507), right femur of a larger individual (LPB [FGGUB] R.2508).

Locality and distribution. The type locality is Locality I (Kadić, 1916), between Vălioara and Ciula Mică villages. This site occurs in the lowermost part of the unnamed middle member of the Densuș-Ciula Formation (Fig. 1E), which is earliest Maastrichtian in age (Fig. 8). Individual E was recovered from the same stratigraphical unit, in the vicinity of Ciula Mică (Figs 1E, 8). Assemblage F is also early Maastrichtian in age, but comes from deposits along the Bărbat River, at Pui, belonging either to the Sînpetru Formation (e.g. Grigorescu, 1992; Mamulea, 1953b), or a different (though penecontemporaneous) unit (Csiki-Sava et al., 2016; Therrien, 2005) (Figs 1E, 8).

Revised diagnosis. *Magyarosaurus dacus* can be diagnosed on the basis of five autapomorphies (marked with an asterisk), as well as six 'local' autapomorphies (defined in Beeston et al., 2024 as an apomorphy that is uniquely present in one taxon within a region of the tree, but that is also convergently present in a phylogenetically distant taxon (or taxa) within the same higher level clade): (1) anterior caudal centra with ventrolateral ridges but without a midline furrow (Individual E and Assemblage A); (2) posterior margin of the proximal articulation of the chevron forms a small 'hook'-like process that overhangs the posterior surface of the ramus (Individual E); (3) chevrons with a proximodistal ridge located on the lateral surface of each ramus (Individual E and Assemblage F); (4) marked prominence extending distally from the humeral head along the

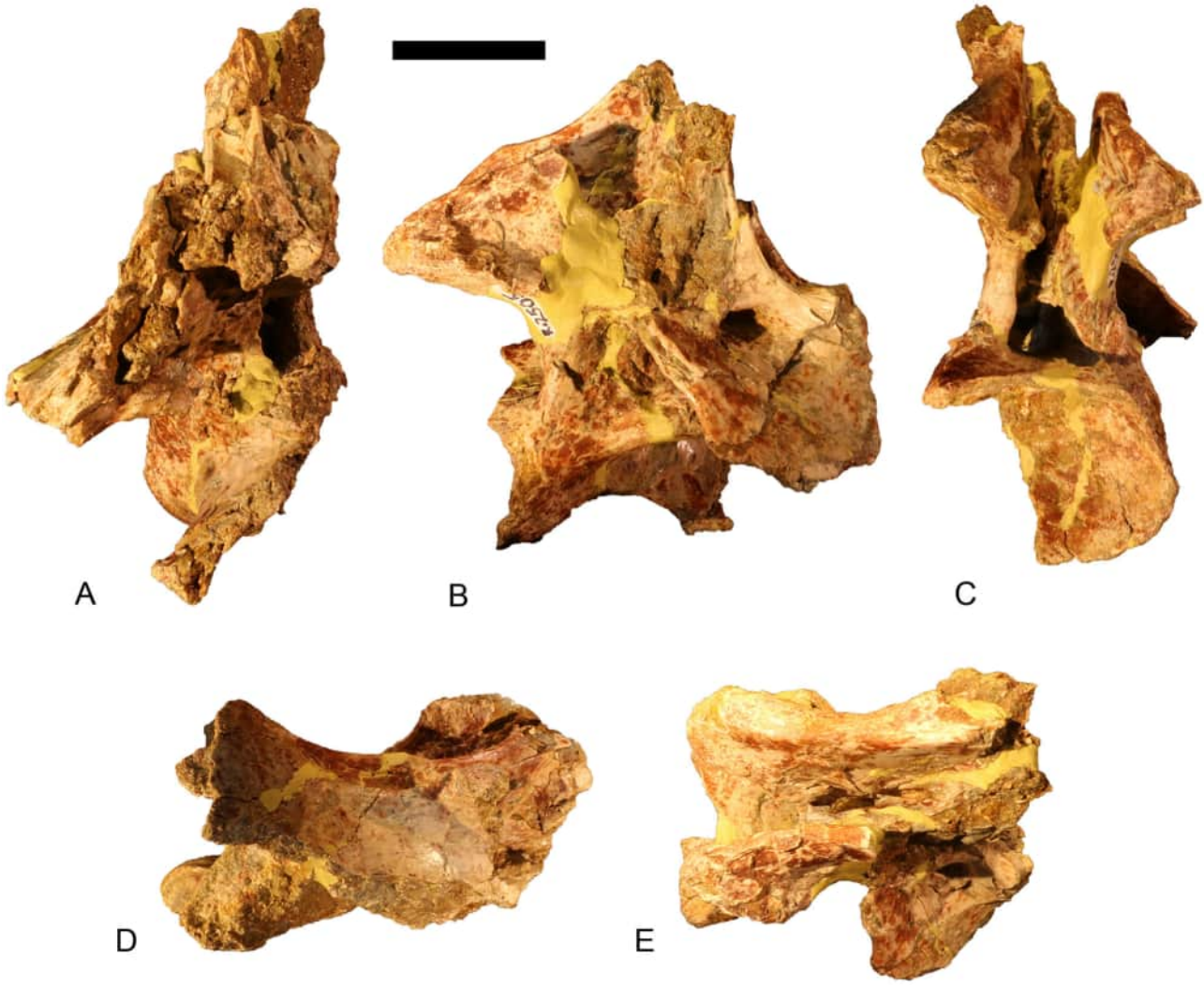

Figure 20. *Magyarosaurus dacus*, cervical vertebra LPB (FGGUB) R.2505 (Assemblage F) in **A,** anterior; **B,** right dorsolateral; **C,** posterior; **D,** ventral; and **E,** dorsal views. Scale bar equals 50 mm.

posterior surface, giving the proximal end a posteriorly deflected aspect in lateral/medial views (Individual E and Assemblage F)*; (5) coracobrachialis fossa divided into a small, shallow dorsomedial region and a large, deep ventrolateral region by an obliquely curved ridge (Individual E and Assemblage F)*; (6) position of the well-developed bulge (presumably site for M. latissimus dorsi) approximately equidistant from medial and lateral margins of posterior surface (Individual E and Assemblages A and F)*; (7) strong distolateral orientation of the interosseous ridge of the ulna, with the proximal end of this ridge intersecting the anteromedial margin of the shaft (Assemblage A)*; (8) shaft of radius displays torsion of approximately 45° (Assemblage A and Individual E); (9) distal end of radius, broader anteroposteriorly on the lateral margin than on the medial one (preservation means that this feature is only visible in the radius of Individual E); (10) low eccentricity of femoral midshaft (1.1–1.4) (Individual E, and Assemblages A and F)*; (11) subtle ridge on the anterior margin of the lateral surface of the fibula, with its proximal tip situated at approximately the level of the distal end of the lateral trochanter (Assemblage A).

Justification for referrals. The type material (Assemblage A) can be diagnosed by autapomorphies present in the anterior caudal vertebra (no. 1), humerus (no. 6), ulna (no. 7), femur (no. 10), and fibula (no. 11). Poor preservation and lack of anatomical overlap means that Individual E and Assemblage F can only be compared to Assemblage A via the humerus and the femur, but here the referrals are supported by the presence of autapomorphies 6 and 10. Moreover, Assemblage A and

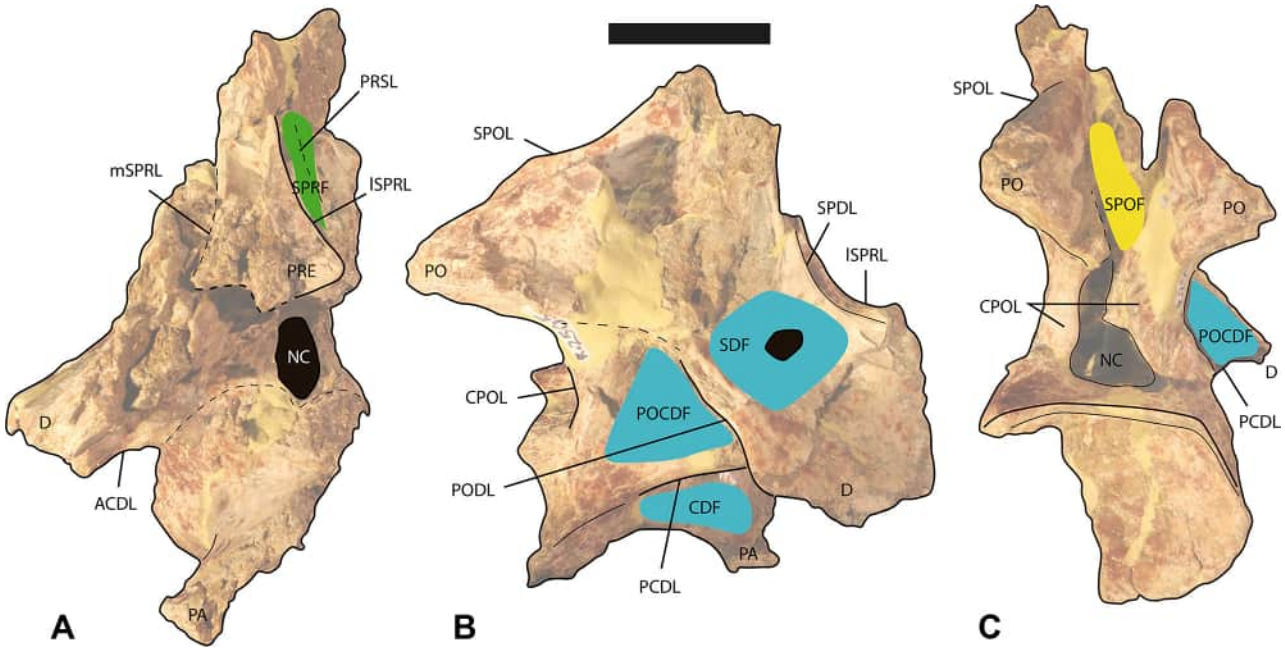

Figure 21. *Magyarosaurus dacus*, interpretive drawing of the cervical vertebra LPB (FGGUB) R.2505 (Assemblage F) in **A,** anterior; **B,** dorsolateral; and **C,** posterior views. **Abbreviations: ACDL**, anterior centrodiapophyseal lamina; **CPOL**, centropostygapophyseal lamina; **D**, diapophysis; **lSPRL**, lateral spinoprezygapophyseal lamina; **mSPRL**, medial spinoprezygapophyseal lamina; **NC**, neural canal; **PA**, parapophysis; **PCDL**, posterior centrodiapophyseal lamina; **PO**, postzygapophysis; **POCDF**, posterior centrodiapophyseal fossa; **PODL**, postzygodiapophyseal lamina; **PRE**, prezygapophysis; **PRSL**, prespinal lamina; **SDF**, spinodiapophyseal fossa; **SPDL**, spinodiapophsyeal lamina; **SPOF**, spinopostzygapophyseal fossa; **SPOL**, spinopostzygapophyseal lamina; **SPRF**, spinoprezygapophyseal fossa. Scale bar equals 50 mm.

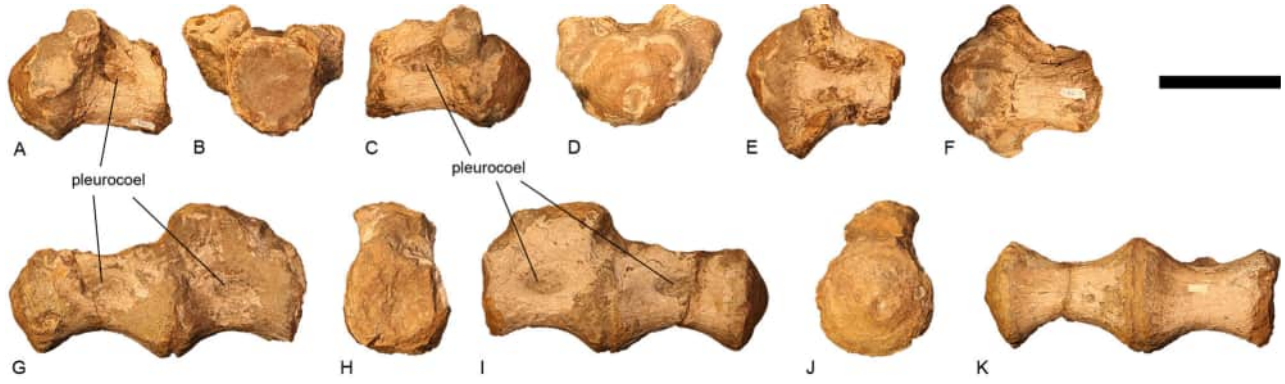

Figure 22. *Magyarosaurus dacus*, dorsal vertebrae. Anterior dorsal vertebra LPB (FGGUB) R.1063 (Individual E) in **A,** left lateral; **B,** posterior; **C,** right lateral; **D,** anterior; **E,** dorsal; and **F,** ventral views. Middle–posterior dorsal vertebrae LPB (FGGUB) R.1061 (Individual E) in **G,** left lateral; **H,** posterior; **I,** right lateral; **J,** anterior; and **K,** ventral views. Scale bar equals 100 mm.

Individual E share an unusual combination of character states in the anterior caudal centra, whereby they lack a ventral midline furrow, but possess distinct ventrolateral ridges (autapomorphy no. 1). Individual E and Assemblage F can be compared directly via the humeri, metacarpals and femora. Some of these elements provide strong evidence that E and F belong to the same taxon, possessing autapomorphy nos. 3 to 6, 8 and 10.

Description and comparisons of *Magyarosaurus dacus*

Cervical vertebra. LPB (FGGUB) R.2505 (Assemblage F) is a poorly preserved cervical vertebra (Figs 20, 21), probably from the posterior region of the neck, based on comparisons with titanosaurs with near-completely known cervical series (e.g. Calvo, Porfiri, et al., 2007; Carballido et al., 2017; Curry Rogers, 2009). Most of

Figure 23. *Magyarosaurus dacus*, dorsal rib fragments. LPB (FGGUB) R.1861 (Individual E) in **A,** lateral/medial? view; and **B,** transverse cross-section. LPB (FGGUB) R.1863 1861 (individual E) in **C,** lateral/medial? view; and **D,** transverse cross-section. Scale bar equals 50 mm.

the left half of the vertebra has been eroded away, and it is missing the condyle, both prezygapophyses, and the dorsal portion of the neural spine. The right side is also incomplete in places, and some areas of the vertebra are partly obscured by matrix. As a consequence of the eroded left side, the internal tissue structure is clearly visible, demonstrating the presence of camellae in both the centrum and neural arch, as in most somphospondylans (Wilson & Sereno, 1998).

Based on the nearly complete parapophysis and a lamina that probably represents part of the anterior centrodiapophyseal lamina (ACDL), little of the non-condylar centrum is missing. The centrum is anteroposteriorly short, with an aEI of approximately 1.74. This value varies between titanosaur taxa and along the posterior cervical series, but an aEI of 1.74 is comparable to that of some of the posterior cervical vertebrae of taxa such as *Alamosaurus* (Tykoski & Fiorillo, 2017), *Patagotitan* (Carballido et al., 2017), and *Savannasaurus* (Poropat et al., 2020). By contrast, the posterior cervical vertebrae of some titanosaurs have a lower aEI, including *Abditosaurus* (aEI = ∼1.1; Vila et al., 2022), and *Saltasaurus* (aEI = 1.03–1.52; Powell, 2003).

The posterior cotyle is deeply concave and, although incomplete, it is mediolaterally wider than dorsoventrally tall (Table S1). The morphology of the lateral pneumatic excavation is difficult to discern because of matrix and preparation: a sharp-lipped excavation is present, but its depth, and whether there were dividing ridges, cannot be determined (Figs 20B, 21B). It is not anteriorly restricted, and it does not extend to near the posterior-most margin of the centrum. There are two pneumatic foramina close to the dorsal surface of the base of the parapophysis, inside the lateral pneumatic excavation. The parapophysis projects ventrolaterally, but it does not extend far beyond the ventral margin of the centrum. In this regard, it differs from *Overosaurus* (Coria et al., 2013) and some members of Lognkosauria (González Riga et al., 2018). In *Magyarosaurus*, the parapophysis appears to occupy more than half of the length of the non-condylar centrum: such parapophyseal elongation is a derived state that also occurs in the middle–posterior cervical vertebrae of the Iberian taxon *Abditosaurus*, as well as *Alamosaurus*, *Bonatitan*, *Mansourasaurus*, saltasaurines and *Yongjinglong* (D'Emic, 2012; Li et al., 2014; Salgado et al., 2015; Sallam et al., 2018; Vila et al., 2022). However, the articular surface of the parapophysis in *Magyarosaurus* is relatively small compared to these taxa, such that much of its anteroposterior extent occurs where it merges with the centrum and it is more akin to a posterior centroparapophyseal-like lamina (PCPL). This lamina fades out posteriorly, such that there are no

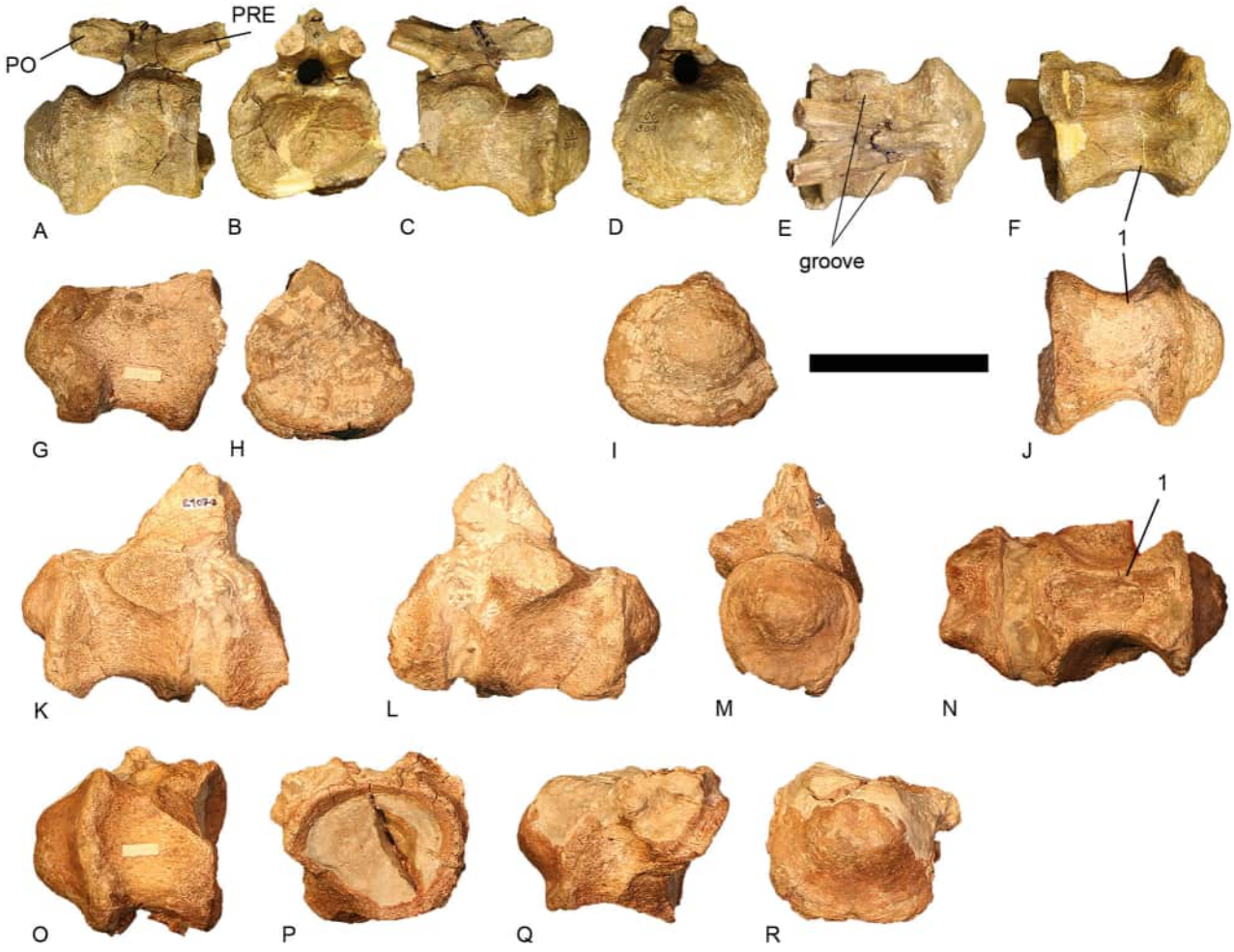

Figure 24. *Magyarosaurus dacus*, anterior caudal vertebrae. Lectotype SZTFH Ob.3091 (Assemblage A) in **A,** right lateral; **B,** anterior; **C,** left lateral; **D,** posterior; **E,** dorsal; and **F,** ventral views. LPB (FGGUB) R.1069 (Individual E) in **G,** right lateral; **H,** anterior; **I,** posterior; and **J,** ventral views. LPB (FGGUB) R.1070 (Individual E) in **K,** right lateral; **L,** left lateral; **M,** posterior; and **N,** ventral views. LPB (FGGUB) R.1071 (Individual E) in **O,** right lateral, **P,** anterior; **Q,** left lateral; and **R,** posterior views. **Abbreviations: PO**, postzygapophysis; **PRE**, prezygapophysis. The number 1 indicates the autapomorphy described in the text: anterior caudal centra with ventrolateral ridges but without a midline furrow. Scale bar equals 100 mm.

ventrolateral ridges along the posterior third of the centrum. As is also the case in most other titanosaurs (Poropat et al., 2016; Upchurch, 1998), the dorsal surface of the parapophysis is unexcavated. The preserved area of the ventral surface of the centrum is transversely flat anteriorly and gently convex posteriorly (Fig. 20D). It is too incomplete to determine if a midline ridge was present.

There is a prominent, posterior centrodiapophyseal lamina (PCDL) that extends posteriorly and slightly ventrally (Fig. 21B). The ACDL is incomplete, but the dorsal-most preserved portion is steeply oriented. These two laminae delimit a deep triangular centrodiapophyseal fossa (CDF), floored by a lamina that extends parallel to the PCDL and roofs the lateral pneumatic excavation on the centrum. The neural arch does not extend to the posterior margin of the centrum. Each centropostzygapophyseal lamina (CPOL) is robust and nearly vertical (Fig. 21C). There is no interpostzygapophyseal lamina (TPOL), but we cannot be certain whether its absence is a preservational artefact. Despite this, there is clearly no vertical midline lamina between the roof of the posterior neural canal opening and the postzygapophyses. The latter processes terminate approximately level with the posterior margin of the cotyle. This morphology characterizes the posterior cervical vertebrae of most titanosaurs, but contrasts with many other sauropods in which the postzygapophyses terminate anterior to the posterior margin of the centrum (Poropat et al., 2016; Tschopp et al., 2015). The postzygapophyses are proportionally large, with articular facets that face ventrally, partly laterally, and slightly

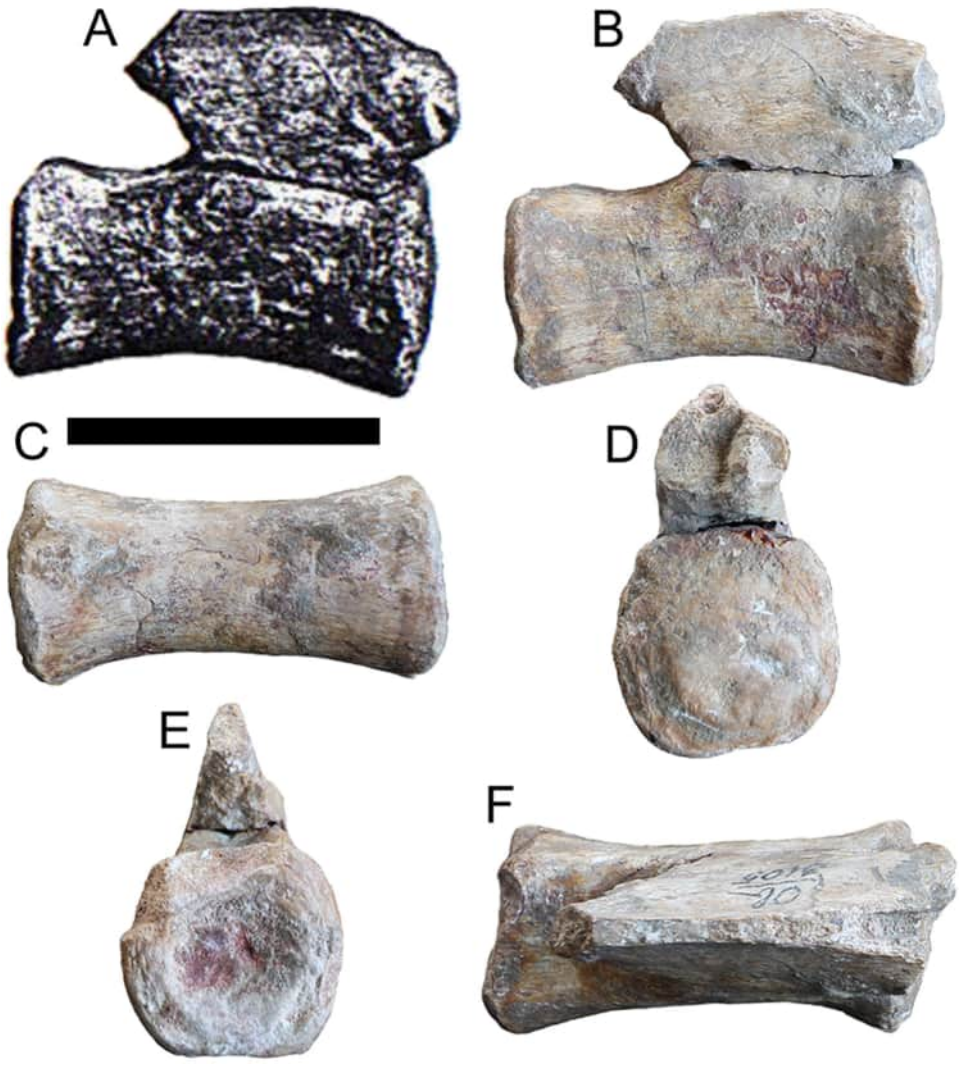

Figure 25. *Magyarosaurus dacus*, posterior caudal vertebra SZTFH Ob.3105 (Assemblage A) in **A,** right lateral view, from Nopcsa (1915); **B,** right lateral; **C,** ventral; **D,** posterior; **E,** anterior; and **F,** dorsal views. Scale bar equals 50 mm.

posteriorly. There appears to be a small epipophysis, at least on the left postzygapophysis. The medial surfaces of the postzygapophyses are not excavated.

The preserved proximal part of the diapophysis projects laterally. Its broad dorsal surface is predominantly flat. A prominent postzygodiapophyseal lamina (PODL), in conjunction with the PCDL and CPOL, define a deep triangular postzygapophyseal centrodiapophyseal fossa (POCDF) (Fig. 21B). Close to the base of the anterior region of the neural spine, there is an elliptical, well-defined foramen within the spinodiapophyseal fossa (SDF). Although the presence of a SDF is common in sauropod cervical vertebrae (Wilson et al., 2011), a comparably deep opening has otherwise only been reported in the posterior cervical vertebrae of *Alamosaurus* (Tykoski & Fiorillo, 2017), *Abditosaurus* (Vila et al., 2022), and some members of Lognkosauria (González Riga et al., 2018) and Aeolosaurini (Coria et al., 2013; Gorscak et al., 2017).

The lower sections of the SPRLs are preserved (Fig. 21A). There is both a medial and lateral SPRL (mSPRL and lSPRL, respectively), although only their bases are preserved (note that the left lSPRL is not preserved). Their distal ends (i.e. the portions of SPRLs that would have ascended to the spine summit) are not preserved, so whether the mSPRLs and lSPRLs continued as separate laminae or merged distally cannot be ascertained. There is a sharp-lipped, oval pneumatic foramen within the resultant SPRL fossa (SPRL-F). The presence of medial and lateral branches of the SPRL is unusual in sauropods, but it has been documented in posterior cervical vertebrae of *Mendozasaurus* (González Riga et al., 2018) and *Neuquensaurus* (Zurriaguz, 2016). However, even in these taxa, a double SPRL is not consistently present in

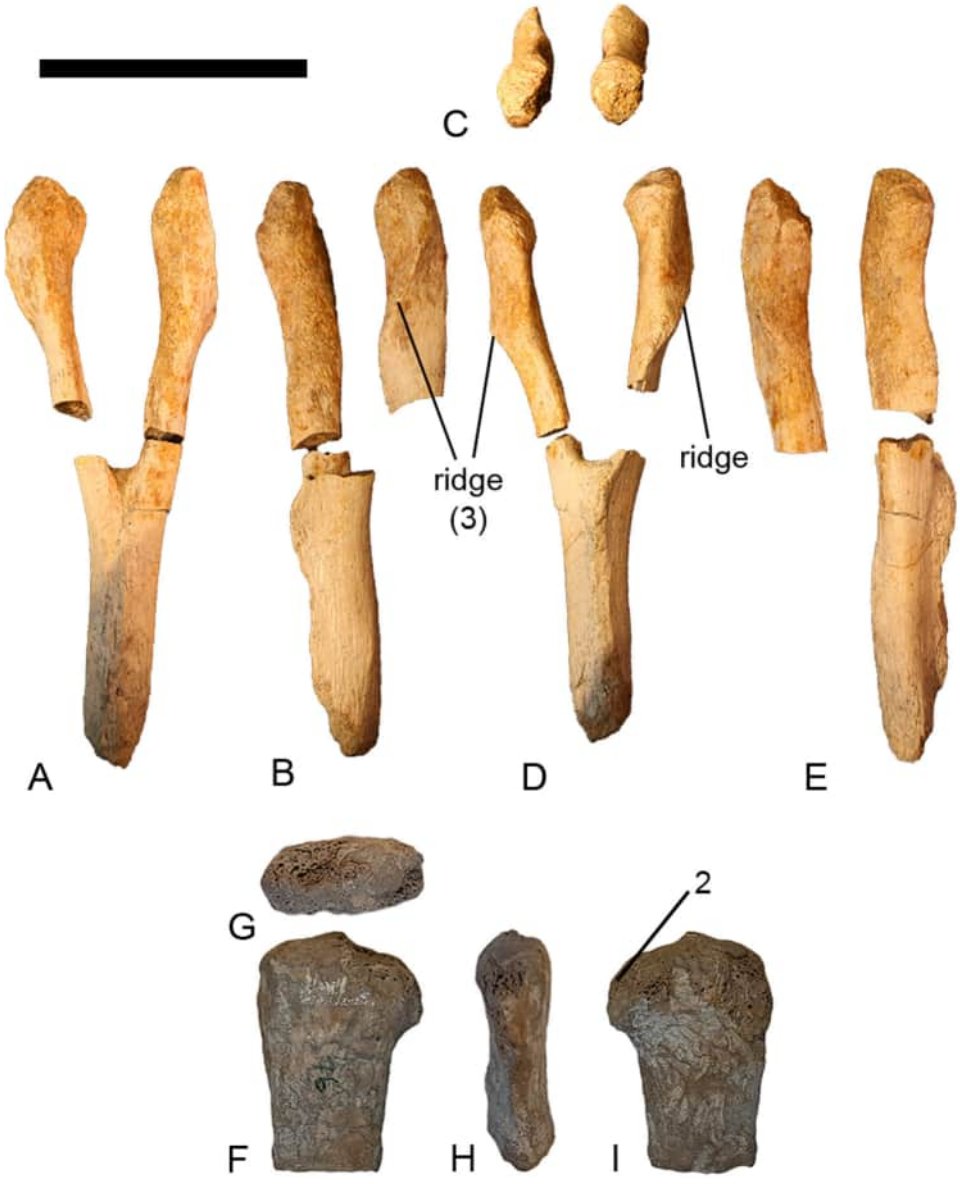

Figure 26. *Magyarosaurus dacus*, chevrons. Chevron LPB (FGGUB) R.2510 (Assemblage F) in **A,** anterior; **B,** right lateral; **C,** proximal (posterior towards top); **D,** posterior; and **E,** left lateral views. Chevron ramus LPB (FGGUB) R.0076 (Individual E) in **F,** left lateral; **G,** proximal (anterior towards left); **H,** posterior; and **I,** right lateral views. The numbers 2 and 3 indicate the autapomorphies described in the text: posterior margin of the proximal articulation of the chevron forms a small 'hook'-like process that overhangs the posterior surface of the ramus; and chevrons with a proximodistal ridge located on the lateral surface of each ramus. Scale bar equals 50 mm.

posterior cervical vertebrae; as such, we do not consider it a diagnostic feature of *Magyarosaurus*, pending the discovery of additional specimens with this feature. Although too poorly preserved to be certain, there is some evidence for a midline prespinal lamina (PRSL) within the spinoprezygapophyseal fossa (SPRF), as is the case in the posterior-most cervical vertebrae of most somphospondylans (D'Emic, 2012; Salgado et al., 1997).

The broad spinopostzygapophyseal laminae (SPOLs) bound a deep, but mediolaterally narrow spinopostzygapophyseal fossa (SPOF), with no evidence for a postspinal lamina (POSL) (Fig. 21C). The narrow SPOF resembles those in the posterior cervical vertebrae of some titanosaurs (e.g. *Atsinganosaurus* [Díez Díaz et al., 2018], *Overosaurus* [Coria et al., 2013, fig. 2], *Trigonosaurus* [Campos et al., 2005, fig. 4], and saltasaurines [e.g. Zurriaguz, 2016, fig. 4]), but differs from the wide fossa that characterizes others, including *Ampelosaurus* (Le Loeuff, 2005b), *Garrigatitan* (Díez Díaz et al., 2021), *Kaijutitan* (Filippi et al., 2019), and

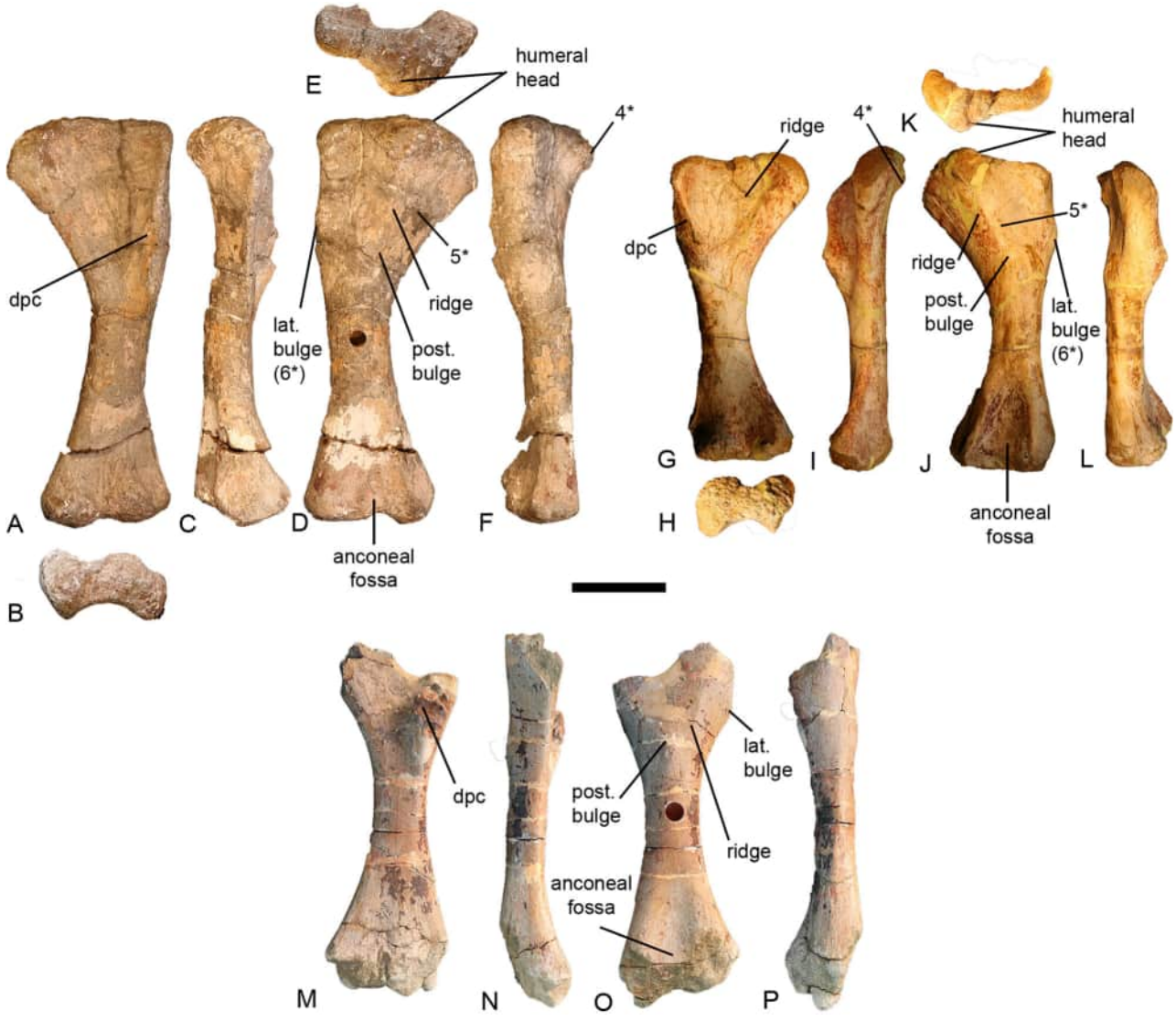

Figure 27. *Magyarosaurus dacus*, humeri. Left humerus LPB (FGGUB) R.1047 (Individual E) in **A,** anterior; **B,** distal (posterior towards bottom); **C,** medial; **D,** posterior; **E,** proximal (anterior towards top); and **F,** lateral views. Right humerus LPB (FGGUB) R.2506 (Assemblage F) in **G,** anterior; **H,** distal (posterior towards bottom); **I,** medial; **J,** posterior; **K,** proximal (anterior towards top); and **L,** lateral views. Left humerus SZTFH Ob.3089 (Assemblage A) in **M,** anterior; **N,** medial; **O,** posterior; and **P,** lateral views. **Abbreviations: dpc**, deltopectoral crest; **lat**, lateral; **post**, posterior. The numbers 4*, 5* and 6* indicate the autapomorphies described in the text: marked prominence extending distally from the humeral head along the posterior surface, giving the proximal end a posteriorly deflected aspect in lateral/medial; coracobrachialis fossa divided into a small, shallow dorsomedial region and a large, deep ventrolateral region by an obliquely curved ridge; and position of the well-developed bulge (presumably site for *M. latissimus dorsi*), which is situated approximately equidistant from medial and lateral margins of posterior surface, level with the distal tip of the deltopectoral crest. Scale bar equals 100 mm.

Mendozasaurus (González Riga et al., 2018). Given the incomplete nature of the specimen, it is not possible to obtain further information on the morphology of the cervical neural spine of *Magyarosaurus*.

Anterior dorsal vertebrae. LPB (FGGUB) R.1063 (Individual E) preserves the centrum and base of the neural arch of an anterior dorsal vertebra, missing material from its posterior surface (Fig. 22A–F). Its internal bone structure is camellate, a derived state that characterizes the presacral vertebrae of somphospondylans (Wilson & Sereno, 1998). The opisthocoelous centrum is mediolaterally wide and dorsoventrally low (Table S1), similar to the morphology of most titanosaurs (Mannion, Upchurch, Schwarz, et al., 2019). Its ventral surface is transversely convex, lacking fossae or ridges (Fig. 22F). In this regard, it differs from the anterior dorsal

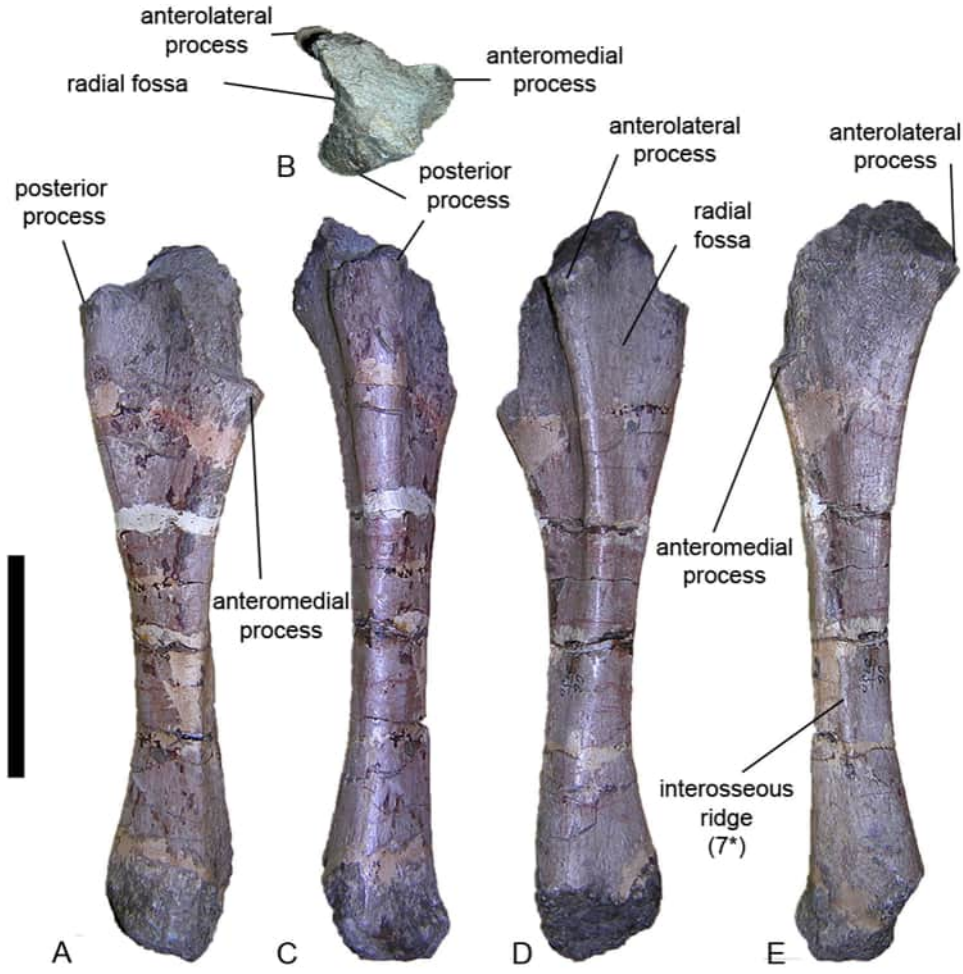

Figure 28. *Magyarosaurus dacus*, left ulna SZTFH Ob.3100 (Assemblage A) in **A,** medial; **B,** proximal (anterior towards top); **C,** posterior; **D,** anterolateral; and **E,** anterior views. The number 7* indicates the autapomorphy described in the text: distolateral orientation of the interosseous ridge of the ulna: proximal end of interosseous ridge, on anterior surface, intersects the anteromedial margin of the shaft and slants distolaterally. Scale bar equals 100 mm.

centra of *Lirainosaurus* (Díez Díaz et al., 2013b, fig. 3a), *Lohuecotitan* (Díez Díaz et al., 2016), and *Opisthocoelicaudia* (Borsuk-Białynicka, 1977), which are characterized by a longitudinal ventral ridge.

The parapophyses are situated mainly on the centrum, extending onto the base of the neural arch (Fig. 22A, C), supporting the inference that this specimen probably represents the second or third dorsal vertebra, based on comparisons with titanosaurs preserving complete dorsal series (e.g. *Rapetosaurus* [Curry Rogers, 2009]) and *Trigonosaurus* [Campos et al., 2005]). In this *Magyarosaurus* specimen, the parapophyses are relatively prominent processes that project quite far laterally. Each lateral surface of the centrum is excavated by a deep pneumatic foramen, located at approximately midheight, lying slightly closer to the anterior margin than the posterior one. This opening is oval, with an acute posterior terminus, as is typical for the anterior dorsal centra of most macronarians (Upchurch, 1998; Upchurch et al., 2004). Unlike the lateral pneumatic openings of the dorsal centra of many titanosaurs (Bonaparte & Coria, 1993; Upchurch et al., 2004), that of LPB (FGGUB) R.1063 is not set within a fossa. The neural arch is anteriorly biased, and the floor of the neural canal is flat and unexcavated.

Middle–posterior dorsal vertebrae. LPB (FGGUB) R.1061 (Individual E) consists of two articulated middle–posterior dorsal centra, with the base of the neural arch preserved in the more posterior element (Fig. 22G-K). The posterior end of the more posterior centrum is slightly incomplete. No parapophyses are present on either centrum or the preserved portion of neural arch, supporting the view that these vertebrae are not from the anterior region of the dorsal series. The aEI of the more anterior of these centra is 1.36, and that of the

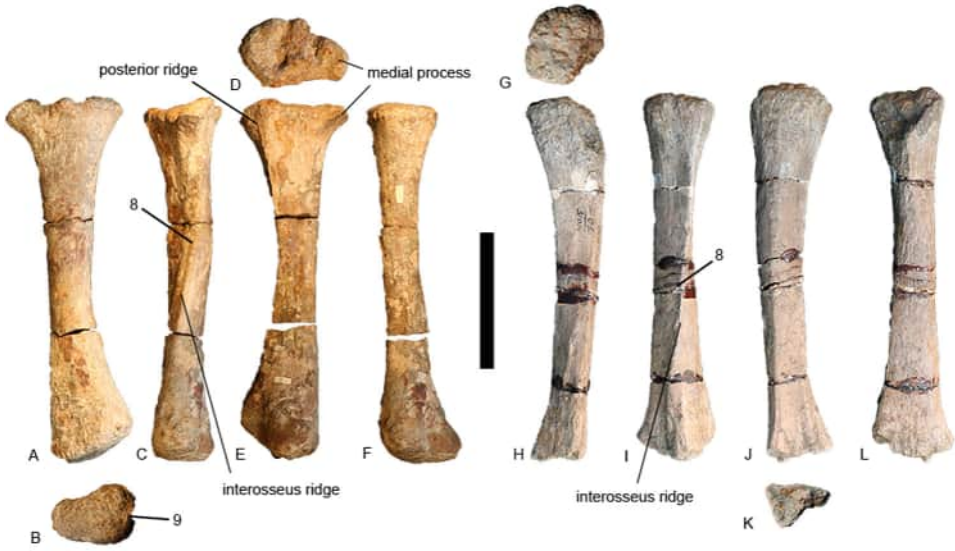

Figure 29. *Magyarosaurus dacus*, radii. Left radius LPB (FGGUB) R.1049 and R.1060 (Individual E) in **A,** anterior; **B,** distal (anterior towards top); **C,** medial; **D,** proximal (posterior towards bottom); **E,** posterior; and **F,** lateral views. Left radius SZTFH Ob.3101 (Assemblage A) in **G,** proximal (posterior towards bottom); **H,** posterior; **I,** medial; **J,** anterior; **K,** distal (anterior towards top); and **L,** lateral views. The numbers 8 and 9 indicate the autapomorphies described in the text: shaft of radius displays torsion of approximately 45°; and distal end of radius, broader anteroposteriorly on the lateral margin than on the medial one. Scale bar equals 100 mm.

more posterior one is 1.34, higher than the values calculated for the middle–posterior dorsal vertebrae of *Lirainosaurus* (Díez Díaz et al., 2013b). The centra have a camellate internal structure. Both centra are strongly opisthocoelous, and there is a slight central depression on each condyle. In lateral view, the ventral margins of the centra are strongly arched upwards. The ventral surface of each centrum is gently convex transversely, lacking ridges or excavations (Fig. 22F, K). This is similar to the condition in most sauropods, but differs from the midline ventral ridge that characterizes the middle–posterior dorsal centra of some titanosaurs, including *Diamantinasaurus* (Poropat, Upchurch, et al., 2015), *Futalognkosaurus* (Calvo, Porfiri, et al., 2007), and *Opisthocoelicaudia* (Borsuk-Białynicka, 1977), and that is variably present in taxa such as *Overosaurus* (Coria et al., 2013) and possibly *Atsinganosaurus* (Díez Díaz et al., 2018). 'Eye'-shaped lateral pneumatic openings are present, extending across approximately the middle third of the anteroposterior length of the non-condylar centrum, at approximately midheight (Fig. 22A, C, G, I). Although filled with matrix, these lateral pneumatic openings appear to be deep, and they are not set in a fossa. The neural arch does not extend to the posterior margin of the centrum.

Thoracic ribs. LPB (FGGUB) R.1861 (in two pieces), R.1863, and R.1865, are small fragments of thoracic rib shafts from Individual E (Fig. 23). There is no clear evidence for pneumaticity, but this is potentially because they are almost certainly quite distal fragments of the shaft. LPB (FGGUB) R.1861 is 'plank'-like, with the anteroposterior width approximately three times that of the mediolateral width (Fig. 23B). Although we cannot be certain of its position in the dorsal series, such 'plank'-like ribs are a derived state of Titanosauriformes when present in the anterior thoracic region (Wilson & Sereno, 1998). By contrast, the anteroposterior to mediolateral width ratio is closer to 2.0 in LPB (FGGUB) R.1863, which has a narrow, 'D'-shaped cross-section (Fig. 23D). The absence of the plank-like structure in LPB (FGGUB) R.1863 potentially indicates that it comes from a more posterior rib within the thoracic region.

Anterior caudal vertebrae. Parts of five anterior caudal vertebrae can currently be referred to *Magyarosaurus* (Fig. 24). Specimens LPB (FGGUB) R.1069 (Fig. 24G–J) and R.1071 (Fig. 24O–R) (Individual E) belong to the proximal section of the tail. However, none of them can be considered as being the first caudal vertebra because of the presence of chevron facets. Their aEI ranges from 0.68 to 0.81, a low value when compared with the anterior-most caudal vertebrae of some early-branching titanosaurs, such as *Andesaurus* (aEI = 0.92, Mannion & Calvo, 2011) and *Malawisaurus* (aEI = 0.96, Gomani, 2005), but closer to the aEI of *Lohuecotitan* (where the aEI of the first six caudal centra ranges from 0.57 to 0.74; Díez Díaz et al., 2016), *Bonitasaura* (aEI = 0.77; Gallina & Apesteguía, 2015), and *Trigonosaurus* (aEI = 0.81; Campos et al., 2005).

Figure 30. *Magyarosaurus dacus*, Individual E metacarpals. Metacarpal LPB (FGGUB) R.0074 in **A,** dorsal; **B,** lateral/medial; **C,** ventral; **D,** medial/lateral; and **E,** distal (ventral towards bottom) views. Metacarpal III? LPB (FGGUB) R.1864 in **F,** ventral; **G,** lateral/medial; **H,** dorsal; **I,** medial/lateral; and **J,** proximal (ventral towards bottom) views; **K,** transverse cross-section at mid-shaft. Left metacarpal IV? LPB (FGGUB) R.1053 in **L,** dorsal; **M,** lateral/medial; **N,** ventral; **O,** medial/lateral; and **P,** distal (ventral towards bottom) views. Metacarpal IV? LPB (FGGUB) R.1862 in **Q,** dorsal; **R,** lateral/medial; **S,** ventral; **T,** medial/lateral; **U,** transverse cross-section of the distal third of the shaft; and **V,** distal (ventral towards bottom) views. Right metacarpal V LPB (FGGUB) R.0077 in **W,** lateral; **X,** ventral; **Y,** medial; **Z,** dorsal; and **A',** distal (ventral towards left) views. Scale bar equals 10 mm.

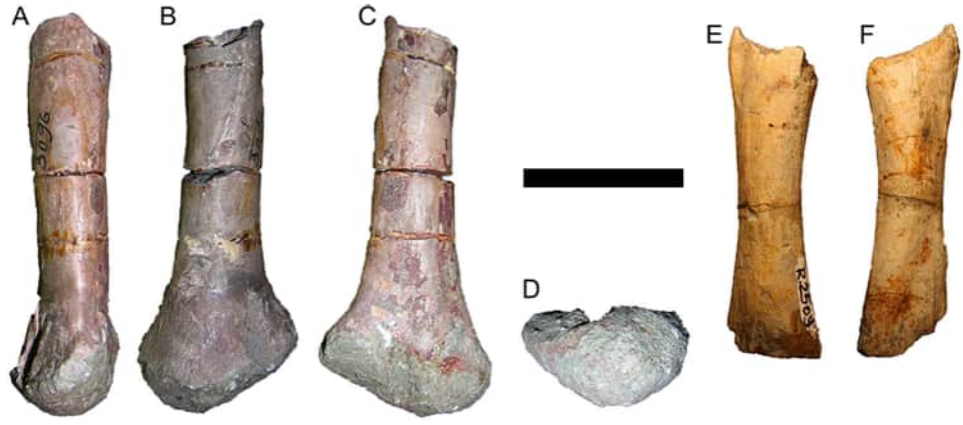

Figure 31. *Magyarosaurus dacus*, Assemblages A and F metacarpals. Metacarpal SZTFH Ob.3096 (Assemblage A) in **A,** lateral/medial; **B,** dorsal?; **C,** ventral?; and **D,** distal (dorsal? towards bottom) views. Metacarpal LPB (FGGUB) R.2509 (Assemblage F) in **E,** ventral; and **F,** dorsal views. Scale bar equals 50 mm.

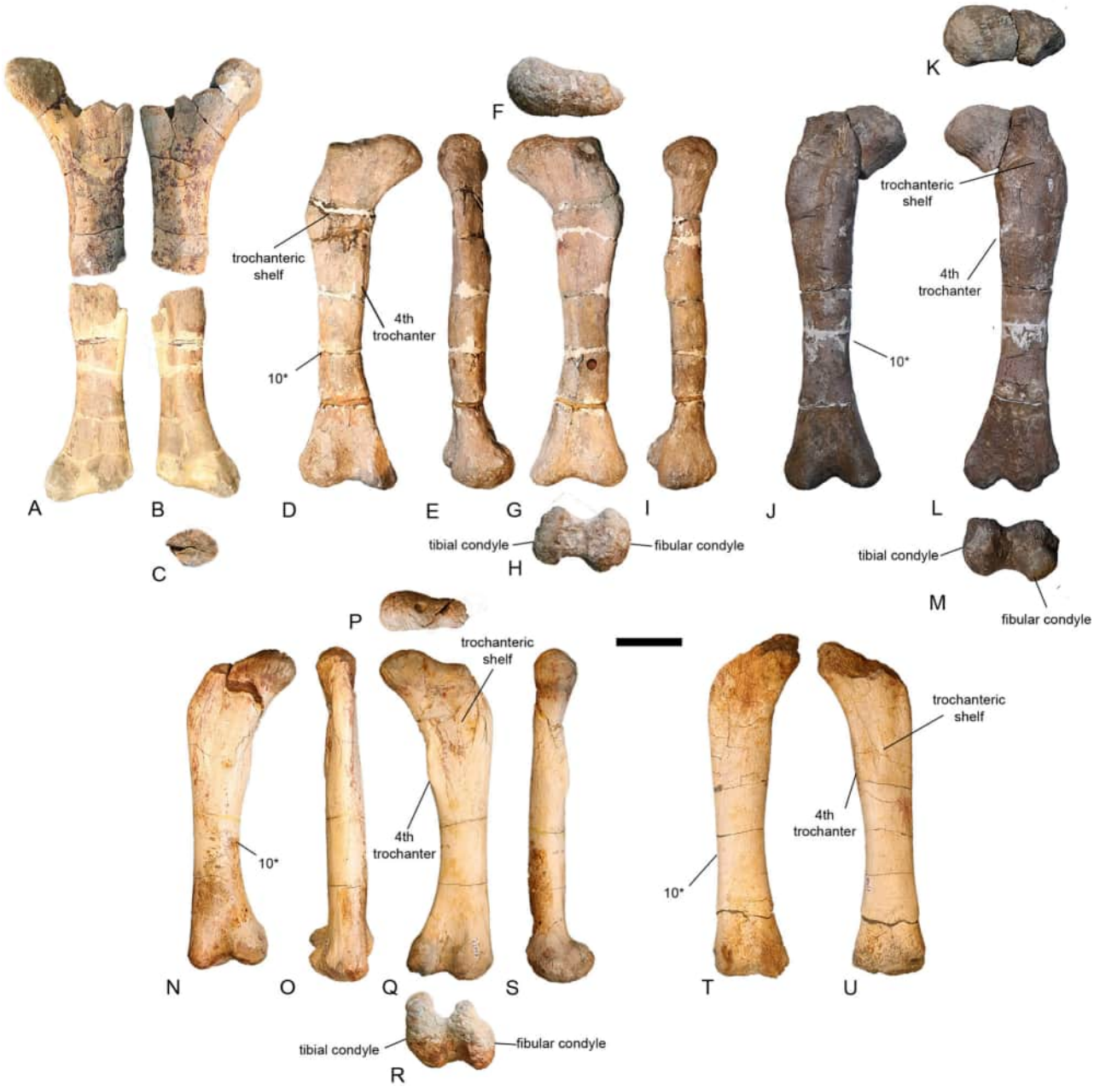

Figure 32. *Magyarosaurus dacus*, femora. Left femur SZTFH Ob.3088 (Assemblage A) in **A,** anterior; **B,** posterior views; and **C,** transverse cross-section (at approximate midshaft). Left femur LPB (FGGUB) R.1046 (Individual E) in **D,** posterior; **E,** lateral, **F,** proximal (posterior towards top); **G,** anterior; **H,** distal (anterior towards top); and **I,** medial views. Right femur LPB (FGGUB) R.1992 (Individual E) in **J,** anterior; **K,** proximal (posterior towards bottom); **L,** posterior; and **M,** distal (posterior towards top) views. Right femur LPB (FGGUB) R.2507 (Assemblage F) in **N,** anterior; **O,** lateral; **P,** proximal (posterior towards bottom); **Q,** posterior; **R,** distal (posterior towards top); and **S,** medial views. Right femur LPB (FGGUB) R.2508 (Assemblage F) in **T,** anterior; and **U,** posterior views. The number 10* indicates the autapomorphy described in the text: low eccentricity of femoral midshaft (1.1–1.4). Scale bar equals 100 mm.

LPB (FGGUB) R.1070 (Fig. 24K–N) (Individual E) is an anterior caudal vertebra, in articulation with the posterior part of the preceding vertebra, that comes from further along the caudal sequence than LPB (FGGUB) R.1069 and R.1071. The lectotype of *Magyarosaurus*, SZTFH Ob.3091 (Fig. 24A–F) (Assemblage A), is probably from the distal part of the anterior series and has an aEI of 1.01.

None of these caudal vertebrae present a camellate internal tissue structure, contrasting with some

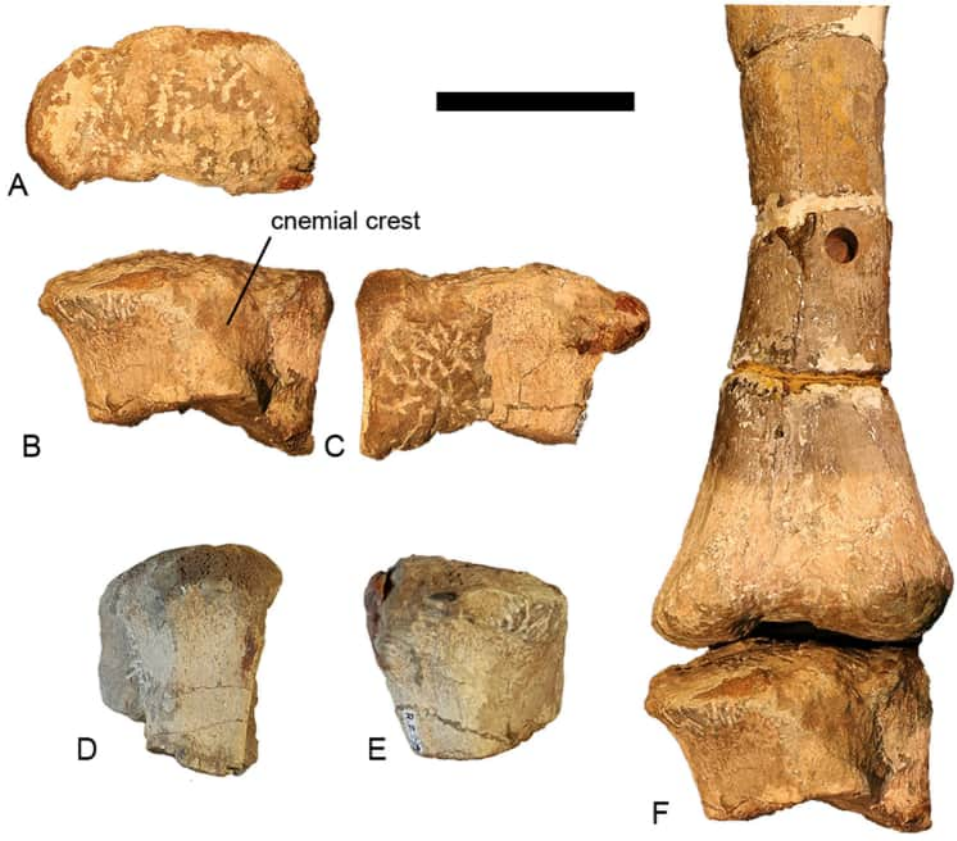

Figure 33. *Magyarosaurus dacus*, left tibia and fibula LPB (FGGUB) R.2299 (Individual E) in **A,** proximal (posterior towards bottom); **B,** anterior; **C,** posterior (fibula barely visible on the left); **D,** lateral (only fibula visible); and **E,** medial (fibula not visible) views. **F,** tibia and fibula articulated with femur LPB (FGGUB) R.1046 in anterior view. Scale bar equals 100 mm.

titanosaurs, in which the neural arch (and sometimes the centrum too) of anterior caudal vertebrae is internally pneumatized (e.g. see Poropat et al., 2020). The concave anterior articular surface of each centrum has a slightly dorsoventrally compressed subcircular outline. The centra are strongly procoelous, and demonstrate that a posterior condyle was present throughout the anterior caudal vertebral series. This feature characterizes nearly all lithostrotians (Mannion et al., 2013). The posterior condyle is prominent in *Magyarosaurus*, but is also constricted because of the presence of a marked ridge on the outer margin of the posterior articular face of the centrum, as in most somphospondylans (Mannion et al., 2013). The condyle is located in the centre of the articulation surface in SZTFH Ob.3091 and LPB (FGGUB) R.1071, whereas it is more dorsally shifted in LPB (FGGUB) R.1069 and 1070. This demonstrates that some of the purported differences in morphotypes amongst Romanian titanosaurian caudal vertebrae identified by Mocho et al. (2023) might instead represent serial variation. In SZTFH Ob.3091 there is a shallow midline groove on the condyle (Fig. 24D).

The ventral surfaces of LPB (FGGUB) R.1069 and R.1071 are transversely wide, whereas they are narrower in SZTFH Ob.3091 and LPB (FGGUB) R.1070, as a result of the ventral half of the centrum being more transversely compressed than in the two more anterior caudal vertebrae. The ventral surface is also flat in all of the anterior caudal vertebrae, lacking a midline furrow. The presence of a ventral midline furrow characterizes the anterior caudal centra of many somphospondylans, including several titanosaurs (e.g. *Alamosaurus*, *Andesaurus*, *Epachthosaurus*, *Malawisaurus*, *Opisthocoelicaudia*, *Saltasaurus*; Mannion & Calvo, 2011; Upchurch, 1998; Wilson, 2002), but many taxa lack this feature. Amongst Titanosauria, a flat ventral surface, without a midline groove, also characterizes the anterior caudal centra of other western Eurasian species (i.e. *Atsinganosaurus*, *Lirainosaurus*, *Lohuecotitan*, *Normanniasaurus*, *Paludititan*, and *Volgatitan*; Averianov & Efimov, 2018; Csiki, Codrea, et al., 2010; Díez Díaz et al., 2013b, 2016, 2018; Mannion, Upchurch, Jin, et al., 2019), as well as several South American taxa, e.g.

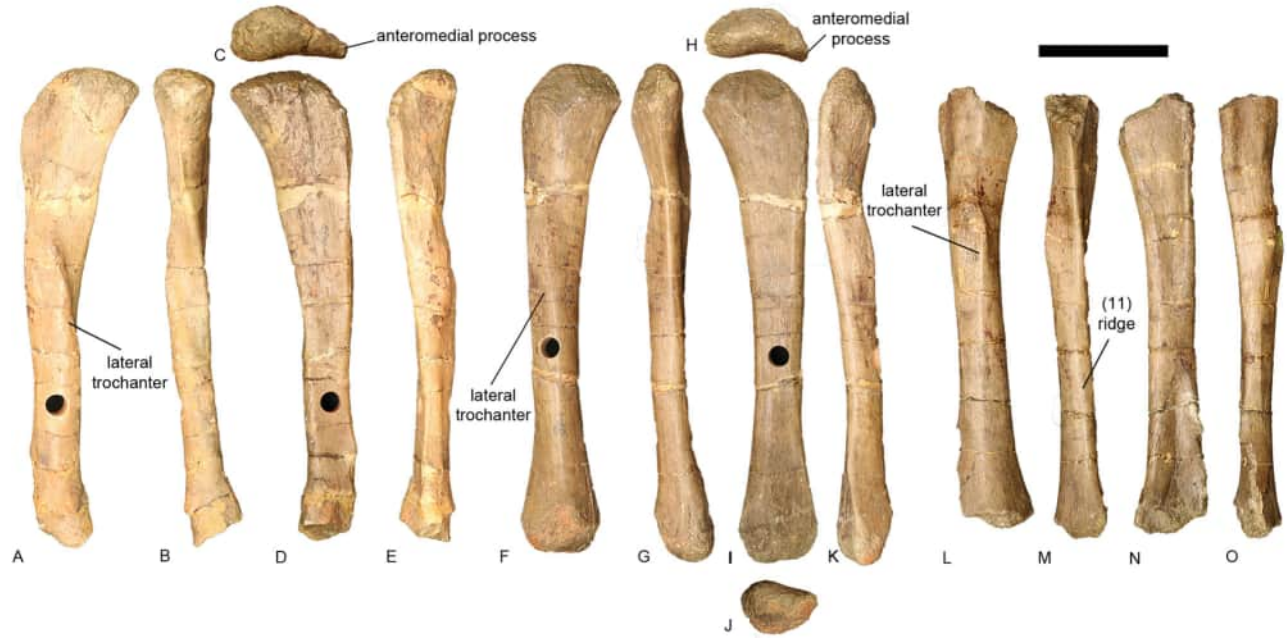

Figure 34. *Magyarosaurus dacus*, fibulae. Left fibula SZTFH Ob.3086a (Assemblage A) in **A,** lateral; **B,** posterior; **C,** proximal (medial towards bottom); **D,** medial; and **E,** anterior views. Left fibula SZTFH Ob.3086b (Assemblage A) in **F,** lateral; **G,** posterior; **H,** proximal (medial towards bottom); **I,** medial; **J,** distal (medial towards top); and **K,** anterior views. Left fibula SZTFH Ob.3102 (Assemblage A) in **L,** lateral; **M,** posterior; **N,** medial; and **O,** anterior views. The number 11 indicates the autapomorphy described in the text: subtle ridge on the anterior margin of the lateral surface of the fibula, with its proximal tip situated at approximately the level of the distal end of the lateral trochanter. Scale bar equals 100 mm.

Baurutitan (Kellner et al., 2005) and *Mendozasaurus* (González Riga et al., 2018). All known anterior caudal centra of *Magyarosaurus* bear anterior and, more prominent, posterior chevron facets, although these are less well-developed in LPB (FGGUB) R.1071. In SZTFH Ob.3091 and LPB (FGGUB) R.1070, the ventral surface is delimited laterally by two longitudinal ridges that connect the anterior and posterior chevron facets (Fig. 24F, N). Taxa that have a midline ventral furrow in their anterior caudal centra typically also have ventrolateral ridges (including most of the taxa mentioned above), though *Lirainosaurus* (Díez Díaz et al., 2013b) and some specimens of *Atsinganosaurus* (Díez Díaz et al., 2018) are also characterized by the combination of ventrolateral ridges without a midline furrow observed in *Magyarosaurus*.

The lateral surfaces of the anterior caudal centra of *Magyarosaurus* lack excavations or ridges. Transverse processes are partially preserved on LPB (FGGUB) R.1070 and 1071, where they are situated at the arch-centrum junction. In SZTFH Ob.3091, they are reduced to low, rugose prominences at the arch-centrum junction, supporting our inference that this specimen comes from the distal part of the anterior tail series. These transverse processes are gently excavated at midheight, forming a shallow, anteroposteriorly oriented groove (Fig. 24E).

The base of the neural arch is anteriorly placed on the centrum. Only SZTFH Ob.3091 preserves enough of the neural arch and spine to provide detailed anatomical information. Although incomplete, the prezygapophyses are slender processes that project anterodorsally beyond the anterior margin of the centrum, as in most titanosaurian anterior caudal vertebrae, including those of other European taxa (Csiki, Codrea, et al., 2010; Díez Díaz et al., 2013b, 2016, 2018; Le Loeuff, 2005b; Le Loeuff et al., 2013). The prezygapophyses are supported by short, stout CPRLs, and are linked to each other by a wide, horizontal TPRL. Each postzygapophysis has a flat oval facet that faces mainly laterally and does not project beyond the posterior margin of the neural spine. Ventrally, the postzygapophyses are each supported by a CPOL. No hyposphene-hypantrum complex is present, an absence that is typical for the caudal vertebrae of most titanosaur taxa (Upchurch, 1998; Upchurch et al., 2011). The neural spine is almost complete and is dorsoventrally short, similar to that of taxa such as *Atsinganosaurus*, *Lirainosaurus*, *Paludititan*, *Rapetosaurus* and *Saltasaurus* (Csiki, Codrea, et al., 2010; Curry Rogers, 2009; Díez Díaz et al., 2013b, 2018; Powell, 1992), but unlike the elongated spines of *Andesaurus*, *Muyelensaurus* and *Lohuecotitan* (Calvo, González Riga, et al., 2007; Díez Díaz et al., 2016;

Mannion & Calvo, 2011). The neural spine of SZTFH Ob.3091 is transversely compressed and posterodorsally oriented, as in many titanosaurs, including *Andesaurus*, *Atsinganosaurus*, *Lirainosaurus* and *Normanniasaurus* (Díez Díaz et al., 2013b, 2018; Le Loeuff et al., 2013; Mannion & Calvo, 2011). It does not extend as far as the posterior margin of the non-condylar centrum. Weakly developed SPRLs define the anterolateral margins of the neural spine. The presence of weakly developed SPOLs can also be inferred, because there is a central depressed area on the posterior surface of the neural spine, between and above the postzygapophyseal surfaces, with raised margins laterally.

Posterior caudal vertebra. SZTFH Ob.3105 (Assemblage A) is an almost complete posterior caudal vertebra (Fig. 25). It has an aEI of 1.99. It is not possible to observe the internal tissue structure anatomy of this specimen. The centrum is spool-like, slightly opisthocoelous, with a poorly developed anterior condyle. A change in the type of articulation within the tail series is not uncommon within Titanosauria, especially in the posterior caudal vertebrae (e.g. *Opisthocoelicaudia*, *Bonitasaura* and *Rinconsaurus*; Borsuk-Białynicka, 1977; Calvo & González Riga, 2003; Gallina & Apesteguía, 2015; Pérez Moreno et al., 2022). The outline of both articular surfaces is slightly sub-quadrangular. No ridges or rugosities are present on the lateral surfaces of the centrum. The ventral surface is flat, and only the posterior articular facets for the chevrons can be seen. The neural arch is short, and is anteriorly placed on the centrum. Only the bases of the prezygapophyses are preserved, and the postzygapophyses are absent. Although not complete, the neural spine was originally anteroposteriorly long and dorsoventrally low. No laminae or fossae are present in this specimen.

Chevrons. LPB (FGGUB) R.2510 (Assemblage F) includes three fragments that come from a single chevron, missing its distal end (Fig. 26). The proximal articular surfaces cannot be assessed because of their poor preservation (Fig. 26C), but the chevron is clearly 'open' proximally (i.e. no bridge of bone links the left and right proximal articulations above the haemal canal), such that it is characterized by the typical open 'Y'-shaped morphology described by Otero et al. (2012, fig. 2), as is also the case in most macronarians (Calvo & Salgado, 1995; Upchurch, 1998). Although the chevron is slightly incomplete, the haemal canal was probably similar in length to the distal blade. Such a relatively deep haemal canal (i.e. at least 40% of total chevron length) is a derived state that occurs in most titanosauriforms (Curry Rogers, 2005; Wilson, 2002). A prominent ridge is present along most of the length of the lateral surface of each ramus (Fig. 26A, D): this starts close to the anterodorsal-most corner of the ramus and extends posteroventrally, forming the posterior margin of the ramus at its distal tip. A similar ridge has been identified on chevrons from the anterior–middle caudal vertebrae of several titanosaurs, including *Alamosaurus*, *Arrudatitan*, *Baurutitan*, *Epachthosaurus* and *Saltasaurus* (Poropat et al., 2016; Santucci & Arruda-Campos, 2011). It is clearly absent from the chevrons of some titanosaurs, including those of other European taxa (i.e. *Abditosaurus*, *Atsinganosaurus*, *Lirainosaurus*, *Lohuecotitan* and *Paludititan*), although it is not always present along all of the anterior–middle caudal series in taxa that possess this feature. Therefore, we consider this feature a 'local' autapomorphy of *Magyarosaurus*. It is possible that this ridge provides an attachment site for M. caudofemoralis longus (Díez Díaz et al., 2020; Otero & Vizcaíno, 2008; Wilhite, 2003). Distal to this ridge, each proximal ramus is transversely compressed. The preserved part of the distal blade has a subtriangular horizontal cross-section, with a prominent posterior midline ridge that forms the apex of this triangle, as well as a less well-developed, broader and flatter anterior counterpart. There are no ridges on the lateral surface of the distal blade.

LPB (FGGUB) R.0076 (Fig. 26G–I) (Individual E) preserves the proximal part of a ramus of a chevron, probably also from the anterior region of the tail. The proximal articular surface is too poorly preserved to fully determine its morphology, but it is clearly anteroposteriorly convex and lacks a transverse groove. The absence of this groove distinguishes the chevrons of *Magyarosaurus* from those of some aeolosaurines (Powell, 2003; Santucci & Arruda-Campos, 2011), *Epachthosaurus* (Poropat et al., 2016), members of Lognkosauria (González Riga et al., 2018), as well as both *Lohuecotitan* (Díez Díaz et al., 2016) and *Paludititan* (see below). The posterior margin of the proximal articulation forms a small 'hook'-like process that overhangs the posterior surface of the ramus. A broadly comparable feature has otherwise only been observed in the non-titanosaurian titanosauriforms *Cedarosaurus* (DMNH 39045: PDM pers. obs. 2008) and *Gobititan* (IVPP 12579: PDM and PU pers. obs. 2007) and, as such, is regarded as a potential local autapomorphy of *Magyarosaurus*. Despite its incomplete state, it seems unlikely that the chevron was 'closed' proximally by a bridge of bone above the haemal canal. There is no posteroventrally oriented ridge on the lateral surface of LPB (FGGUB) R.0076, such as that seen in LPB (FGGUB) R.2510, but this could be because only the proximal-most portion of the ramus is preserved, or might reflect serial variation given that this feature is

often absent in the anterior-most chevrons of those titanosaurs that otherwise display it.

Humerus. LPB (FGGUB) R.1047 (Fig. 27A–F) (left element, Individual E) and R.2506 (Fig. 27G–L) (right element, Assemblage F) are virtually complete and well-preserved humeri, with the former approximately 25% longer than the latter. LPB (FGGUB) R.1047 is abraded at its articular ends, and the tip of the deltopectoral crest is damaged. SZTFH Ob.3089 (Fig. 27M–P) (Assemblage A) is a left humerus that is incomplete proximally and distally.

The *Magyarosaurus* humerus has a mediolaterally constricted shaft and articular ends that are markedly expanded relative to the shaft. The robusticity index (RI) is approximately 0.28–0.30. There is a small degree of torsion between the proximal and distal ends. The proximal end is approximately 22% wider transversely than the distal one, and is more than twice as wide as the midshaft. As is the case in nearly all titanosauriforms (Poropat et al., 2016), most of this proximal expansion occurs along the medial margin, with little expansion of the lateral margin relative to the shaft. The expansion of the proximal end gives the humerus a proximal width index (PWI) of 0.33–0.44. As such, the proximal end of the humerus does not conform to those of titanosaur taxa typically regarded as having more gracile humeri, such as *Isisaurus* (PWI = 0.31; Jain & Bandyopadhyay, 1997), nor to those that have extremely robust humeri, e.g. *Neuquensaurus* (PWI = 0.48; Otero, 2010) and *Opisthocoelicaudia* (PWI = 0.51; Borsuk-Białynicka, 1977). Instead, in this respect, the proximal end is more similar to those found in taxa such as *Futalognkosaurus* (PWI = 0.38; González Riga et al., 2016) and *Lirainosaurus* (PWI = 0.39; Díez Díaz et al., 2013a).

In anterior view, the profile of the proximal end is slightly sinusoidal, with this feature being most noticeable in LPB (FGGUB) R.2506 (Fig. 27G). This condition is similar to that in titanosaur taxa such as *Mansourasaurus* (Sallam et al., 2018), *Opisthocoelicaudia* (Borsuk-Białynicka, 1977), and *Saltasaurus* (Powell, 1992), but contrasts with the convex or straight margin that characterizes most sauropods (González Riga, 2003; Upchurch, 1998), including *Ampelosaurus* (Le Loeuff, 2005b) and *Lirainosaurus* (Díez Díaz et al., 2013a). The proximolateral corner of the humerus has a 'squared' morphology in anterior/posterior view, as is the case in nearly all somphospondylans (Carballido et al., 2012; Wilson, 2002). By contrast, the proximal and medial surfaces converge to form an acute, triangular projection, similar to those observed in *Angolatitan*, *Mendozasaurus*, and *Paralatitan* (González Riga et al., 2018; Mateus et al., 2011; Smith et al., 2001).

In *Magyarosaurus*, the humeral head is situated closer to the medial margin than the lateral one, and it is strongly expanded posteriorly. A marked posterior prominence characterizes the humeral head of most neosauropods, although it is absent in many titanosaurs and close relatives, including *Alamosaurus*, *Diamantinasaurus*, *Jainosaurus*, *Rapetosaurus* and saltasaurines (Bonaparte et al., 2006; Curry Rogers, 2009; Mannion, Upchurch, Jin, et al., 2019; Poropat et al., 2016; Smith et al., 2001; Upchurch et al., 2015). A steeply oriented ridge extends distally and slightly laterally from the humeral head along the posterior surface, fading out at approximately the level of the deltopectoral crest. The posterior surface of the proximal end of the humerus is transversely convex medial to this ridge, and concave lateral to it. This prominent ridge is not present in other titanosaurs or close relatives, e.g. *Diamantinasaurus*, *Mansourasaurus*, *Rapetosaurus* and *Saltasaurus* (Curry Rogers, 2009; Poropat, Upchurch, et al., 2015; Powell, 2003; Sallam et al., 2018), including European taxa that have well-preserved humeri, i.e. *Ampelosaurus*, *Atsinganosaurus*, *Garrigatitan* and *Lirainosaurus* (Díez Díaz et al., 2013a, 2018, 2021; Le Loeuff, 2005b). Therefore, this ridge is regarded as an autapomorphy of *Magyarosaurus*.

The anterior surface of the proximal third of the humerus is concave, with the coracobrachialis fossa bounded laterally by the deltopectoral crest. The humerus of *Magyarosaurus* displays an autapomorphic morphology in this region, with the coracobrachialis fossa divided into a small, shallow dorsomedial region and a larger, deeper ventrolateral region by an obliquely curved, stepped ridge. Such division of this fossa is not present in other titanosaurs, including European taxa with well-preserved humeri (Díez Díaz et al., 2013a, 2018, 2021; Le Loeuff, 2005b). Given that no other tuberosities or distinct rugosities are present in this area, it is possible that this ridge served as the insertion site for M. coracobrachialis. Distally, the coracobrachialis fossa is demarcated by a curved ridge.

The deltopectoral crest is anteromedially deflected, slightly overhanging the anterior concavity. It is similarly oriented in most titanosauriforms, including *Abditosaurus*, *Atsinganosaurus* and *Lirainosaurus* (Díez Díaz et al., 2013a, 2018; Vila et al., 2022), although it projects mainly anteriorly in saltasaurines, *Diamantinasaurus*, *Mansourasaurus* and Rinconsauria (Mannion et al., 2013; Poropat et al., 2016; Sallam et al., 2018). The most prominent part of the deltopectoral crest is missing in most *Magyarosaurus* specimens, with the exception of LPB (FGGUB) R.2506 (Fig. 27I).

In this specimen, the crest widens transversely towards its distal end. This approximate doubling in width is a feature of most saltasaurids, as well as some members of Lognkosauria and Rinconsauria (González Riga et al., 2018; Poropat et al., 2016; Wilson, 2002), and it also characterizes *Ampelosaurus*, *Atsinganosaurus* and *Lirainosaurus* (Le Loeuff, 2005b; Díez Díaz et al., 2013a, 2018). The deltopectoral crest terminates well above the midlength of the humerus in *Magyarosaurus*.

The lateral surface of the deltopectoral crest is rugose, becoming heavily striated distally, at least in LPB (FGGUB) R.2506, which could indicate the insertion area for M. deltoideus clavicularis and/or M. pectoralis (Otero, 2018; Voegele et al., 2020). A short vertical ridge extends from the proximal end of the humerus along the lateral margin of the posterior surface. Such a ridge is present in some other titanosaur taxa (e.g. *Diamantinasaurus*, *Epachthosaurus*, *Rapetosaurus* and *Saltasaurus*; Poropat et al., 2016). At the approximate level of the most prominent portion of the deltopectoral crest, there is a well-developed bulge on the lateral margin of the posterior surface that is visible in anterior view. This characterizes nearly all titanosaurs (Mannion, Upchurch, Schwarz, et al., 2019) and probably represents the insertion site for M. scapulohumeralis anterior (Borsuk-Białynicka, 1977; Upchurch et al., 2015; Voegele et al., 2020) or possibly M. deltoideus clavicularis (Otero, 2018). There is a further prominence approximately equidistant from the medial and lateral margins of the posterior surface, level with the distal tip of the deltopectoral crest. This presumably represents the insertion site for M. latissimus dorsi, which characterizes several other titanosaurs, namely *Alamosaurus*, *Opisthocoelicaudia*, *Patagotitan*, *Rukwatitan* and saltasaurines (Borsuk-Białynicka, 1977; Carballido et al., 2017; D'Emic, 2012; Gorscak et al., 2014; Otero, 2010; Voegele et al., 2020), as well as the European taxa *Atsinganosaurus*, *Garrigatitan* and *Lirainosaurus* (Díez Díaz et al., 2013a, 2018, 2021). However, only in *Garrigatitan* and *Lirainosaurus* is it also situated closer to the midline than the lateral margin (VDD pers. obs.), and in those two it is a hypertrophied longitudinal bulge and a subtly expressed ridge, respectively: thus, the shape, development, and central position of this feature is regarded as an autapomorphy of *Magyarosaurus*. In the humeri referred to *Magyarosaurus*, this prominence is confluent with the distal-most part of the subvertical posterior ridge that extends from the humeral head.

Distal to the base of the deltopectoral crest, the humerus constricts markedly into an anteroposteriorly compressed oval shaft (the eccentricity index [ECC] ranges from 1.26 to 1.44). The anterior surface of the shaft is relatively flat, whereas the posterior one is transversely convex, and these surfaces slightly converge medially to form a rounded but angular medial margin. In anterior/posterior view, the medial margin of the shaft is strongly concave. By contrast, the lateral margin is only slightly concave, or nearly straight, giving the humerus a canted aspect, resembling the morphology in most titanosaurs, including *Ampelosaurus*, *Atsinganosaurus* and *Lirainosaurus* (Le Loeuff, 2005b; Díez Díaz et al., 2013a, 2018).

The shaft expands gradually transversely as it approaches the distal end of the humerus. Its degree of expansion is moderate, as expressed by a distal width index (DWI) of 0.31–0.36, similar to that reported in *Ampelosaurus* (DWI = 0.33), *Mendozasaurus* (DWI = 0.31), *Isisaurus* (DWI = 0.30) and *Lirainosaurus* (DWI = *c*. 0.30) (González Riga, 2003; Le Loeuff, 2005b; (Díez Díaz et al., 2013a; Wilson et al., 2009). The distal articular condyles extend to some degree onto the anterior surface of the humerus, which is a feature primarily restricted to taxa close to or within Saltasauridae, including *Alamosaurus*, *Opisthocoelicaudia* and saltasaurines (Wilson, 2002). As is also the case in nearly all titanosaurs (D'Emic, 2012), the anterior surface of the distal lateral condyle of the *Magyarosaurus* humerus is undivided. On the anterior surface, the distal condyles are separated by an intercondylar groove that deepens laterally. The medial part of this intercondylar groove is rugose. The lateral surface of the lateral condyle is excavated by a longitudinal depression that faces anterolaterally, such that this region is divided into an anteriorly projecting lateral distal condyle, and a laterally projecting ectepicondyle. The ectepicondyle is wide and rounded, with a flattened, scarred, anterolaterally facing surface. In most preserved *Magyarosaurus* humeri, the lateral surface of the distal end is slightly abraded; nevertheless, a distinct, elongated and rugose anterolateral surface can be discerned.

The distal condyles are shallowly but clearly divided from one another along the distal surface, at least in LPB (FGGUB) R.1047, such that the distal margin of the humerus is concave in anterior/posterior view. This is a feature that is otherwise known only in *Abditosaurus*, *Alamosaurus*, *Lirainosaurus*, *Opisthocoelicaudia* and saltasaurines (Díez Díaz et al., 2013a; Vila et al., 2022; Wilson, 2002), as well as possibly *Paralititan* (Smith et al., 2001, fig. 2). In distal end view, these condyles are oval to subquadrangular in outline, with anteromedially to posterolaterally oriented long axes. The medial condyle is somewhat smaller, but more distally projected, compared to its lateral counterpart. Such bevelling of the distal end is also present in several other titanosaurs, including saltasaurines and some members of Lognkosauria (Mannion, Upchurch,

Jin, et al., 2019), as well as *Lirainosaurus* (Díez Díaz et al., 2013a, fig. 3b), *Mansourasaurus* (Sallam et al., 2018, fig. 2), and *Rukwatitan* (Gorscak et al., 2014, fig. 10). On the posterior surface of the distal end of the *Magyarosaurus* humerus, the olecranon (= supracondylar or anconeal) fossa is wide and deep, bordered by well-developed supracondylar crests, as is the case in most titanosaurs (Upchurch et al., 2004, 2015). The medial supracondylar crest is more acute, and has a slightly depressed posteromedial flattened surface. The proximal portion of this shallowly depressed area, as well as the medial surface of the medial supracondylar crest, is rugose.

Ulna. The left ulna belonging to Assemblage A (SZTFH Ob.3100), the only such element known for *Magyarosaurus*, is essentially complete in terms of its length, but there is material missing from the proximal end, as well as a small anterior portion of the distal one (Fig. 28). Despite its incomplete nature, the ulna is clearly gracile, with an estimated maximum proximal mediolateral width to ulna length ratio of less than 0.3. As such, it differs notably from the robust ulnae of many titanosaurs (e.g. *Diamantinasaurus*, *Epachthosaurus*, *Lirainosaurus*, *Opisthocoelicaudia* and *Saltasaurus*), in which this ratio equals or exceeds 0.4 (Curry Rogers, 2005; Mannion et al., 2013; Wilson, 2002). In the *Magyarosaurus* ulna, the near-complete anterolateral proximal process is short, whereas the incomplete anteromedial process was clearly much longer. The posterior process is prominent and of comparable size to the anterolateral one, as is the case in most titanosaurs (Upchurch et al., 2015; Poropat et al., 2016), including *Lirainosaurus* and *Lohuecotitan* (Díez Díaz et al., 2013a, 2016). Relative to the long axis of the anterolateral process, the posterior process is deflected posterolaterally. The proximal surface is mostly incomplete, except for the anterolateral process, and this missing material might have exaggerated the apparent prominence of the olecranon process.

The anterior surface (radial fossa) is the most strongly concave of the surfaces of the proximal third of the ulna, but the anterolateral and posterior surfaces are also transversely concave. The anteromedial process is supported by a ridge that extends distally for most of the length of the ulna. This anteromedial ridge appears to bifurcate at approximately midlength of the ulna, or this could be interpreted as the development of a second ridge at this point. This results in a more posteriorly placed ridge forming the anteromedial margin of the shaft, and an anterior ridge that is deflected laterally and terminates a short distance from the distal end. Following Otero (2018) and Voegele et al. (2020), we interpret this anterior lateral (interosseous) ridge to be the origin of *M. pronator quadratus* that in life would be connected by ligaments to a similar structure on the radius. The distal end of this interosseous ridge lies almost equidistant from the medial and lateral margins of the ulna. Although the presence of an interosseous ridge on the ulna is typical for virtually all sauropods, its slanting orientation in *Magyarosaurus* appears to be unique, given that this ridge typically follows the long axis of the shaft in other taxa; consequently, we regard this as an autapomorphy of *Magyarosaurus*.

The distal end of the ulna expands posteriorly. In *Malawisaurus* and some saltasaurids (and closely related taxa), the ulna lacks such a distal expansion (D'Emic, 2012), but *Magyarosaurus* shares a distally expanded ulna with the majority of titanosaurs, including taxa such as *Lirainosaurus* (Díez Díaz et al., 2013a), *Opisthocoelicaudia* (Borsuk-Białynicka, 1977), and *Mendozasaurus* (Poropat et al., 2016; González Riga et al., 2018). In *Magyarosaurus*, the distal end of the ulna has an oval outline, but it is possible that it was 'comma'-shaped, with an anterior process that has not been preserved. The morphology of the distal ulna generally resembles those of *Diamantinasaurus*, *Neuquensaurus*, *Rapetosaurus*, and *Lirainosaurus* (Curry Rogers, 2009, fig. 38E; Díez Díaz et al., 2013a, fig. 3.5-6; Otero, 2010, fig. 4; Poropat, Upchurch, et al., 2015, fig. 11H), but it is less transversely compressed than those of some specimens referred to *Ampelosaurus* (e.g. MDE C3-1296; Le Loeuff, 2005b, fig. 4.15a-b), *Atsinganosaurus* (Díez Díaz et al., 2018, fig. 10L–P), *Garrigatitan* (Díez Díaz et al., 2021, fig. 8), and *Lohuecotitan* (Díez Díaz et al., 2016, fig. 5B).

Radius. The best-preserved radii are LPB (FGGUB) R.1049 and R.1060 (Fig. 29A–F), which are portions of a single left radius from Individual E, and SZTFH Ob.3101, which is a left radius from Assemblage A (Fig. 29G–L). LPB (FGGUB) R.1049 comprises the proximal two-thirds (in two pieces), whereas LPB (FGGUB) R.1060 preserves the distal end. There is a small amount of material missing in between these segments, and the posterior surface is poorly preserved throughout much of the element's length. However, SZTFH Ob.3101 is fairly complete, only missing small fragments close to the distal edge, and the lateral border of the proximal end.

The radius to humerus length ratio varies from *c*. 0.65 (Individual E) to *c*. 0.72 (Assemblage A). The ratio of Individual E lies within the typical titanosaur range (Mannion et al., 2013; Mannion, Upchurch, Schwarz, et al., 2019), whereas that of Assemblage A is slightly higher. However, it is important to note that the elements from Assemblage A might not be from the same individual. There is a strong degree of torsion

between the proximal and distal ends of the radius, accentuated by the prominent interosseus ridge (see below), such that their long axes are approximately 45° to one another. A similarly twisted radius also characterizes several other titanosaurs, including *Epachthosaurus*, *Malawisaurus*, *Rapetosaurus*, *Savannasaurus* and *Uberabatitan* (Silva Junior et al., 2019; Mannion et al., 2013; Poropat et al., 2016), whereas the shaft is much straighter in most other taxa, including the only other European taxon with a sufficiently well-preserved radius, *Ampelosaurus* (Le Loeuff, 2005b). The proximal articular surface is slightly deformed in LPB (FGGUB) R.1049 (Fig. 29D), but has a 'comma'-shaped outline, with a prominent medial process that is anteroposteriorly narrower than the remainder of the proximal end, as is also the case in nearly all titanosauriforms (Poropat et al., 2016; Upchurch et al., 2015). This also appears to be the case in SZTFH Ob.3101, although the lateral portion is incomplete (Fig. 29G). It is not possible to determine whether a medial ridge for attachment of the combined M. biceps brachii and M. brachialis inferior (see Otero, 2018; Upchurch et al., 2015; Voegele et al., 2020) is present along the proximal quarter of the shaft.

A proximodistally oriented interosseus ridge is present on the posterolateral surface and extends for most of the radius length (though note that preservation is poor at its proximal part and along the distal third of the radius in LPB [FGGUB] R.1049), as is the case in all titanosaurs (Curry Rogers, 2005), as well as in several non-titanosaurian titanosauriform taxa (Mannion et al., 2013). As preserved, this ridge remains largely on the posterolateral margin throughout the length of the radius, despite the torsion between the proximal and distal ends. This ridge marks the probable insertion of M. pronator quadratus (Otero, 2018; Voegele et al., 2020). In the radius of Individual E, a subtle, vertical ridge is also present on the posterior surface, close to the medial margin, extending along the middle third of the shaft. This ridge appears to be absent in SZTFH Ob.3101. The posterolateral margin of the midshaft also forms a ridge in both radii.

The lateral two-thirds of the distal end surface are strongly bevelled (approximately 30°) relative to a plane perpendicular to the proximodistal axis of the radius. Comparable bevelling characterizes the radius of nearly all titanosaurs, although in saltasaurines and *Argyrosaurus* this extends across the entire distal surface (Mannion & Otero, 2012; Poropat et al., 2016; Wilson, 2002). The posterior surface of the distal end is gently concave, forming a fossa between two subtle condyles. This morphology characterizes most neosauropods, but is lost in some titanosaurs, including *Malawisaurus*, *Opisthocoelicaudia*, and saltasaurines (Upchurch et al., 2015). In distal end view, the *Magyarosaurus* radius has a flat anterior margin and the lateral half is notably wider anteroposteriorly than the medial half (Fig. 29B), especially when compared to the radius of *Abditosaurus* (Vila et al., 2022). This feature is a local autapomorphy of *Magyarosaurus* that also occurs in *Neuquensaurus* (Upchurch et al., 2015, fig. 9P).

Metacarpals. Several fragments of metacarpals are preserved as part of Individual E (Fig. 30), and there is one metacarpal from each of Assemblage A and F (Fig. 31), although their incomplete nature makes their identification difficult.

LPB (FGGUB) R.0074 (Individual E) is the distal end of a metacarpal (Fig. 30A–E). In distal view, it has a transversely elongated elliptical or 'D'-shaped outline, with a mildly concave ventral margin. The distal articular surface does not extend onto the dorsal surface of the metacarpal.

LPB (FGGUB) R.1864 (Individual E) is the proximal end of a possible metacarpal III (Fig. 30F–K). It has a subtriangular outline in proximal view, although the cross-section of the shaft becomes elliptical a short distance from this end.

LPB (FGGUB) R.1053 (Individual E) is another distal end of a metacarpal (Fig. 30L–P). It is poorly preserved, with some incomplete margins, but probably represents a left metacarpal IV. It has a transversely elongate trapezoidal outline in distal view, with a dorsal margin that is wider than the ventral one. The latter margin is mildly concave along its midline. One of the distal condyles of LPB (FGGUB) R.1053 is incomplete, but its lateral margin appears to be straight, whereas the other margin clearly slopes to face partly ventrally, forming a ventromedial ridge.

LPB (FGGUB) R.1862 (Individual E) is the distal end of a metacarpal (Fig. 30Q–V). It has a trapezoidal outline in distal view, with a dorsal margin that is slightly wider transversely than the ventral one. Such a morphology characterizes the distal end of metacarpal IV in many titanosaurs, e.g. *Diamantinasaurus*, *Epachthosaurus*, *Rapetosaurus* and *Saltasaurus* (Poropat et al., 2016), and thus we tentatively identify LPB (FGGUB) R.1862 as such. One of this specimen's distal condyles (probably the medial) is slightly taller dorsoventrally than the other. This taller margin is deflected such that it partly faces ventrally. The distal articular surface is convex dorsoventrally, but it does not extend onto the dorsal surface of the metacarpal. This restriction of the distal articulation is consistent with the derived condition in nearly all titanosauriforms (D'Emic, 2012; Salgado et al., 1997).

LPB (FGGUB) R.0077 (Individual E) consists of the proximal end of a right metacarpal V (Fig. 30W-A'). In proximal view, it has a dorsoventrally tall, subtriangular outline that is more widely rounded ventrally, with only one long and flat articular surface (the latter presumably for metacarpal IV).

SZTFH Ob.3096 (Assemblage A) consists of the distal half of a metacarpal (Fig. 31A–D). The bevelling of the distal articular end is similar to that present in LPB (FGGUB) R.0074, although the outline of the distal articular surface is different. The cross-section of the shaft of SZTFH Ob.3096 is sub-circular. We are unable to identify where LPB (FGGUB) R.0074 and SZTFH Ob.3096 belong in the metacarpus.

LPB (FGGUB) R.2509 (Assemblage F) lacks both its proximal and distal ends, limiting its identification and interpretation (Fig. 31E–F). The preserved proximal and distal parts are twisted relative to one another. A ridge is present on the ventral surface, close to the midline of the distal (?) portion. The medial and lateral margins of the shaft are mostly straight in dorsal view.

Femur. Assemblage A preserves a partial left femur (SZTFH Ob.3088; Fig. 32A–C). The proximal end is missing, and the distal articulation is damaged. Individual E preserves a pair of complete femora (left, LPB [FGGUB] R.1046 [Fig. 32D–I] and right, LPB [FGGUB] R.1992 [Fig. 32J–M]), and Assemblage F includes two right femora (LPB [FGGUB] R.2507 [Fig. 32O–T] and R.2508 [Fig. 32U–V]). The proximal end of LPB (FGGUB) R.2508 is missing, and the distal condyles are eroded, whereas LPB (FGGUB) R.2507 is largely complete.

Based on Individual E, the humerus to femur length ratio for *Magyarosaurus* is 0.8. This ratio is similar to that of the titanosaurs *Diamantinasaurus* (0.79; Poropat, Upchurch, et al., 2015), *Futalognkosaurus* (0.79; Calvo, 2014), and *Rapetosaurus* (0.80; Curry Rogers, 2009), whereas other titanosaurs for which this can be assessed have notably lower (*Opisthocoelicaudia* = 0.72 [Borsuk-Białynicka, 1977]; *Jainosaurus* = 0.74 [Wilson et al., 2011]) or higher values (*Dreadnoughtus* = 0.84 [Lacovara et al., 2014]; *Epachthosaurus* = 0.88 [UNPSJB-PV 920; PDM and PU pers. obs., 2013]).

The femoral head projects primarily medially, such that it is approximately perpendicular to the long axis of the shaft. This is the plesiomorphic eusauropod condition, that also characterizes some titanosaurs (Curry Rogers, 2005; Upchurch et al., 2004), including *Ampelosaurus* (Le Loeuff, 2005b), *Diamantinasaurus* (Poropat, Upchurch, et al., 2015), *Lohuecotitan* (Díez Díaz et al., 2016), and *Mendozasaurus* (González Riga et al., 2018). By contrast, most titanosaurs, including *Lirainosaurus* (Díez Díaz et al., 2013a), *Opisthocoelicaudia* (Borsuk-Białynicka, 1977), *Patagotitan* (Carballido et al., 2017), and saltasaurines (Curry Rogers, 2005), have a more dorsally directed femoral head that is separated from the poorly developed greater trochanter by a shallow sulcus on the proximal surface. Proximally, the lateral margin of the *Magyarosaurus* femur is medially deflected, and there is a well-developed and robust lateral bulge (although these two features are less developed in the Assemblage F specimens [Fig. 31O–V]). The lateral bulge of *Magyarosaurus* is similar to that of the femoral fragment referred to *Abditosaurus* (Vila et al., 2022), and is more prominent than in *Ampelosaurus*, *Lirainosaurus*, and *Lohuecotitan* (Díez Díaz et al., 2013a, 2016; Le Loeuff, 2005b). As in all titanosaurs (Díez Díaz et al., 2013a; Mannion et al., 2013; Otero, 2010), the femur of *Magyarosaurus* is characterized by a trochanteric shelf located on the proximal third of the lateral portion of the posterior surface, commencing below the greater trochanter. This mediolaterally wide, but shallow shelf disappears at the same level as the proximal tip of the fourth trochanter. The latter process is a well-developed, mediolaterally expanded, longitudinal ridge located on the posterior surface of the shaft, close to the medial margin. Its prominence distinguishes it from the barely discernible fourth trochanters of saltasaurines (Mannion, Upchurch, Jin, et al., 2019; Otero, 2010) and *Atsinganosaurus* (Díez Díaz et al., 2018). The distal end of the fourth trochanter of the *Magyarosaurus* femur does not extend as far as the femoral midlength. The medial surface of the femur, level with the fourth trochanter, is rugose, probably for the insertion of M. caudofemoralis longus (Díez Díaz et al., 2020; Ibiricu et al., 2013).

The femoral shaft is mostly straight, with little curvature. The anterior surface of the shaft is mildly convex transversely, whereas the posterior one is flat. This anterior convexity is primarily generated by a faint, longitudinal linea intermuscularis cranialis, which fades out towards the distal end of the shaft. This feature is most marked in the middle section of the shaft of LPB (FGGUB) R.2507. Such a crest is absent in most sauropods, but is present in several titanosaurs, including *Alamosaurus* (D'Emic, 2012), diamantinasaurians (Hocknull et al., 2021; Poropat, Upchurch, et al., 2015), *Lohuecotitan* (Díez Díaz et al., 2016), *Pellegrinisaurus* (Cerda et al., 2021), saltasaurines (Otero, 2010), and *Uberabatitan* (Silva Junior et al., 2019). Although often a subtle feature, it is clearly absent in most other titanosaurs (Mannion, Upchurch, Schwarz, et al., 2019; Poropat et al., 2016), including *Atsinganosaurus* and *Lirainosaurus* (Díez Díaz et al., 2013a, 2018). The *Magyarosaurus* femoral shaft is only slightly

anteroposteriorly compressed at midlength, with a subcircular cross-section (the ECC value ranges from 1.14 to 1.4). This midshaft eccentricity value is notably lower than that in all other macronarians (Mannion et al., 2013; Wilson & Sereno, 1998), including penecontemporaneous European taxa that preserve femora, i.e. *Garrigatitan* (1.5), *Lohuecotitan* (1.6), *Paludititan* (>1.7, although the femoral fragment is close to the distal end), *Abditosaurus* (>1.85), and especially *Ampelosaurus* (>2.0), *Lirainosaurus* (mean average of 2.2), and *Atsinganosaurus* (2.6) (Díez Díaz et al., 2013a, 2016, 2018, 2021; Le Loeuff, 2005b; Vila et al., 2022). As such, we regard a subcircular femoral midshaft as an autapomorphy of *Magyarosaurus*.

The posterior surface of the distal condyles is damaged in the available specimens. The distal condyles are proximomedially bevelled, such that the fibular condyle extends further distally than the tibial one (Fig. 32E, I, P, T), a derived state that characterizes most titanosaurs (Wilson, 2002). Intercondylar fossae separate the tibial and fibular condyles on both the anterior and posterior surfaces, continuous with the deep and wide intercondylar groove on the distal articular surface itself. A shallower sulcus is present between the main fibular condyle and the posterolaterally oriented fibular epicondyle, as is the case in nearly all eusauropods, with the exception of saltasaurines (Beeston et al., 2024; Carballido et al., 2017). The tibial condyle is transversely narrower than the fibular condyle (tibial to fibular condyle width ratio ranges from 0.78 to 0.96), similar to other titanosaurs, including *Lirainosaurus*, *Lohuecotitan*, and some femora ascribed to *Ampelosaurus*, in which this ratio is ≤0.8 (Poropat et al., 2016; this study). In *Magyarosaurus*, the long axis of each distal condyle is anteroposteriorly oriented, and the articulations do not curve noticeably onto the anterior surface. The latter feature contrasts with the condition in saltasaurines, *Alamosaurus*, *Opisthocoelicaudia* and *Lirainosaurus* (Díez Díaz et al., 2013a; Wilson, 2002).

Tibia. The only specimen known to document this skeletal element in *Magyarosaurus*, LPB (FGGUB) R.2299 (belonging to Individual E), comprises the poorly preserved proximal ends of a left tibia and fibula in semi-articulation, which are obscured by matrix in places (Fig. 33). However, this specimen is important in that it demonstrates clear anatomical differences with NHMUK R.3853, i.e. the paralectotype of '*Magyarosaurus*' *hungaricus* (see below). By contrast with the latter species, the long axis of the proximal articular surface of the *Magyarosaurus dacus* tibia is oriented mediolaterally (Fig. 33A), and the cnemial crest projects laterally, roughly aligned with this long axis (Fig. 33C). The proximal end of the tibia has an approximately 'D'-shaped outline, with a flat and transversely wider posterior margin (Fig. 33A), similar to that of many titanosaurs, including *Abditosaurus* (Vila et al., 2022). It differs from the transversely compressed proximal tibiae of *Atsinganosaurus* and *Lirainosaurus* (Díez Díaz et al., 2013a, 2018), as well as the subcircular morphology of the proximal end that characterizes *Ampelosaurus* and *Lohuecotitan* (Díez Díaz et al., 2016; Le Loeuff, 2005b).

Fibula. Three left fibulae are represented within Assemblage A (two registered under SZTFH Ob.3086, and Ob.3102). SZTFH Ob.3086a (Fig. 34A–E) lacks the distal end, but otherwise is nearly complete. SZTFH Ob.3086b (Fig. 34F–K) is largely complete, although the proximal and distal ends are poorly preserved. SZTFH Ob.3102 (Fig. 34L–O) lacks the proximal end and its distal-most tip. As noted above, Individual E includes the poorly preserved proximal end of a left fibula (LPB [FGGUB] R.2299) (Fig. 33D, E).

In lateral view, the shaft of SZTFH Ob.3086a is sigmoidal (Fig. 34A), whereas it is straighter in SZTFH Ob.3086b and Ob.3102 (Fig. 34F, L). Otherwise, the fibulae are broadly comparable in shape. There is clear torsion of approximately 20° between the long axes of the proximal and distal ends. In general, the lateral surface is anteroposteriorly convex, whereas the medial surface is flat, giving the fibula a D-shaped cross-section throughout most of its length. In lateral view, the proximal end is anteroposteriorly expanded relative to the shaft, with this expansion primarily occurring along the posterior margin.

At the proximal end, the fibula has an anteroposteriorly elongate comma-shaped profile, narrowing anteriorly (Fig. 34C, H). The proximal articular surface is mildly bevelled along its anterior half, such that it faces slightly anteriorly. The posterior margin of the proximal half forms a ridge that broadens towards its distal end. Although slightly incomplete, an anteromedial proximal process is clearly present in SZTFH Ob.3086a and b (and probably also LPB [FGGUB] R.2299). Such a process characterizes nearly all somphospondylans (D'Emic, 2012; Mannion et al., 2013; Wilson & Upchurch, 2003). There is no anterolateral trochanter, such as that present in *Jainosaurus* (Wilson et al., 2009), *Laplatasaurus* (Gallina & Otero, 2015), *Lohuecotitan* (Díez Díaz et al., 2016), *Mendozasaurus* (González Riga, 2003), and *Uberabatitan* (Salgado & Carvalho, 2008). There is a break of slope on the lateral surface of SZTFH Ob.3086a and Ob.3102, close to the anterior margin, just posterior to the distal portion of the anteromedial projection. The medial surface of the proximal end of the fibula is only subtly striated and is not

raised, as is also the case in most titanosauriforms (D'Emic, 2012).

Although none of the fibulae preserve their entire length, the lateral trochanter almost certainly did not extend to midlength of the shaft. This trochanter is composed of a prominent, proximodistally elongate, posterior ridge (less well developed in SZTFH Ob.3102), and a shorter, less prominent anterior ridge. There is a striated, gentle concavity in between these two ridges. A similar morphology characterizes most titanosaurs (Upchurch, 1998), including *Epachthosaurus* (Martínez et al., 2004), *Lohuecotitan* (Díez Díaz et al., 2016), *Opisthocoelicaudia* (Borsuk-Białynicka, 1977), and *Saltasaurus* (Powell, 1992). By contrast, there is a single oval trochanter in a small number of titanosaurs, including *Dreadnoughtus* (Ullmann & Lacovara, 2016) and *Jainosaurus* (Wilson et al., 2009). A subtle ridge is present on the anterior margin of the lateral surface of the fibula of *Magyarosaurus*, with its proximal tip situated at approximately the level of the distal end of the lateral trochanter. This ridge is directed steeply posterodistally, and it fades out before it reaches the distal-most preserved portions of the fibula. It is absent in other titanosaurs, including European taxa with well-preserved fibulae, i.e. *Abditosaurus* (Vila et al., 2022), *Ampelosaurus* (VDD pers. obs., 2024), *Lirainosaurus* (Díez Díaz et al., 2013a), and *Lohuecotitan* (VDD pers. obs., 2014). As such, we regard this ridge as an autapomorphy of *Magyarosaurus*. The anterior margin of the distal third of the shaft, as preserved, forms a ridge. Distally, the fibula expands anteroposteriorly. In distal view, the fibula has a tear-drop-shaped outline, with a flat medial surface and an acute anterior edge (Fig. 34J).

Titanosauria Bonaparte & Coria, 1993
Lithostrotia Upchurch, Barrett & Dodson, 2004
Eutitanosauria Sanz, Powell, Le Loeuff, Martínez & Pereda Suberbiola, 1999
Petrustitan n. gen.
(Figs. 35–40)

Type species. *Petrustitan hungaricus* (Huene, 1932) n. comb. (see below).

Etymology. The genus name, which translates roughly as 'stone titan', derives from the Greek words pétra (πετρα), meaning 'stone, rock', alluding both to the place of its type locality, Sânpetru (a shorthand for Saint Peter, in Romanian) village in the central Hațeg Basin (Fig. 3), as well as to the origin of the holotype, coming from the rocky outcrops of the Sînpetru Formation exposed in this area, and the Greek word 'titan', a term often used to name titanosaurian sauropods.

Generic diagnosis. As for the type (and only known) species.

Petrustitan hungaricus (Huene, 1932) n. comb.
1932 *Magyarosaurus hungaricus*; Huene: 269
1970 *Titanosaurus hungaricus*: Steel: 77

Lectotype and paralectotype. NHMUK R.3853, Individual B: associated left fibula (holotype) and tibia (paratype).

Comment. Although not formally designating a holotype, Huene (1932, p. 269) referred only one specimen, an almost completely preserved fibula (NHMUK R.3853), to his new taxon '*Magyarosaurus*' *hungaricus*. Moreover, he briefly described this specimen (albeit incorrectly citing it as Brit. Mus. N. H. No. 3833 in the text as well as in the caption to his plate 47), and briefly compared it to other titanosaur fibulae: thus, this specimen is here chosen as the lectotype of *Petrustitan hungaricus* (Huene, 1932) n. comb. The left fibula NHMUK R.3853 described by Huene can be positively identified based on its figure (Huene, 1932, pl. 47, fig. 1a–c) and his comment that it has the same number as one of the other titanosaur specimens from Transylvania: the paralectotype left tibia NHMUK R.3853 (also briefly described and figured as Brit. Mus. N. H. R. 3853 by Huene, 1932, pp. 273–274, pl. 48, fig. 3a–c). As we argued above, these two elements were almost certainly found associated and belong to the same individual, identified here as Individual B.

Type locality. Sibișel River Valley, south of Sânpetru locality, central Hațeg Basin, Hunedoara County, Romania (Fig. 1E). More precise locality information is unavailable.

Type stratum and age. The holotype comes from the stratotype section of the uppermost Cretaceous continental Sînpetru Formation. The age of this succession was estimated to the early to late Maastrichtian (Csiki-Sava et al., 2016; Panaiotu & Panaiotu, 2010). As more precise locality data are not known, neither is a more precise age assessment possible for the type locality, although it is most probably located within the informal lower subunit of the formation (dated as early to early late Maastrichtian), because the upper subunit is almost completely barren as far as vertebrate remains are concerned (Csiki-Sava et al., 2016).

Referred specimens. Individual G: six caudal vertebrae, although only five appear to be accessioned (MCDRD 255, MCDRD 266, MCDRD 267, MCDRD 268, MCDRD 269) and only the latter four specimens can now be located, right ulna (MCDRD 149), right radius

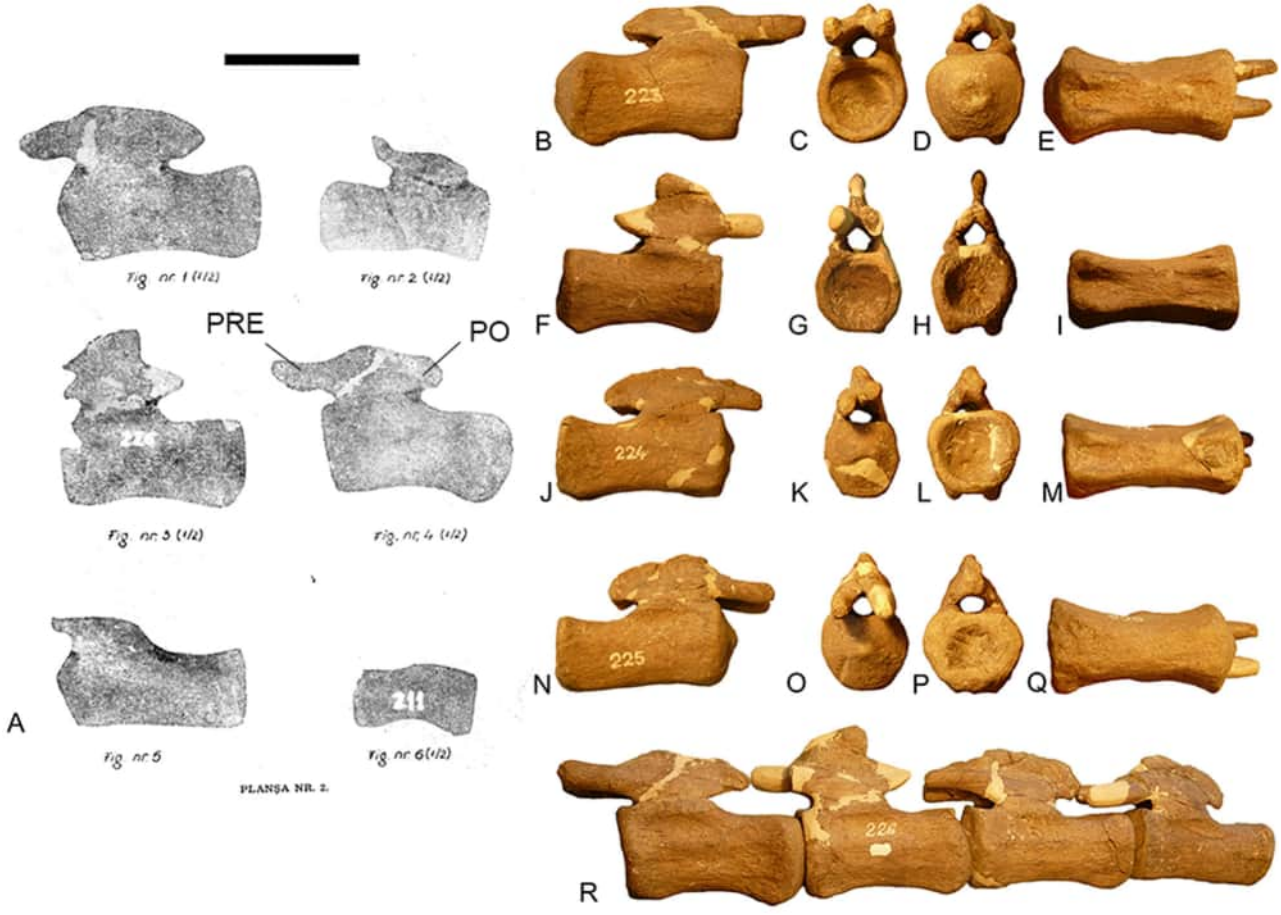

Figure 35. *Petrustitan hungaricus* n. gen., posterior caudal vertebrae. **A,** posterior caudal vertebrae reported by Groza (1983). MCDRD 266 (Individual G) in **B,** right lateral; **C,** anterior; **D,** posterior; and **E,** ventral views. MCDRD 269 (Individual G) in **F,** right lateral; **G,** anterior; **H,** posterior; and **I,** ventral views. MCDRD 267 (Individual G) in **J,** right lateral; **K,** anterior; **L,** posterior; and **M,** ventral views. MCDRD 268 (Individual G) in **N,** right lateral; **O,** anterior; **P,** posterior; and **Q,** ventral views. **R,** MCDRD 266, 269, 267 and 268 (from left to right) in articulation, left view. Abbreviations: **PO**, postzygapophysis, **PRE**, prezygapophysis. Scale bar equals 100 mm.

(MCDRD 150), right metacarpal I (MCDRD 152), right ilium (MCDRD 148), left fibula (MCDRD 153).

Locality and distribution. The geographical and stratigraphical locus of Individual G is broadly consistent with those of the type specimen, but is known more precisely: Râpa Mocioconilor (= *Mocioconilor ravine*), informal lower subunit of the Sânpetru Formation (early, or earliest late, Maastrichtian), Sibișel Valley, between Sânpetru and Săcel villages (Fig. 1E; Csiki, Grigorescu, et al., 2010, fig. 1C; Csiki-Sava et al., 2016; Grigorescu, 1992; Therrien et al., 2009).

Revised species diagnosis. *Petrustitan hungaricus* can be diagnosed on the basis of one autapomorphy (marked with an asterisk), as well as two 'local' autapomorphies: (1) tibia drawn out into slender laterodistal process that inserts into a socket on the medial surface of the distal fibula; (2) proximal end of the fibula with a subtriangular outline*; (3) posterodistally oriented accessory ridge on lateral surface of fibula, extending from midlength to one-quarter of fibula length from distal end.

Justification for referrals. Individuals B and G can be compared directly via the fibula. These fibulae share autapomorphies 2 and 3 above, although the posterior expansion of the proximal end is less well marked in Individual G.

It is worth noting that Huene (1932, p. 274) tentatively referred a number of other Transylvanian titanosaur specimens to his new species '*Magyarosaurus' hungaricus* besides the NHMUK R.3853 fibula, mainly based on their assessed larger size and Huene's opinion that '*M.*' *hungaricus* was 'THE large' Transylvanian

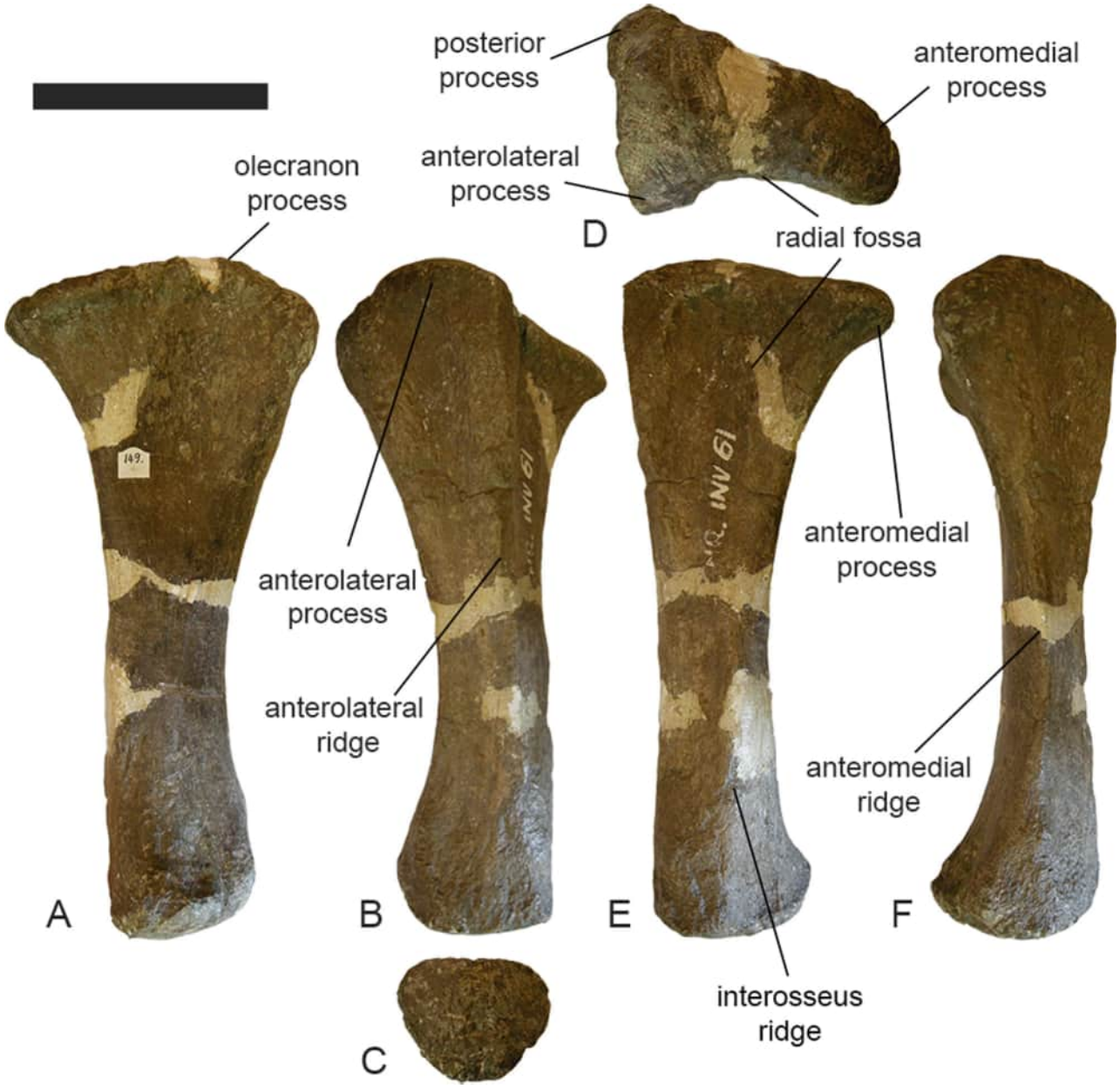

Figure 36. *Petrustitan hungaricus* n. gen., right ulna MCDRD 149 (Individual G) in **A,** posterior; **B,** lateral; **C,** distal (lateral towards top); **D,** proximal (posterior towards top); **E,** anterior; and **F,** medial views. Scale bar equals 100 mm.

titanosaur. However, from these specimens, only the NHMUK R.3853 tibia can be referred with any certainty to this taxon based on its highly probable association with the lectotype fibula. The other specimens (dorsal ribs, caudal centra, sternum, coracoid, ulna, metacarpal, pubis, femur, tibiae; housed in the London and Budapest collections) lack information on their potential field association with the lectotype, and either do not overlap with the lectotype material or else do not share its autapomorphies. Indeed, some of these specimens are here identified as parts of other, more complete skeletal associations, designated as individual C (caudal centra; see below), Individual H (dorsal ribs, sternum), and Individual O (pubis), whereas others appear to be isolated elements whose precise taxonomic affinities remain currently undecided (see the 'Additional individuals and assemblages' section, and the Supplemental Material). Thus, these specimens are here excluded from *Petrustitan hungaricus* n. comb. pending further, more complete discoveries.

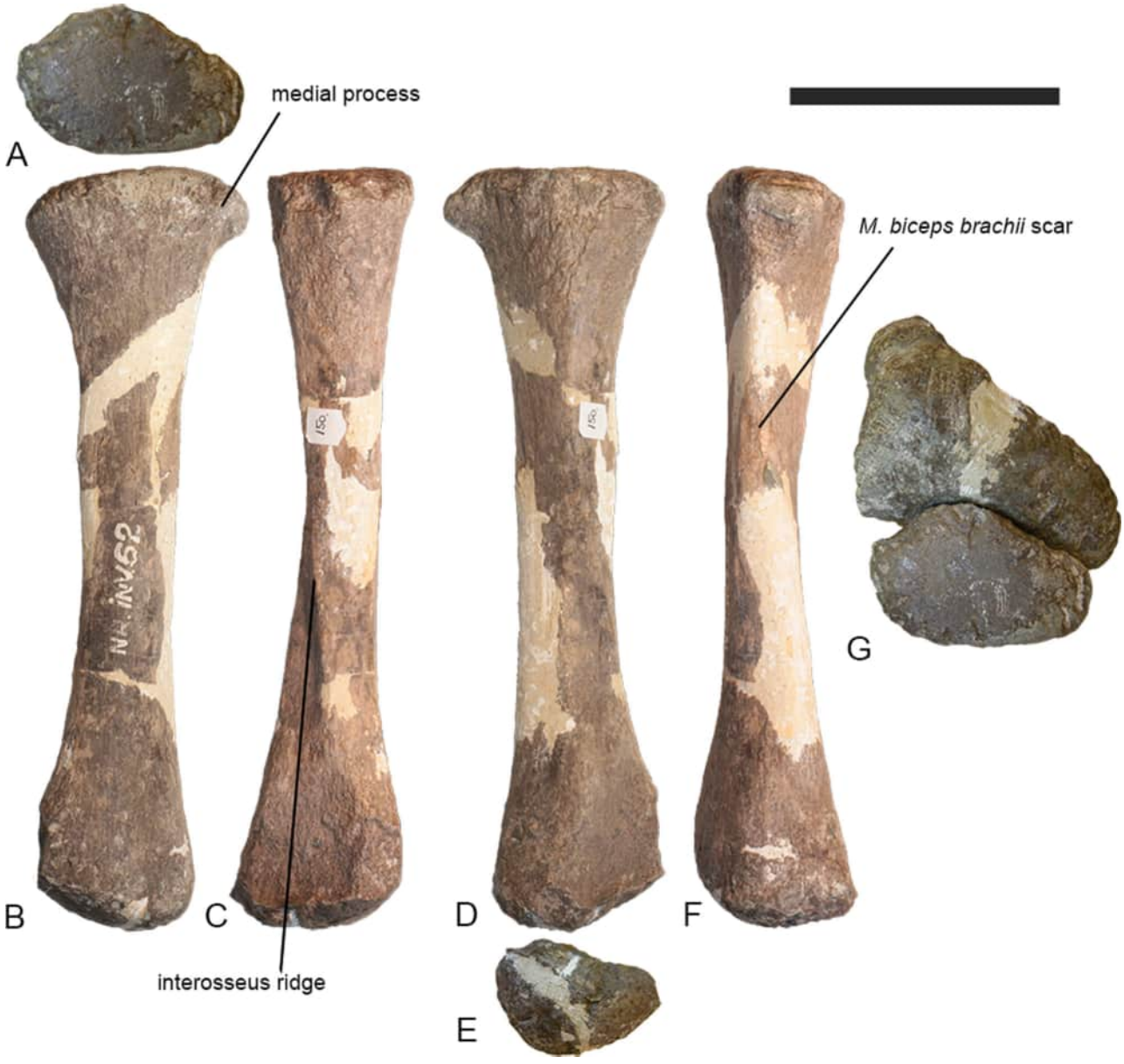

Figure 37. *Petrustitan hungaricus* n. gen., right radius MCDRD 150 (Individual G) in **A,** proximal (posterior towards to); **B,** anterior; **C,** lateral; **D,** posterior; **E,** distal (posterior towards top); and **F,** medial views. **G,** proximal ends of the right ulna MCDRD 149 and radius MCDRD 150 in articulation. Scale bar equals 100 mm.

Description and comparisons of *Petrustitan hungaricus*

Posterior caudal vertebrae. Groza (1983) reported six caudal vertebrae found in articulation as part of Individual G (Fig. 35A), but only four could be located in the MCDRD collections (Fig. 35R). The first in the series (MCDRD 266; Fig. 35B–E) is procoelous, with MCDRD 269 (the second in the series) amphicoelous (Fig. 35F–I), and the last two (MCDRD 267 [Fig. 35J–M] and 268 [Fig. 35N–Q]) mildly opisthocoelous. The centra are spool-like, with a subcircular profile in transverse cross-section, and a slightly constricted central region compared to the articular ends. This morphology differs from the dorsoventrally compressed posterior caudal centra of *Lirainosaurus*, *Muyelensaurus*, *Rinconsaurus* and *Saltasaurus* (Calvo, Porfiri, et al., 2007; Calvo, González Riga, et al., 2007; Calvo & González Riga, 2003; Díez Díaz et al., 2013b). The centra of *Petrustitan* are elongate, with aEI values of 1.76–1.87, similar to the posterior caudal vertebra of *Magyarosaurus* and most titanosaurs, with the exception of *Isisaurus* and *Opisthocoelicaudia*, which have

Figure 38. *Petrustitan hungaricus* n. gen., right metacarpal I MCDRD 152 (Individual G) in **A,** proximal (dorsal towards top); **B,** ventral, **C,** lateral; **D,** distal (lateral towards top); **E,** dorsal; and **F,** medial views. Scale bar equals 50 mm.

Figure 39. *Petrustitan hungaricus* n. gen., right ilium MCDRD 148 (Individual G) in **A,** posterior; **B,** lateral; and **C,** medial views. Scale bar equals 100 mm.

anteroposteriorly shorter centra (Poropat et al., 2016). In *Petrustitan*, the ventral surfaces of the centra are flat (Fig. 35E, I, M, Q). Chevron facets are present, but poorly developed, especially the anterior ones. No ridges or excavations occur on either the ventral or lateral surfaces of the centra.

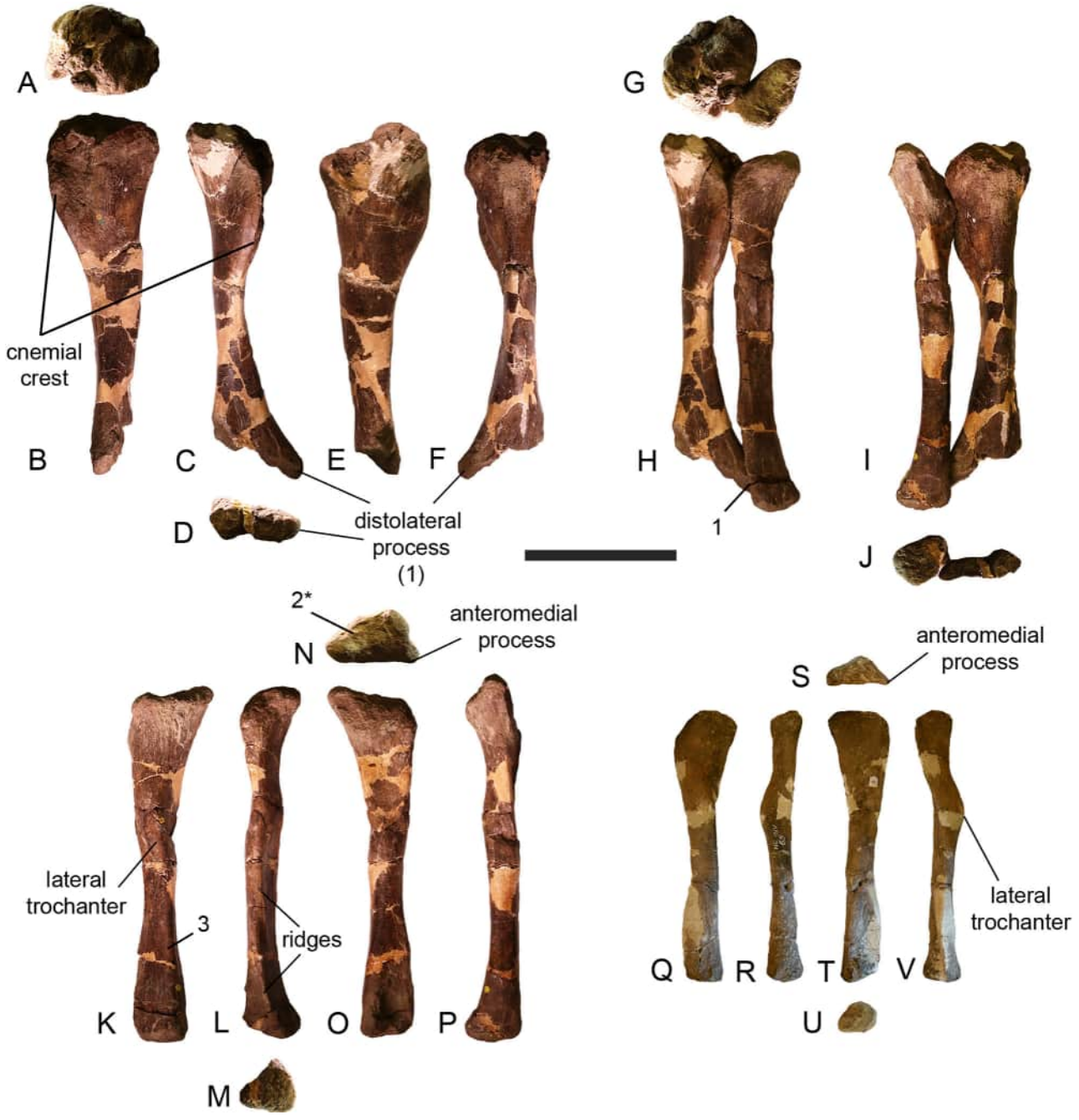

Figure 40. *Petrustitan hungaricus* n. gen., tibia and fibulae. Paralectotype left tibia NHMUK R.3853 (Individual B) in **A,** proximal (lateral towards bottom); **B,** lateral; **C,** anterior; **D,** distal (anterior towards top); **E,** medial; and **F,** posterior views. Paralectotype left tibia and lectotype left fibula NHMUK R.3853 (Individual B) in articulation in **G,** proximal (anterior towards bottom); **H,** anterior; **I,** posterior; and **J,** distal (posterior towards top) views. Lectotype left fibula NHMUK R.3853 (Individual B) in **K,** lateral; **L,** anterior; **M,** distal (anterior towards top); **N,** proximal (medial towards bottom); **O,** medial; and **P,** posterior views. Left fibula MCDRD 153 (Individual G) in **Q,** lateral; **R,** posterior; **S,** proximal (medial towards bottom); **T,** medial; **U,** distal (medial towards top); and **V,** anterior views. The numbers 1, 2*, and 3 indicate the autapomorphies described in the text: tibia drawn out into slender laterodistal process that inserts into a socket on the medial surface of the distal fibula; proximal end of the fibula with a subtriangular outline; and posterodistally oriented accessory ridge on lateral surface of fibula, extending from midlength to one-quarter of fibula length from distal end. Scale bar equals 200 mm.

Longitudinal ridges are present at the junction between the centrum and neural arch (Fig. 35B, F, J, N, R). The neural arch is situated on the anterior half of the centrum. The prezygapophyses are slender and elongate, projecting primarily anteriorly, well beyond the anterior margins of their respective centra. Postzygapophyses do not project as distinct processes: rather, they form laterally facing oval articular surfaces. The neural spines are incomplete and abraded at their apices. Nevertheless, the spines are well enough preserved to determine that they are simple, dorsoventrally low projections.

Ulna. A right ulna (MCDRD 149) is preserved as part of Individual G (Fig. 36). The maximum proximal mediolateral width to proximodistal length ratio is 0.39. Thus, this is a relatively robust element, similar to the ulnae of titanosaurs such as *Diamantinasaurus* (Poropat, Upchurch, et al., 2015), *Isisaurus* (Jain & Bandyopadhyay, 1997), *Lirainosaurus* (Díez Díaz et al., 2013a), and saltasaurines (Otero, 2010; Powell, 1992), and differing substantially from that of *Magyarosaurus* (<0.3). In *Petrustitan*, the proximal articulation surface is gently convex, with only a weakly developed olecranon process. In this regard, *Petrustitan* differs from most titanosaurs, in which the olecranon is a prominent process (Wilson & Sereno, 1998), although the ulnae of *Lirainosaurus* (Díez Díaz et al., 2013a) and *Patagotitan* (Otero et al., 2020) also lack a well-developed olecranon. Although the anterolateral process is incomplete in this *Petrustitan* specimen, it is clear that the anteromedial process of the proximal end was considerably longer (Fig. 36D). This differs from *Magyarosaurus*, in which the proximal processes are more similar in length to one another (Fig. 28B). The lateral surface of the anteromedial process is concave, and its distal tip is gently deflected laterally. The proximal articular surface of this process has a convex outline in lateral/medial views. The posterior process is rounded and only slightly developed when compared to the other two processes. A ridge extends distally from the anteromedial process along the entirety of the shaft. Although less well developed, another ridge extends distally from the anterolateral process and merges into the shaft at approximately midlength. These anteromedial and anterolateral ridges are less conspicuous than in the ulnae referred to *Atsinganosaurus* and *Lirainosaurus* (Díez Díaz et al., 2013a, 2018). The posterior process is buttressed by a thickened edge that develops distally into a thinner ridge.

The anteromedial surface of the shaft, for articulation with the radius, is relatively shallowly concave (Fig. 36D, E) and thus contrasts with the deeper radial articulations of *Magyarosaurus* (Fig. 28B, D), *Atsinganosaurus*, *Lirainosaurus* and *Lohuecotitan* (Díez Díaz et al., 2013a, 2016, 2018). In *Petrustitan*, as in most sauropods, this surface bears an interosseous ridge along its distal half. This ridge extends subparallel to the long axis of the shaft, as is typical for other sauropods, rather than apomorphically slanting across the anterior surface, as in *Magyarosaurus* (see above). The overall shape of the shaft differs from the more slender ulna of *Atsinganosaurus* (Díez Díaz et al., 2018), but also from the transversely compressed ulnae of *Ampelosaurus* (C3-1296; Le Loeuff, 2005b) and *Garrigatitan* (Díez Díaz et al., 2021).

In *Petrustitan*, the distal articular surface of the ulna is convex, with a rounded subtriangular outline, and little posterior expansion (Fig. 36C), differing from the probable 'comma'-shaped distal end in *Magyarosaurus*. This distal morphology in *Petrustitan* is similar to that of *Diamantinasaurus* (Poropat, Upchurch, et al., 2015), but differs from the more angular distal ends seen in *Atsinganosaurus* (Díez Díaz et al., 2018, fig. 10O), *Lirainosaurus* (Díez Díaz et al., 2013a, fig. 3.8), and *Ampelosaurus* (C3-1000; Le Loeuff, 2005b, fig. 4.19D).

Radius. A right radius (MCDRD 150) (Fig. 37), associated with the ulna MCDRD 149 (Figs 36, 37G), has been recovered as part of Individual G. The proximal articular surface is slightly convex, with an oval outline, as a result of a prominent medial process (Fig. 37A, B, D). The shaft is slender, almost straight, with a subcircular cross-section at midshaft. A slight torsion is present in the shaft; however, this is not as marked as in the radius of *Magyarosaurus.* There is a medially placed ridge, located slightly above midlength, that probably represents the M. biceps brachii scar. On the posterolateral surface, the interosseous ridge extends from the proximal end. However, it is not possible to determine the distal extent of these medial and posterolateral ridges, because part of the shaft has been reconstructed in plaster. The posterolateral surface of the distal end is shallowly concave for articulation with the ulna. In distal view (Fig. 37E), the radius has a rounded/oval outline, with a lateral prominence. The lateral two-thirds of the distal end surface are bevelled at an angle of *c.* 33° to a plane perpendicular to the proximodistal axis of the radius. The distal articular surface is gently convex, contrasting with the relatively flat one in *Magyarosaurus.*

Metacarpal. The right metacarpal I (MCDRD 152) of Individual G is preserved (Fig. 38). This element is incomplete and slightly eroded. The shaft is straight and has a circular cross-section, with the proximal and distal thirds twisted relative to each other. It lacks the lateral bowing that characterizes the first metacarpal of the titanosaurs *Andesaurus* and *Argyrosaurus*

(Apesteguía, 2005; Mannion & Calvo, 2011). In *Petrustitan*, the proximal and distal regions of metacarpal I are transversely expanded in comparison to the shaft. Both the proximal and distal articular surfaces are convex and have rounded subrectangular outlines. The distal articular surface does not extend onto the dorsal surface of the metacarpal. As is the case in most titanosauriforms, the distal end is approximately perpendicular to the long axis of the metacarpal (Mannion et al., 2013; Wilson, 2002).

Ilium. A partial right ilium of Individual G (MCDRD 148) preserves most of the ventral portion of the preacetabular process, as well as the pubic peduncle (Fig. 39). The preacetabular process clearly projects anterolaterally, but the ilium is too incomplete to determine whether this formed a sub-horizontal platform, such as that seen in many titanosaurs (Powell, 2003). There is some indication of a 'kink' on the ventral margin of the preacetabular process, similar to that seen in some titanosaurs, including saltasaurines, *Alamosaurus* and *Dreadnoughtus* (D'Emic, 2012; Ullmann & Lacovara, 2016), but its presence in *Petrustitan* is not certain given the incomplete nature of the element. The pubic peduncle is short and robust, contrasting with the relatively more slender peduncles of many titanosaurs, including *Diamantinasaurus*, *Overosaurus*, *Rapetosaurus*, *Atsinganosaurus*, *Garrigatitan*, *Lirainosaurus*, *Normanniasaurus* and *Paludititan* (Coria et al., 2013; Csiki, Codrea, et al., 2010; Curry Rogers, 2009; Díez Díaz et al., 2013a, 2018, 2021; Le Loeuff et al., 2013; Otero, 2010; Poropat, Upchurch, et al., 2015). In *Petrustitan*, this process projects primarily perpendicular to the long axis of the preacetabular process. Its posterior margin is dorsoventrally concave in lateral view. The distal articular surface of the pubic peduncle is anteroposteriorly convex, such that the posterior half of the distal surface faces ventrally and posteriorly. There is no evidence for a triangular excavation on the lateral surface of the upper part of the pubic peduncle, such as that seen in *Lirainosaurus* (Díez Díaz et al., 2013a), *Dreadnoughtus* (Ullmann & Lacovara, 2016), and *Rocasaurus* (Salgado & Azpilicueta, 2000). It is not possible to ascertain the internal tissue structure of the *Petrustitan* ilium.

Tibia. NHMUK R.3853 is a left tibia (Fig. 40A–F) associated with the holotype fibula, together representing Individual B (Fig. 40G–J). The tibia is described with the flat subtriangular anterior surface at the distal end of the shaft facing directly anteriorly. The proximal end is equidimensional (Table S1), forming a rounded, quadrangular outline (Fig. 40A). This morphology differs from that seen in the proximal tibia of *Magyarosaurus*, which presents a relatively narrower, sub-rectangular to 'D'-shaped profile (Fig. 33A). In *Petrustitan*, the cnemial crest expands anterolaterally and is curved only very mildly along its length. In proximal view, the cnemial crest projects less markedly outward relative to the dimensions of the proximal end, differing from the condition in *Magyarosaurus*. Furthermore, whereas the latter taxon has a cnemial crest that is approximately aligned with the long mediolateral axis of the proximal tibia, in *Petrustitan* the crest extends perpendicular to the long axis of the proximal tibial surface (the latter being oriented anteromedially–posterolaterally). The embayment enclosed by the cnemial crest on the anterolateral surface, that receives the head of the fibula, is shallow and relatively small because of the transverse widening of the proximal end. A similar condition is present in some other titanosaurs, including *Diamantinasaurus*, *Saltasaurus*, *Atsinganosaurus* and *Lirainosaurus* (Powell, 1992; Díez Díaz et al., 2013a, 2018; Poropat, Upchurch, et al., 2015). The cnemial crest of *Petrustitan* fades out before reaching the midlength of the tibia.

At midlength, the shaft is constricted, especially transversely. At this point, the shaft has an anteroposteriorly elongated oval cross-section. Although incompletely preserved, it is nevertheless clear that the distal end expands strongly transversely, such that its distal-most preserved mediolateral width is more than twice that of the shaft at midlength. The anteroposterior expansion of the distal end is slight, and the anterior face is wide and flat. As a result, the distal articular end has a laterally elongated and pointed subtriangular profile. Essentially, the lateral malleolus projects as a prominent distolateral process. The tip of this triangular process inserts into a medial fossa at the distal end of the fibula (see below; Fig. 40H–J, O), forming an unusual interlocking contact between the tibia and fibula distally. This morphology also occurs in the saltasaurines *Neuquensaurus* (e.g. MCS – 5 [PDM pers. obs., 2009] and MLP-CS 1264 [PDM & PU pers. obs., 2013]; see also Otero, 2010, figs 11, 12) and *Saltasaurus* (PVL 4017: PDM & PU pers. obs., 2013; see also Powell, 2003, pls 45, 46), but is clearly absent in other sauropods for which this feature can be assessed, including the penecontemporaneous Iberoarmorican taxa *Abditosaurus*, *Ampelosaurus*, *Atsinganosaurus*, *Lirainosaurus*, and *Lohuecotitan* (Díez Díaz et al., 2013a, 2016, 2018; Le Loeuff, 2005b; Vila et al., 2022). As such, we regard this unusual morphology of the distal tibia and fibula as a local autapomorphy of *Petrustitan*. As already noted, the distal-most articular portion of the tibia is not preserved in NHMUK R.3853. There is no evidence for a prominent ridge on the anteromedial margin of the preserved distal tibia; such a ridge characterizes the distal

quarter of the tibiae of *Atsinganosaurus*, *Lirainosaurus*, *Abditosaurus* and *Uberabatitan* (Díez Díaz et al., 2013a, 2018; Silva Junior et al., 2019, fig. 23; Vila et al., 2022), although it remains possible that the tibia of *Petrustitan* is too incomplete to preserve this feature.

Fibula. The fibula of *Petrustitan* is represented by two left elements, NHMUK R.3853 (the holotype, Individual B; Fig. 40K–P) and MCDRD 153 (belonging to Individual G; Fig. 40Q–V). NHMUK R.3853 is essentially complete, whereas MCDRD 153, though almost complete, has missing parts of the shaft and a distal third restored with plaster. In lateral view, the proximodistal axis of the fibula follows a gentle sigmoidal curve (Fig. 40L, R), as is the case in most somphospondylans (Canudo et al., 2008). The proximal and distal ends are slightly twisted relative to one another, such that the medial surfaces at each end are not quite in the same plane. Although the proximal end is slightly worn in the available specimens, this region is characterized by the presence of an anteromedially directed crest that extends into a notch behind the cnemial crest of the tibia, as also occurs in *Magyarosaurus*. Excluding the anteromedial process, the proximal articular surface of the fibula has an anteroposteriorly elongate subtriangular outline in *Petrustitan* (Fig. 40K, Q). This proximal profile is formed by a nearly straight medial margin, and a transverse narrowing towards its posterior end. Such a proximal end outline differs from the 'D'-shaped one in *Magyarosaurus* (Fig. 40N, S) and the D-shaped to elliptical outline in other titanosaurs, including *Ampelosaurus* (VDD pers. obs., 2024) and *Lohuecotitan* (Díez Díaz et al., 2016). It is therefore regarded as autapomorphic for *Petrustitan.* In the fibula of *Petrustitan*, the proximal end is strongly expanded posteriorly relative to the shaft, such that the proximal half of the posterior margin of the fibula is concave in lateral view. This is an unusual condition that we regard as a possible autapomorphy of *Petrustitan*. However, this feature is not as hooked or as prominent in (the more poorly preserved) MCDRD 153 specimen (Fig. 40S), and thus we have provisionally excluded this feature from our diagnosis. The proximal articular surface of the fibula is irregular, and is bevelled such that it faces proximally and also slightly anteriorly. The medial surface of the proximal end appears to be striated, although not especially raised, as is also the case in other titanosauriforms (D'Emic, 2012; Wilson & Sereno, 1998).

The fibula of *Petrustitan* lacks an anterolateral trochanter along its proximal third. The lateral trochanter extends distally to at least midlength of the fibula in NHMUK R.3853 (Fig. 40K), but does not reach so far distally in MCDRD 153 (Fig. 40Q, R, V). Most eusauropods are characterized by the former condition (Whitlock, 2011), although the lateral trochanter is more proximally restricted in some titanosaurs, including *Epachthosaurus*, *Lohuecotitan* and *Mendozasaurus* (Díez Díaz et al., 2016; Mannion, Upchurch, Jin, et al., 2019). The lateral trochanter is composed of two subparallel ridges: a prominent one (more laterally developed in MCDRD 153) that extends along the posterior margin of the lateral surface, and a less developed one that is situated more anteriorly (this ridge is less obvious in MCDRD 153 because of its poorer preservation and partial restoration in plaster). Although prominent, the lateral trochanter of *Petrustitan* is not hypertrophied to the same extent as those of the fibulae of *Laplatasaurus* and *Uberabatitan* (Gallina & Otero, 2015). An additional ridge is present on the anterior margin of the lateral surface in NHMUK R.3853 (this feature cannot be ascertained in MCDRD 153). Its proximal tip is situated at approximately the midlength of the fibula. It is directed steeply posterodistally, terminating distally at about three-quarters of fibula length. This ridge is similar to that described in the fibula of *Magyarosaurus* but appears to represent a convergently developed feature (supported by our phylogenetic analyses – see below) that we herein regard as a local autapomorphy of both *Petrustitan* and *Magyarosaurus*. Just proximal to the distal tip of this ridge in *Petrustitan*, the anterior margin of the distal third of the fibula forms a well-developed ridge, as in most eusauropods (Upchurch et al., 2004), although this is poorly preserved in NHMUK R.3853.

The medial surface of the distal end is strongly concave for reception of the laterodistal expansion of the tibia (see above; Fig. 40O). As noted above, a similar concavity on the distal fibula is otherwise only known in *Neuquensaurus* and *Saltasaurus*. In distal view, the fibula has a subtriangular outline, with flattened medial, anterolateral and posterolateral margins (although the latter two margins meet at a rounded corner) (Fig. 40M, U). The anterior apex of this triangle is incomplete in NHMUK R.3853. The distal end has a more rounded outline in MCDRD 153, but this is likely to be the result of poor preservation. This outline differs from the tear-drop-shaped distal end present in *Magyarosaurus* (Fig. 34J). A subtriangular distal fibular outline is a derived state that occurs in several other titanosaurs, such as *Lirainosaurus* (Díez Díaz et al., 2013a) and *Diamantinasaurus* (Poropat, Upchurch, et al., 2015).

Titanosauria Bonaparte & Coria, 1993
Lithostrotia Upchurch, Barrett & Dodson, 2004
Uriash n. gen.
Figs 41–45

Type species. *Uriash kadici* sp. nov.

Etymology. The genus name comes from the Romanian word 'uriaș' (pronounced 'uriash') that refers to gigantic humanoid fairy-tale characters in Romanian folk-lore (see also the Hungarian term 'óriás'), but also, generally, to something or someone colossal, gigantic. It alludes to the large body size of this titanosaur taxon, significantly larger than the other Transylvanian taxa.

Generic diagnosis. As for the type (and only known) species.

Uriash kadici *n. gen.* n. sp.

1932 *Magyarosaurus hungaricus* Huene: 269
1970 *Titanosaurus hungaricus* Steel: 77
2005a *Magyarosaurus dacus* Le Loeuff: 15–16
2010 '*Magyarosaurus*' *hungaricus* Stein *et al.*: 9259

Holotype. Individual C: four posterior–distal caudal vertebrae (SZTFH Ob.3090B, D, G, H; originally eight vertebrae collected, but four are missing); incomplete right humerus (SZTFH Ob.3104); incomplete right femur and one small fragment (region of the fourth trochanter) of the left femur (SZTFH Ob.3103); left metatarsal I (SZTFH Ob.3095).

Etymology. The species name honours Ottokár Kadić (1876–1957), geologist and palaeontologist of the Royal Geological Survey of Hungary and discoverer of several continental vertebrate-bearing fossil localities in the north-western Hațeg Basin, including the type locality of *Uriash*, between 1909 and 1915.

Type locality. Locality VI of Kadić (see Kadić, 1916) in the Budurone ravine (Pârâul Budurone), south-east of Vălioara locality, north-western Hațeg Basin, Hunedoara County, Romania (Fig. 71). The approximate position of the original locality was recently relocated in the field by Botfalvai et al. (2021).

Type stratum and age. The holotype comes from the lower part of the unnamed middle member of the uppermost Cretaceous continental Densuș-Ciula Formation (Csiki-Sava et al., 2016; Grigorescu, 1992). The age of the local succession, once considered to be late Maastrichtian (e.g. Antonescu et al., 1983), was recently

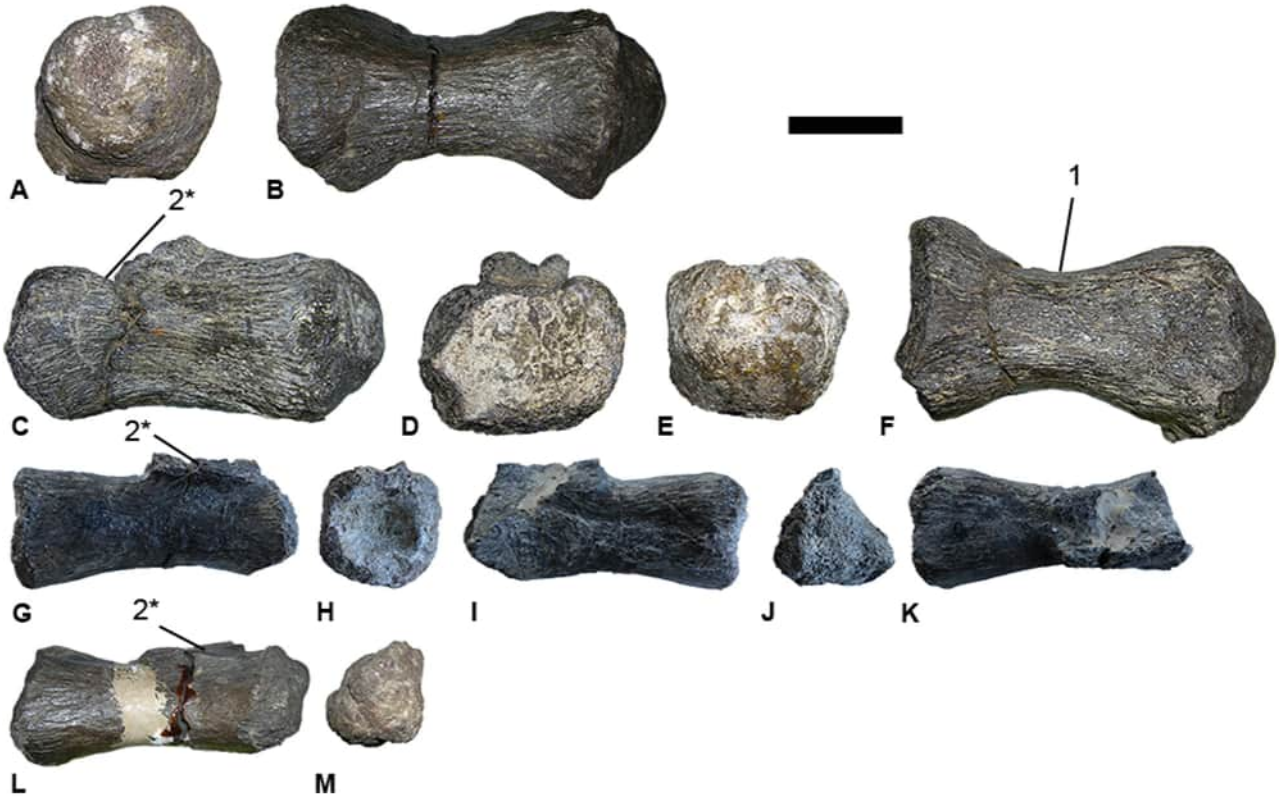

Figure 41. *Uriash kadici* n. gen. n. sp. holotype, posterior caudal vertebrae SZTFH Ob.3090 (Individual C). SZTFH Ob.3090B in **A,** anterior; and **B,** ventral views. SZTFH Ob.3090D in **C,** left lateral; D; anterior; **E,** posterior; and **F,** ventral views. SZTFH Ob.3090G in **G,** right lateral; **H,** posterior; **I,** left lateral; **J,** anterior; and **K,** dorsal views. SZTFH Ob.3090H in **L,** right lateral; and **M,** anterior views. The numbers 1 and 2* indicate the autapomorphies described in the text: posterior caudal vertebrae with a markedly procoelous centrum and a distinctive hour-glass shaped contour in ventral view; and posterior caudal vertebrae with anteroposteriorly elongated neural arch pedicels. Scale bar equals 50 mm.

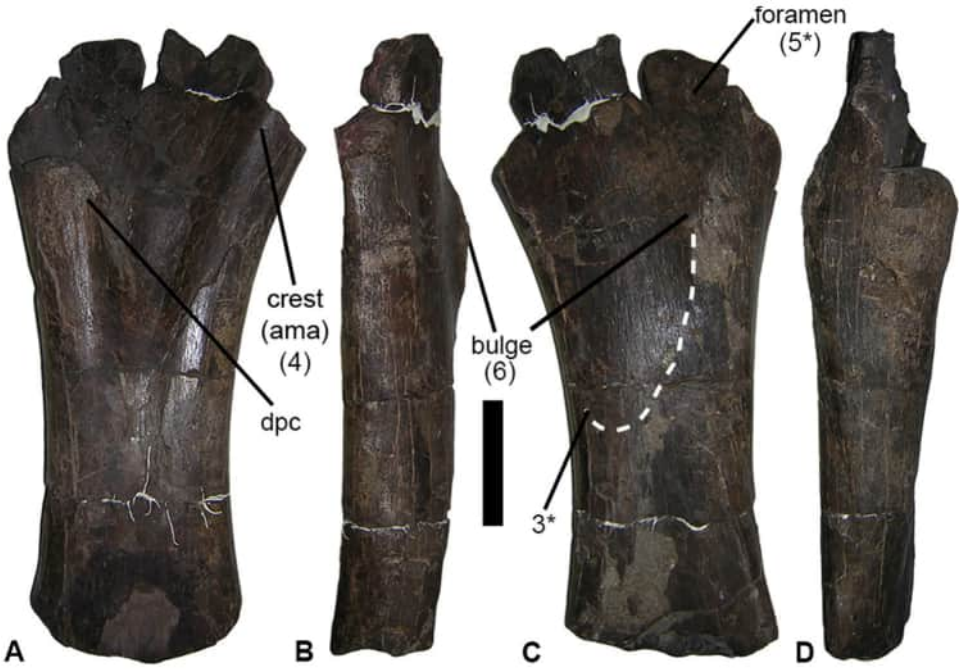

Figure 42. *Uriash kadici* n. gen. n. sp. holotype, right humerus SZTFH Ob.3104 (Individual C) in **A,** anterior; **B,** medial; **C,** posterior; and **D,** lateral views. **Abbreviations: ama**, anteromedial arm; **dpc**, deltopectoral crest. The dashed line represents the area of the posterior longitudinal convexity. The numbers 3*, 4, 5* and 6 indicate the autapomorphies described in the text: presence of a midline longitudinal convexity along the posterior humeral shaft curving distally towards the medial edge; proximal half of humerus with an 'anteromedial arm'; large and proximodistally elongated oval foramen in the posterolateral depression of the proximal humerus; and respectively hypertrophied bulge for insertion site of *M. latissimus dorsi*. Scale bar equals 100 mm.

reassessed as early Maastrichtian (Fig. 10; Botfalvai et al., 2021; Csiki et al., 2007; Csiki-Sava et al., 2016).

Diagnosis. *Uriash kadici* n. gen. sp. can be diagnosed on the basis of four autapomorphies (marked with an asterisk), as well as four 'local' autapomorphies: (1) posterior caudal vertebrae with a markedly procoelous centrum and a distinctive hour-glass shaped contour in ventral view; (2) posterior caudal vertebrae with anteroposteriorly elongated neural arch pedicels*; (3) presence of a midline longitudinal convexity along the posterior humeral shaft curving distally towards the medial edge*; (4) proximal half of humerus with an 'anteromedial arm'; (5) large and proximodistally elongated oval foramen in the posterolateral depression of the proximal humerus*; (6) hypertrophied bulge for insertion site of M. latissimus dorsi; (7) femoral shaft starts to transversely expand distally at a point close to its midlength*; (8) hypertrophied femoral fourth trochanter.

Comment. As noted above, skeletal elements belonging to Individual C had been briefly discussed by Huene (1932) and Le Loeuff (2005a), without these authors recognizing that these may represent parts of the same incomplete skeleton. Huene (1932, p. 271, pl. 47, figs 4, 5) briefly described and figured two of the SZTFH Ob.3090 posterior caudal centra and, again based on their large size, tentatively referred them to his new species '*M.*' *hungaricus* (here reassigned as *Petrustitan hungaricus* nov. comb). Le Loeuff (2005a) discussed the large size of the humerus specimen SZTFH Ob.3104 (referred by him to *Magyarosaurus dacus*, under specimen number MAFI V13491) as evidence of the non-dwarfed status of this taxon. Our detailed comparisons (see below) show that Individual C does not share any of the autapomorphies used to diagnose *Magyarosaurus*, *Petrustitan* and/or *Paludititan*, instead presenting a set of autapomorphies of skeletal elements that can be directly compared with those of the former three taxa, thus precluding its referral to any of these other Transylvanian titanosaurs.

Description and comparisons of *Uriash kadici*

Caudal vertebrae. As noted above, the lettering sequence of the individual vertebrae appears to reflect their relative position within the tail, with vertebrae SZTFH Ob.3090B and Ob.3090D being more anteriorly situated than Ob.3090G and Ob.3090H (Fig. 41). The former pair have an approximately comparable morphology, but one that is clearly distinct from that of the latter pair, suggesting a substantial morphological change along the tail within its posterior segment. None

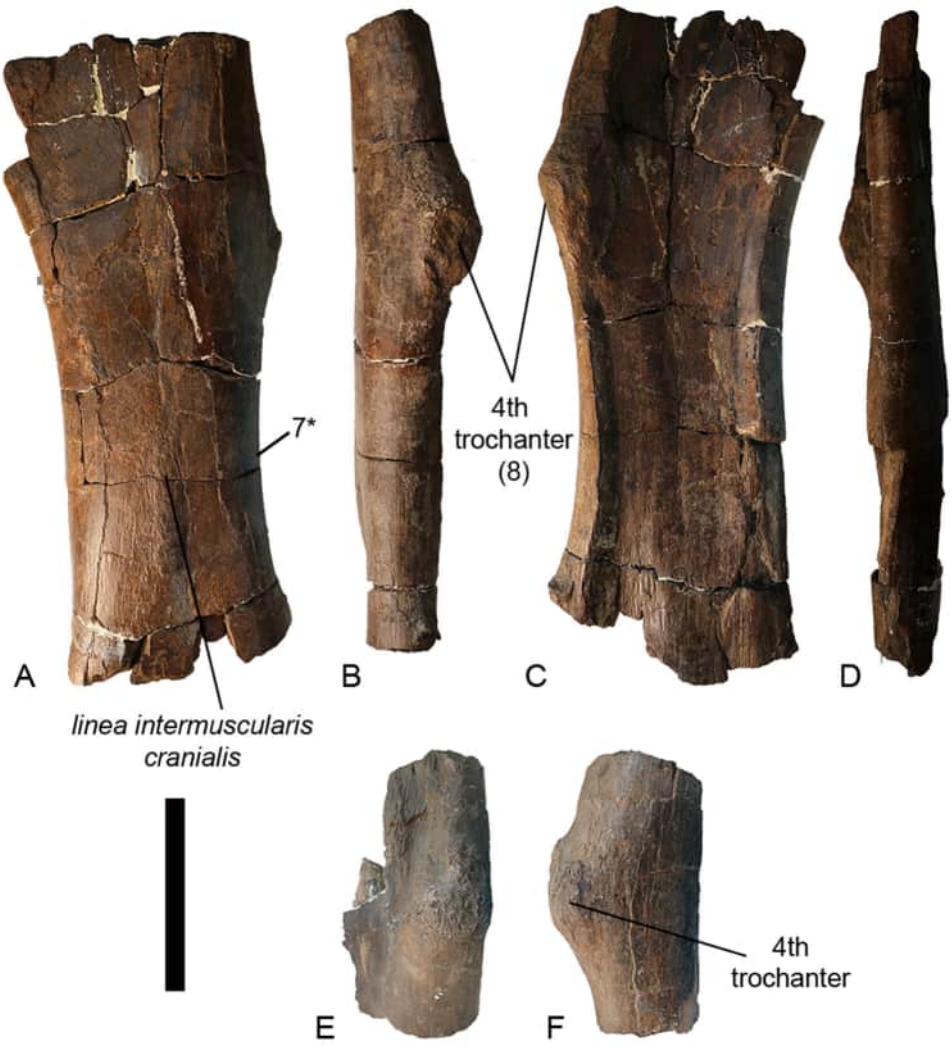

Figure 43. *Uriash kadici* n. gen. n. sp. holotype, femora. Large fragment of right femur SZRFH Ob.3103 (individual C) in **A,** anterior; **B,** medial; **C,** posterior; and **D,** lateral views. Small fragment of left femur SZRFH Ob.3103 (individual C) in **E,** posterior; and **F,** medial views. The numbers 7* and 8 indicate the autapomorphies described in the text: femoral shaft starts to transversely expand distally at a point close to its midlength; and hypertrophied femoral fourth trochanter. Scale bar equals 200 mm.

of the four remaining vertebrae of the series is complete, preserving only the centra and bases of the neural arches; furthermore, the articular ends of the centra are often heavily damaged (especially those of G and H), making the assessment of the type of articular surface difficult in some of them. The vertebrae are all from the posterior to distal region of the tail, as suggested by features such as the absence of transverse processes, relative elongation of the centra, and absence of articular facets for the chevrons (Mannion et al., 2013).

The first two vertebrae in this series (B and D) are both strongly procoelous (Fig. 41A–F), with a deeply concave anterior articular cotyle, differing from the posterior caudal vertebrae of *Magyarosaurus* and *Petrustitan*. The posterior articular surfaces of SZTFH Ob.3090B and D are markedly convex and somewhat wider than high. The 'apex' of the posterior condyle is located dorsally relative to the mid-height of the centrum. In vertebra D, the centre of the condyle is excavated by a circular pit (Fig. 41E). Vertebrae B and D are both characterized by an hourglass-shaped morphology in dorsal/ventral view, which results from an elongated centrum that is strongly laterally constricted at midlength (Fig. 41B, F). The lateral sides of the centrum are consequently deeply concave anteroposteriorly, but mildly convex dorsoventrally. A similar hourglass morphology can be observed in the posterior caudal centra of *Lirainosaurus* and *Atsinganosaurus* (Díez Díaz et al., 2013b, 2018), but the specific anatomy of the caudal vertebrae of *Uriash* – a combination of an

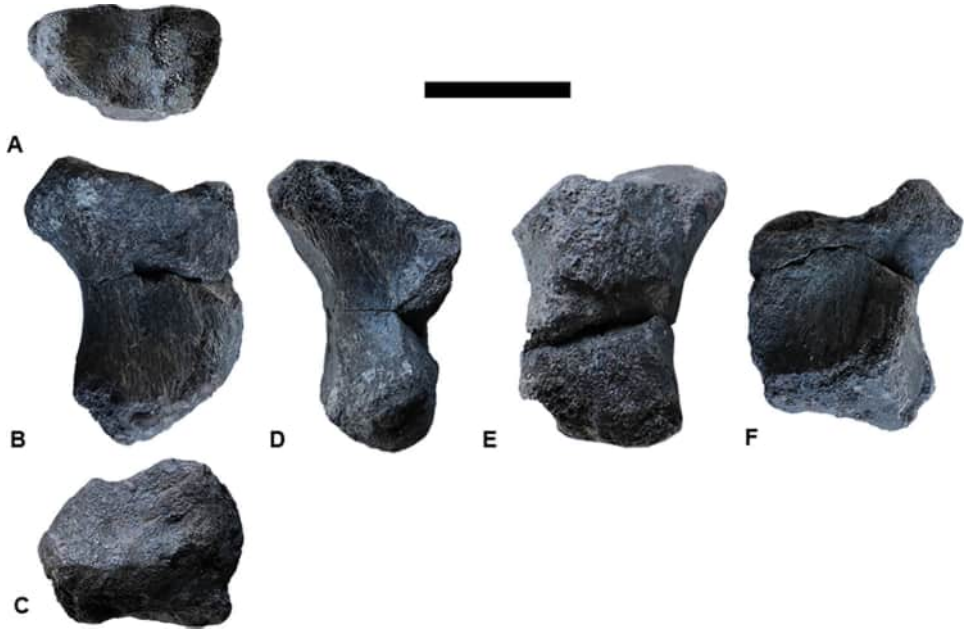

Figure 44. *Uriash kadici* n. gen. n. sp. holotype, left metatarsal I SZTFH Ob.3095 (individual C) in **A,** proximal (ventral towards bottom); **B,** ventral; **C,** distal (ventral towards top); **D,** medial; **E,** dorsal; and **F,** lateral views. Scale bar equals 50 mm.

hourglass-shaped cross-section and strong procoely – has not been found in any other titanosaurs, including the European taxa (Díez Díaz et al., 2013b, 2016, 2018; Le Loeuff, 2005b). In *Uriash*, the dorsal and ventral surfaces of the centrum are approximately equal in transverse width, although the maximum transverse width occurs at the level of the aforementioned longitudinal lateral crest. The ventral surface of the centrum is flat to slightly convex transversely, and lacks a midline furrow and ventrolateral ridges connecting chevron facets; only the remnants of very short and low crests can be seen near the posterior articular margin. The position of the neural arch is clearly biased towards the anterior end of the centrum; however, the neural arch pedicels are elongated, extending for over half the length of the centrum (Fig. 41C). Such arch elongation is not present, as far as we are aware, in the posterior caudal vertebrae of other Transylvanian specimens, or other Late Cretaceous European titanosaurian taxa either, and might ultimately represent an autapomorphy. The neural canals are transversely narrow.

The morphology of the other two vertebrae of the series (G and H, Fig. 41G–N) differs from that described in vertebrae B and D. Vertebrae G and H have more elongated, spool-like centra, that are not so markedly constricted at midlength. Furthermore, these two distal posterior or distal caudal vertebrae are not procoelous, and are either amphicoelous or opisthocoelous (N.B. given the damaged nature of the articular ends, especially the anterior ones, this is difficult to ascertain). The posterior articular surfaces are slightly concave (deeper in G than in H), surrounded by a stout, rounded rim. This morphology is shared with *Petrustitan*, but clearly differs from the generally procoelous-to-platycoelous posterior caudal vertebrae of most titanosaurs, including *Muyelensaurus*, *Rapetosaurus* and *Saltasaurus*, as well as the European titanosaurs *Magyarosaurus*, *Ampelosaurus*, *Atsinganosaurus* and *Lirainosaurus* (Calvo, Porfiri, et al., 2007; Calvo, González Riga, et al., 2007; Curry Rogers, 2009; Díez Díaz et al., 2013b, 2018; Le Loeuff, 2005b). The ventral surface is transversely flat and slightly dorsally arched along its length, lacking ventrolateral longitudinal ridges. The lateral sides of the centra are subparallel, dorsoventrally flat, and slightly concave anteroposteriorly. A rounded protuberance lies at the level of the junction between the neural arch and the centrum. Neural arch pedicels are restricted to the anterior half of the centrum, extending almost to the anterior margin of the latter (Fig. 41G, M). The neural canal is reduced, especially in vertebra H.

Humerus. The right humerus (SZTFH Ob.3104) preserves the major part of the diaphysis, extending from the region of the deltopectoral crest to close to the distal epiphysis; thus, both the proximal and distal articulations are missing (Fig. 42). Despite its incomplete preservation, this humerus displays several unusual features, aside from its very large size, compared to most other titanosaur remains from Transylvania, as also noted by Le Loeuff (2005a).

The preserved proximal segment of the humerus is anteroposteriorly flattened, with a rounded and narrow lateral margin and a wider, largely convex medial margin. Immediately distal to the broken proximal region, a longitudinal angular crest appears on the medial edge of the anterior surface, merging with the shaft distally (Fig. 42A). This crest is not present in *Magyarosaurus*, but is similar to the 'anteromedial arm' that characterizes the titanosaurs *Argyrosaurus*, *Gondwanatitan*, *Muyelensaurus*, *Paralititan* and *Rukwatitan* (Gorscak et al., 2017; Mannion & Otero, 2012). The anterior face of the proximal end is generally concave. Only the distal half of the deltopectoral crest (approximately from the most prominent anteromedial part [= tip] of the crest to its distal base) is preserved. This crest projects mainly medially, rather than anteromedially, overhanging the anterior face, as in the humeri of *Magyarosaurus* and *Lirainosaurus* (Díez Díaz et al., 2013a). However, it is not as medially deflected as in the humerus of *Abditosaurus* (Vila et al., 2022). The lateral side of the distal part of the deltopectoral crest has a coarse texture. Distal to the tip of the deltopectoral crest, there is a weak prominence on the anterolateral edge of the humerus: this potentially represents the insertion of M. brachialis inferior. Distal to the most prominent part of the deltopectoral crest, the shaft of the humerus narrows gradually. This constriction of the shaft is relatively mild compared to that seen in *Magyarosaurus*: the ratio between the minimum shaft width and the mediolateral width at the level of the deltopectoral crest tip is approximately 0.73 in SZTFH Ob.3104, whereas it is as low as 0.63 in the humerus LPB (FGGUB) R.1047 of *Magyarosaurus*.

The posterior face of the proximal end is broadly flat in SZTFH Ob.3104, but has a complex morphology (Fig. 42C). In particular, this surface bears a proximodistally elongated depressed area in its lateral part, a similarly elongated midline prominence, and another shallowly concave area medially. The midline longitudinal convexity continues distally along the shaft, curving towards the medial edge and gradually attenuating. Within the lateral depression, just below the broken proximal edge, there is a large and proximodistally elongated oval foramen, which might represent an autapomorphy, as it has not been described in any other titanosaur. Lateral and distal to this foramen, there is a rugose, prominent, proximodistally elongated bulge (insertion site of M. latissimus dorsi) on the posterior face of the proximal end. This bulge starts slightly proximal to the most prominent part of the deltopectoral crest, and extends distally, approximately parallel to the lateral margin, to a point level with where the distal part of the deltopectoral crest merges into the humeral shaft. The strongest projection of this bulge, which is also where it reaches its greatest mediolateral width, is approximately level with the most prominent part of the deltopectoral crest. This bulge is so well developed that it is clearly visible in both medial and lateral views (Fig. 42B, D). A similarly well-developed posterior longitudinal bulge is present in the large humerus ascribed to *Garrigatitan*, although it is more centrally located in the latter taxon (Díez Díaz et al., 2021, fig. 5F). Given that the corresponding feature in *Magyarosaurus* is less well developed and centrally placed, we regard the extreme prominence of this laterally positioned bulge in the humerus of *Uriash* as a potential autapomorphy. Medial to the proximal part of the bulge, the posterior surface of the proximal end is excavated by a rugose, elongated oval depression, bordered proximally by a small sharp lip. A narrow angular crest originates lateral and distal to the prominent bulge; this extends obliquely distally for approximately 140 mm, merging with the lateral margin of the shaft at a point level with the latter's minimum transverse width. The proximal part of this crest is unevenly rugose, whereas its distal half is covered by coarse longitudinal striae, suggesting it was probably a muscle insertion site. Level with this angular crest, but on the midline of the posterior face, there is a proximodistally elongated flat region marked by coarse vertical striae.

The humeral shaft is relatively robust, with a moderately flattened, transversely elongate oval cross-section and an ECC of 1.65, higher than in *Magyarosaurus* (in which ECC values range between 1.26 and 1.44). In SZTFH Ob.3104, the lateral and medial surfaces of the shaft are broadly rounded, the posterior face is mildly convex transversely, and the anterior one is slightly concave on the midline proximally and then flattens distally.

Distal to the point of minimum shaft circumference, the humerus expands again, but this is rather mild in the preserved segment. In the distal-most preserved part of the humerus, its posterior face becomes somewhat concave because of the presence of the bases of the supracondylar ridges. The medial surface remains largely rounded anteroposteriorly, whereas the lateral one bears an angular crest covered by longitudinal striae (possibly the area of origin for the M. flexor carpi ulnaris and radialis; Voegele et al., 2020).

Femur. The femur is known from a large fragment (most of the shaft, including the fourth trochanter) of a right element (Fig. 43A–D), and a small fragment preserving the region of the fourth trochanter from the left element (Fig. 43E–F), both registered under the same specimen number (SZTFH Ob.3103). Although the proximal and distal ends are absent, the preserved length

of the right femur suggests an estimated original length of more than one metre, which is about twice the size of the next largest femur known from the Transylvanian area (LPB [FGGUB] R.1046, a specimen referred to *Magyarosaurus*); this suggests an individual comparable in size with the Argentinean early-branching titanosaur *Epachthosaurus* (Martínez et al., 2004). The right femur is badly preserved and severely crushed anteroposteriorly. The femur was probably robust, with a highly anteroposteriorly compressed shaft, even taking into account the crushing of the bone that might have exaggerated this feature. It has an ECC of 2.48, much higher than the values calculated for the femora of *Magyarosaurus* (ECC range = 1.14–1.17). The better preserved, less crushed anterior surface of the shaft is transversely rounded, being more convex in its medial half and slightly depressed in its lateral half. As a result, the greatest anteroposterior width of the shaft lies medial to the midline. The anterior surface of the shaft changes from transversely flat proximally to slightly convex distally. A longitudinal rugose crest arises distal to the midlength of the anterior surface and extends distally, which might be the linea intermuscularis cranialis.

The posterior face of the shaft is heavily crushed inward. A weak angular crest is present near the medial margin of the posterior surface, but it is unclear whether or not this is a taphonomic artefact. The shaft starts to expand transversely at a point close to its midlength, contrasting with the condition present in most titanosaurs, including *Ampelosaurus*, *Atsinganosaurus*, *Garrigatitan*, *Lirainosaurus* and *Lohuecotitan* (Díez Díaz et al., 2013a, 2016, 2018, 2021), as well as *Magyarosaurus*, in which the femur starts to expand transversely closer to the distal extremity.

A notable feature of the femur, seen in both the left and right element, is its extremely well developed, prominent fourth trochanter, clearly differing from those of most titanosaurs. This is located on the posteromedial margin, as in most sauropods, but its great development means that it is clearly visible in anterior, posterior, lateral and medial views (Fig. 43). As such, we regard this hypertrophied fourth trochanter as a potential autapomorphy. Two distinct rugose areas are present on the fourth trochanter of both femoral fragments, which we interpret as the insertion areas for M. caudofemoralis longus and brevis. One of these is oval and located on the medial tip of the fourth trochanter, covering its distal two-thirds. The second muscle insertion is positioned in the proximal third of the fourth trochanter, and runs distally posteriorly. The elongated rugosity on the medial edge, proximal to the fourth trochanter, probably forms the insertion area for M. puboischiofemoralis externus (Voegele et al., 2021).

The flaring of the shaft in the distal-most preserved part of the right femoral fragment suggests that the breakage occurred near the base of the distal articular end. At the broken distal end, the beginning of a longitudinally elongated crest can be observed near the lateral edge of the posterior surface. This represents the proximal-most termination of the lateral (fibular) supracondylar crest (Fig. 43C). The surface of this crest is marked by coarse longitudinal striations. The posterior face of the shaft is flattened, but the proximal portion of the medial (tibial) supracondylar crest is also visible, close to the medial margin.

Metatarsal. SZTFH Ob.3095 is a left metatarsal I (Fig. 44). This element is nearly complete, but lacks some of the medial margin and small portions of the lateral margin of the proximal end. It has been broken into two pieces and glued back together. The proximal end is bevelled relative to the long axis of the element, such that it faces slightly medially. The proximal articular surface is flat to mildly concave. Although incomplete, the metatarsal has a ‘D’-shaped outline in proximal view, with the dorsoventrally tall, flat margin facing steeply ventrolaterally. The dorsal surface of the shaft lacks the foramina and the dorsolateral rugosity seen in several diplodocoids (Tschopp et al., 2015; Upchurch, 1998). In dorsal view, the lateral margin is concave, but the medial margin is too incomplete to assess its profile. The metatarsal decreases in dorsoventral height distally, with the lateral surface of the proximal half being gently concave dorsoventrally.

The distal end is bevelled relative to the long axis of the metatarsal, with the lateral condyle extending further distally than the medial one. It also bears a ventrolateral projection that results in the laterodistal condyle extending further laterally than the proximal end of the element in dorsal view. In distal view, the metatarsal has a mediolaterally elongated oval profile, decreasing in dorsoventral height towards its lateral margin. The distal articular surface is mediolaterally concave over most of its extent, becoming convex towards its medial and lateral margins. This surface is dorsoventrally convex, although it flattens centrally.

Additional anatomical information on *Paludititan nalatzensis*

Although *Paludititan* was described only just over a decade ago (Csiki, Codrea, et al., 2010), additional insights into its anatomy arise from both the new information provided in the current work and also the numerous other studies of titanosaur taxa published recently. Therefore, below we provide an update on the

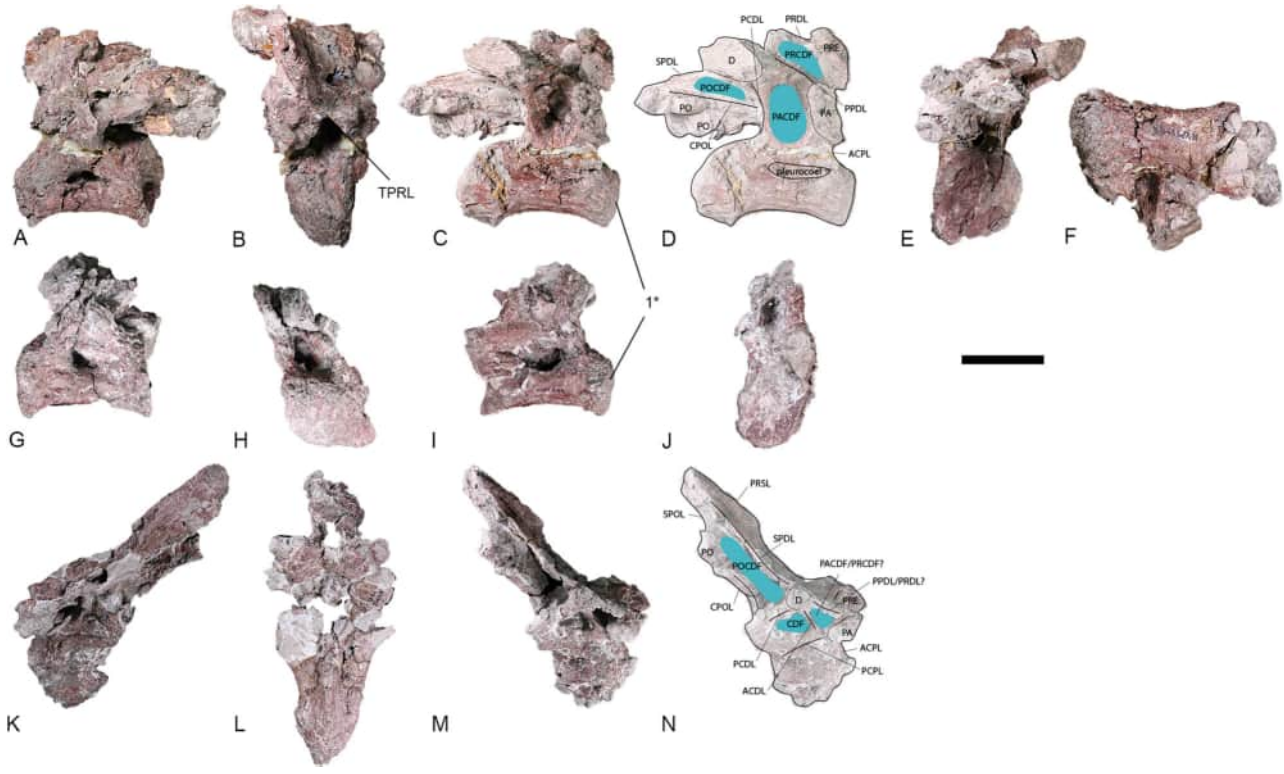

Figure 45. *Paludititan nalatzensis* holotype, dorsal vertebrae (Individual D). Anterior dorsal vertebra UBB NVM 1-43 in **A,** left lateral; **B,** anterodorsal; **C,** right lateral; **D,** right lateral (interpretive drawing); **E,** posterior; and **F,** ventral views. Middle–posterior dorsal vertebra UBB NVM 1-44 in **G,** left lateral; **H,** anterior; **I,** right lateral; and **J,** posterior views. Middle–posterior dorsal vertebra UBB NVM 1-45 in **K,** left lateral; **L,** anterior; **M,** right lateral; and **N,** right lateral (interpretive drawing) views. **Abbreviations: ACDL**, anterior centrodiapophyseal lamina; **ACPL**, anterior centroparapophyseal lamina; **CDF**, centrodiapophyseal fossa; **CPOL**, centropostygapophyseal lamina; **D**, diapophysis; **PA**, parapophysis; **PACDF**, parapocentrodiapophyseal fossa; **PCDL**, posterior centrodiapophyseal lamina; **PCPL**, posterior centroparapophyseal lamina; **PPDL**, paradiapophyseal lamina; **PO**, postzygapophysis; **POCDF**, posterior centrodiapophyseal fossa; **PRCDF**, prezygocentrodiapophsyeal fossa; **PRDL**, prezygodiapophyseal lamina; **PRE**, prezygapophysis; **PRSL**, prespinal lamina; **SPDL**, spinodiapophsyeal lamina; **SPOL**, spinopostzygapophyseal lamina. The number 1* indicates the autapomorphy described in the text: dorsal centra with weakly developed anterior condyle. Scale bar equals 100 mm.

diagnostic characters of *Paludititan*, together with a more detailed anatomical description and comparison.

Titanosauria Bonaparte & Coria, 1993
Lithostrotia Upchurch, Barrett & Dodson, 2004
Eutitanosauria Sanz, Powell, Le Loeuff, Martínez & Pereda Suberbiola, 1999
Paludititan Csiki, Codrea, Jipa-Murzea & Godefroit, 2010
Paludititan nalatzensis Csiki, Codrea, Jipa-Murzea & Godefroit, 2010
(Figs. 45–50)

Holotype. Individual D: three dorsal vertebrae (UBB NVM 1-43, UBB NVM 1-44, UBB NVM 1-45), several ribs and rib fragments (UBB NVM 1-12, UBB NVM 1-20, UBB NVM 1-22 to UBB NVM 1-25, UBB NVM 1-27 to UBB NVM 1-42), three anterior caudal vertebrae (UBB NVM 1-3, UBB NVM 1-50, UBB NVM 1-58), three anterior mid-caudal vertebrae (UBB NVM 1-1 – two vertebrae in connection, UBB NVM 1-2), six mid-posterior caudal vertebrae (UBB NVM 1-21, UBB NVM 1-26, UBB NVM 1-46, UBB NVM 1-47, UBB NVM 1-48, UBB NVM 1-49), several fragments of caudal vertebrae (UBB NVM 1-19, UBB NVM 1-57), 12 incomplete chevrons (UBB NVM 1-4 to UBB NVM 1-9, UBB NVM 1-15 to UBB NVM 1-18, UBB NVM 1-24), partial right pelvis including almost complete pubis, ischium and acetabular part of the ilium, in articulation (UBB NVM 1-13), left ischium (UBB NVM 1-45), fragment of right femur (UBB NVM 1-53), and two ungual phalanges (UBB NVM 1-10, UBB NVM 1-11). Several other fragments are either incompletely prepared (e.g. UBB NVM 1-59) or unidentified in the original publication (UBB NVM 1-51, UBB NVM 1-52, here we identify them as clavicles).

Locality and distribution. Sânpetru Formation, Nălaț-Vad, Haţeg Basin, Romania. The UBB NVM 1

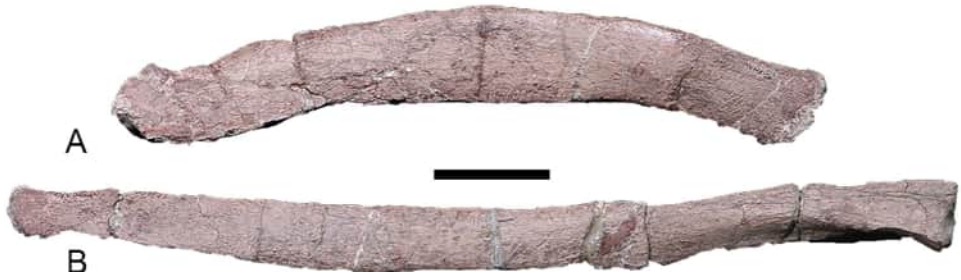

Figure 46. *Paludititan nalatzensis*, thoracic ribs (Individual D) in **A,** lateral?; and **B,** medial views. Scale bar equals 100 mm.

specimen comes from site 10 of Smith et al. (2002); according to van Itterbeeck et al. (2004), the position of site 10 corresponds to the dark palaeosoil horizon at 56–58 metres.

Revised diagnosis. *Paludititan nalatzensis* can be diagnosed on the basis of two autapomorphies (marked with an asterisk), as well as two 'local' autapomorphies: (1) dorsal centra with weakly developed anterior condyle*; (2) ischiadic peduncle of the ilium unusually well developed dorsoventrally, with an anteroposteriorly elongate distal end*; (3) iliac peduncle of ischium bearing a posterolateral buttress (i.e. a raised area on the posterolateral margin of its proximal part); (4) non-coplanar distal ischia.

Comment. Csiki, Codrea, et al. (2010) proposed a list of four autapomorphies (comprising three vertebral features and one corresponding to the ischium) and two putative ones (pertaining to the lamination of the posterior dorsal vertebrae and the pubis). These authors also noted that *Paludititan* possesses a unique combination of three character states pertaining to the axial skeleton. All of these character states have been reviewed in the current work: although some are no longer recognized as autapomorphies, additional autapomorphies have been newly identified.

Individual V (LPB [FGGUB] R.2715), comprising 10 caudal vertebrae and one chevron, recovered from the lower part of the unnamed middle member of the Densuș-Ciula Formation (lower part of the lower Maastrichtian) at locality K2, was preliminarily suggested to be closely comparable to *Paludititan* (Botfalvai et al., 2021). This assessment was based on a caudal vertebral feature ("presence of amphiplatyan and platycoelous caudal vertebrae intercalated between procoelous caudal vertebrae in the mid-section of the tail"; Csiki, Codrea, et al., 2010, p. 302) that is no longer regarded as an autapomorphy of *Paludititan* in our revised diagnosis, and thus cannot be used as a unique feature to unite these two individuals. Furthermore, the K2 titanosaur material requires further preparation and detailed study before such a referral can be supported.

Description and comparisons of *Paludititan nalatzensis*

Dorsal vertebrae. One anterior (UBB NVM 1-43) and two middle–posterior (UBB NVM 1-44 and 1-45) dorsal vertebrae of *Paludititan* are known (Fig. 45). UBB NVM 1-43 is the most complete specimen (Fig. 45A–F), preserving the centrum and much of the neural arch and spine (though lacking most of the processes), with details visible mostly only on the right side (Fig. 45C, D). However, it is poorly preserved in many places, and somewhat deformed (e.g. the neural spine has been distorted to project almost entirely posteriorly). UBB NVM 1-44 (Fig. 45G–J) preserves the centrum and base of the neural arch; the right side has been partly sheared, such that it is dorsally displaced relative to the left side. UBB NVM 1-45 preserves the anterior half of the centrum and most of the neural arch and spine, although the latter is now separated from the rest (Fig. 45K–N).

The internal camellate structure of the vertebra is clearly visible in UBB NVM 1-43. The elongated nature of each centrum can be confirmed, mainly because of the better preservation of the two more anterior dorsal vertebrae. All of the centra are opisthocoelous, although the anterior surfaces are only gently convex. This distinguishes them from the dorsal vertebrae of *Magyarosaurus*, as well as most somphospondylans, which are characterized by a prominent anterior condyle throughout the dorsal series (Salgado et al., 1997). As such, the presence of a mildly convex anterior condyle is regarded as a local autapomorphy of *Paludititan*. The ventral surface of each centrum is transversely convex and lacks ridges or fossae (Fig. 45F). In lateral view, the ventral margin of UBB NVM 1-43 is concave. Generally, the single lateral pneumatic openings are eye-shaped and occupy most of the length of the non-condylar centrum; they extend over approximately the dorsal two-thirds in UBB NVM 1-43 (Fig. 45A, C, D), and the dorsal half of the UBB NVM 1-44 centrum (Fig. 45G, I). These pneumatic openings are deep but do not seem to ramify dorsally or ventrally. There is no clear evidence that these pneumatic spaces were divided by a ridge internally, but they are not well enough

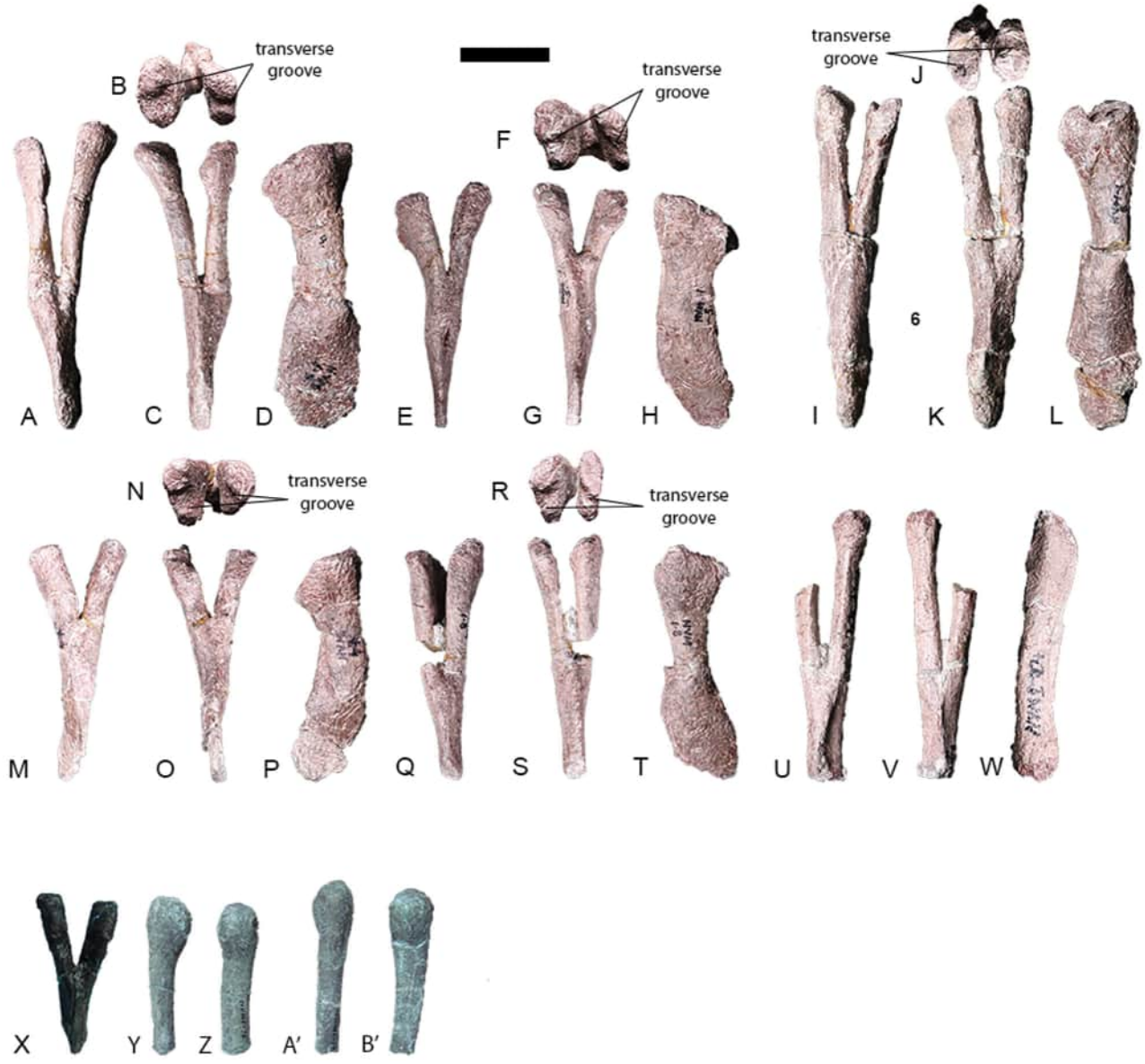

Figure 47. *Paludititan nalatzensis*, chevrons (Individual D). UBB NVM 1-4 in **A,** anterior; **B,** proximal (posterior towards bottom); **C,** posterior; and **D,** right lateral views. UBB NVM 1-5 in **E,** anterior; **F,** proximal (posterior towards bottom); **G,** posterior; and **H,** left lateral views. UBB NVM 1-6 in **I,** anterior; **J,** proximal (posterior towards bottom); **K,** posterior; and **L,** right lateral views. UBB NVM 1-7 in **M,** anterior; **N,** proximal (posterior towards bottom); **O,** posterior; and **P,** right lateral views. UBB NVM 1-8 in **Q,** anterior; **R,** proximal (posterior towards bottom); **S,** posterior; and **T,** left lateral views. UBB NVM 1-15 in **U,** anterior; **V,** posterior; and **W,** left lateral views. UBB NVM 1-9 in **X,** posterior view. UBB NVM 1-16 in **Y,** anterior; and **Z,** posterior views. UBB NVM 1-17 in **A′**, anterior; and **B′**, posterior views. Scale bar equals 50 mm.

preserved for this to be determined with certainty. The lateral pneumatic opening of UBB NVM 1-43 does not seem to be set within a wider fossa; that in UBB NVM 1-44 probably was set within such a fossa, although it is difficult to discern.

No hyposphene-hypantrum complex is present, as is also typical of the dorsal vertebrae of nearly all titanosaurs, with the exception of *Andesaurus* and *Epachthosaurus* (Martínez et al., 2004; Salgado et al., 1997; Upchurch, 1998), as well as some specimens of *Patagotitan* (Carballido et al., 2017). In UBB NVM 1-43, the neural arch does not extend to the posterior margin of the centrum. Neither the anterior or posterior neural canal openings are well enough preserved in this vertebra to be entirely certain of their outlines, but they were probably dorsoventrally tall and elliptical. Poor preservation in most specimens means that it is not possible to unequivocally determine whether the anterior

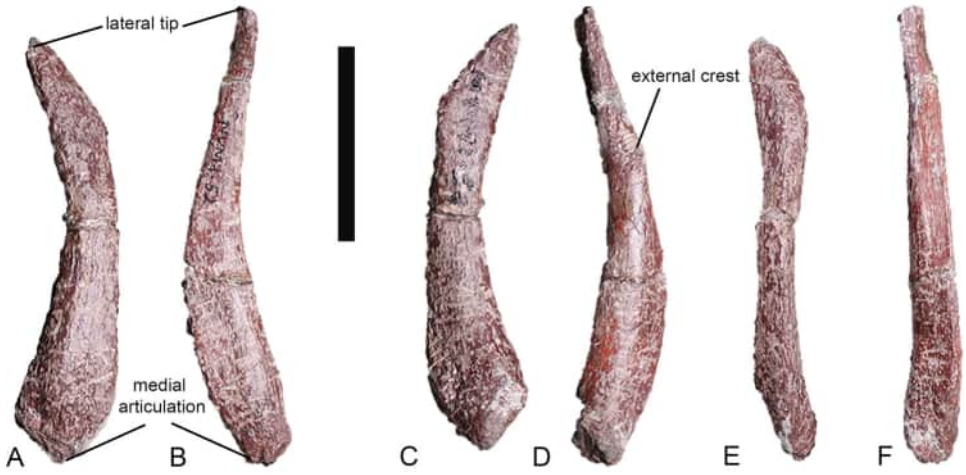

Figure 48. *Paludititan nalatzensis*, clavicles (Individual D). UBB NVM 1-51 in **A,** internal; **C,** external; and **E,** anterior? views. UBB NVM 1-52 in **B,** internal; **D,** external; and **F,** anterior? views. Scale bar equals 50 mm.

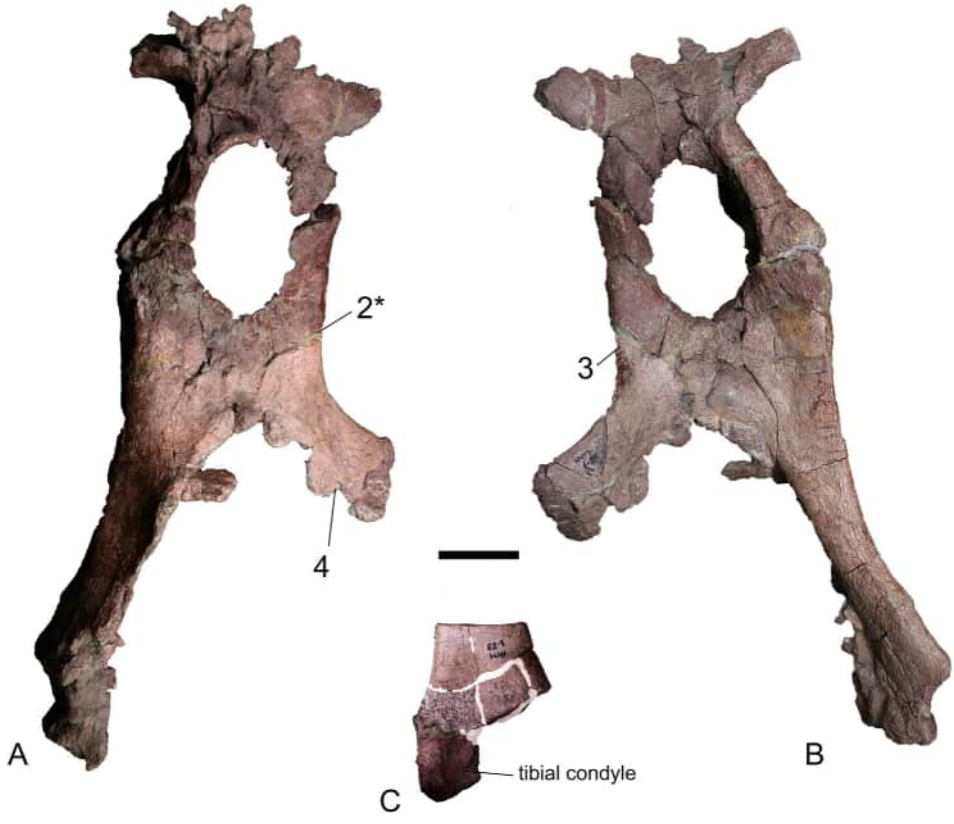

Figure 49. *Paludititan nalatzensis*, partial right pelvis (Individual D) including an almost complete pubis, ischium and acetabular part of the ilium, in articulation (UBB NVM 1-13) in **A,** medial; and **B,** lateral views. Right femur UBB NVM 1-53 (Individual D) in **C,** posterior view. The numbers 2*, 3 and 4 indicate the autapomorphies described in the text: ischiadic peduncle of the ilium unusually well developed dorsoventrally, with an anteroposteriorly elongate distal end; iliac peduncle of ischium bears a posterolateral buttress (i.e. a raised area on the posterolateral margin of its proximal part; and respectively non-coplanar distal ischia. Scale bar equals 100 mm.

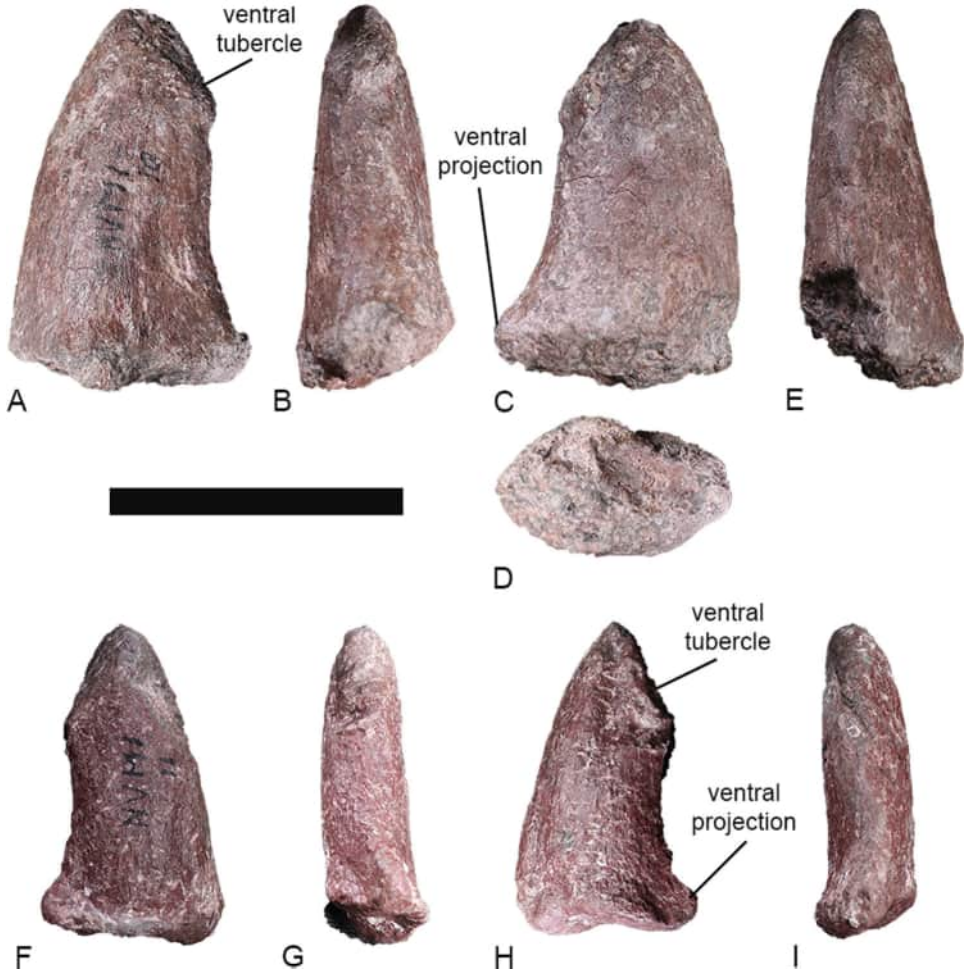

Figure 50. *Paludititan nalatzensis*, pedal unguals (Individual D). Right pedal ungual from digit I or II UBB NVM 1-10 in **A,** lateral; **B,** ventral; **C,** medial; **D,** distal (medial towards top); and **E,** dorsal views. Left pedal ungual from digit III UBB NVM 1-10 in **F,** lateral; **G,** dorsal; **H,** medial; and **I,** ventral views. Scale bar equals 50 mm.

neural canal opening was set within a fossa, but this does seem to be the case in UBB NVM 1-45, in which the anterior neural canal opening is clearly dorsoventrally tall and elliptical. The right prezygapophysis is preserved in UBB NVM 1-43 (Fig. 45C, D); although almost certainly accentuated by crushing, its flat articular surface is strongly tilted to face dorsomedially. A PRDL is preserved, but little information can be ascertained regarding its morphology (Fig. 45D). The prezygapophyseal articular surfaces in UBB NVM 1-45 are flat and much more gently inclined (less than 30° to the horizontal) than in UVV NVM 1-43. It is not possible to fully determine the morphology of the CPRL. Although each CPRL appears to be single in UBB NVM 1-45, poor preservation of their anterior surfaces makes this uncertain. A small, poorly preserved TPRL, which is 'V'-shaped in anterior view, is present in UBB NVM 1-43 (Fig. 45B).

Parapophyses are only preserved in specimens UBB NVM 1-43 (the right parapophysis) and NVM 1-45. The parapophysis of UBB NVM 1-43 is situated on the lower part of the arch, extending ventrally to the centrum-arch junction (Fig. 45D), suggesting that this was an anterior dorsal vertebra, in approximately position D3. This parapophysis has a dorsoventrally tall, elliptical shape, and does not seem to extend beyond the anterior margin of the non-condylar centrum. By contrast, the parapophyses are situated at the level of the ventral margin of the prezygapophyseal articular surfaces in UBB NVM 1-45 (Fig. 45N), suggesting that this specimen is a middle or posterior dorsal vertebra. The parapophyses in the latter specimen are much shorter dorsoventrally than in UBB NVM 1-43. Each parapophysis is supported from below by a steep, anterodorsally oriented ACPL. PCPLs are present on both sides of UBB NVM 1-45, where they appear to be singular,

although neither side is well enough preserved to confirm the latter. A PPDL is present on both sides in UBB NVM 1-43, extending posterodorsally at approximately 45° to the horizontal. The PCDL, PPDL and parapophysis bound a parapophyseal centrodiapophyseal fossa (PACDF). The diapophyses are preserved in UBB NVM 1-43, and project dorsolaterally (Fig. 45B, E); although this seems to be slightly more lateral than normal, this is almost certainly the result of dorsoventral crushing of the neural spine, and the diapophysis has also been very slightly displaced. The distal end of the diapophysis of UBB NVM 1-43 is incomplete, and therefore we cannot determine the morphology of its dorsal surface. ACDLs are present in UBB NVM 1-44 and 45. These laminae are posterodorsally directed (most clearly seen on the right side) in UBB NVM 1-44, and are distinct from the ventral expansion of the PCDL. The ACDL curves posterodorsally, rather than being straight, in UBB NVM 1-45. Csiki, Codrea, et al. (2010, p. 302, fig. 2C1) regarded the morphology of the ACDL as an autapomorphy of *Paludititan*: 'the dorsal segment of the anterior centrodiapophyseal lamina curves anterodorsally and extends parallel to the dorsal segment of the posterior centrodiapophyseal lamina', which led those authors to interpret the presence of an accessory ACDL. However, we re-interpret this as a taphonomic artefact, resulting in the posteroventral displacement of the ACDL, with no evidence for an accessory lamina (Fig. 45N); as such, we exclude this feature from our revised diagnosis of *Paludititan*. The ACDL and PCDL define a CDF. A PACDF or PRCDF (it is not certain which fossa is present because of the poor preservation of the roofing lamina, i.e. PPDL or PRDL) is present in UBB NVM 1-45, anterior to the ACDL, and bounded anteriorly by the ACPL and parapophysis/prezygapophysis. The PCDL is near-vertical in UBB NVM 1-45, whereas it is steeply oriented anterodorsally in the middle–posterior dorsal vertebrae. It is slightly expanded at its ventral end, but it is not bifurcated.

The left postzygapophysis is partially preserved in UBB NVM 1-43, though distorted, whereas only the very base of the right postzygapophysis remains (Fig. 45C–E). Because of the distortion to the spine, the articular surface of the right postzygapophysis faces primarily medially. The postzygapophyseal articular surfaces are flat and face posteroventrally, as well as partly laterally, in UBB NVM 1-45 (Fig. 45M, N). Neither CPOL is clearly preserved in UBB NVM 1-43, although it is possible to trace their approximate positions. The bases of the CPOLs are preserved in UBB NVM 1-44, where they project posterodorsally. In UBB NVM 1-45, each CPOL appears to be single (i.e. unbifurcated) and vertical (Fig. 45M, N). No PODLs are present in any of these vertebrae, but this absence could reflect poor preservation. A POCDF is defined by the PCDL, CPOL and SPDL in UBB NVM 1-43 and 45 (Fig. 45D, N).

The neural spine of UBB NVM 1-45 is the best-preserved of the three dorsal vertebrae, and it projects strongly posterodorsally (Fig. 45K, M, N). In lateral view, it has approximately parallel anterior and posterior margins, with a slight degree of anteroposterior shortening dorsally. Its dorsal tip is not preserved, but probably only a small amount of bone is missing, and clearly it was not bifurcated. In anterior view, the neural spine of UBB NVM 1-45 has a subtriangular outline, narrowing in transverse width dorsally (Fig. 45L). There is evidence for weakly developed aliform processes where the SPOLs and SPDLs probably converge, a short distance from the spine summit. The distal neural spine morphology is very unclear because of its poor preservation in all three dorsal vertebrae. There is no clear evidence for SPRLs as a result of the poor preservation of much of the anterior surface of the neural spine of UBB NVM 1-43. These laminae are also not preserved in UBB NVM 1-45, but it is unlikely that they were prominent structures in life. There are remnants of what could be portions of a possible midline PRSL at the base of the spine, and again just above midheight of the latter, but both areas might just be broken surfaces. A prominent midline PRSL is present along the length of the neural spine of UBB NVM 1-45 (Fig. 45N), although this flattens close to the spine summit, with the anterior surface of the spine becoming strongly convex transversely in this region. A midline POSL is present in UBB NVM 1-43 and 45. The SPOLs of UBB NVM 1-43 are mainly vertically oriented (with a slight medial deflection), and are clearly restricted to the posterolateral margins of the neural spine (Fig. 45D, N). In UBB NVM 1-45, these laminae are poorly preserved, and it is not possible to determine if they were bifid. One prominent, unbifurcated SPDL is present on each side in UBB NVM 1-45. As preserved, the long axis of the SDF is essentially horizontal, but this is clearly the result of taphonomic damage.

Thoracic ribs. Csiki, Codrea, et al. (2010) reported that a number of plank-like ribs are preserved in *Paludititan* (Fig. 46). No pneumatic features are visible, although no proximal ends are preserved. There is a hollow filled with matrix visible in the cross-section in some of these elements, which was interpreted as evidence for pneumaticity by Csiki, Codrea, et al. (2010), but this is present in many sauropod ribs and appears to have been non-pneumatic (Waskow & Sander, 2014).

Caudal vertebrae. Seven anterior caudal vertebrae are preserved in *Paludititan*, and can be ordered into a

series: UBB NVM 1-58, 1-50, 1-3, 1-2, 1-1 (the latter specimen comprises two articulated caudal vertebrae), and 1-21 (Csiki, Codrea, et al., 2010, fig. 3). Of these, UBB NVM 1-58 and 50 are more poorly preserved than the others. Although from the anterior region of the tail, none of these specimens represent the anterior-most caudal vertebrae. The aEI of these seven vertebrae ranges from 0.94 to 1.33, encompassing the typical range of aEI values of anterior caudal centra observed in several early-branching titanosaur taxa (see above). All of the centra are procoelous, with a deeply concave anterior articular surface that has a circular profile (Csiki, Codrea, et al., 2010, fig. 3E), with the exception of UBB NVM 1-21, which is elliptical. The posterior condyle is prominent but has a constricted base, shifted slightly dorsally (Csiki, Codrea, et al., 2010, fig. 3D, F), and those of UBB NVM 1-1 and 21 are less well developed than the others. The ventral surface of each centrum is flat (Csiki, Codrea, et al., 2010, fig. 3G, I), rather than possessing a ventral hollow as described by Mocho et al. (2023), and becomes more transversely compressed passing distally along the series. Ventrolateral longitudinal ridges are only present on the centrum of some anterior caudal vertebrae (i.e. UBB NMV 1-1 and 3). The posterior chevron facets are more developed than the anterior ones. The articular surfaces of the posterior chevron facets face posteroventrally, and project far below the condyle, especially in UBB NVM 1-3. In the more anteriorly placed UBB NVM 1-1 vertebra, there is a low longitudinal ridge on the lateral surface of the centrum at approximately midheight. This ridge demarcates where the lateral surface meets the ventrolaterally facing surface that extends toward the ventral midline (see also Salgado & García, 2002). However, there is no equivalent morphology in the more posterior caudal vertebra UBB NVM 1-3.

The transverse processes are located below the junction between the neural arch and the centrum (Csiki, Codrea, et al., 2010, fig. 3C, D, H). These processes are large rounded bulges in UBB NVM 1-3 and 1-1, whereas they are smaller and posterolaterally oriented in UBB NVM 1-2. In the latter vertebra, and in UBB NVM 1-50, the transverse processes are dorsally delimited by a prominent ridge. The prezygapophyses are long, and become more anterodorsally directed passing distally along the series. They are not connected by a distinct TPRL at their bases, unlike those of middle caudal vertebrae (see below). The articular surfaces of the prezygapophyses face dorsomedially in UBB NVM 1-3, and entirely medially in UBB NVM 1-1. In UBB NVM 1-3 and 1-1, the postzygapophyses are short, with laterally facing surfaces with a circular outline. The neural spine is low and nearly vertical, being slightly posterodorsally inclined. Both SPRLs and SPOLs are present on the neural spine as single (i.e. unbifurcated) laminae (Csiki, Codrea, et al., 2010, fig. 3D, H). SPRLs arise on the dorsal aspect of the prezygapophyses laterally, and the next end posteriorly and medially to meet the PRSL approximately at its midlength. The SPOLs extend lateral to the POSL. The PRSL and POSL are wide and rugose laminae that extend over almost the complete length of the neural spine. The dorsal tips of the PRSL and POSL are slightly anteriorly and posteriorly extended as ‘spurs’, probably for the attachment of the deep epaxial musculature. In the plate-like neural spines of UBB NVM 1-3 and 1, a deep SPRF is present between the SPRLs. A deep SPOF is also present between the two vertical SPOLs.

Four middle caudal vertebrae are preserved in *Paludititan* (UBB NVM 1-46, 1-47, 1-48 and 1-49) (Csiki, Codrea, et al., 2010, fig. 4A–F). The centra have a concave to flattened anterior surface. UBB NVM 1-48 is procoelous, whereas UBB NVM 1-49 has a flat posterior articular surface. UBB NVM 1-46 is a slightly procoelous to amphyplatyan caudal vertebra, and UBB NVM 1-47 is platycoelous. UBB NVM 1-46 and 1-47 have articular surfaces with circular outlines, whereas the centrum is transversely compressed in UBB NVM 1-48 and 1-49. The posterior articular surfaces of UBB NVM 1-46, 1-47 and 1-49 have a heart-shaped outline, but with a rounded ventral edge (Csiki, Codrea, et al., 2010, fig. 4C). The ventral surface of the centrum is flat and slightly transversely constricted in UBB NVM 1-47, 1-48 and 1-49, whereas no transverse constriction is present in the similarly flat ventral surface of UBB NVM 1-46. No ridges are present on the ventral surface of any specimen. A prominent longitudinal ridge is present close to the midheight of the lateral surface of the centrum in UBB NVM 1-49. All specimens possess a longitudinal ridge demarcating the junction between the centrum and the anteriorly located neural arch. In UBB NVM 1-47 and 1-49, these ridges are approximately half the length of the base of the neural arch, but they are more posteriorly extensive in UBB NVM 1-46. The prezygapophyses are short, oriented almost horizontally, and are joined at their bases by a well-developed TPRL. The postzygapophyseal articular facets, preserved in UBB NVM 1-46 and 49, are ellipsoidal, with their articular surfaces oriented ventrolaterally. The neural spine is not complete in any of the four specimens, but was probably low, long and posteriorly directed, with a slight dorsal deflection. Two sharp SPRLs delimit a deep SPRF in UBB NVM 1-49 (Csiki, Codrea, et al., 2010, fig. 4F). Between the short and almost vertical SPOLs, a deep SPOF is also present in this specimen.

Chevrons. Of the 12 chevrons described by Csiki, Codrea, et al. (2010), 10 could be located by us in the UBB collections (UBB NVM 1-4, -5, -6, -7, -8, -9, -16, -17, -18 and -24, Fig. 47). UBB NVM 1-6 is the largest chevron of the available sample (Fig. 47I–L), whereas UBB NVM 1-9 seems to have been the smallest chevron, although it is not complete (Fig. 47X). Only the proximal part of a transversely compressed blade is preserved of chevron UBB NVM 1-18. Although the anatomical order of these chevrons is not known on the basis of articulation with caudal vertebrae or other field associations, a combination of relative size and morphological gradients can be used to infer an approximate sequence. From anterior-most to posterior-most, this inferred sequence is: UBB NVM 1-16, 1-17, 1-24, 1-6, 1-4, 1-5, 1-9 (N.B. the relative positions of the remaining three available chevrons are more uncertain, but they are likely to have been located between 1-5 and 1-9). These elements sample those ranging from near the anterior end of the tail to approximately its middle (which is consistent with the seven anterior and four middle caudal vertebrae preserved in this partial skeleton), but are unlikely to represent a continuous series. If our estimated sequence is correct, it seems that the chevrons increased in length from UBB NVM 1-16 (Fig. 47Y, Z) to UBB NVM 1-6 (Fig. 47I–L), and then shortened again towards the middle of the tail.

All preserved chevrons are 'Y'-shaped in anterior/posterior view (i.e. the haemal canal is not bridged by bone proximally), although the proximal rami diverge only slightly from one another. The ratio between the proximodistal length of the haemal canal and that of the entire chevron varies between 0.36 and 0.57, with higher ratios in the more anteriorly placed elements. The anterior-most chevrons (UBB NVM 1-16 and 1-17, Fig. 47Y–AB) have single articular facets, whereas the other elements have proximal facets that are divided by a transverse groove that is anteroposteriorly widest at its medial end. The resultant anterodorsal articular surface is slightly larger than its posterodorsal counterpart, except in UBB NVM 1-7 (Fig. 47N) and 8 (Fig. 47J), where these facets are equidimensional. As noted above, such a groove is absent from the chevrons of *Magyarosaurus*, but *Paludititan* shares this feature with several South American titanosaurs (Poropat et al., 2016; Powell, 2003; Santucci & Arruda-Campos, 2011), as well as *Lohuecotitan* (Díez Díaz et al., 2016). The proximal rami of *Paludititan* chevrons lack the lateral ridges present in *Magyarosaurus* and several other titanosaurs (see above). In the anterior-most chevrons (UBB NVM 1-16 and 1-17), the distal blade has a subcircular cross-section. The next two chevrons in our inferred sequence (UBB NVM 1-24 and 1-6) display the onset of more transverse compression of the distal blade, but retain strongly convex (anteroposteriorly) lateral surfaces. This trend continues in the remaining chevrons, such that the distal blade is transversely compressed and anteroposteriorly expanded, with a rounded distal end profile. The more anterior chevrons (UBB NVM 1-16, 1-17, 1-24, 1-6 and 1-4) are nearly straight in lateral view, but the distal blade starts to curve more posteriorly relative to the proximal rami from UBB NVM 1-5 onwards. From this list of anterior chevrons only UBB NVM 1-24 presents a rounded, slightly anteriorly located, prominence on the lateral surface at the junction of the ramus and the blade, probably for the attachment of the ventral part of the M. caudofemoralis longus. Anterior and posterior midline crests are present along the length of the distal blade of this chevron. However, in UBB NVM 1-5 (Fig. 47H) no bulges or rugosities are visible, which could indicate that the distal tip of the M. caudofemoralis longus was located anteriorly to this section of the tail.

The best-preserved and most complete chevrons in the sample present the 'open Y'-shaped morphology described by Otero et al. (2012, fig. 2).

Clavicle. Two unidentified bones (UBB NVM 1-51, 52, Fig. 48) were included within the holotype, but not described by Csiki, Codrea, et al. (2010). Following Tschopp and Mateus (2013), we tentatively interpret these specimens as 'morphotype B'-type clavicles. Both are slender, elongate, curved elements. These taper at their lateral (?) tip and expand transversely as they approach the medial (?) articulation. UBB NVM 1-51 (Fig. 48A, C, E) is more anteroposteriorly compressed than UBB NVM 1-52 (Fig. 48B, D, F). The medial (?) half of UBB NVM 1-52 has a convex external surface (Fig. 48D), whereas the internal one is flat (*sensu* Tschopp & Mateus, 2013) (Fig. 48B). The specimen is gently curved, and the convex edge has a crest that terminates before reaching the lateral (?) tip. The lateral (?) half has a more subcircular cross-section. The general morphology of these specimens contrasts with the typical 'L'-shaped clavicles found in some diplodocids (Schwarz et al., 2007; Tschopp & Mateus, 2013), but they are not as straight as that in the non-neosauropod eusauropod *Spinophorosaurus* (Remes et al., 2009). This is the first report of a clavicle in a titanosauriform sauropod.

Ilium. The right ilium UBB NVM 1-13 (Fig. 49A, B) preserves the acetabular region, as well as portions of the preacetabulum and postacetabulum (Csiki, Codrea, et al., 2010, fig. 5). Because the specimen is very incompletely preserved, it is not possible to determine the orientation of the preacetabular process, nor is it

possible to be entirely certain of the orientation of the pubic peduncle relative to the long axis of the ilium. No triangular fossa is present on the lateral surface of the upper portion of the pubic peduncle. The distal end of this peduncle has a comma-shaped outline that tapers in anteroposterior width medially, with a transversely long, straight to mildly concave posterior margin. In this regard, it clearly differs from the distal pubic peduncle of *Petrustitan* (see above, Fig. 39). The pubic peduncle appears to be unusually dorsoventrally elongate in *Paludititan*, but this might be a false impression given by the incomplete nature of the main body of the ilium. The ischiadic peduncle is unusually well developed in terms of dorsoventral extent and distal anteroposterior width compared to other eusauropods (see also Csiki, Codrea, et al., 2010, fig. 5A, C), which we regard as an autapomorphic feature of *Paludititan*. The distal end of the ischiadic peduncle has a comma-shaped outline, decreasing in anteroposterior width medially. This transversely convex articular surface is strongly deflected to face laterally, as well as ventrally and very slightly posteriorly. No tubercles are present on the lateral surface of the ischiadic peduncle, such as those described in *Diamantinasaurus*, *Opisthocoelicaudia* and *Rapetosaurus* (Borsuk-Białynicka, 1977; Curry Rogers, 2009; Poropat, Upchurch, et al., 2015). There is some evidence for pneumatic pockets on the broken dorsal margin of the element, suggesting that *Paludititan* possessed the derived pneumatized ilium seen in many other somphospondylans (Mannion et al., 2013; Wilson & Sereno, 1998).

Pubis. The right pubis UBB NVM 1-13 (Fig. 49A, B) is almost complete in terms of length (Csiki, Codrea, et al., 2010, fig. 5), but its distal end is poorly preserved, and the posterior margin is incomplete distal to the ischiadic articulation. Despite the relevant area being preserved, albeit fractured, the obturator foramen cannot be observed. The anterior margin of the proximal end is too poorly preserved to determine whether or not an ambiens process was present. The pubic blade is strongly twisted relative to the proximal end, such that what would usually be described as the lateral surface faces primarily posteriorly. This posterolateral surface is gently convex anteroposteriorly along its proximal half, but flattens distally. It lacks any distinct longitudinal ridge and groove, contrasting with the lateral surface of the pubis of several titanosaurs, including *Epachthosaurus*, *Isisaurus*, saltasaurines and *Uberabatitan* (Otero, 2010; Poropat et al., 2016; Powell, 2003; Salgado & Carvalho, 2008). The distal end is too poorly preserved to unequivocally state that it did not expand mediolaterally, although such an expansion seems unlikely.

Ischium. The right ischium UBB NVM 1-13 (Fig. 49A, B) is essentially complete (Csiki, Codrea, et al., 2010, fig. 5), with only the very distal end poorly preserved, and some of the anteroventral margin of the distal blade missing. The iliac peduncle has a raised area on the posterolateral margin of its proximal end, described as a posterolateral buttress by Csiki, Codrea, et al. (2010), who noted that this feature is otherwise only known in a specimen attributed to *Ampelosaurus*. We herein follow these authors in regarding this as a local autapomorphy of *Paludititan*. The medial margin of the acetabulum is broken away, such that the presence of an anteromedial flange on the iliac peduncle cannot be ascertained, and it is also uncertain whether the acetabulum maintained a constant mediolateral width. It appears that there is no prominent upturning of the anterodorsal corner of the acetabulum, such as that which characterizes many titanosaurs (D'Emic, 2012), although this region is not fully preserved. On the lateral surface of the ischium, close to its posterior margin and situated at approximately mid-height of the pubic plate, a very prominent ridge marks the attachment of M. flexor tibialis internus III. This ridge projects laterally and is not associated with a groove. The long axis of the distal blade, if extrapolated anteriorly, passes through the pubic articular surface, and forms a right angle with a line drawn between the anterior margin of the proximal end of the iliac peduncle and the anterodorsal corner of the pubic peduncle. The ventral margin of the blade is too incomplete to determine the nature of the symphysis between the ischia. The distal end of the ischium is little expanded mediolaterally or dorsoventrally relative to the more proximal part of the blade. Based on the orientation of the ischium with the iliac articular surface held in a horizontal plane, it seems unlikely that the long axes of the distal end surfaces of the ischia would have been coplanar. This contrasts with most somphospondylans (Upchurch, 1998; Wilson & Sereno, 1998), in which the derived coplanar condition is present, although *Muyelensaurus*, *Neuquensaurus*, *Patagotitan* and *Rinconsaurus* also lack coplanar distal ischia (Mannion, Upchurch, Jin, et al., 2019).

Femur. The distal end of a femur (UBB NVM 1-53) was recovered, although it is poorly preserved (Fig. 49C). It is probably a right element, although this is difficult to confirm because it is missing a large amount of the distal articular region, only preserving the posteromedial portion of what we interpret as the tibial condyle. If correct, then the tibial condyle is narrower mediolaterally than the fibular distal condyle, almost certainly displaying the derived state that characterizes most somphospondylans, wherein the tibial to fibular condyle width ratio is <0.8 (Poropat et al., 2016). The distal articular surface is strongly convex anteroposteriorly, curving up onto the

posterior surface. Although Csiki, Codrea, et al. (2010) noted that the shaft cross-section is not as anteroposteriorly compressed (ECC = 1.69) as occurs in some titanosaurs, this fragment does not preserve the midshaft where the measurements for calculating eccentricity are normally taken.

Pedal unguals. Two pedal unguals are known; UBB NVM 1-10 (Fig. 50A–E), a right pedal ungual from either digit I or II (Csiki, Codrea, et al., 2010); and UBB NVM 1-11 (Fig. 50F–I), a left pedal ungual from digit III. The general morphology of both unguals, crescent-shaped and transversely compressed, is typical for eusauropods (Wilson & Sereno, 1998), and is retained by most titanosaurs, e.g. *Dreadnoughtus*, *Rapetosaurus* and *Mendozasaurus* (Curry Rogers, 2009; González Riga et al., 2018; Ullmann & Lacovara, 2016). It is not possible to discern the nature of the proximal bevelling of UBB NVM 1-10, because its proximal articular surface is poorly preserved along its medial half. However, the proximal articular surface of UBB NVM 1-11 faces proximolaterally relative to the long axis of the ungual, such that it would have projected anterolaterally in life, as is typical for most eusauropods (Poropat et al., 2016; Wilson & Upchurch, 2009). The proximal ends have dorsoventrally elongated elliptical outlines (Fig. 50D). The ventral margin of the proximal end forms a projection (flexor tubercle) that is somewhat more prominent in UBB NVM 1-11 than in UBB NVM 1-10. The dorsal margin of the proximal end is incomplete in the latter specimen, but is preserved in the former, where it projects less prominently than the ventral one. In medial/lateral views, the dorsal margin of each ungual is convex. The ventral surfaces are rugose on the distal third of the claw, with a well-developed tubercle, as in other somphospondylans (Canudo et al., 2008; Mannion et al., 2013), including the titanosaurs *Dreadnoughtus* (Ullmann & Lacovara, 2016), *Epachthosaurus* (Martínez et al., 2004), *Malawisaurus* (Gomani, 2005), and *Mendozasaurus* (González Riga et al., 2018). Distal to this ventral tubercle, both the dorsal and the ventral margins narrow dorsoventrally towards the distal tip in UBB NVM 1-10. The ventral margin is concave throughout its length in UBB NVM 1-10 in lateral/medial views, whereas it is only concave proximal to the ventral tubercle in UBB NVM 1-11. Distal to this tubercle, in the latter ungual, the ventral margin is deflected to face anteroventrally.

Additional individuals and assemblages

In this section we describe individuals and assemblages whose elements do not present sufficient similarities with those referred to the nominal titanosaur taxa described above to justify referral, and/or whose remains are not diagnostic enough to erect new taxa. Nonetheless, they help to understand the titanosaurian diversity of the Haţeg Basin and are worth reporting here in case more complete and associated material is found in the future.

Individual H (Green Four titanosaur)

All of the specimens referred to Individual H (see 'Key localities and skeletal associations' section) are accessioned as NHMUK R.4891, and comprise a partial dorsal vertebra, two partial dorsal ribs, a left scapula, coracoid and sternal plate, and three right metacarpals.

Dorsal vertebra. This specimen preserves the posterior end of the centrum and part of the arch (Fig. 51A, B). The centrum is camellate throughout. Despite the centrum being heart-shaped in posterior view, there is no ventral midline keel. The posterior end of the lateral pneumatic opening is preserved. This opening is deep, although the midline septum appears to have been mediolaterally thick, but it is possible that the septum thinned anteriorly. No further detailed comparisons with remains attributed to the named titanosaurs of the Haţeg Basin can be made.

Dorsal ribs. Both dorsal ribs are broken into two portions that fit together (Fig. 51C–F). First, we describe the best-preserved element (Fig. 51C, D), which probably came from the left side and is likely to have been either the most anterior rib or a very posterior one, based on its non-plank-like shaft. The capitulum and tuberculum are nearly equally prominent, and diverge from each other at approximately 80°. Thus, with the tuberculum directed dorsally, the capitulum projects medially and slightly upwards. Both of these articulations are compressed anteroposteriorly, but much of this is due to crushing. The tuberculum is slightly shorter and somewhat wider than the capitulum. Although damaged, there appears to have been a prominent vertical plate-like ridge on the anterior surface of the proximal end, extending distally from the base of the tuberculum, and curving slightly medially towards its distal end. This ridge is deflected anteromedially, creating a groove between itself and the anterior face of the base of the capitulum. This ridge fades out rapidly distally and does not extend onto the shaft. There is damage to the anterior and posterior faces of the proximal end, but there is some indication of a pocket-like depression on the posterior surface below the base of the tuberculum. In anterior/posterior views, the lateral margin of the proximal end is concave over the transition from shaft to tuberculum. Below the proximal end, the shaft starts

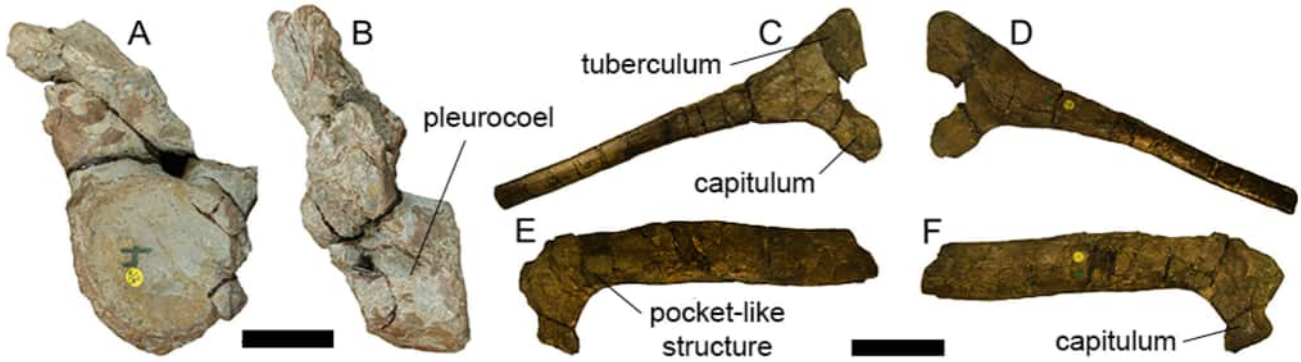

Figure 51. Lithostrotia *incertae sedis*, Individual H, dorsal vertebra and ribs NHMUK R.4891. Dorsal vertebra in **A,** posterior; and **B,** left views. ?Left dorsal rib in **C,** posterior; and **D,** anterior views. ?Left dorsal rib in **E,** anterior; and **F,** posterior views. Scale bar equals 50 mm in A, B and 100 mm in C–F.

with an anteroposteriorly compressed 'D'-shaped horizontal cross-section, with convex anterior and flat to medially concave posterior surfaces. This rapidly narrows in transverse width as it extends distally, though it maintains a cross-section that is wider transversely than anteroposteriorly throughout its length. The broken distal portion has an oval cross-section, with an anteroposteriorly wider and more rounded medial margin and a narrower sharper lateral one.

The second, less well-preserved rib preserves the damaged bases of the tuberculum and capitulum (Fig. 51E, F). Again, this is a left rib, probably from the anterior part of the series. The proximal shaft is plank-like, being at least three times wider transversely than anteroposteriorly. There is again evidence of a pocket-like structure on the posterior surface of the proximal end, below the base of the tuberculum. There is a low rounded ridge, trending in the same direction, as the plate-like structure seen on the anterior surface of the proximal end in the previous rib. The distal blade is strongly compressed anteroposteriorly and again has a more rounded medial and sharper lateral margin.

Scapula. This specimen is a left scapula missing the dorsal portion of the acromion and the distal tip of the blade (Fig. 52A–D). There are large amounts of plaster reconstruction, especially along the blade: therefore, it is difficult to be confident about the anatomy of the dorsal and ventral margins. The acromial plate seems to have been thin transversely over most of its extent, apart from the stout region posteriorly formed from the acromial ridge. It is not possible to determine the orientation of the coracoid articular surface due to incompleteness. The glenoid articular surface has a dorsoventrally elongated 'D'-shaped outline (with a flat lateral margin) and is deflected to face medially as well as anteroventrally. The medial edge of the glenoid forms a slightly projecting lip. Anterior to the acromial ridge, the lateral surface of the acromion is gently concave and featureless. The medial surface of the acromial plate is moderately concave over most of its preserved extent. The acromial ridge is anteroposteriorly broad, but not especially prominent, and is incomplete dorsally. There is no evidence for a fossa posterior to the acromial ridge. The angle between the long axes of the acromial ridge and the blade is acute, approximately 70°, but caution is required because most of the ridge is absent. There is a small tubercle on the ventral margin of the posterior end of the acromion; a subtle additional tubercle is also situated slightly anteriorly, on the medial margin of the ventral surface. No tubercle on the ventral margin of the anterior end of the blade is evident, but this region is heavily reconstructed with plaster. There are no tubercles on the medial surface of the acromion, or in the region where the acromion meets the blade.

The scapular blade is straight, projecting posteriorly and slightly medially relative to the acromial plate. It is dorsoventrally narrow, with no indication of expansion towards its distal end, but this is possibly due to damage in this area. The ventral margin of the blade is concave in lateral view, and the dorsal margin is slightly sinuous, but we cannot be certain that either morphology is accurate because of the large amount of plaster reconstruction. The lateral surface of the proximal third of the blade is gently convex dorsoventrally. Consequently, the cross-section through the base of the blade is weakly 'D'-shaped. The convexity of the lateral surface of the blade does not create a clear longitudinal ridge, and distally this surface becomes predominantly flat. The medial surface of the blade is dorsoventrally concave proximally, but is flat for most of its length. Just distal to the acromial plate, the dorsal margin of the blade gives rise to a prominent but short ridge on the medial surface, forming a short dorsal platform. A similar ridge characterizes the scapula of several titanosaurs,

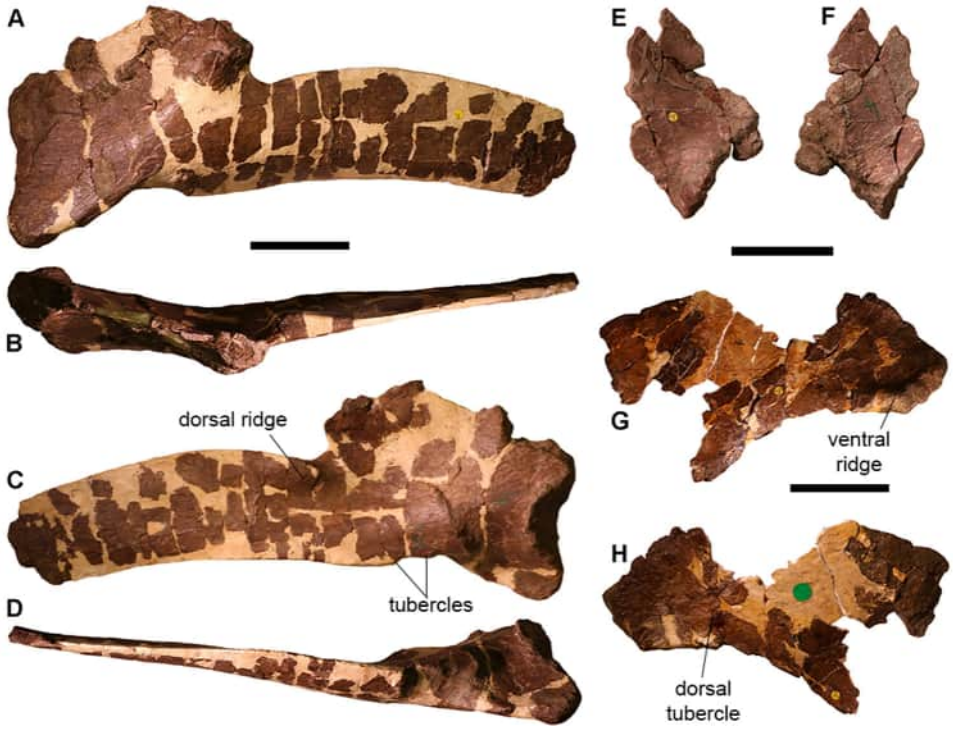

Figure 52. Lithostrotia *incertae sedis*, Individual H, scapular girdle elements NHMUK R.4891. Left scapula in **A,** lateral; **B,** dorsal; **C,** medial; and **D,** ventral views. Left coracoid in **E,** lateral; and **F,** medial views. Left sternal plate in **G,** ventral; and **H,** dorsal views. Scale bars equal 100 mm.

including *Abditosaurus*, *Lirainosaurus* and saltasaurines (Sanz et al., 1999; Vila et al., 2022). Unlike the pectoral girdles of saltasaurines (Cerda et al., 2012), there is no evidence of pneumaticity.

Coracoid. This specimen is a left coracoid that preserves the glenoid and parts of the main body (Fig. 52E, F). The only anatomical information that can be gleaned is that the glenoid articular surface does not extend onto the lateral surface of the coracoid. In this regard the coracoid is similar to that of several other titanosaurs, including *Lirainosaurus* and saltasaurines (Poropat et al., 2016).

Sternal plate. This specimen was figured by Huene (1932, pl. 47, fig. 11), who identified it as a left sternal plate, an identification that we follow here. It is preserved in three pieces (along with several small fragments) and lacks its posterior end (Fig. 52G, H). The lateral margin is concave, whereas the medial margin is convex. Although incomplete posteriorly, there is a strong posterolateral expansion: thus, the sternal plate clearly had the kidney-shape typical of later-diverging titanosaurs (Upchurch, 1998). The sternal plate thickens dorsoventrally anteriorly, with a prominent ventral ridge situated close to the lateral margin. Generally, the dorsal surface is gently convex anteroposteriorly. There is evidence for a ridge-like tubercle on the dorsal surface, situated a short distance from the medial margin and at approximately one-third of the element length from the anterior end, but the sternal plate is heavily damaged in this region.

Metacarpals I–III. These three right metacarpals were figured by Huene (1932, pl. 46, fig. 10) (Fig. 53). They are largely complete and articulated, although metacarpal I is now separated from the other elements. All three have been broken into several pieces and subsequently re-glued and their relative positions differ from that described by Huene (1932). Although it is possible that they have been reassembled incorrectly, we follow their current condition in our interpretation of their identification. The metacarpals are straight and expanded at their ends relative to their shafts. No channel-like ventral concavities are visible. The distal articular surfaces do not extend onto the dorsal sides of the metacarpals. Metacarpal II is the longest of the three, and metacarpal I is also slightly longer than metacarpal III. This feature – with metacarpal II being the longest, then metacarpal I and metacarpal III the shortest of the three – is also observable in the titanosaur *Epachtosaurus*, while *Alamosaurus* and *Opisthocoelicaudia* present both metacarpal I and II of almost equal proximodistal lengths,

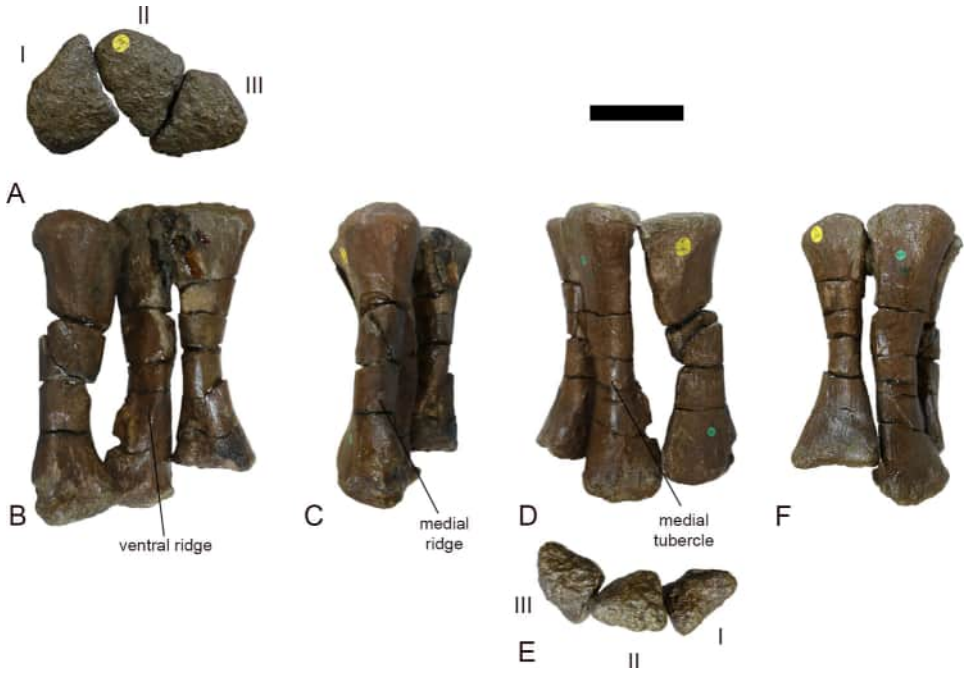

Figure 53. Lithostrotia *incertae sedis*, Individual H, right metacarpals I to III in articulation, NHMUK R.4891. **A,** proximal (ventral towards bottom); **B,** ventral; **C,** medial; **D,** dorsomedial; **E,** distal (ventral towards top); and **F,** dorsolateral views. Scale bar equals 50 mm.

and longer than metacarpal III (Poropat, Mannion, et al., 2015, table 13).

Metacarpal I. The proximal end of this metacarpal has a 'D'- or comma-shaped outline, with a prominent dorsolateral projection (Fig. 53A). This profile is created by: a dorsoventrally elongate, mildly concave, lateral margin; a straight ventral margin; a convex medial margin; and a dorsal margin that slopes to face dorsomedially. This proximal morphology contrasts with that of the metacarpal I (MCDRD 152) referred to *Petrustitan* (Fig. 38A). In the current specimen, the proximal articular surface is gently convex in all directions. The ventrolateral corner of the proximal end continues distally as a low rounded ventral ridge, fading out at approximately two-thirds of the element length from the proximal end, at which point it is situated equidistant from the medial and lateral margins. In dorsal view, the medial margin of the metacarpal is fairly straight whereas the lateral margin is concave. The metacarpal appears to bow slightly medially in dorsal view, although breaks in the shaft mean that this morphology might not be reliable. There are no marked ridges or bumps on the shaft other than the ventrolateral ridge noted above. The shaft rapidly contracts to form a rounded subtriangular cross-section in the proximal part, contrasting with the circular one in *Petrustitan*.

A short distance from the distal end, the medial margin forms a small concavity (clearly visible in both dorsal and ventral views). The bone texture differs on either side of this concavity, potentially marking a healed break. Distally, the shaft becomes subtriangular in cross-section. In distal view, the metacarpal has a subtriangular profile, with a long, gently convex dorsal margin, and sloping, gently concave medial and lateral margins (Fig. 53E). The ventrolateral corner of this triangle forms a small but distinct process that would have projected into the central cavity of the manus formed by all five metacarpals when articulated in life (i.e. the central hollow within the tubular manus). This projection makes the ventral, and especially the lateral margins, moderately concave in outline.

Metacarpal II. In proximal view, this metacarpal has a mildly asymmetrical subtriangular shape, with the medial margin slightly longer than the lateral one (Fig. 53A). The dorsal and lateral margins meet at a near right angle, whereas the dorsomedial corner is rounded, and the apex of the triangular proximal profile projects primarily ventrally. The proximal articular surface is gently convex in all directions. The triangular cross-section is maintained over the proximal four-fifths of the metacarpal, with a prominent ridge along the ventral margin (Fig. 53B). This ridge terminates close to the distal end, approximately equidistant from the medial and lateral margins, at the point where the metacarpal broadens mediolaterally. In dorsal view, both the medial and lateral margins of the metacarpal are concave. The

dorsal surface is concave proximodistally, giving the metacarpal a bowed appearance in medial view. Just proximal to midlength, there is a prominent, anteroposteriorly elongate tubercle on the medial surface – this extends to the dorsal margin (and is visible in dorsal view, Fig. 53D), but it is not possible to determine its ventral extent because the bone surface is missing. The medial margin of the distal third of the metacarpal forms a prominent ridge, although this is broken distally (Fig. 53C). In distal view, the metacarpal has a mediolaterally elongate 'D'-shaped outline created by a vertical lateral margin, and sloping dorsal and ventral edges that form a rounded medial margin (Fig. 53E). The distal articular surface is strongly convex in all directions. As in metacarpal I, the ventrolateral corner of the distal end forms a distinct projection that extends towards the centre of the tubular manus.

Metacarpal III. This specimen is attached to metacarpal II and so aspects of its medial, as well as the latter's lateral surface are obscured, especially where they articulate proximally and distally. There are breaks and glued repairs throughout the shaft in at least three places. The proximal end has a nearly symmetrical, dorsoventrally tall, triangular outline, with the apex of this triangle projecting ventromedially (Fig. 53A). A triangular cross-section is maintained for approximately the proximal three-quarters of the metacarpal length, although the ventral margin is broad, rather than forming a distinct ridge (N.B. this surface is not preserved along the proximal third). By mid-length the shaft is more rounded in cross-section, being subrectangular and slightly transversely compressed. The medial margin of the metacarpal is fairly straight in dorsal view, whereas the lateral margin is concave. As in metacarpal II, metacarpal III is bowed in medial/lateral view, with the dorsal surface concave anteroposteriorly. There are no clear additional ridges or bumps on the shaft. The distal end is expanded, especially transversely, compared to the mid-shaft. In distal view, the metacarpal has a trapezoidal outline, created by: a long, flat dorsal margin; a medial margin that is nearly vertical and dorsoventrally taller than the lateral margin; a lateral margin that slopes such that it faces ventrolaterally; and a ventral margin that is gently concave (Fig. 53E). The distal articular surface is gently convex dorsoventrally, and mildly concave mediolaterally.

Individual I (Tuștea titanosaur)

The most important element preserved for this individual (see the 'Key localities and skeletal associations' section) is the sacrum (currently only observable in ventral view) in articulation with the partial right ilium (LPB [FGGUB] R.2345), alongside two posterior caudal vertebrae (LPB [FGGUB] R.2027 and 2028), and four chevrons (LPB [FGGUB] R.1881, 2025, 2026 and 2184).

Sacrum. The sacrum (LPB [FGGUB] R.2345) comprises five vertebrae (Fig. 54). The original sacral vertebra 1 is probably missing, given that somphospondylan sacra usually possess six vertebrae (Upchurch, 1998; Wilson & Sereno, 1998), although it is possible that some titanosaur taxa could have presented the plesiomorphic condition of a sacrum with five vertebrae (Averianov et al., 2023). The total preserved anteroposterior length of the sacrum is *c*. 290 mm. It is dorsoventrally compressed, with this compression also visible in the horizontal preacetabular process of the ilium. The centra are fused, although the sutures between them are visible. The most anterior centrum (S2?) presents a condyle on its anterior articular surface, and the posterior-most centrum (S6?) has a concave posterior articular surface. On the ventrally exposed parts of the first preserved vertebra (S2?), long oval longitudinal pneumatic structures can be observed on the lateral and ventral sides. The ventral surfaces of the centra vary through the series: only the first one (S2?) is flat, the second and third (S3? and S4?) have an irregular surface, the fourth (S5?) presents a narrow and shallow, longitudinally elongated concave surface on the midline bounded by two poorly developed ridges, and the fifth (S6?) has a subtriangular outline with a concave area on its posterior part. The lateral edges of this 'triangle' form smooth ventrolateral ridges on the posterior-most centrum. The lateral surfaces of the centra bear anterodorsally placed, deep pneumatic openings, most clearly observed in the first preserved sacral vertebra (S2?). In S2?, the prezygapophyses are wide and short, and anterodorsally directed, with the articular facets facing dorsomedially. Below the prezygapophyses, a CPRF is present.

No transverse foramina are present between the centra and the ribs. The sacral ribs are anteroposteriorly compressed and dorsoventrally expanded, especially in their distal part, where they form the sacricostal yoke and connect to the ilium. There were probably intercostal junctions between the ribs forming the sacricostal yoke, as can be observed between the first (S2?) and second (S3?) right sacral ribs, whose distal ends are connected. The presence of intercostal foramina cannot be assessed because of the state of preservation.

Caudal vertebrae. LPB (FGGUB) 2027 is a posterior caudal centrum (Fig. 55A–E). It is procoelous, with a weakly developed posterior condyle. Although slightly affected by taphonomic deformation, this centrum is probably genuinely dorsoventrally compressed: the

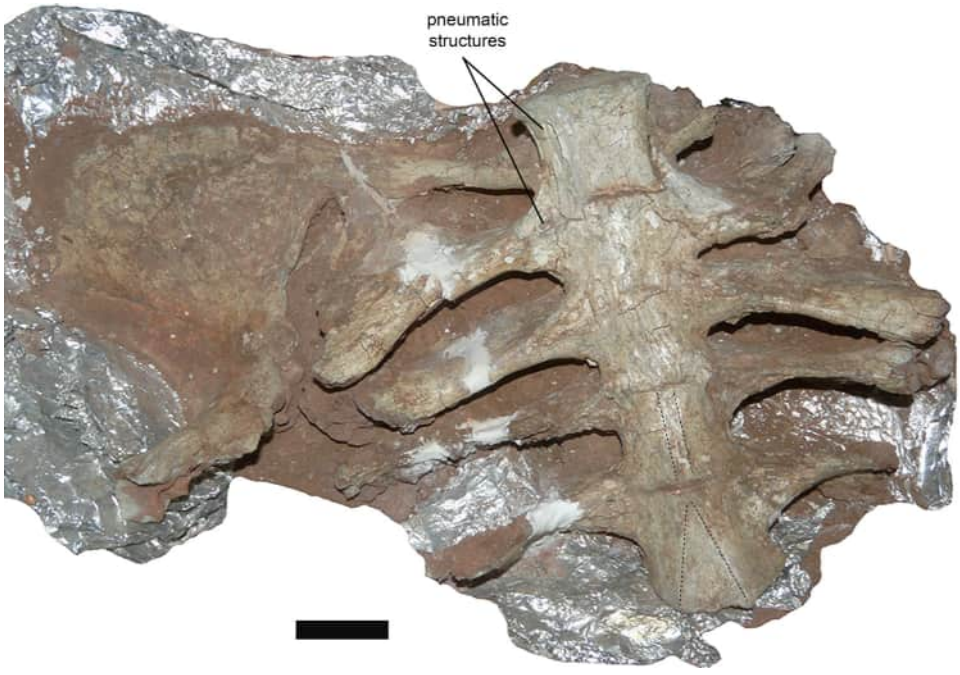

Figure 54. Individual I sacrum LPB (FGGUB) R.2345 in ventral view. The dotted lines highlight the ventral ridges. Scale bar equals 100 mm.

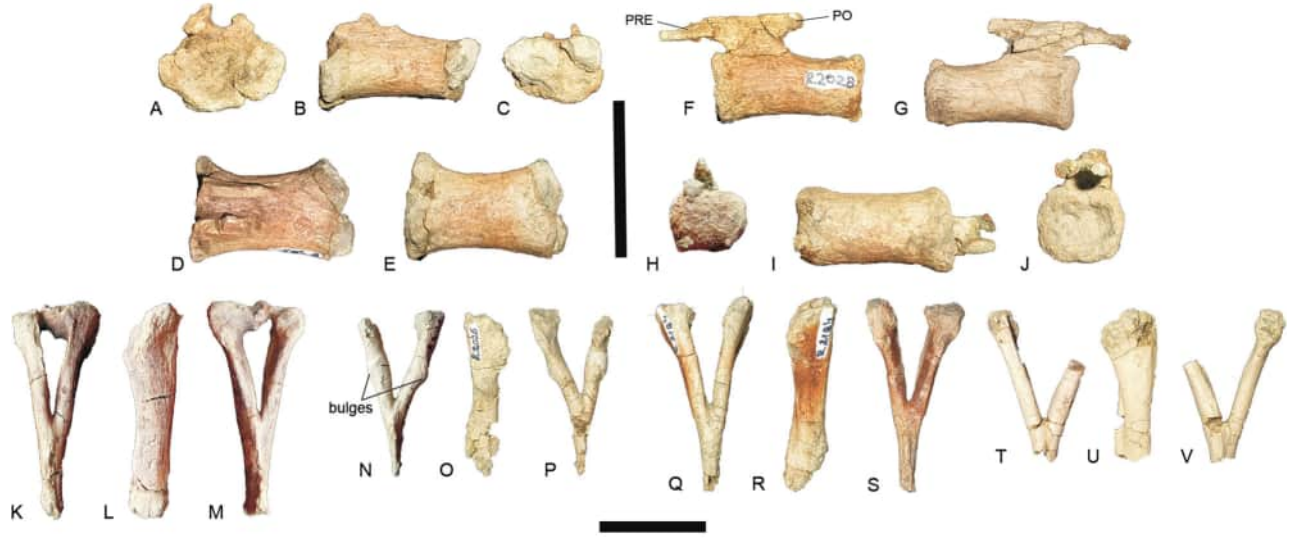

Figure 55. Lithostrotia *incertae sedis*, Individual I, posterior caudal vertebrae and chevrons. Posterior caudal vertebra LPB (FGGUB) R.2027 in **A,** anterior; **B,** left lateral; **C,** posterior; **D,** dorsal; and **E,** ventral views. Posterior caudal vertebra LPB (FGGUB) R.2028 in **F,** left lateral; **G,** right lateral; **H,** posterior; **I,** ventral; and **J,** anterior views. Chevron LPB (FGGUB) R.1881 in **K,** anterior; **L,** right lateral; and **M,** posterior views. Chevron LPB (FGGUB) R.2026 in **N,** anterior; **O,** left lateral; and **P,** posterior views. Chevron LPB (FGGUB) R.2184 in **Q,** anterior; **R,** right lateral; and **S,** posterior views. Chevron LPB (FGGUB) R.2025 in **T,** anterior; **U,** right lateral; and **V,** posterior views. **Abbreviations: PO**, postzygapophysis; **PRE**, prezygapophysis. Scale bars equal 40 mm.

height to width ratio of the anterior articular surface is 0.61, whereas most of the other titanosaurian posterior caudal vertebrae from the Haţeg Basin show values closer to 1 (Table S1). This is the only posterior caudal vertebra to display such an advanced degree of vertical compression out of all those from the Haţeg Basin studied in this work, as well as in the large sample surveyed by Mocho et al. (2023). Some posterior caudal vertebrae with strongly dorsoventrally compressed centra have also been described previously for

Atsinganosaurus (Garcia et al., 2010, fig. 4D–G) and *Lirainosaurus* (Díez Díaz et al., 2013b, fig. 6K–R). Indeed, a dorsoventral compression of the centrum of the first posterior caudal vertebra is one of the changes that can occur in the caudal series, as observed in the tails of *Bonitasaura salgadoi* (Gallina & Apesteguía, 2015) and *Rinconsaurus caudamirus* (Pérez Moreno et al., 2022). In LPB (FGGUB) 2027, the ventral surface is slightly convex transversely (Fig. 55E). The base of the neural arch is placed anteriorly (Fig. 55D).

LPB (FGGUB) 2028 (Fig. 55F–J) is a caudal vertebra that is somewhat smaller and located more posteriorly in the vertebral series than LPB (FGGUB) 2027, and the main difference between them is that the former has a more subcircular (albeit still somewhat dorsoventrally compressed) cross-section through the centrum. In LPB (FGGUB) 2028, the ventral profile of the centrum is subrectangular (Fig. 55I), contrasting with the more spool-like shape (i.e. expanded articular ends and constricted central region) that characterizes the posterior caudal vertebra SZTFH Ob.3105 of *Magyarosaurus* (Fig. 25C) and those of *Uriash* (Fig. 41). The neural arch is anteriorly placed on the centrum. There are long, slender, anteriorly directed prezygapophyses (differing from the more robust ones of *Petrustitan*, Fig. 35), and postzygapophyseal facets are still present. The TPRL extends beyond the anterior margin of the centrum (clearly observable in ventral view), a morphology that is not present in *Petrustitan*.

Chevrons. None of the chevrons are complete (Fig. 55K–V). They have the typical 'Y'-shaped morphology (i.e. not bridged proximally), with the exception of LPB (FGGUB) R.1881, in which there is an incomplete dorsal bridge (Fig. 55K–M); however, the clearly asymmetrical development of this bony bridge, originating from the proximal articular face of one ramus, but unevenly developed and not reaching the articular surface of the opposite ramus, suggests that it might represent a pathological bony outgrowth instead of a genuine anatomical feature bridging the haemal canal. It is difficult to assess the morphology of the proximal articular facets, because of poor preservation, but they appear to be divided into anterior and posterior articular surfaces, better observed in in LPB (FGGUB) R.1881 and R.2025. This is a similar condition to that seen in *Paludititan*, but differing from the chevrons referred to *Magyarosaurus* (Fig. 26). In the more anterior chevrons of Individual I, the anterior articular facet faces dorsally and is larger than the posterior facet, which faces posterodorsally. Those chevrons that preserve part of the distal blade demonstrate that it was transversely compressed, whereas the proximal rami have a more circular cross-section. LPB (FGGUB) R.2026 (Fig. 55N–P) bears a prominent bulge on the lateral surface of the proximal ramus, as is also the case in *Magyarosaurus*.

Ilium. Only the right ilium is preserved in Individual I (Fig. 54). It is fairly complete, although further preparation is needed to fully understand its anatomy. The ilium is not well preserved where it articulates with the sacral ribs. The dorsal margin of the preacetabular process is gently curved and rounded in lateral view, and its horizontal orientation and lateral deflection could have been exaggerated by dorsoventral taphonomic compression. The pubic peduncle is incomplete, obfuscating a detailed comparison with those of *Petrustitan* and *Paludititan*. Nevertheless, enough of the pubic process is preserved in Individual I to determine that its base is robust. The highest part of the dorsal margin of the preacetabular process seems to have been located anterior to the base of the pubic peduncle, as is typical for titanosauriforms (Upchurch, 1998).

Assemblage J (the Groapă assemblage)

This assemblage includes axial and appendicular remains, although not all of them are well preserved. Part of the material collected at this locality (recovered mainly during the 1980s) is in the collections of the MCDRD in Deva, Romania, and was inaccessible to us during this study. However, more recently collected specimens are deposited in the collections of the LPB (FGGUB), and comprise one cervical vertebra (LPB [FGGUB] R.1073), one dorsal vertebra (LPB [FGGUB]R.1854), and over 50 caudal vertebrae that are mostly isolated (e.g. LPB [FGGUB]R.1148, R.1184, R.1187, R.1191, R.1193, R.1202–R.1217, R.1232–R.1238, R.1240–R.1245, R.1512, R.1515–R.1522, R.1540, R.1569, R.1813], but can also occur occasionally articulated, with four (LPB [FGGUB] R.1254], or five (LPB [FGGUB] R.1568) elements, a dorsal rib fragment (LPB [FGGUB] R.1795), one chevron (LPB [FGGUB] R.1597), three humeri (LPB [FGGUB]R.1246, R.1257, R.1528), two ulnae (LPB [FGGUB] R. 1514, R.1598), one radius (LPB [FGGUB] R.1248), four femora (LPB [FGGUB]R.1220, R.1511. R.1513, R.1578), four tibiae (LPB [FGGUB] R.1182, R.1219, R.1252, R.1301), two fibulae (LPB [FGGUB] R.1221, R.1263), two metapodial elements (LPB [FGGUB] R.1185, R.1564) and one phalanx (LPB [FGGUB] R.1222). From this large sample, only the best-preserved and most informative specimens are described here.

Cervical vertebra. LPB (FGGUB) R.1073 (Fig. 56) is an opisthocoelous posterior cervical vertebra, better preserved on its right side. Erosion reveals that the internal tissue structure is camellate. The centrum is slightly

transversely compressed. It has an aEI of 2.08, which is slightly higher than that of the known posterior cervical vertebra of *Magyarosaurus*. There is a weakly developed midline ridge along the anterior three-quarters of the ventral surface of the centrum. On either side of this ridge, the ventral surface is shallowly concave transversely, flattening posteriorly. The parapophysis is anteroventrally located on the lateral surface of the centrum and merges with a posteriorly directed PCPL-like lamina that extends along the ventrolateral edge of the centrum. The lateral surface of the centrum bears a deep oval lateral pneumatic opening.

The neural arch occupies most of the centrum length. As a result of poor preservation, the transition between the diapophysis and the prezygapophysis is not clearly discernible. The prezygapophysis is short and slightly anterodorsally directed, such that it does not project beyond the anterior edge of the condyle. The prezygapophyseal articular surface faces dorsomedially. The diapophysis is only slightly laterally developed, although this could be due to poor preservation. In overall morphology and orientation, the diapophyses are different in LPB [FGGUB] R.1073 relative to the cervical vertebra of *Magyarosaurus* (LPB [FGGUB] R.2505, Fig. 20); they are shorter, dorsoventrally thicker, laterally oriented, with a rounded profile in the former, whereas they are ventrally directed in the latter. In LPB (FGGUB) R.1073, a prominent PCDL extends posteroventrally from the diapophysis, and a short ACDL is also present (Fig. 56F). Posterior to the PODL and below the postzygapophysis, a deep POCDF is present. The postzygapophysis is relatively shorter than that of the cervical vertebra of *Magyarosaurus*, and its articular surface (although eroded) is dorsolaterally oriented. Matrix means that it is not possible to observe whether a TPRL and TPOL are present (Fig. 56G).

The summit of the neural spine is not complete, although it appears to have been low, with a triangular outline in lateral view. It was probably lower than the incomplete neural spine of the cervical vertebra of *Magyarosaurus.* The dorsoventral extent of the PRSL cannot be assessed because of the presence of matrix (although the most distal tip is visible), as is also the

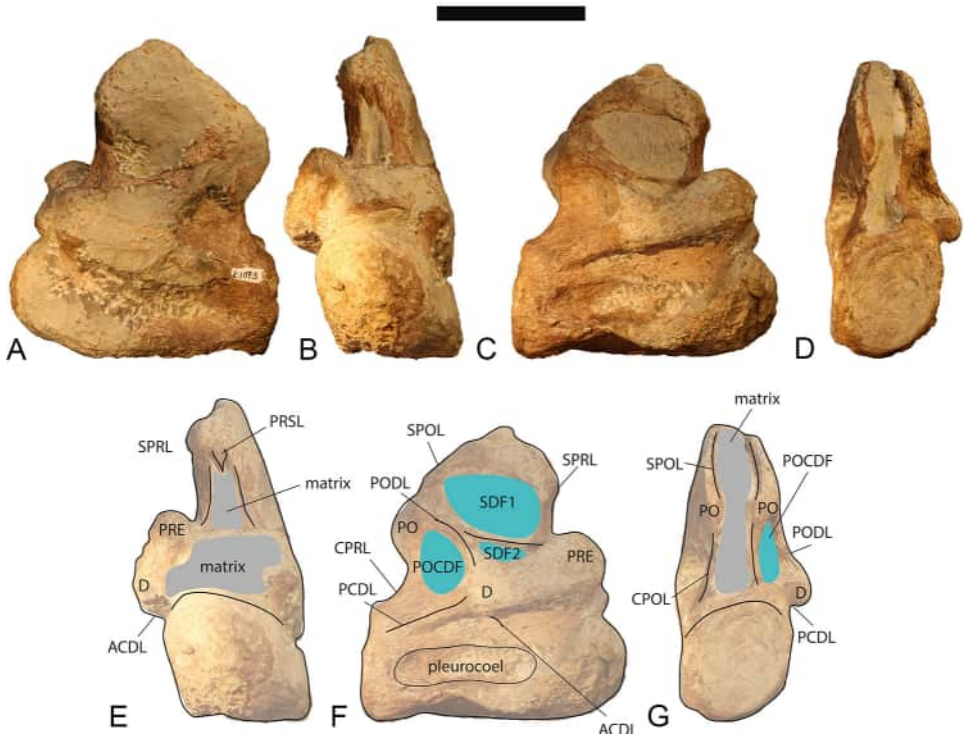

Figure 56. Lithostrotia *incertae sedis*, Assemblage J, posterior cervical vertebra LPB (FGGUB) R.1073 in **A,** left lateral; **B,** anterior; **C,** right lateral; and **D,** posterior views. Interpretive drawings in **E,** anterior; **F,** right lateral; and **G,** posterior views. **Abbreviations: ACDL**, anterior centrodiapophyseal lamina; **CPOL**, centropostygapophyseal lamina; **CPRL**, centroprezygapophyseal lamina; **D**, diapophysis; **PCDL**, posterior centrodiapophyseal lamina; **PO**, postzygapophysis; **POCDF**, posterior centrodiapophyseal fossa; **PODL**, postzygodiapophyseal lamina; **PRE**, prezygapophysis; **PRSL**, prespinal lamina; **SDF**, spinodiapophyseal fossa; **SPOL**, spinopostzygapophyseal lamina; **SPRL**, spinoprezygapophyseal lamina. Scale bar equals 100 mm.

case for the POSL (Fig. 56E, G). Both the SPRL and SPOL are single (i.e. unbifurcated), robust, and vertically oriented in lateral view. The latter lamina shows a slight ventrolateral orientation in posterior view.

Caudal vertebrae. Anterior caudal vertebrae. LPB (FGGUB) R.1813 (Fig. 57A–C) is the most completely preserved anterior caudal vertebra in this assemblage, but the neural arch and part of the eroded condyle are obscured by matrix. The centrum is procoelous and slightly dorsoventrally compressed. Its anterior surface has a subcircular outline, with the ventral margin shorter than the dorsal one because of transverse compression ventrally. The shape of the posterior surface is difficult to assess due to damage and concretionary matrix that is adhered to this region, but it appears to be more quadrangular. The posterior condyle is dorsally displaced and, although incomplete at its tip, it is conical and relatively prominent. The anterior half of the centrum appears to have been more transversely expanded than the rest of the centrum. The lateral sides of the centrum are very mildly convex dorsoventrally and concave anteroposteriorly. The ventral surface is both longitudinally dorsally arched and transversely concave, with a wide and relatively shallow median groove bordered by similarly wide and rounded margins (Fig. 57C). This median groove attenuates towards the anterior and posterior ends. The articular facets for the chevrons are not preserved because of damage to both anterior and posterior margins of the ventral surface. The transverse processes have large rounded bases that are situated above the junction between the anterior neural arch and the centrum. There is a well-developed PRDL that extends laterally, suggesting that this specimen probably comes from a relatively anterior position in the tail. Anterior to the PRDL, there is a PRCDF. The preserved bases of the prezygapophyses indicate that they were directed anterodorsally, as in the lectotype of *Magyarosaurus* (SZTFH Ob.3091). Only the base of the neural spine is preserved, and it is covered

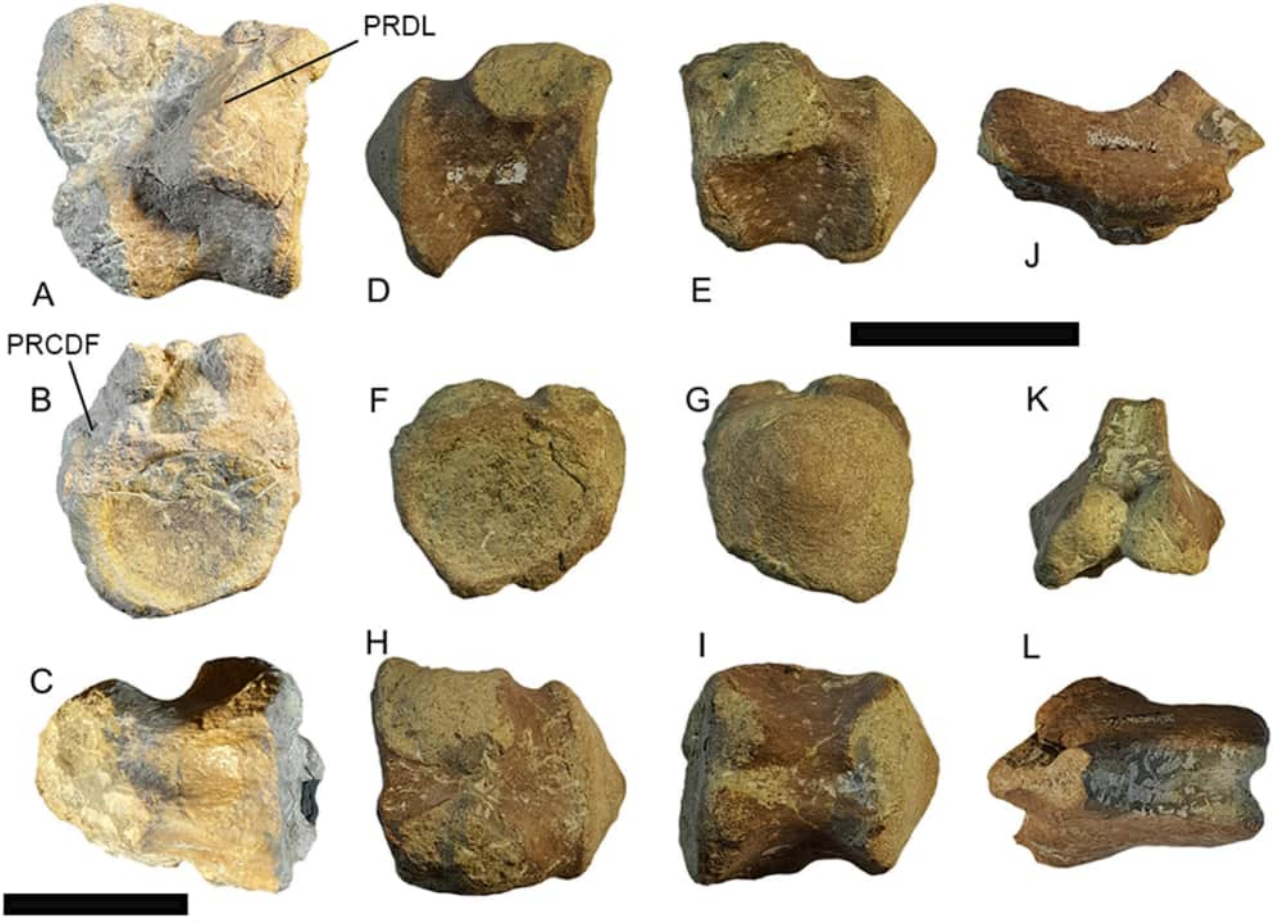

Figure 57. Lithostrotia *incertae sedis*, Assemblage J, anterior caudal vertebrae. LPB (FGGUB) R.1813 in **A,** right lateral; **B,** anterior; and **C,** ventral views. LPB (FGGUB) unnumbered in **D,** right lateral, **E,** left lateral; **F,** anterior; **G,** posterior; **H,** dorsal; and **I,** ventral views. Neural arch LPB (FGGUB) R.1184 in **J,** left lateral; **K,** anterior; and **L,** dorsal views. **Abbreviations: PRCDF**, prezygocentrodiapophyseal fossa; **PRDL**, prezygodiapophyseal lamina. Scale bars equal 50 mm.

in hard matrix, hindering observation of its morphology as well as that of the postzygapophyseal region.

A second, somewhat smaller, procoelous anterior caudal centrum (unnumbered) (Fig. 57D–I) is better preserved, but less complete, with breaks marking the bases of the neural pedicels. It is similar in most respects to the centrum of R.1813, including the dorsally wider subcircular anterior surface, and the presence of a dorsally displaced, conical (albeit less protruding) condyle on the posterior surface. On the ventral surface, the median groove is relatively deeper, and the bounding ventrolateral ridges are narrower and more pronounced (Fig. 57I).

LPB (FGGUB) R.1184 preserves the base of a caudal neural arch (Fig. 57J–L). The prezygapophyses are short and anterodorsally directed. A rounded and shallow fossa is present posteriorly at the base of the neural spine. A SPRL originates from the angular dorsal margin of each prezygapophysis, together delimiting a shallow longitudinal depression along the anterior base of the neural spine. As a result, the basal horizontal cross-section through the spine is approximately 'Y'-shaped, with a very short anterior 'fork' and a distally expanded base. These features suggest that this specimen comes from an anterior caudal vertebra, although probably from a more distal position than R.1813.

Middle caudal vertebrae. Middle caudal vertebrae are represented by a number of well-preserved specimens in the Groapă sample, including LPB (FGGUB) R.1202, R.1203, R.1204, R.1210 and R.1512 (Fig. 58). Although none of these specimens have their articular surfaces completely exposed from under the hard matrix, it is nevertheless clear that their centra were largely platycelous, with a relatively shallowly excavated anterior surface and a posterior surface that appears to vary from very mildly convex, and apparently centrally excavated by a depression (R.1202, R.1204), to flat and centrally hollowed (R.1512). The centra are anteroposteriorly longer than dorsoventrally high and markedly transversely compressed, especially at midlength where the height of the centrum can be more than 1.5 times its width. Both the anterior and posterior articular surfaces have tall, evenly rounded subquadrangular contours. The ventral surface is narrow and flat centrally, strongly concave in lateral view, and transversely concave between the ventrolateral ridges that connect the weak (when preserved and visible) articulations for the chevrons. The lateral sides of the centra are dorsoventrally flat, but concave anteroposteriorly. A sharp anteroposteriorly oriented ridge, located at the base of the neural arch pedicels, represents the remnant of the transverse process. This ridge extends along almost the entire length of the neural arch pedicels, and is more pronounced posteriorly. Only the basal parts of the prezygapophyses can be seen in R.1202, R.1204 and R.1210; these appear to be rod-like, and are anteriorly and only very slightly dorsally oriented. Their bases appear to be bridged medially above the neural canal. Based on partial preservation in different specimens, the neural spine was a transversely compressed, dorsoventrally low and posteriorly elongated blade, overhanging the posterior half of the centrum.

More distally placed in the middle caudal series, specimens such as LPB (FGGUB) R.1190, R.1191 and R.1569 (Fig. 59) have very mildly procoelous to platycoelous/amphicoelous, spool-like centra. These centra are not transversely compressed to any significant amount, with their width and height being approximately equal at mid-length. These specimens are relatively more elongated than those from more proximal positions in the middle tail. The articular surfaces are rounded subquadrangular, often with a central concavity. The ventral surface is slightly narrowed at mid-length, but otherwise generally wider than in the more proximal middle caudal vertebrae. This ventral surface is only mildly concave both anteroposteriorly and transversely, with a very weak midline furrow bounded by two ridges connecting the poorly expressed articular facets for the chevrons. The ventral furrow is better developed near the articular ends, but almost flattens out and disappears at mid-length. The lateral surfaces are weakly concave longitudinally. Rugose bumps appear below the junction between the anteriorly placed neural arch and the centrum, marking the position of the even more weakly developed, vestigial transverse processes. LPB (FGGUB) R.1191 preserves parts of a low and long neural spine with a sharp dorsal margin.

Posterior and distal caudal vertebrae. Several isolated caudal vertebrae (LPB [FGGUB] R.1212–R.1215, 1516) (Fig. 60) will be described for Assemblage J. LPB (FGGUB) R.1516 is a posterior caudal vertebra. The spool-like centrum is incomplete (damaged at both ends), so aspects of its morphology and proportions cannot be ascertained. It has a transversely flat ventral surface that lacks longitudinal ridges, although it shows very short and shallow depressions near the articular surfaces. The long neural arch is located anteriorly on the centrum. A low, weakly rugose longitudinal ridge marks the arch–centrum junction. The neural spine is low and long, with a narrow and somewhat sharp horizontal dorsal edge. The other specimens have better-preserved centra with a morphology reminiscent of that in R.1516, but preserve only parts of the neural arch or only the neural arch pedicels. Their centra are spool-shaped and relatively more elongated than those from the middle section of the tail. They document a variety

Figure 58. Lithostrotia *incertae sedis*, Assemblage J, middle caudal vertebrae. LPB (FGGUB) R.1203 in **A,** right lateral; **B,** anterior; **C,** left lateral; **D,** posterior; **E,** dorsal; and **F,** ventral views. LPB (FGGUB) R.1204 in **G,** right lateral; **H,** anterior; **I,** left lateral; **J,** dorsal; and **K,** ventral views. LPB (FGGUB) R.1512 in **L,** right lateral; **M,** anterior; **N,** left lateral; **O,** posterior; **P,** dorsal; and **Q,** ventral views. **Abbreviation: PO**, postzygapophysis. Scale bar equals 50 mm.

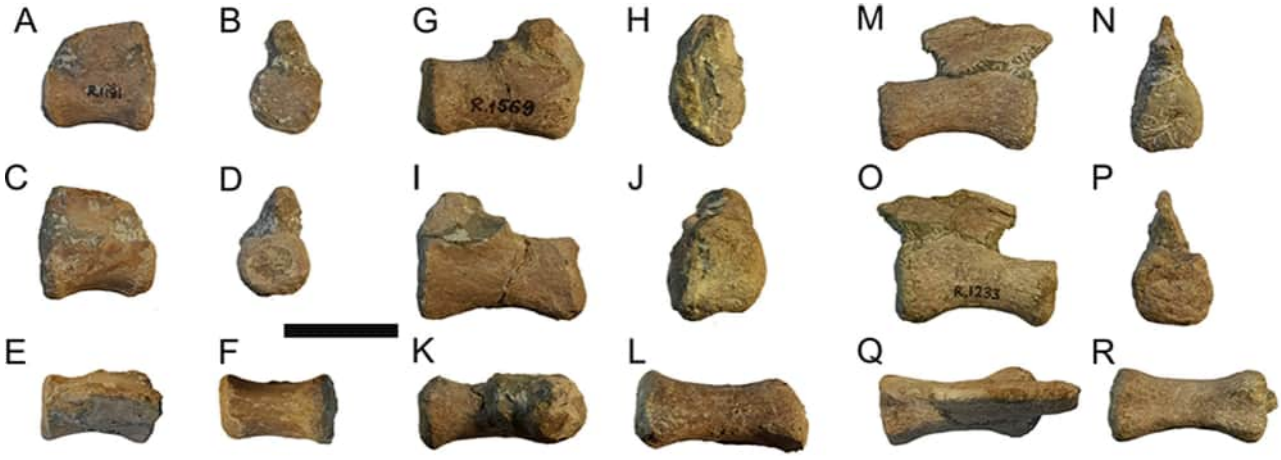

Figure 59. Lithostrotia *incertae sedis*, Assemblage J, middle caudal vertebrae. LPB (FGGUB) R.1191 in **A,** right lateral; **B,** anterior; **C,** left lateral; **D,** posterior; **E,** dorsal; and **F,** ventral views. LPB (FGGUB) R.1569 in **G,** right lateral; **H,** anterior; **I,** left lateral; **J,** posterior; **K,** dorsal; and **L,** ventral views. LPB (FGGUB) R.1233 in **M,** right lateral; **N,** anterior; **O,** left lateral; **P,** posterior; **Q,** dorsal; and **R,** ventral views. Scale bar equals 50 mm.

of articular surface morphologies, including platycoelous-amphiplatyan (R.1212, R.1215), mildly biconvex (R.1214), and even weakly opisthocoelous as seen in specimen R.1213, where in the posterior surface is mildly excavated centrally and the anterior one has a centrally placed low and conical condyle. The proportions of these centra also vary, from ones with a quadrangular cross-section at mid-length, and articular faces that are highly rectangular (R.1213), to ones that are moderately dorsoventrally compressed at both the mid-section and at their articular surfaces that can be as much as 1.5 times wider than tall (e.g. R.1215). The ventral surfaces are slightly arched longitudinally, but mainly flat transversely, with weak central depressions bordered by short triangular ridges near the articular ends. There are no distinct chevron facets. The lateral surfaces of the centra are convex dorsoventrally, sometimes with a weak longitudinal ridge at the base of the neural arch pedicels. The neural arches are anteriorly situated and relatively long, amounting to about half of the centrum length. One further specimen (R.1216, Fig. 60M–R), although significantly smaller in size, has the same general centrum morphology, being mildly opisthocoelous and dorsoventrally compressed. Its anteriorly positioned neural arch is better preserved, with relatively long and slightly anterodorsally projecting

Figure 60. Lithostrotia *incertae sedis*, Assemblage J, posterior caudal vertebrae. LPB (FGGUB) R.1214 in **A,** right lateral; **B,** anterior; **C,** left lateral; **D,** posterior; **E,** dorsal; and **F,** ventral views. LPB (FGGUB) R.1215 in **G,** right lateral; **H,** anterior; **I,** left lateral; **J,** posterior; **K,** dorsal; and **L,** ventral views. LPB (FGGUB) R.1216 in **M,** right lateral; **N,** anterior; **O,** left lateral; **P,** posterior; **Q,** dorsal; and **R,** ventral views. **Abbreviations: PRE**, prezygapophysis. Scale bar equals 50 mm.

Figure 61. Lithostrotia *incertae sedis*, Assemblage J, distal caudal vertebrae. LPB (FGGUB) R.1237 in **A,** anterior; **B,** right lateral; **C,** posterior; **D,** dorsal; and **E,** ventral views. Five distal caudal vertebrae in articulation LPB (FGGUB) R.1568 in **F,** dorsal view; and detail of the first two vertebrae in **G,** dorsolateral; and **H,** dorsal views. The arrow indicates the vestigial pedicel. Scale bar equals 50 mm.

prezygapophyses that are bridged medially along their preserved length above the neural canal.

Another set of isolated caudal vertebrae (LPB [FGGUB] R.1236-R.1238), alongside a string of five vertebrae preserved in articulation (LPB [FGGUB] R.1568), are identified as distal caudal vertebrae. These have elongated, dorsoventrally compressed cylindrical centra that flare out in all directions towards their articular ends. The centra are elongated, although relatively less so than those from the preceding, posterior series (e.g. LPB [FGGUB] R.1214 and R.1215; see Fig. S1). Their morphology varies from amphiplatyan (R.1237) to mildly procoelous (R.1238) to biconvex (R.1568). The ventral and dorsal surfaces are flat transversely, although the former is somewhat dorsally arched longitudinally. The lateral sides are dorsoventrally convex. Some of the specimens (e.g. R.1237; Fig. 61A–E) are slightly asymmetrical, laterally deflected along their length, so that one of the sides is convex and the opposite one is concave in ventral/dorsal view. Neural arches are no longer present in these vertebrae, although one (but not both) of the pedicels may sometimes be present in the form of an anteriorly and marginally placed short and rounded dorsal ridge (e.g. R.1238). In the first two vertebrae of the articulated series R.1568 (Fig. 61F–H), this vestigial pedicel is present only on the right side, appears only on the left side in the third, and may be missing entirely in the last two caudal vertebrae (although this is difficult to ascertain because the centra are still partly embedded in the matrix).

A few minute rod-like elements represent distal-most caudal vertebrae. These are approximately similar to the distal ones described previously in being dorsoventrally compressed cylinders, but are significantly smaller (11–50 mm in length, and less than 5 mm in width). No other features, such as traces of the pedicels, can be seen on these very anatomically 'simple' elements.

Ulna. The right ulna LPB (FGGUB) R.1598 is complete and fairly well preserved (Fig. 62). The estimated maximum proximal mediolateral width to ulna length ratio is 0.39, indicating a relatively robust element, as in *Petrustitan*. The long axes of the anteromedial and anterolateral processes form an angle of approximately 80° (Fig. 62D). The anteromedial process of the

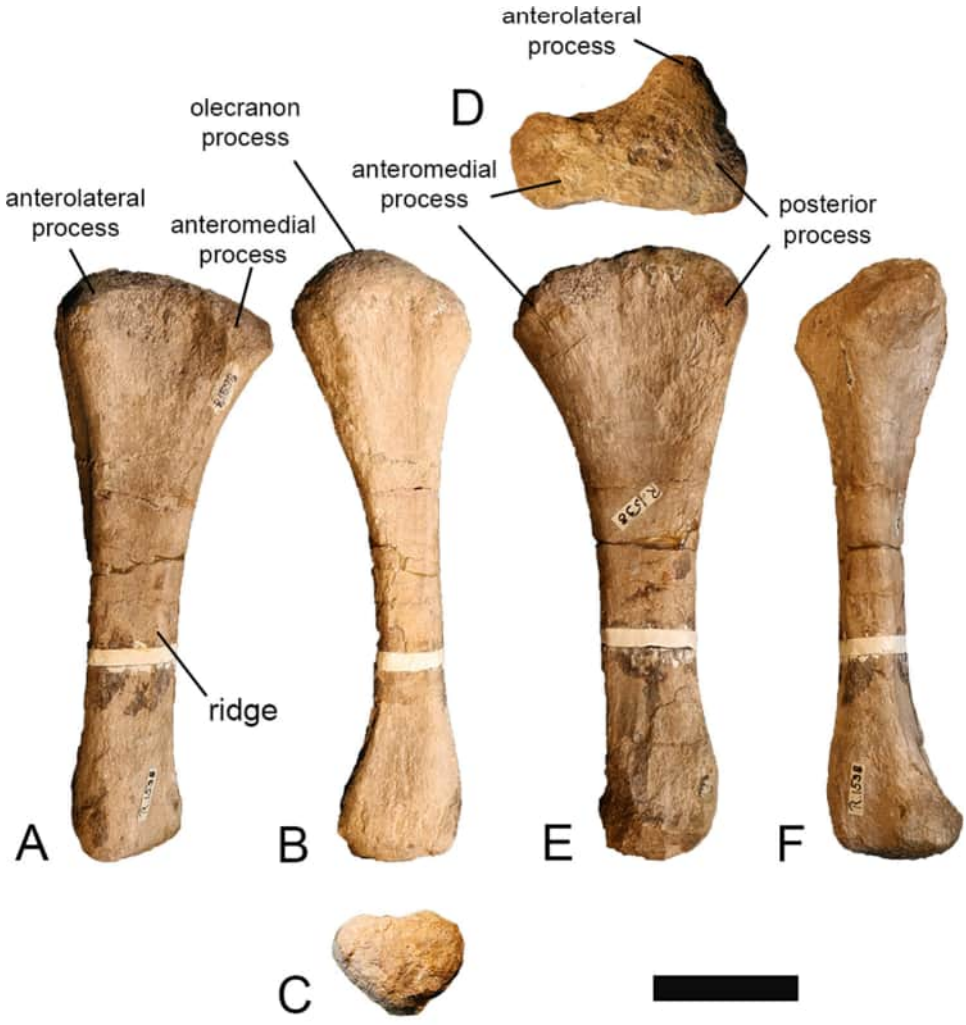

Figure 62. Lithostrotia *incertae sedis*, Assemblage J, right ulna LPB (FGGUB) R.1598 in **A,** anterior; **B,** lateral; **C,** distal (lateral towards top); **D,** proximal (anterior towards top); **E,** posterior; and **F,** medial views. Scale bar equals 50 mm.

proximal end is much longer than that of the anterolateral process, similar to *Petrustitan* (Fig. 36D). The posterior process of the proximal end is only moderately developed, and its long axis is offset from that of the anterolateral process, such that it projects posterolaterally. Only a weakly developed olecranon process is present. The proximal surface of the anteromedial process is flat, lacking any concave profile. The posterior surface of the proximal end is concave mediolaterally. The proximal processes extend distally as weakly developed ridges. A proximodistally oriented ridge is present along the distal third of the anteromedial surface, for articulation with the radius (Fig. 62A). This ridge extends obliquely relative to the long-axis of the shaft, such that it trends laterodistally, similar to the condition in *Magyarosaurus*. Posterior to this ridge, the distal-most portion of the anteromedial surface is gently concave. The ulna expands posteriorly at its distal end. In distal view, the ulna has a subtriangular or 'D'-shaped outline, with a flat to mildly concave medial margin (Fig. 62C). The ulna shares similar anatomical features of the distal end with that of *Petrustitan*, with a convex articular surface with rounded edges, and little posterior expansion.

Femur. None of the femora are complete. Specimen LPB (FGGUB) R.1578 is the proximal end of a right femur. Apart from the dorsomedial orientation of the femoral head, no other informative anatomical features can be discerned. LPB (FGGUB) R.1511 (Fig. 63A) and R.1513 are left femoral shafts, lacking the proximal and distal ends. The best-preserved specimen (LPB [FGGUB] R.1220, Fig. 63B-E) is also the smallest one from the Groapă sample, lacking the distal condylar region and the extreme proximal end. Both LPB (FGGUB) R.1220 and R.1511 were histologically

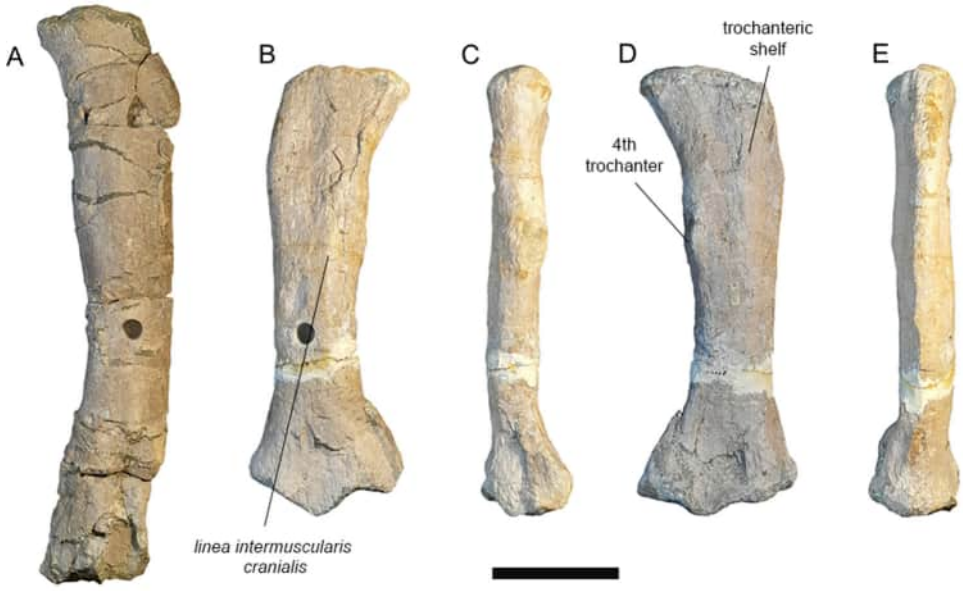

Figure 63. Lithostrotia *incertae sedis*, Assemblage J, femora. **A,** left femur LPB (FGGUB) R.1511 in anterior view. Right femur LPB (FGGUB) R.1220 in **B,** anterior; **C,** medial; **D,** posterior; and **E,** lateral views. Scale bar equals 100 mm.

sampled by Stein et al. (2010), who assigned them to HOS 13. The anterior face is more convex transversely than the flatter posterior one, especially in LPB (FGGUB) R.1513, because of the wide and well developed linea intermuscularis cranialis. It is more difficult to assess the presence of this ridge in LPB (FGGUB) R.1511, although this structure is potentially represented by a rugose surface in the middle of the anterior face of the shaft. In LPB (FGGUB) R.1220, a moderate degree of lateral bulging of the lateral edge is present near the proximal end. On the posterior surface, a wide trochanteric shelf extends ventrally from the preserved part of the proximal end, parallel to the lateral edge of the shaft (Fig. 63D). This shelf ends approximately level with the distal tip of the fourth trochanter, as in the femur of *Magyarosaurus*. The shelf and fourth trochanter are separated by a shallow concave surface. The fourth trochanter is a poorly developed ridge close to the medial edge of the shaft (Fig. 63D), differing from the more developed ones of *Magyarosaurus* (Fig. 32) and, especially, *Uriash* (Fig. 43). In the Assemblage J femora, there is a rugose oval area located on the medial surface, close to the fourth trochanter. Specimens LPB (FGGUB) R.1220 and R.1511 have ECC values of 1.47 and 1.45, respectively – higher than in the femora of *Magyarosaurus* – whereas that of LPB (FGGUB) R.1513 is 1.24, similar to *Magyarosaurus*. All of these femora show much lower ECC values when compared to the femur of *Uriash*.

Phylogenetic analysis

Phylogenetic dataset

We utilized the phylogenetic data matrix presented by Poropat et al. (2023), which is the most recent iteration of the matrix originally presented by Mannion et al. (2013), and which has undergone numerous updates and expansions (e.g. Mannion, Upchurch, Schwarz, et al., 2019; Poropat et al., 2016). Character scores for the existing OTU of *Ligabuesaurus leanzai* were revised based on additional remains described by Bellardini et al. (2022), as were those of *Patagotitan mayorum* based on new information presented by Otero et al. (2020) and personal observations (PDM 2018: MPEF-PV specimens). We also made a small number of character score changes to several other existing OTUs. These changes are all documented in the Supplemental Material.

We added *Magyarosaurus dacus*, *Paludititan nalatzensis* and *Petrustitan hungaricus* as new OTUs based on the information presented herein and personal observations. We did not include *Uriash kadici* given its incompleteness and the limited number of characters for which it could be scored (~1%). As noted by Gorscak et al. (2023), one potential driver of inconsistency between phylogenetic analyses using different datasets might be variation in spatial sampling of taxa. Those authors commented upon the underrepresentation of European and African titanosaurs in most analyses

(including previous iterations of the data matrix used in the present study), as well as poor sampling of Australian taxa in datasets other than the one used herein. Consequently, we also included a further 23 Cretaceous titanosaurian OTUs. These comprise taxa from Africa, Europe and South America, scored based on a combination of personal observations and the published literature, as documented in Table 1. Although we do not disagree *a priori* with the conclusions of Silva Junior, Martinelli, Marinho, et al. (2022) that the latest Cretaceous Brazilian species *Trigonosaurus pricei* might be a junior synonym of the sympatric species *Baurutitan britoi*, the presented evidence is limited in terms of identified anatomically overlapping autapomorphies. As such, we retain these two taxa as separate OTUs. Following Silva Junior, Martinelli, Marinho, et al. (2022), we exclude the caudal vertebrae previously referred to the paratype of *Trigonosaurus pricei* (MCT 1719-R), but that are now assigned to *Caieiria allocaudata*, and analyse this taxon as an additional OTU. In total, the updated data matrix consists of 152 OTUs. Our resultant data matrix therefore goes some way to alleviating the problem highlighted by Gorscak et al. (2023), such that our data matrix includes the majority of named titanosaur taxa from Africa, Asia, Australia, Europe, Indo-Madagascar and North America, as well as a large sampling of South American taxa (30 taxa). In total, we sample 50 unequivocal titanosaurs, with a further 40 OTUs representing additional somphospondylans; furthermore, a large proportion of this subset of taxa (>60%) is scored first-hand based on personal observations.

Our character sampling universe is also extensive, building upon previous iterations of this data matrix. Taxa are scored for 570 phylogenetically informative characters (see the Supplemental Material for the complete character list), with a large proportion of these not included in other data matrices. Of these, we modified character 122, which pertains to the morphology of the lateral excavation of the cervical centra, separating depth (a revised character 122, with new scores documented in the Supplemental Material) and division of this feature (newly added character 557). Also, characters 558–570 are newly added to the dataset, based on the literature and personal observations:

C122. Postaxial cervical centra, lateral surfaces: lack an excavation or have a shallow fossa (0); possess a deep foramen with clearly defined margins (1) (McIntosh, 1990; Russell & Zheng, 1993; Upchurch, 1995, 1998; revised here).

C557. Postaxial cervical centra, lateral surfaces: undivided (0); fossa or foramen divided into separate portions by one or more laminae (1) (McIntosh, 1990; Russell & Zheng, 1993; Upchurch, 1995, 1998; revised here).

C558. Middle–posterior cervical centra, paired pneumatic fossae on the anterior third of the ventral surface, level with the parapophyses: absent (0); present (1) (new character: based on (Coria et al., 2013; Gorscak et al., 2014).

C559. Posterior cervical centra, posterior margin of parapophysis–capitulum suture forms a tubercle: absent (0); present (1) (new character: based on Gorscak et al., 2014; note that this is most clearly seen in ventral view).

C560. Postaxial cervical neural arches, prezygapophyseal articular surfaces situated dorsal to the anterior portion of the diapophyses: absent (0); present (1) (Salgado et al., 1997; modified here).

C561. Middle–posterior cervical neural spines, 'bulbous' lateral expansions at apex: absent (0); present (1) (Campos et al., 2005; Gorscak & O'Connor, 2016; modified here; note that these expansions are not formed by laminae).

C562. Middle–posterior caudal vertebrae, internal tissue structure: solid (0); camellate (1) (new character: based on Cerda et al., 2012).

C563. Scapulocoracoid, internal tissue structure: solid (0); camellate (1) (new character: based on Cerda et al., 2012).

C564. Scapular blade, ventrally located ridge or tuberosity on medial surface of proximal half: absent (0); present (1) (Sanz et al., 1999).

C565. Humerus, medial margin of anterior surface forms a ridge ('anteromedial arm') along the proximal half: absent (0); present (1) (new character: based on Gorscak et al., 2017; Mannion & Otero, 2012).

C566. Femur, fibular condyle, posterior surface: single condyle, with the lateral portion of the posterior surface merging smoothly into the lateral surface of the distal end (0); divided, forming two distinct condylar processes (i.e. a well-developed epicondyle) (1) (Beeston et al., 2024; Carballido et al., 2017; Sekiya, 2011; modified here).

C567. Tibia, anteromedial margin of distal quarter forms a sharp, prominent ridge, delimiting concave anterior and medial surfaces: absent (0); present (1) (new character: based on (Díez Díaz et al., 2013a, 2018).

C568. Tibia and fibula, distal articulation, tibia with a laterally expanded distal end (extending further laterally than the remainder of the tibia, creating a concave

Table 1. List of taxa added to the data matrix (in addition to the three Romanian taxa), along with their spatiotemporal distribution and the basis for their scoring.

Taxon	Spatiotemporal distribution	Reference/source
Africa		
Mansourasaurus shahinae	Middle Campanian, Egypt	Sallam et al. (2018)
Mnyamawamtuka moyowamkia	Aptian to Cenomanian, Tanzania	Gorscak and O'Connor (2019)
Paralititan stromeri	Cenomanian, Egypt	Smith et al. (2001)
Rukwatitan bisepultus	Cenomanian to Campanian, Tanzania	Gorscak et al. (2014)
Shingopana songwensis	Cenomanian to Campanian, Tanzania	Gorscak et al. (2017)
Europe		
Abditosaurus kuehnei	Early Maastrichtian, Spain	Vila et al. (2022); B. Vila and A. Sellés, pers. comm.
Atsinganosaurus velauciensis	Late Campanian, France	Garcia et al. (2010); Díez Díaz et al. (2018); VDD pers. obs.
Lirainosaurus astibiae	Late Campanian, Spain	Sanz et al. (1999); Díez Díaz et al. (2011); Díez Díaz et al., 2013a, 2013b); VDD, PDM & PU pers. obs. (2009)
Lohuecotitan pandafilandi	Late Campanian to early Maastrichtian, Spain	Díez Díaz et al. (2016); VDD pers. obs.
South America		
Argyrosaurus superbus	Coniacianh to Campanian, Argentina	Mannion and Otero (2012)
Arrudatitan maximus	Late Campanian to early Maastrichtian, Brazil	Santucci and Arruda-Campos (2011); Silva Junior, Martinelli, Marinho, et al. (2022)
Baurutitan britoi	Maastrichtian, Brazil	Kellner et al. (2005); PDM pers. obs. (2019)
Bonatitan reigi	Late Campanian to early Maastrichtian, Argentina	Martinelli and Forasiepi (2004); Salgado et al. (2015); PDM pers. obs. (2013, 2018)
Caieiria allocaudata	Maastrichtian, Brazil	Campos et al. (2005); Silva Junior, Martinelli, Iori, et al. (2022); PDM pers. obs. (2019)
Dreadnoughtus schrani	Campanian to Maastrichtian, Argentina	Lacovara et al. (2014); Ullmann and Lacovara (2016); Voegele et al. (2017, 2020)
Elaltitan lilloi	Coniacian, Argentina	Mannion and Otero (2012); PDM pers. obs. (2013)
Gondwanatitan faustoi	Late Campanian to early Maastrichtian, Brazil	Kellner and Azevedo (1999); PDM pers. obs. (2009)
Narambuenatitan palomoi	Early to middle Campanian, Argentina	Filippi et al. (2011); Paulina Carabajal et al. (2020); PDM pers. obs. (2014)
Neuquensaurus australis	Early to middle Campanian, Argentina	Salgado et al. (2005); Otero (2010); D'Emic and Wilson (2011); PDM pers. obs. (2013, 2018)
Overosaurus paradasorum	Santonian, Argentina	Coria et al. (2013); PDM pers. obs. (2014)
Pellegrinisaurus powelli	Early to middle Campanian, Argentina	Cerda et al. (2021); VDD pers. obs. (2011)
Trigonosaurus pricei	Maastrichtian, Brazil	Campos et al. (2005); PDM pers. obs. (2019)
Uberabatitan ribeiroi	Maastrichtian, Brazil	Salgado and Carvalho (2008); Silva Junior et al. (2019)

margin along the distal half of the tibia in anterior view) that articulates with a concave medial surface on the distal end of the fibula: absent (0); present (1) (new character).

C569. Fibula, posterodistally oriented accessory ridge on lateral surface of fibula, extending from mid-length to approximately one-quarter of fibula length from distal end: absent (0); present (1) (new character).

C570. Osteoderms, keeled morphology (subcircular to oval in external or internal view and bear one or more longitudinal keels on their internal surfaces): absent (0); present (1) (Curry Rogers, 2005; D'Emic et al., 2009).

Phylogenetic analysis

Phylogenetic analyses under a parsimony framework were run in TNT v1.6 (Goloboff et al., 2008; Goloboff & Morales, 2023). Following previous iterations of this data matrix (e.g. Mannion et al., 2013; Mannion, Upchurch, Schwarz, et al., 2019; Poropat et al., 2023), 17 of the 574 characters were treated as ordered (characters 11, 14, 15, 27, 40, 51, 104, 147, 148, 195, 205, 259, 297, 426, 435, 472 and 510; note that revision to character 122 means that this is no longer an ordered character) and eight OTUs identified as highly unstable were excluded *a priori* (*Astrophocaudia*, *Australodocus*, *Brontomerus*, *Fukuititan*, *Fusuisaurus*, *Liubangosaurus*, *Malarguesaurus* and *Mongolosaurus*). Under a 'New

Technology Search', we used the 'Stabilize Consensus' option with sectorial searches, drift and tree fusing. After five rounds of consensus stabilizing, the resultant trees were used as the starting topologies for a 'Traditional Search', utilizing tree bisection–reconnection. Two versions of the analysis were run: one in which equal character weighting (EQW) was applied, and a second in which extended implied weighting (EIW) was implemented (Goloboff, 2014; Goloboff et al., 2018), using a *k*-value of 9 (see Mannion, Upchurch, Jin, et al., 2019; Tschopp & Upchurch, 2018). As with recent iterations of this data matrix (Poropat et al., 2021, 2023), two further OTUs (the 'Cloverly titanosauriform' and *Ruyangosaurus*) were excluded *a priori* from the analysis applying equal character weighting, although they were retained in the extended implied weighting analysis.

Phylogenetic results

Our EQW analysis results in more MPTs than TNT can hold, with a large polytomy for much of Titanosauria. As such, we used the Iterative PCR approach of Pol and Escapa (2009) to identify additional unstable taxa, with this implemented via the IterPCR option in TNT (Goloboff & Szumik, 2015). This was supplemented by several preliminary analyses, as well as use of the Pruned Trees option in TNT. These combined approaches highlighted *Puertasaurus* and five of the newly incorporated taxa (*Arrudatitan*, *Caieiria*, *Paralititan*, *Shingopana* and *Trigonosaurus*) as unstable. Exclusion of these six OTUs, along with the 10 OTUs from the initial analysis, *a priori*, yields 304,128 MPTs of length 2996 steps (CI = 0.200, RI = 0.613), and results in a fairly well-resolved strict consensus tree (Fig. 64). Relationships outside of Titanosauria are largely congruent with those produced through previous iterations of this data matrix, but there are numerous differences in terms of titanosaurian interrelationships, including: (1) Diamantinasauria is recovered as the sister taxon of Titanosauria; (2) *Malawisaurus* is the sister taxon of a clade composed of *Andesaurus* and several East Asian sauropods (*Baotianmansaurus*, *Daxiatitan*, *Dongyangosaurus*, *Huabeisaurus*, *Xianshanosaurus*), with *Rapetosaurus* + Aeolosaurini (= *Aeolosaurus* + *Gondwanatitan*) as the successive sister taxon to this grouping (the preliminary analysis also suggests that *Arrudatitan* and *Caieiria* are additional members of the Aeolosaurini + *Rapetosaurus* clade); *Mnyamawamtuka* is the earliest diverging member of this clade, which is the sister taxon to a clade comprising all other titanosaurs (= Eutitanosauria *sensu* Carballido et al., 2022); (3) the usual members of Lognkosauria are divided into two clades, with *Abditosaurus* and *Atsinganosaurus* clustering with *Argentinosaurus* and *Patagotitan*, whereas *Lohuecotitan* and *Paludititan* form a more phylogenetically nested clade with *Futalognkosaurus*, *Mendozasaurus* and *Notocolossus*, and neither clade clusters with Rinconsauria (which includes *Baurutitan*, *Normanniasaurus*, and *Rukwatitan*, as well as the two clade specifiers) to form Colossosauria; (4) *Nemegtosaurus* is recovered as a relatively early diverging titanosaur and does not cluster with *Tapuiasaurus*, with the latter taxon instead forming a clade with *Dreadnoughtus*, *Epachthosaurus* and *Uberabatitan*; (5) *Petrustitan* is most closely related to *Narambuenatitan* and *Pitekunsaurus*, with these taxa forming a clade with *Antarctosaurus*, *Argyrosaurus*, *Jainosaurus* and *Vahiny*; (6) *Bonatitan* and *Elaltitan* are sister taxa and are the earliest diverging members of the clade that includes saltasaurids, which comprises *Neuquensaurus* + *Saltasaurus* (= Saltasaurinae) as the sister taxon to a polytomy formed of *Isisaurus*, *Opisthocoelicaudia* and *Overosaurus* (= Opisthocoelicaudiinae); *Alamosaurus*, *Pellegrinisaurus*, *Magyarosaurus*, and a clade consisting of *Lirainosaurus* + *Mansourasaurus*, form successively distant sister taxa to Saltasauridae (our preliminary analyses suggest that *Shingopana* and *Trigonosaurus* are also part of this broader clade). Bremer supports are low across the tree (values of 1–4), with values of 1 or 2 for most titanosaurian clades, although values of 3 characterize Titanosauria, the early diverging titanosaur clade that includes *Andesaurus* and *Mnyamawamtuka*, as well as Saltasaurinae.

Under EIW, our analysis produces 90,720 MPTs of length 154.7 steps (CI = 0.194, RI = 0.599), with a generally well-resolved strict consensus tree (Fig. 65). As with the EQW analysis, relationships outside of Titanosauria are largely unchanged from those produced using the most recent previous iteration of this data matrix (Poropat et al., 2023). This includes the recovery of Diamantinasauria as a clade closely related to, but outside of, Titanosauria. Relationships at the base of Titanosauria are more consistent with recent iterations of this data matrix than the results from the EQW analysis, with *Andesaurus* clustering with only two other taxa (*Huabeisaurus* and *Ruyangosaurus*), and most titanosaurs recovered within Lithostrotia as a result of *Malawisaurus* occupying its 'typical' position, such that Lithostrotia excludes *Andesaurus*. *Daxiatitan* and *Xianshanosaurus* are sister taxa, forming a clade with *Malawisaurus*. As with the EQW analysis, Aeolosaurini occupies a notably different position to its usual placement, recovered as a diverse clade that is outside Eutitanosauria (*sensu* Carballido et al., 2022). Aeolosaurini is divided into two subclades: one is composed of *Aeolosaurus* and *Arrudatitan* as sister taxa,

with *Rapetosaurus* and *Nemegtosaurus* + *Tapuiasaurus* recovered as successively more distant taxa; the second clade comprises *Caieiria* and *Overosaurus* as sister taxa, with *Gondwanatitan*, *Trigonosaurus*, *Shingopana* and *Uberabatitan* placed as successively more distant taxa. *Argyrosaurus* is placed as the sister taxon to Eutitanosauria. As with the EQW analysis, the taxa usually recovered within Lognkosauria form two clades, and neither of these clades clusters with Rinconsauria. *Argentinosaurus*, *Patagosaurus* and *Puertasaurus* form a clade with *Petrustitan*, whereas *Futalognkosaurus*, *Mendozasaurus* and *Notocolossus* form a more phylogenetically nested clade with *Antarctosaurus*, *Jainosaurus* and *Vahiny*, as well as *Lohuecotitan* and *Paludititan*. Other early diverging eutitanosaurian clades consist of *Narambuenatitan* as the sister taxon of *Mnyamawamtuka* + *Pitekunsaurus*, as well as another distinct lineage in which *Dreadnoughtus* and *Epachthosaurus* form a monophyletic group. As well as the clade specifiers, Rinconsauria includes

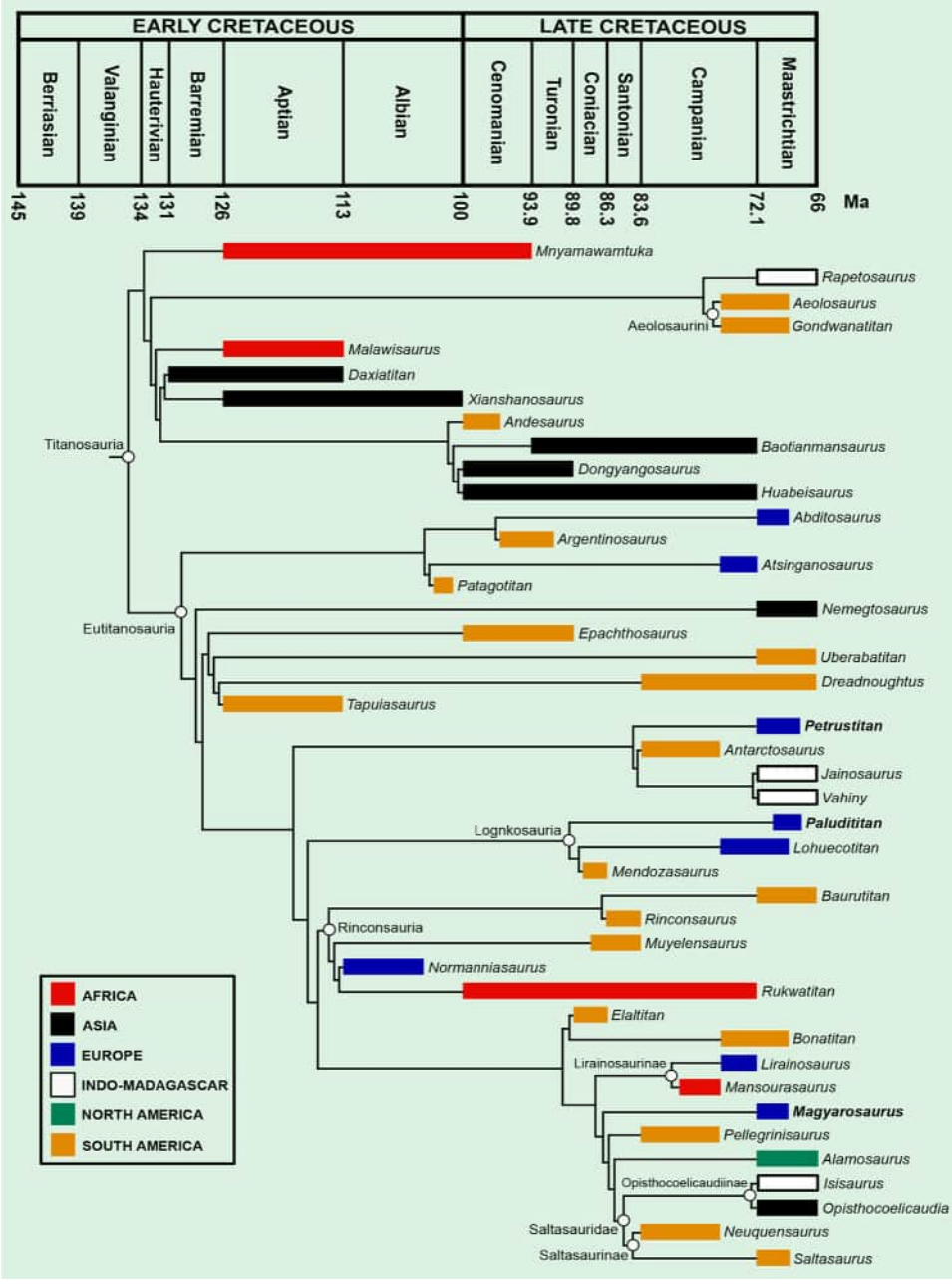

Figure 64. Time-calibrated agreement subtree based on the equal weights analysis, showing the phylogenetic relationships and palaeobiogeographical distribution of Titanosauria. Romanian genus names emboldened.

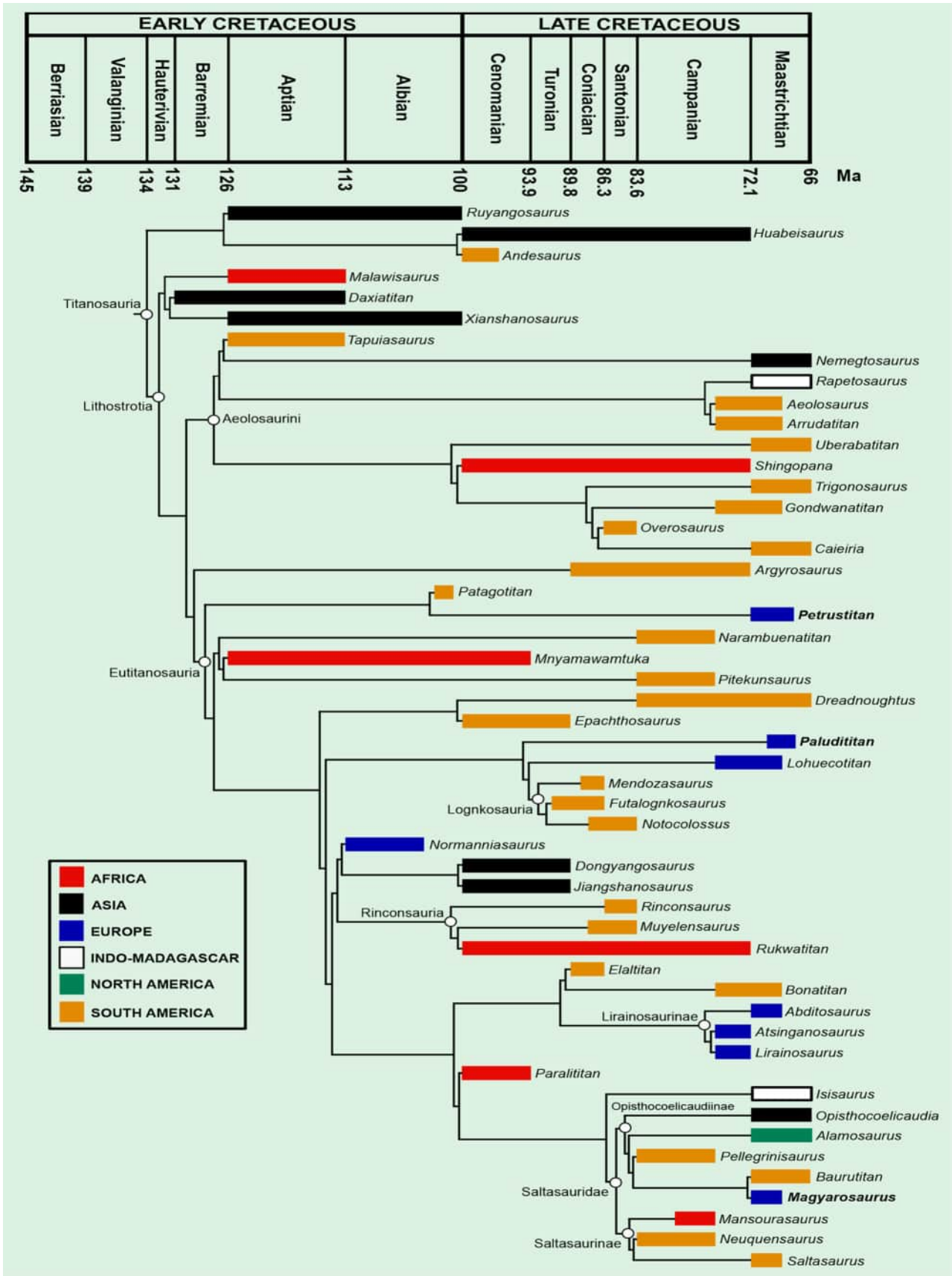

Figure 65. Time-calibrated agreement subtree based on the extended implied weights analysis, showing the phylogenetic relationships and palaeobiogeographical distribution of Titanosauria. Romanian genus names emboldened.

Table 2. Body size and mass of the titanosaurian taxa from the Haţeg Basin described in this work. Maximum and minimum sizes were calculated using results from the formulae of both Packard et al. (2009) and Benson et al. (2018). It is important to remember that calculations derived from assemblages only provide approximate results, as their elements do not belong to a single individual.

		Specimens	PerH + F (mm)	$3.352 \times PerH + F^{2.125}$ (gr) (Packard et al., 2009)	Weight (kg) (Packard et al., 2009)	Weight (kg) Benson et al. (2018)	$M/214.44 = L^{1.46}$ (Seebacher, 2001)	
Magyarosaurus dacus	*Assemblage A*	Left humerus (MBFSZ Ob.3089) + left femur (MBFSZ Ob.3088)	330?	753,609.1	753.61	659.77	2.37 m	2.16 m
	Individual E	Left humerus (LPB [FGGUB] R.1047) + left femur (LPB [FGGUB] R.1046)	372	972,092.86	972.09	917.11	2.82 m	2.71 m
	Assemblage G	Right humerus (LPB [FGGUB] R.2506) + right femur (LPB [FGGUB] R.2507)	341.5	810,511.65	810.51	724.92	2.49 m	2.3 m
Uriash kadici	*Individual C*	Right humerus (MBFSZ Ob.3104) + right femur (MBFSZ Ob.3103)	816	5,159,951.23	5159.95	7947.6	8.83 m	11.87 m

Abbreviations: L, body length; **M**, body mass; **PerH + F**, sum of the perimeters of the humerus and femur in mm.

Rukwatitan, forming the sister taxon to a clade comprising *Normanniasaurus* + (*Dongyangosaurus* + *Jiangshanosaurus*). Rinconsauria is the sister taxon to a clade of the remaining titanosaurs in the data matrix. *Bonatitan* + *Elaltitan* forms a clade with Lirainosaurinae, which consists of *Abditosaurus* as the sister taxon to *Atsinganosaurus* + *Lirainosaurus*. This is in turn the sister taxon to a clade comprising *Paralititan* + (*Isisaurus* + Saltasauridae). Within Saltasauridae, we recover *Mansourasaurus* as the sister taxon to *Neuquensaurus* + *Saltasaurus*, forming Saltasaurinae. A relatively diverse Opisthocoelicaudiinae is composed of *Opisthocoelicaudia*, *Alamosaurus*, *Pellegrinisaurus* and *Baurutitan* + *Magyarosaurus* as successively more phylogenetically nested taxa.

Estimation of body size and mass

Table 2 summarizes the body mass and size estimations for *Magyarosaurus dacus* and *Uriash kadici* obtained by the equations of Benson et al. (2018), Packard et al. (2009) and Seebacher (2001), and the humeri and femora used for those calculations. For *Magyarosaurus dacus* we have obtained masses between 660 and 972 kg. The mass calculated by Benson et al. (2018) for *Magyarosaurus* (750 kg) falls within the ranges obtained in this work, being closer to the values calculated for the specimens referred to Assemblage G. Benson et al.'s (2018) estimation was based on specimens that we are not currently able to assign to *Magyarosaurus dacus* with confidence, but their value is consistent with ours. Body length ranges from 2.16 to 2.82 m for this taxon. Thus, *Magyarosaurus dacus* is still one of the smallest titanosaur taxa described so far, even within the Late Cretaceous of Europe (see Díez Díaz et al., 2021).

Concerning *Uriash kadici*, the body mass estimates range from 5 to 8 tonnes, with lengths between 8.83 and 11.87 m. Benson et al. (2018) calculated a body mass of 10.5 tonnes for the titanosaur *Epachthosaurus*, whose femur has a length of 988 mm. The *Uriash* holotype Individual C could have had a body size similar to this taxon.

Discussion

Titanosaurian diversity in the Haţeg Basin

This work provides an extensive and updated revision of numerous sites from the continental uppermost Cretaceous of the Haţeg Basin and surrounding regions, and the titanosaurian individuals and assemblages found therein, but it also highlights the complexity in objectively assessing the actual diversity of this group of sauropods in this area. With more than 20 individuals/monospecific assemblages identified and described here, four taxa can be confidently recognized at present: *Magyarosaurus dacus*, *Paludititan nalatzensis*, *Petrustitan hungaricus* n. gen., and *Uriash kadici* n. gen. n. sp. These four taxa exhibit significant size

Table 3. List of the specimens described and figured by Huene (1932) and their referral to individuals and assemblages in this work.

Huene (1932)			This work		
Taxon	Specimen no.	Element	Individual/assemblage	Taxon	Notes
M. dacus	NHMUK R.3861a	Dorsal vertebra	Not assigned	Titanosauria indet	
	NHMUK R.3851	Anterior caudal vertebra	Not assigned	Titanosauria indet	
	SZTFH Ob.3091	Middle caudal vertebra	**Assemblage A**	***Magyarosaurus dacus*** (lectotype)	Figured and assigned to *Titanosaurus dacus* by Nopcsa, 1915.
	SZTFH v.10339	Posterior caudal vertebra	Not assigned	Titanosauria indet	
	NHMUK R.3849	Humerus	**Individual L**	Titanosauria indet	
	SZTFH Ob.3099	Ulna	**Assemblage M**	Titanosauria indet	
	SZTFH Ob.3086a	Fibula	**Assemblage A**	***Magyarosaurus dacus***	
M. transsylvanicus	NHMUK R.3896	2 articulated dorsal vertebrae	Not assigned	Titanosauria indet	
	SZTFH v.10341	Anterior caudal vertebra	Not assigned	Titanosauria indet	
	Cd. Pl.46 fig. 5	Anterior caudal vertebra	Not assigned	Titanosauria indet	
	SZTFH v.13520b	Posterior caudal vertebra	Not assigned	Titanosauria indet	
	SZTFH Ob.4215b	Posterior caudal vertebra	Not assigned	Titanosauria indet	Figured and assigned to *Titanosaurus dacus* by Nopcsa, 1915.
	SZTFH v.13469	Anterior caudal vertebra	Not assigned	Titanosauria indet	
	SZTFH v.10342	Anterior caudal vertebra	Not assigned	Titanosauria indet	
	SZTFH v.13520a	Posterior caudal vertebra	Not assigned	Titanosauria indet	
	SZTFH v.13492	Humerus	**Assemblage M**	Titanosauria indet	
	SZTFH Ob.3100	Ulna	**Assemblage A**	***Magyarosaurus dacus***	
	SZTFH R.4891	Metacarpals I–II–III	**Individual H**	Titanosauria indet	
	SZTFH Ob.3086b	Fibula	**Assemblage A**	***Magyarosaurus dacus***	
	SZTFH Ob.3102	Fibula	**Assemblage A**	***Magyarosaurus dacus***	
M. hungaricus	NHMUK R.3833	Fibula	**Individual B**	***Petrustitan hungaricus***	
Tentatively assigned					
M. dacus ?	SZTHF unknown	Cervical neural arch	??	**??**	No specimen number given, we were unable to identify this specimen in the Budapest collection
M. hungaricus ?	NHMUK R.4891	2 dorsal ribs	**Individual H**	Titanosauria indet	
M. hungaricus ?	SZTFH Ob.3130b	Dorsal rib	Not assigned	Titanosauria indet	
M. dacus or M. transylvanicus ?	NHMUK R.3898	Sacrum			Titanosaur?
M. hungaricus ?	SZTFH Ob.3090b	Middle caudal vertebra	**Individual C**	***Uriash kadici***	

(*Continued*)

Table 3. (*Continued*).

Huene (1932)			This work		
Taxon	Specimen no.	Element	Individual/assemblage	Taxon	Notes
M. hungaricus ?	SZTFH Ob.3090d	Posterior caudal vertebra	**Individual C**	***Uriash kadici***	
M. hungaricus ?	NHMUK R.3858	Distal caudal vertebra	Not assigned	Titanosauria indet	
M. dacus ?	SZTFH v.10345	Distal caudal vertebra	Not assigned	Titanosauria indet	
M. hungaricus ?	NHMUK R.4891	Sternum	**Individual H**	Titanosauria indet	
M. hungaricus ?	NHMUK unnumbered	Coracoid	Not assigned	Titanosauria indet	
M. hungaricus ?	NHMUK unnumbered	Ulna	Not assigned	Titanosauria indet	
M. hungaricus ?	NHMUK unnumbered	Metacarpal III	Not assigned	Titanosauria indet	
M. hungaricus ?	NHMUK R.3852	Right pubis	**Individual P**	Titanosauria indet	
M. hungaricus ?	NHMUK unnumbered	Distal femur	Not assigned	Titanosauria indet	No specimen number given, hard to identify.
M. dacus ?	NHMUK R.3856	Femur	Not assigned	Titanosauria indet	
M. hungaricus ?	NHMUK R.3853	Tibia	**Individual B**	***Petrustitan hungaricus*** (para-lectotype)	
M. hungaricus ?	NHMUK R.3850	Tibia	Not assigned	Titanosauria indet	
M. hungaricus ?	NHMUK unnumbered	Tibia	Not assigned	Titanosauria indet	Not figured, not described, no specimen number given - cannot be identified.

Note: In bold, those specimens assigned to a specific Individual, Assemblage or taxon.

disparities, in addition to their anatomical differences, ranging from a dwarf taxon weighing less than 1 tonne and achieving an adult body length of no more than 3 metres, to a large-bodied taxon weighing up to approximately 10 tonnes and a length of nearly 12 metres.

We have demonstrated the validity and diagnostic nature of *Magyarosaurus dacus* – one of the first titanosaurs to be described – with 11 autapomorphies distributed across the axial and appendicular skeleton. Nopcsa (1915) did not describe diagnostic features for this species, although he gave a brief description of some axial remains, as well as the scapula and the femur. Huene (1932), on the other hand, did provide descriptions, measurements and figures of several individual skeletal elements from Transylvania that allowed him to differentiate between two approximately similarly sized species of his newly erected genus *Magyarosaurus*, *M. dacus* and *M. transsylvanicus*, with a third, larger taxon referred to the same genus only tentatively as *M.* (?) *hungaricus* (see the 'History of titanosaur discoveries and research in Transylvania' section). In summary, Huene (1932) regarded *M. dacus* as a more robustly built taxon compared to *M. transsylvanicus*, based on the caudal vertebrae, humerus, ulna, metacarpals, and fibula, with the bones of the former species also assessed to have more prominently marked muscle scars. By contrast, he differentiated *M.* (?) *hungaricus* from *M. dacus* and *M. transsylvanicus* mainly on the basis of its larger size and the distinct anatomy of its fibula. Subsequently, the validity of these three Transylvanian titanosaur taxa has been either accepted (e.g. Curry Rogers, 2005; Steel, 1970) or tentatively refuted (e.g. Le Loeuff, 1993; McIntosh, 1990; Upchurch et al., 2004), although usually without supportive argumentation, with Upchurch et al. (2004) also noting that *Magyarosaurus* itself required a major revision.

In the current work, in line with Huene's (1932, p. 274) tentative suggestion concerning the potential generic distinctiveness of *M. dacus* and *M.* (?) *hungaricus*, we have identified enough differences between these species to establish the latter as a new genus, *Petrustitan*. However, the situation is markedly different in the case of *M. transsylvanicus*. As noted above, McIntosh (1990) and Le Loeuff (1993) considered this species as invalid, although without clear arguments presented in support of such a decision. Our re-study of the Transylvanian titanosaur material presents evidence that helps to resolve this issue more decisively. According to Huene (1932), although the two taxa were remarkably similar to each other both in their dimensions and overall morphology, two lines of evidence supported their

separation: the more robust nature of the bones of *M. dacus*, displaying better-developed muscle scars, compared to *M. transsylvanicus*; and the morphology of the caudal vertebral centra. Regarding the morphological differences between the caudal vertebrae, Huene (1932) alluded to the presence of two different morphotypes that he considered could not be present in the tail of a single species: (1) a morphotype with centra possessing subparallel and slightly concave lateral surfaces, such that the dorsal and ventral surfaces of the centrum are of similar width (considered to characterize *M. dacus*); and (2) one with slightly convex lateral surfaces that converge ventrally, such that the ventral surface is narrower than the dorsal one (corresponding to *M. transsylvanicus*). However, our results indicate that both the diagnostic nature and conspecificity of the purported *M. transsylvanicus* specimens are far from being firmly established. Indeed, several of the specimens that Huene (1932) referred to this taxon are identified here as belonging to different key individuals and assemblages (some of which we can even refer to other nominal taxa). Moreover, some of these specimens actually belong to individuals/assemblages whose other skeletal elements were referred by Huene (1932) to *M. dacus* (e.g. assemblages A and M) or, tentatively, even to *M.* (?) *hungaricus* (Individual H). Such a mixing of specimens makes *M. transsylvanicus* chimaeric, and renders the purported differences in relative robustness of the appendicular elements (considered to be diagnostic by Huene, but here recognized to occur within the same individual/assemblage) taxonomically meaningless. Other specimens referred to *M. transsylvanicus*, most of them isolated caudal vertebrae, have been shown by us to be currently taxonomically indeterminate, often being identified no more precisely than 'Titanosauria indet.' (see Table 3). It is also worth emphasizing that our survey of associated titanosaur material demonstrates that caudal vertebrae belonging to the same taxon (even to the same individual) can display both *dacus*-type parallel-sided and *transsylvanicus*-type wedge-shaped morphologies, depending on their position within the tail (e.g. Individual E and Assemblage J) – an observation that further reduces the support for separating *M. dacus* and *M. transsylvanicus*. To conclude, all currently available information argues against maintaining *M. transsylvanicus* as a valid species, so here we follow McIntosh (1990), Le Loeuff (1993), and Upchurch et al. (2004) in considering this species as invalid and, at least in part, a junior synonym of *M. dacus*.

Regarding the erection of the new genus and species *Uriash kadici*, we consider this justifiable and useful despite the fact that the material from Individual C is scarce and poorly preserved. The type material belongs to a single individual and displays eight autapomorphies, which are widely distributed among the recovered skeletal remains and are absent in the corresponding overlapping elements of *Magyarosaurus*, *Paludititan*, and *Petrustitan*. Moreover, *Uriash* can be definitively distinguished from other Late Cretaceous Transylvanian taxa because of its larger size, which cannot be accounted for by interpreting Individual C as a more mature member of *Magyarosaurus*, *Paludititan* or *Petrustitan*, as was suggested previously by Le Loeuff (2005a; see below). Indeed, *Uriash* is one of the largest titanosaurs recovered to date from the Upper Cretaceous of Europe, surpassed in size only by *Abditosaurus*. All these reasons support the recognition of Individual C as a new taxon.

As previously indicated, there are three further individuals/assemblages (Individuals H and I, and Assemblage J) that provide important information on the anatomy of Transylvanian titanosaurs, even though there is currently insufficient evidence to either refer them to one of the four named Haţeg taxa or make them the basis of new taxa. Of these three sets of specimens, Assemblage J is the only one with several elements that can be compared with any of the named taxa, and it presents anatomical similarities with both *Petrustitan* (in the ulna) and *Magyarosaurus* (in the femur; note, however, that the femur of *Petrustitan* is currently unknown).

Similarly, because of the lack of sufficient comparative data and diagnostic features for the remainder of the individuals and assemblages identified in this survey (see descriptions and comments in the Supplemental Material), we refrain from referring them to any of the four named Transylvanian titanosaur taxa recognized here, or using them to erect new taxa, at least for the time being. Thus, we maintain a working hypothesis of a minimum diversity of four titanosaurian taxa in the Maastrichtian of the Haţeg Basin, pending further discoveries. These conclusions are broadly congruent with those presented by Mocho et al. (2023), in which they suggested that there is evidence for four different caudal vertebral morphotypes for the titanosaurs of the Haţeg and Transylvanian basins. However, it is important to note that some of the differences between morphotypes recognized by those authors might represent serial variation along the tail, rather than being indicators of taxonomic separation (see the 'Systematic palaeontology' section, and the Supplemental Material).

One final comment regarding the diversity of Haţeg titanosaurs concerns their spatial and temporal distribution. According to our survey of the occurrences of individuals/assemblages that can be positively referred to one or another of the currently recognized four nominal

taxa, these appear to show spatiotemporally distinct distributions (Figs 1, 8). Specimens of *Magyarosaurus dacus* occur between Ciula Mică and Vălioara in the north-western Haţeg Basin, in beds assigned to the lowermost part of the middle member of the Densuș-Ciula Formation, and also at Pui in the central-eastern Haţeg Basin, in beds belonging to the lower part of the 'Pui beds' cropping out in this area (Csiki-Sava et al., 2016; Therrien, 2005). *Uriash* is currently only known from east of Vălioara in the north-eastern Haţeg Basin, also from the lower part of the middle member of the Densuș-Ciula Formation, albeit from beds that are marginally younger than those yielding the remains of *Magyarosaurus* (e.g. Botfalvai et al., 2021). All of these occurrences are probably early Maastrichtian in age (some perhaps as old as earliest Maastrichtian), and thus fall into chronostratigraphical Tier 2 (or tiers 1/2 to 2) of the Transylvanian faunal assemblages defined by Csiki-Sava et al. (2016).

By contrast, the holotype and only known specimen of *Paludititan nalatzensis* was discovered in the lower part of the 'Râul Mare beds' (see Csiki-Sava et al., 2016), corresponding to chronostratigraphical Tier 3 (i.e. late early to early late Maastrichtian in age). Botfalvai et al. (2021) reported currently taxonomically indeterminate titanosaur specimens from site K2 near Vălioara (here designated Individual V) that they assessed as potentially referable to *Paludititan* or a closely related taxon, despite coming from beds roughly contemporaneous with those yielding specimens of *Magyarosaurus dacus*. Their suggestion was based on the presence of non-procoelous caudal vertebrae within the middle part of the tail of the K2 titanosaur, previously considered a diagnostic feature of *Paludititan* (Csiki, Codrea, et al., 2010). However, our survey of Haţeg titanosaur material has revealed the presence of this feature in several other, currently taxonomically indeterminate titanosaur specimens (e.g. Assemblage J) and it can no longer be used to unequivocally support referral to *Paludititan*. As such, this removes the evidence supporting the possible co-occurrence of *Paludititan* and *Magyarosaurus* within the same unit/time interval.

Finally, specimens of *Petrustitan hungaricus* are documented solely from the Sibișel Valley outcrops of the Sînpetru Formation, although whether these come from Tier 2 (earliest Maastrichtian), Tier 3 (late early to early late Maastrichtian), or span the Tier 2–3 intervals, is currently uncertain because of the scarcity of constraints on the relative stratigraphical positions of these deposits compared to those from around Vălioara, Pui and Nălaţ-Vad (Csiki-Sava et al., 2016). Nevertheless, it appears likely that these Sibișel Valley occurrences are somewhat older than that of *Paludititan*, although they may be at least in part broadly synchronous with *Magyarosaurus* and/or *Uriash* (Csiki-Sava et al., 2016; Fig. 8).

To conclude, the currently recognized higher taxic diversity of Haţeg titanosaurs (at least four different taxa) does not translate automatically into a high diversity of sympatric titanosaurs; to the contrary, it appears that these taxa had largely non-overlapping areal and/or temporal ranges, possibly representing members of distinct chrono- and/or eco-faunas. However, it should be borne in mind that this clear-cut picture of differential titanosaur distribution in the Haţeg Basin may result at least in part from our current inability to refer further individuals to one or another of these nominal taxa from among the large amount of known titanosaur remains that for the moment are left indeterminate.

Indeed, each of these nominal taxa are currently known from a very small number (1 to at most 3) of occurrences, which suggests that we might greatly underestimate the range of their temporal (and probably also spatial) distribution (e.g. Marshall, 1990). Thus, their perceived chronostratigraphical and geographical separateness may in fact simply be a by-product of their currently limited fossil record instead of reflecting a real-life distributional pattern. These adverse effects of a limited fossil record may be alleviated in the future through the discovery of new, more complete, associated and diagnostic specimens, which should improve our ability to refer further remains to these taxa.

The phylogenetic affinities of latest Cretaceous European titanosaurs

In both sets of phylogenetic analyses, *Magyarosaurus dacus*, *Paludititan nalatzensis* and *Petrustitan hungaricus* are not closely related to one another (note that *Uriash kadici* was not included in these analyses because of its incompleteness, but there is evidence to suggest it is also not closely related to the other three taxa – see below). This lends further support to our retention of *Paludititan nalatzensis* as a taxon distinct from *Magyarosaurus dacus*, and our removal of '*Magyarosaurus*' (?) *hungaricus* from this genus and the erection of *Petrustitan hungaricus*.

As a result of its uncertain taxonomic status and chimaeric nature, *Magyarosaurus* has largely been excluded from previous phylogenetic analyses. The sole exception is the study of Curry Rogers (2005), along with subsequent analyses that reran this matrix (e.g. Csiki, Codrea, et al., 2010; Mannion & Upchurch, 2011). The position of *Magyarosaurus* was poorly constrained in these studies: such results potentially reflect the impact of phylogenetic character scores obtained from remains that can no longer be attributed with any

certainty to this taxon. Here, *Magyarosaurus* is placed either as a member of, or a close relative of, Saltasauridae.

In their original description of *Paludititan*, Csiki, Codrea, et al. (2010) recovered it in a range of positions dependent on the underlying phylogenetic dataset, including placing it as an early diverging titanosaur and as a saltasaurid. A sister taxon relationship between *Paludititan* and the Spanish genus *Lohuecotitan* was identified by Díez Díaz et al. (2018), with this clade positioned close to the 'base' of Lithostrotia. A similar position for *Paludititan* was supported by Navarro et al. (2022), although those authors identified *Lohuecotitan* as being phylogenetically deeply nested within the Lirainosaurinae instead. Sallam et al. (2018) placed both *Lohuecotitan* and *Paludititan* in a clade comprising Lirainosaurinae and closely related titanosaurs, with broadly similar results in other iterations of this matrix (Gorscak et al., 2023; Gorscak & O'Connor, 2016, 2019; Vila et al., 2022). In our analyses, *Paludititan* is consistently recovered either as a member of Lognkosauria, or just outside of this clade, albeit still closely related to *Lohuecotitan*. As such, our results differ, at least with respect to the wider phylogenetic position of this taxon, from those of all previous studies, while seemingly upholding a close *Paludititan*–*Lohuecotitan* relationship.

The phylogenetic position of *Petrustitan* has not been previously evaluated or discussed. This taxon has a less consistent placement than *Magyarosaurus* and *Paludititan*, although it is most closely related to South American early diverging eutitanosaurian taxa in both sets of analyses. Whereas *Petrustitan* groups with *Narambuenatitan* and *Pitekunsaurus* in our EQW analysis, it clusters with *Argentinosaurus*, *Patagotitan* and *Puertasaurus* in the EIW analysis.

Although it is not possible to quantitatively test the phylogenetic affinities of *Uriash* at this stage, at least one feature of this taxon is otherwise known only in Gondwanan lithostrotian titanosaurs. This pertains to the 'anteromedial arm' that characterizes the proximal half of the humerus, which is a feature that had previously been identified in the Argentinean genus *Argyrosaurus* (Mannion & Otero, 2012), as well as the African genera *Paralititan* and *Rukwatitan* (Gorscak et al., 2017), and which we newly document in *Gondwanatitan* and *Muyelensaurus*, from Brazil and Argentina, respectively (PDM pers. obs.). As these Gondwanan taxa are recovered in different parts of our trees, it is not possible to narrow down the phylogenetic affinities of *Uriash*, but it is noteworthy that none of the other European taxa cluster with any of these five Gondwanan genera, providing tentative support to the idea that *Uriash* belongs to a distinct lineage.

Most previous studies have tended to place the late Campanian Spanish genus *Lirainosaurus* either within, or close to, the saltasaurid radiation (e.g. Calvo, Porfiri, et al., 2007; Calvo, González Riga, et al., 2007; Curry Rogers, 2005; Gorscak & O'Connor, 2016; Navarro et al., 2022; Sanz et al., 1999; Upchurch et al., 2004), although it has been recovered as an early diverging lithostrotian or eutitanosaurian in some analyses (Díez Díaz et al., 2018; Gallina & Apesteguía, 2011; Salgado et al., 2015). The contemporaneous French genus *Atsinganosaurus* has been recovered as a member of Lirainosaurinae in some studies (Díez Díaz et al., 2018, 2021; Navarro et al., 2022), whereas it has clustered with Lognkosauria in others (Gorscak et al., 2023; Gorscak & O'Connor, 2019; Sallam et al., 2018; Vila et al., 2022). The early Maastrichtian Spanish taxon *Abditosaurus* has previously been recovered as a saltasaurid (Gorscak et al., 2023; Vila et al., 2022), without close affinities to any other European titanosaur. In our EQW analysis, *Lirainosaurus* is closely related to Saltasauridae, forming a clade with the African taxon *Mansourasaurus*, whereas *Abditosaurus* and *Atsinganosaurus* form an early diverging lithostrotian clade with the South American titanosaurs *Argentinosaurus* and *Patagotitan*. By contrast, in our EIW analysis, *Atsinganosaurus* is the sister taxon of *Lirainosaurus*, forming a lirainosaurine clade with *Abditosaurus*, with these taxa just outside the saltasaurid radiation. The overall position of *Lirainosaurus* in our analyses is broadly congruent with previous studies that have supported close affinities with saltasaurids, whereas the inconsistent placement of *Atsinganosaurus* mirrors the contrasting positions recovered by other authors. Both of our analyses support novel positions for *Abditosaurus*. The incorporation of the early Maastrichtian French titanosaur *Ampelosaurus*, which is known from multiple individuals, preserving much of the skeleton (Le Loeuff, 1995, 2005b), might help to better constrain the relationships of these western European taxa. *Ampelosaurus* has been recovered as a lirainosaurine in certain previous studies (Díez Díaz et al., 2018, 2021; Navarro et al., 2022; Vila et al., 2022), but was excluded here from the phylogenetic analyses given that it probably represents a chimaera and is in need of revision (VDD pers. obs.).

Broader implications for the evolutionary relationships of titanosaurs

There are a large number of additional novel results pertaining to the evolutionary relationships of Titanosauria. Here, we focus on several results that are broadly

consistent across equal and extended weights analyses, and that have implications for titanosaurian systematics.

Using a previous iteration of this data matrix, Poropat et al. (2023) recovered Diamantinasauria as a titanosaurian clade in their EQW analysis, but it fell outside of Titanosauria when EIW was applied. In the present study, both analyses support a non-titanosaurian placement for this clade (see also Beeston et al., 2024). With *Diamantinasaurus* now one of the most completely known somphospondylans (Beeston et al., 2024; Hocknull et al., 2009; Poropat, Upchurch, et al., 2015; Poropat et al., 2016, 2021, 2022, 2023; Rigby et al., 2022), this taxon potentially plays a pivotal role in determining the polarity and acquisition of character states at the base of Titanosauria.

In all of our analyses, the commonly recovered members of Colossosauria (see Carballido et al., 2022) are polyphyletic, forming three non-closely related clades. Lognkosauria includes its two clade specifiers, *Futalognkosaurus* and *Mendozasaurus*, as well as *Notocolossus* and the European taxa *Lohuecotitan* and *Paludititan*, but excludes *Argentinosaurus*, *Patagotitan* and *Puertasaurus*. The latter three taxa form a clade of early diverging lithostrotians, whereas Lognkosauria is more deeply phylogenetically nested within Lithostrotia (Figs 64, 65). This disruption of Lognkosauria contrasts with most recent analyses that have sampled a broad array of these taxa, including previous iterations of this data matrix (e.g. Agnolin et al., 2023; Carballido et al., 2017; González Riga et al., 2018; Hechenleitner et al., 2020; Mannion, Upchurch, Jin, et al., 2019), although not all analyses have supported the recovery of a diverse Lognkosauria (e.g. Gorscak & O'Connor, 2016, 2019; Navarro et al., 2022). The inclusion of non-South American taxa within Lognkosauria is not novel to our analysis. Previous iterations of the data matrix used herein provided some support for a position at the 'base' of Lognkosauria for the Early Cretaceous French sauropod *Normanniasaurus* (Averianov et al., 2021; Mannion, Upchurch, Jin, et al., 2019), although this is not supported in the present study. Material assigned to the latest Cretaceous North American genus *Alamosaurus* was recovered within this clade by some authors (Navarro et al., 2022; Tykoski & Fiorillo, 2017), a configuration which requires further testing. Lerzo et al. (2021) also found support for a lognkosaurian position for the early Late Cretaceous *Dzharatitanis* from Uzbekistan, although we contend that this taxon is much more likely to be a close relative of approximately contemporaneous somphospondylans from East Asia, such as *Dongyangosaurus* (e.g. see Mannion, Upchurch, Jin, et al., 2019; Sues et al., 2015), to which those authors made no comparisons. Nevertheless, our consistent recovery of the European taxa *Lohuecotitan* and *Paludititan*, as well as that of some Indo-Madagascan taxa (*Jainosaurus* and *Vahiny*) in our EIW analysis, within this clade provides support for a more widespread distribution of Lognkosauria.

A close relationship between Lognkosauria and Rinconsauria has also been found in a large number of studies (e.g. Carballido et al., 2017; Gallina & Apesteguía, 2011; Gallina & Otero, 2015; González Riga et al., 2018; Hechenleitner et al., 2020; Navarro et al., 2022; Pérez Moreno et al., 2023; Salgado et al., 2015), leading González Riga et al. (2019) to erect Colossosauria to unite the two clades. By contrast, the analyses of Gorscak and O'Connor (2016) and subsequent iterations of that data matrix (e.g. Gorscak & O'Connor, 2019; Sallam et al., 2018; Vila et al., 2022) recovered Rinconsauria and Lognkosauria as distantly related lineages, with the latter clade more closely related to Saltasauridae. Our analyses also support their phylogenetic separation, but here it is Rinconsauria that is consistently placed as more closely related to Saltasauridae. Both sets of our analyses recover the African titanosaur *Rukwatitan* within Rinconsauria for the first time, with unequivocal members otherwise represented by the two South American clade specifiers, *Rinconsaurus* and *Muyelensaurus*. The Early Cretaceous European taxon, *Normanniasaurus*, is placed either as an additional rinconsaurian or a close relative, providing further support for a broader spatiotemporal distribution of this clade.

The relationships of the South American titanosaur *Aeolosaurus* have been inconsistent across previous studies (Carballido et al., 2022), with most analyses placing it close to or within Rinconsauria (e.g. Calvo, Porfiri, et al., 2007; Calvo, González Riga, et al., 2007; Gorscak & O'Connor, 2019; Hechenleitner et al., 2020; Navarro et al., 2022; Poropat et al., 2023; Salgado et al., 2015; Santucci & Arruda-Campos, 2011), and some supporting closer affinities with saltasaurids (González Riga et al., 2018; Poropat et al., 2016). Nevertheless, regardless of its relationship with other taxa, in all cases, *Aeolosaurus* has been recovered as a relatively later-diverging titanosaur. Our analyses therefore stand out notably in placing *Aeolosaurus* and closely related taxa ('aeolosaurines') as a clade of early diverging titanosaurs. Aeolosaurini is currently defined as the most recent common ancestor of *Aeolosaurus* and *Gondwanatitan* and all of its descendants (Carballido et al., 2017; Franco-Rosas et al., 2004). Our EQW analysis restricts Aeolosaurini to the clade specifiers and probably *Arrudatitan* and *Caieiria*, all of which are from South America, with the Malagasy titanosaur *Rapetosaurus* recovered as the sister taxon to the clade. A more diverse Aeolosaurini is recovered in our EIW

analysis, including additional South American taxa (e.g. *Tapuiasaurus*), *Rapetosaurus*, the African titanosaur *Shingopana*, and the Mongolian taxon *Nemegtosaurus*. The position of *Shingopana* as a member of Aeolosaurini is consistent with some of the few analyses that have previously considered this taxon (Gorscak et al., 2017; Gorscak & O'Connor, 2019). Although the recovery of *Nemegtosaurus* as a member of Aeolosaurini may appear extremely unexpected, it has often been positioned as the sister taxon to *Tapuiasaurus*, a South American taxon that had not been recovered in this part of the tree prior to our analyses. However, this particular grouping may potentially be driven by a 'monophyly of the preserved' effect, rather than a genuinely close relationship (see e.g. D'Emic, 2012; Poropat et al., 2023; Wilson et al., 2016). Furthermore, neither *Nemegtosaurus* nor *Tapuiasaurus* are recovered as closely related to Aeolosaurini in our EQW analysis.

The analyses of Carballido et al. (2022) suggested that Colossosauria was one of the more stable groups inside Titanosauria, and those authors redefined it as the most inclusive clade containing *Patagotitan*, but not *Saltasaurus*. They also used *Patagotitan* as a clade specifier for two already existing, but largely unused clade names, Eutitanosauria and Saltasauroidea. Carballido et al. (2022) redefined Eutitanosauria as the most recent common ancestor of *Patagotitan* and *Saltasaurus* and all of its descendants, and Saltasauroidea as the most inclusive clade containing *Saltasaurus*, but not *Patagotitan*. The results from our analyses do not have a substantial impact upon the content of Eutitanosauria, the most notable outcome being the placement of *Aeolosaurus* outside of this clade. However, Colossosauria is now a depauperate clade, consisting of just a few taxa, whereas nearly all eutitanosaurians belong to Saltasauroidea. In parallel, Navarro et al. (2022) proposed an alternative definition for Saltasauroidea, as the most recent common ancestor of *Lirainosaurus*, *Opisthocoelicaudia* and *Saltasaurus*, and all of its descendants. Under this definition, the saltasauroid clade in our analyses would be much closer to the taxonomic composition envisaged by Carballido et al. (2022). However, rather than choosing between definitions, or proposing further changes, we suggest that further work is first required to test the robustness and consistency of these different alternative phylogenetic topologies.

Biogeographical implications for the assembly of the European titanosaur fauna

A survey of the literature suggests that there are three key hypotheses that could account for the presence of titanosaurs in Europe during the latest Cretaceous: Hypothesis 1 [H1] – sauropods died out in Europe during the early Late Cretaceous and then re-invaded from Africa in the Campanian–Maastrichtian; Hypothesis 2 [H2] – Early Cretaceous European titanosaurs gave rise to lineages that persisted into the latest Cretaceous; and Hypothesis 3 [H3] – titanosaurs were involved in faunal exchange between Europe and Asia during the Late Cretaceous. H2 can be regarded as having two variants: H2.1 – Early Cretaceous European titanosaurs were members of Gondwanan lineages that invaded the former area during the Barremian–Albian; and H2.2 – Titanosauria, or at least some of its major clades, originated in Eurasia and gave rise to the Early Cretaceous European fauna '*in situ*'. It should be noted that these hypotheses are not necessarily mutually exclusive: with multiple distinct titanosaur lineages present in latest Cretaceous European faunas, it is conceivable that different groups had distinct biogeographical histories (e.g. Díez Díaz et al., 2018). Moreover, some aspects of these hypotheses can be combined: for example, titanosaurs could have crossed from Africa to Europe (in the late Early Cretaceous and/or the latest Cretaceous) and then dispersed from the latter area to Asia (e.g. Upchurch, in press).

Our revised Romanian titanosaur taxonomy and updated phylogeny has produced evolutionary trees containing seven Late Cretaceous European sauropod genera (as well as *Normanniasaurus* from the Albian) distributed across five (EIW) or seven (EQW) lineages, providing a fresh opportunity to evaluate these biogeographical hypotheses. We have not carried out a quantitative phylogenetic biogeographical analysis (such as BioGeoBEARS; Matzke, 2013, 2014): this is partly because this would substantially increase the length of an already long study, and partly because we believe that such analysis should wait until further planned work on titanosaurian phylogeny is completed. Instead, below we first offer some caveats regarding fossil record sampling, and then explore the key biogeographical hypotheses in more detail and determine to what extent they are supported or contradicted by our new insights into European sauropod lineages.

Fossil record sampling. Before examining individual titanosaur relationships and assessing their biogeographical implications, an important caveat concerning fossil record sampling must be discussed. In our assessments below, we make the assumption that a ghost lineage occupied the same geographical area as its terminal taxon. This is reasonable in terms of Occam's Razor – without additional evidence, we cannot justify more complex assumptions of area occupancy. Thus, if we have a European taxon X of Maastrichtian age that is

the sister taxon of a South American taxon Y of Albian age, the implied ghost range would be inferred as occupying Europe from the Albian to the Maastrichtian. The problem is that such assumptions can easily be invalidated by uneven fossil record sampling. If, for example, taxon Z from Campanian age deposits in Africa is more closely related to taxon X than is taxon Y, then the lineage extending from X + Z back to the Albian might have included taxa living in Europe, or Africa, or both. Failure to sample taxon Z could thus have a significant impact on the inferred biogeographical history. This is more than just a hypothetical example: the Late Cretaceous dinosaur fossil record of Africa is particularly poorly sampled (Gorscak et al., 2023; Krause et al., 2019; Mannion & Barrett, 2013; Sereno & Brusatte, 2008; Tortosa et al., 2014; Vila et al., 2022; Upchurch, in press), as illustrated by the relatively low numbers of such taxa in our data set. The deleterious effects of sampling failures can be partially alleviated by applying quantitative phylogenetic biogeographical methods such as BioGeoBEARS, but even these approaches are not immune to sampling issues (e.g. Mannion, Upchurch, Jin, et al., 2019; Poropat et al., 2016). This issue, combined with the observation that our EQW and EIW trees have different topologies and therefore imply different biogeographical histories, demonstrates the need to regard the following discussion as presenting working hypotheses that should be tested through new specimens and further work on titanosaur phylogenetic relationships.

H1: Late Out of Africa, and the 'sauropod hiatus'. During the 1980s and 1990s, two linked ideas were proposed to explain the presence of titanosaurs in latest Cretaceous European faunas. First, several studies noted the apparent absence of sauropods in North America and Europe throughout most of the Late Cretaceous, the so-called 'sauropod hiatus' (Le Loeuff, 1993; Le Loeuff & Buffetaut, 1995; Lucas & Hunt, 1989; see reviews in D'Emic et al., 2010; Mannion & Upchurch, 2011; Upchurch, in press). Second, if the hiatus hypothesis is correct, then the latest Cretaceous European titanosaurs must have invaded from another region during the Campanian and/or Maastrichtian. Titanosaurs have long been regarded as an essentially Gondwanan radiation (e.g. Wilson & Upchurch, 2003; see also Mocho et al., 2019), and, even today with much better sampling from Laurasia (e.g. Mannion, Upchurch, Jin, et al., 2019), the clade remains dominated by taxa from South America, augmented by taxa from Indo-Madagascar, with recently described contributions from Africa and Australia (e.g. Carballido et al., 2017; Curry Rogers, 2009; Curry Rogers & Wilson, 2014; Gallina et al., 2022; Gorscak et al., 2023; Gorscak & O'Connor, 2016; Hocknull et al., 2009; Poropat et al., 2016; Sallam et al., 2018; Santucci & Filippi, 2022; Wilson et al., 2009). Consequently, the latest Cretaceous European titanosaurs have been interpreted as invaders from Gondwana, and the palaeogeographically most probable source area for such dispersals has been identified as Africa (Astibia et al., 1990; Buffetaut, 1989; Buffetaut et al., 1988; Csiki, 1997; Csiki-Sava et al., 2015; Ezcurra & Agnolin, 2012; Gheerbrant & Rage, 2006; Le Loeuff, 1991, 1993, 1997; Le Loeuff & Buffetaut, 1995; Novas et al., 2013; Pereda-Suberbiola, 2009; Rage, 1996, 2002; Vila et al., 2022; Weishampel et al., 2010).

More recently, the validity of the sauropod hiatus has been questioned (Mannion & Upchurch, 2011), especially regarding Europe (e.g. Pereda-Suberbiola, 2009; Wilson & Upchurch, 2003). Although sauropods remain unknown in North America from the late Cenomanian to end-Campanian (inclusive) (D'Emic et al., 2010), there is now strong evidence that they were present in Europe during this time interval. In particular, a number of Turonian–Santonian tracksites, as well as a tooth, indicate the presence of sauropods in Europe at this time (Mezga et al., 2006; Nicosia et al., 2007; Ősi et al., 2017b; Solt et al., 2020). This opens up the possibility that at least parts of Europe were occupied by sauropods continuously from the Early Cretaceous through to the Maastrichtian, and that at least some of the latest Cretaceous titanosaurs could be descendants of earlier European forms rather than recent immigrants from Africa or elsewhere (see below).

Palaeogeography provides another line of evidence that potentially mitigates against the latest Cretaceous 'out of Africa' explanation for European titanosaurs. Recent palaeogeographical maps depict an extensive marine barrier between Africa and various European islands during the Campanian–Maastrichtian (Longrich et al., 2021, 2024; Scotese, 2016). This does not necessarily falsify H1 if sauropods were capable of transoceanic dispersal. Some workers have advocated that such dispersals were feasible for sauropods and other large-bodied dinosaurs (e.g. Dunhill et al., 2016; Longrich et al., 2021, 2024), but others have considered this unlikely (Mannion, Upchurch, Schwarz, et al., 2019; Poropat et al., 2016; Xu et al., 2018; Upchurch, in press). Ezcurra and Agnolin (2012) and Vila et al. (2022) argued for a landbridge linking Africa and Europe via a re-emergent Apulian carbonate platform during the latest Cretaceous. However, a continuous Europe–Africa land route at this time seems unlikely given current palaeogeographical data (Gheerbrant & Rage, 2006; Longrich et al., 2021, 2024; Upchurch, in press). Dispersals of sauropods via 'island hopping'

seem more feasible, especially at times of lower sea level, such as in the mid-Campanian and at the Campanian/Maastrichtian boundary (Csiki-Sava et al., 2015; Gheerbrant & Rage, 2006; Le Loeuff, 1991; Longrich et al., 2021, 2024; Ősi, Apesteguía, et al., 2010; Vila et al., 2022), although this would still require sauropods to have crossed some open bodies of water.

Recent support for the occurrence of latest Cretaceous sauropod dispersals between Europe and Africa has come from studies by Sallam et al. (2018), Vila et al. (2022), and Gorscak et al. (2023). Sallam et al. (2018) and Gorscak et al. (2023) described the titanosaurs *Mansourasaurus* and *Igai*, respectively, from mid-Campanian deposits in Egypt, and assessed their phylogenetic relationships and biogeographical histories via Bayesian tip-dating methods and BioGeoBEARS. Sallam et al.'s (2018) results suggested that *Mansourasaurus* was nested in a latest Cretaceous clade of European and Asian titanosaurs, and its ancestral lineage had probably dispersed from Europe at approximately 75 Ma. This implies the existence of a viable crossing between Europe and Africa, and it is interesting that the inferred timing of this dispersal lies close to the mid-Campanian KCa6 sea-level lowstand event (see Haq, 2014) mentioned above. Gorscak et al. (2023) found a similar topology, although they estimated that the divergence of *Mansourasaurus* occurred at ∼80 Ma, disrupting the previously proposed correlation with the KCa6 sea-level lowstand; nevertheless, such an earlier dispersal coincides with the more substantial earliest late Campanian (∼80 Ma) KCa3 sea-level drop of (Haq, 2014). Our results are partially compatible with these previous works. In particular, the EQW topology includes *Lirainosaurus* and *Mansourasaurus* as sister taxa (see also Navarro et al., 2022), supporting dispersal between Europe and Africa prior to the late Campanian (though the direction of this dispersal is currently uncertain). By contrast, *Mansourasaurus* is the sister taxon of latest Cretaceous South American saltasaurines in our EIW trees. If the latter is correct, this would remove the necessity to infer a latest Cretaceous Europe to Africa dispersal event, and instead the presence of *Mansourasaurus* could be interpreted as part of a South America/Africa vicariance pattern resulting from their final separation at ∼100 Ma (see Gorscak & O'Connor, 2016; Upchurch, in press [and references therein]). *Igai* was placed as the sister taxon of a European lineage (*Lirainosaurus*+*Lohuecotitan*) in the analyses of Gorscak et al. (2023), with their divergence time estimated as close to the Santonian/Campanian boundary. As *Igai* is not included in our phylogenetic data set, we provisionally accept Gorscak et al.'s (2023) view that it supports dispersal between Europe and Africa during the latest Cretaceous: we note, however, that the 95% highest posterior density for this node age extends as far back as the earliest Late Cretaceous and thus does not definitively contradict H2.1.

Perhaps the strongest recent case for latest Cretaceous dispersal of titanosaurs from Africa to Europe was presented by Vila et al. (2022). That study described the early Maastrichtian Ibero-Armorican titanosaur *Abditosaurus* and found support for a sister taxon relationship with the Cenomanian African form *Paralititan*. BioGeoBEARS ancestral area estimation suggested that the most recent common ancestor (MRCA) of *Paralititan* and *Abditosaurus* lived either in Africa or was widespread across the latter continent and Europe, and that the ancestor of the lineage leading solely to *Abditosaurus* occurred in Africa, or Europe, or both. Vila et al. (2022) interpreted these results as supporting dispersal from Africa to Europe during an earliest Maastrichtian (∼70.6 Ma) sea-level lowstand. Additional support for this scenario, based on sauropod body mass variation and their egg fossil record, was also presented by Vila et al. (2022), and linked to faunal turnover in the middle part of the Maastrichtian. Essentially, Vila et al. (2022) suggested that Europe was characterized by a Campanian–early Maastrichtian sauropod fauna comprising small-bodied island dwarf forms (such as *Ampelosaurus*, *Atsinganosaurus*, *Lirainosaurus* and *Lohuecotitan*) that probably produced the endemic oospecies *Megaloolithus aureliensis* and *Megaloolithus siruguei*. During the early Maastrichtian, larger-bodied titanosaurs from Africa, such as the *Abditosaurus* lineage, invaded western Europe and replaced the dwarfed forms as part of the 'Maastrichtian Dinosaur Turnover' (MDT) that also involved a shift away from sauropod-dominated faunas to ones with a higher abundance and diversity of ornithopods (especially lambeosaurine hadrosaurs) (Csiki-Sava et al., 2015; Mocho et al., 2019). Moreover, *Abditosaurus* was found in association with the oospecies *Fusioolithus baghensis*. This oospecies, and also *Megaloolithus mamillare*, are known from Campanian and Maastrichtian age deposits in South America and India (and potentially also Africa in the case of the former egg type), but do not occur in Europe until the early Maastrichtian. Vila et al. (2022) therefore proposed that the transition from the *Megaloolithus aureliensis*+*Megaloolithus siruguei* assemblage to the *Fusioolithus baghensis*+*Megaloolithus mamillare* one in Europe during the early Maastrichtian marks the invasion of non-dwarfed titanosaurs from Gondwana. Given that *Abditosaurus* is an Ibero-Armorican taxon, the focus of Vila et al.'s (2022) study was on that area; however, they speculated that their invasion and replacement scenario might also

apply to the Haţeg region where it could explain the presence of dwarf forms such as *Magyarosaurus* and large ones such as the taxon represented by *Uriash* (but see below). In addition, although not specifically highlighted by Vila et al. (2022), the occurrence of the Transylvanian *Paludititan*, recovered in their study as the sister-taxon of the north African *Mansourasaurus*, could represent a potential second example of such an early Maastrichtian out-of-Africa titanosaur dispersal.

Vila et al.'s (2022) study provides an elegant and unifying explanation of several disparate aspects of latest Cretaceous European dinosaur biogeography. However, closer scrutiny reveals a number of difficulties, especially in light of our revision of Haţeg titanosaur taxonomy and broader phylogenetic results. First, Vila et al.'s (2022) own BioGeoBEARS results are more compatible with H2.1 than H1: most estimates suggest that *Abditosaurus* was descended from an ancestor that lived in Europe, or Europe + Africa, during the Cenomanian. However, in any case, an augmented and updated version of the Vila et al. (2022) data set was analysed by Gorscak et al. (2023), resulting in the disruption of the *Paralititan-Abditosaurus* clade, with the latter genus instead being placed as the sister taxon of the South American early–middle Campanian titanosaur *Pellegrinisaurus*. Second, our phylogenetic results also do not support a sister taxon relationship between *Abditosaurus* and an African form. Our EQW trees place *Abditosaurus* as a member of an endemic latest Cretaceous European lirainosaurine clade (with *Atsinganosaurus* and *Lirainosaurus*), which is the sister taxon of a South American lineage comprising the Coniacian taxon *Elaltitan* and the late Campanian–early Maastrichtian genus *Bonatitan*. These relationships are not decisive with regard to choosing between H1 and H2.1: the latter hypothesis would be favoured if we assume that terrestrial dispersal between South America and Africa ended around 100 Ma, when the Central Atlantic Ocean severed their last remaining land connection (see Upchurch, in press and references therein), but H1 can still be supported if we accept the feasibility of transoceanic dispersal for sauropods or the presence of land connections persisting much later into the Cretaceous (e.g. Ezcurra & Agnolin, 2012; Sereno et al., 2004). By contrast, our EIW trees place *Abditosaurus* as the sister taxon of the late Cenomanian *Argentinosaurus*: given the minimum age of their MRCA, such a relationship is more consistent with H2.1. Third, significant spatiotemporal gaps in the fossil record of sauropod eggs mean that it is difficult to test the proposition that the producers of *Fusioolithus baghensis* and *Megaloolithus mamillare* originated in Gondwana and dispersed into Europe during the early Maastrichtian. For example, despite the presence of taxa such as *Alamosaurus* in North America and *Opisthocoelicaudia* in East Asia during the Maastrichtian, no fossil eggs referable to titanosaurs are known from these regions at present. Finally, our revised taxonomy and chronostratigraphical framework for Haţeg titanosaurs does not lend support to the proposal that large-bodied forms replaced dwarf forms, and, when considered together with data concerning other dinosaurian taxa, also casts some doubt on the occurrence of a MDT in Transylvania (see the 'Body size evolution and island dwarfism in Transylvanian titanosaurs' section below).

Aside from the *Lirainosaurus*+*Mansourasaurus* sister taxon relationship in the EQW trees (see above), the strongest (although still relatively weak) support for H1 in our results involves *Magyarosaurus* and *Petrustitan*. In the EQW trees, *Magyarosaurus* is the sister taxon of the widespread clade containing *Pellegrinisaurus*, *Alamosaurus*, saltasaurines, *Isisaurus*, and *Opisthocoelicaudia*, with all of these taxa being Campanian or Maastrichtian in age. However, given that this clade contains both Laurasian and Gondwanan forms, it is difficult to determine the ancestral area for the lineage leading to *Magyarosaurus* without applying a more quantitative method. In the EIW trees, *Magyarosaurus* is nested in a South American clade as the sister taxon of the Maastrichtian Brazilian taxon *Baurutitan*; and in the EQW trees, *Petrustitan* is the sister taxon of a clade containing the early–middle Campanian South American taxa *Narambuenatitan* and *Pitekunsaurus*. Although no African taxa are associated with these portions of our trees, some support for H1 can be claimed on the basis that *Magyarosaurus* and *Petrustitan* typically have their closest relatives in latest Cretaceous South American faunas, implying potential Gondwana to Europe dispersals during this interval. Such an interpretation requires either: direct dispersal to Europe from South America (or via Africa) during the latest Cretaceous, which seems unlikely given the width and depth of the North and Central Atlantic in the latest Cretaceous (Upchurch, in press and references therein); or a substantial amount of sampling failure in the European, South American, and especially African Late Cretaceous terrestrial fossil records, which is a more plausible explanation (see above).

H2: Descendants of an Early Cretaceous European fauna. The fossil record clearly demonstrates the presence of titanosaurs in Early Cretaceous faunas in Europe and western Asia, including *Volgatitan* from the upper Hauterivian of western Russia (Averianov & Efimov, 2018), fragmentary remains from the Barremian Wessex Formation of the Isle of Wight, UK (D'Emic, 2012; Le Loeuff, 1993; Mannion et al., 2013; Upchurch et al., 2011; Wilson & Upchurch, 2003), a *Malawisaurus*-like taxon from the upper Aptian–lower

Albian of Italy (Dal Sasso et al., 2016), and *Normanniasaurus* from the lower Albian of France (Le Loeuff et al., 2013). Given the evidence cited above for the presence of sauropods in Europe during the Turonian–Santonian, it is conceivable that latest Cretaceous titanosaurs represent direct descendants of these Early Cretaceous European faunas. The latter faunas appear to include immigrants from Gondwana, as indicated by several recent discoveries and phylogenetic studies (Dal Sasso et al., 2016; Gorscak & O'Connor, 2016; Holwerda et al., 2018; Mocho et al., 2019; Weishampel et al., 2010; Upchurch, in press), giving rise to the H2.1 variant of H2. For example, the Bayesian phylogenies and BioGeoBEARS analyses presented by Gorscak and O'Connor (2016) and Sallam et al. (2018) supported the presence of a latest Cretaceous Eurasian clade whose ancestral lineage dispersed from Gondwana at approximately 93 Ma. Moreover, Dal Sasso et al. (2016) and Mocho et al. (2019) reported titanosaur remains from the Albian of Italy and Cenomanian of Spain, respectively, and showed that these taxa had close affinities with Gondwanan lineages. These putative dispersal events coincide with the probable presence of a land connection (via the Apulian Route) during the Barremian–early Albian.

The most frequently observed pattern in our results is one in which one or more latest Cretaceous European taxa are the sister taxa of a Gondwanan (typically South American) form that occurred during the late Early or early Late Cretaceous. This pattern is indeed most consistent with H2.1. Such lineages include: (1) the *Abditosaurus-Argentinosaurus* clade in the EIW tree (see above); (2) the late Campanian *Atsinganosaurus* (EQW) or the early–early late Maastrichtian *Petrustitan* (EIW) clustering with the late Albian *Patagotitan* and late Cenomanian *Argentinosaurus*; (3) the late Campanian–early Maastrichtian *Lohuecotitan* and the 'mid'-Maastrichtian *Paludititan* clustering with late Turonian–Santonian members of Lognkosauria (EQW and EIW); and (4) the lirainosaurine clade which diverged from a South American lineage (including *Elaltitan*) prior to the Coniacian (EQW). The early Albian *Normanniasaurus* is the sister taxon of the putatively Cenomanian African taxon *Rukwatitan* (EQW), and, although not directly informative regarding the latest Cretaceous sauropods of Europe, does also support faunal exchange between these two areas in the late Early Cretaceous. Recently, the possibility that *Rukwatitan* is Campanian in age has been raised (Widlansky et al., 2018), but the Albian age of *Normanniasaurus* would still favour a late Early Cretaceous Europe–Africa dispersal rather than a latest Cretaceous one.

Although not mutually exclusive of Barremian–Albian dispersals from Africa to Europe, it is also conceivable that at least some components of the Early Cretaceous European titanosaur fauna had occupied that region since the earliest Cretaceous or even the Late Jurassic (H2.2) (see e.g. Averianov & Efimov, 2018). Indeed, the observation that the stratigraphically oldest members of Titanosauria are typically Eurasian (with the exception of the late Berriasian–Valanginian *Ninjatitan* from Argentina; Gallina et al., 2021), could be interpreted as indicating that this clade originated there. If correct, then at least some of the latest Cretaceous European titanosaur lineages might be direct descendants of this initial radiation, either persisting *in situ* in Europe or invading from Asia (see H3 below). For example, the late Hauterivian *Volgatitan* from Russia (Averianov & Efimov, 2018) potentially predates the sea-level lowstands that apparently generated the Apulian landbridge during the Barremian–early Albian (Upchurch, in press): as such, the occurrence of this Russian taxon is more consistent with H2.2 than H2.1. Similarly, stratigraphically older taxa such as the Valanginian *Tengrisaurus* (from Asiatic Russia; Averianov et al., 2021) and *Volgatitan* have been placed in early diverging positions in the titanosaurian clades Lognkosauria, Colossosauria and Rinconsauria, suggesting that these groups originated in Asia according to Averianov and Efimov (2018) and Averianov et al. (2021). Moreover, as noted above, there are several instances of apparent dispersal involving Europe and Africa during the middle or latest Cretaceous that can be interpreted as Laurasian lineages invading Gondwana.

Although a Eurasian origin of titanosaurs around approximately the Jurassic/Cretaceous boundary cannot be ruled out, there are some lines of evidence that suggest this is a less likely scenario than a Gondwanan origin. In particular, there are far more Gondwanan titanosaurs than Laurasian ones, and this results in most of the Eurasian taxa being deeply nested within Gondwanan clades. Such a recurrent topology might be interpreted as the result of a sampling bias, but this explanation seems unlikely given that current data suggest that any such bias is in favour of Laurasia. For example, inspection of *The Paleobiology Database* (https://paleobiodb.org/, accessed on 15 August 2023), indicates that 84% of Cretaceous dinosaur-bearing collections, and 82% of Cretaceous tetrapod-bearing collections, have been recovered from Laurasian landmasses. In short, although H2.2 cannot be rejected at this time (especially given the difficulties of estimating

phylogenetic relationships accurately for the often very fragmentary earliest titanosaur specimens), a Eurasian origin for titanosaurs followed by numerous earliest Cretaceous dispersals to Gondwana seems less likely than other scenarios based on current evidence.

H3: Europe-Asia faunal interchange in the Late Cretaceous. Putative dispersals between Europe and Asia during the Late Cretaceous have played an important role in explaining several aspects of dinosaurian biogeographical history, although this has largely applied to non-sauropod groups such as dromaeosaurid theropods, lambeosaurine hadrosaurs, and ceratopsians (Csiki, Vremir, et al., 2010; Gierliński, 2015; Prieto-Márquez et al., 2013; Prieto-Marquez & Wagner, 2009; Ősi, Butler, et al., 2010; Sellés et al., 2021; see review in Upchurch in press). Recently, however, several phylogenetic studies have also found evidence for a latest Cretaceous opisthocoelicaudine clade comprising European and Asian taxa (Gorscak & O'Connor, 2016; Gorscak et al., 2023; Sallam et al., 2018; Vila et al., 2022). Divergence time estimation and BioGeoBEARS analysis by Sallam et al. (2018) generated a biogeographical scenario that fits well with our current understanding of palaeogeographical history. Essentially, having crossed from Gondwana at around 93 Ma (see above), a lineage of titanosaurs apparently gave rise to a clade that became widespread across Eurasia in the mid-Santonian (~85 Ma). This geodispersal event coincided approximately with a late Coniacian–early Santonian drop in sea level that created a land connection between Europe and Asia across the Turgai Sea (Baraboshkin et al., 2003; Longrich et al., 2021, 2024; Poropat et al., 2016; Upchurch, in press). Subsequently, it appears that this clade underwent two Europe/Asia vicariance events in the early part of the Campanian (~78–80 Ma), reflecting increasing sea levels during the late Santonian and early Campanian that severed the land connection across the Turgai Sea and made the latter a more significant marine barrier to terrestrial dispersal (Baraboshkin et al., 2003; Upchurch, in press).

However, evidence for a Eurasian opisthocoelicaudine clade is not present in either the EQW or EIW topologies. Indeed, the only sister-taxon relationships between European and Asian titanosaurs are seen in the EIW trees, involving taxa of Early/Late Cretaceous boundary age (i.e. the Albian *Normanniasaurus* from France, and the Cenomanian *Dongyangosaurus* and *Jiangshanosaurus* from China) (see also Averianov et al., 2021, who recognized a close relationship between *Normanniasaurus* and *Tengrisaurus*). Although this represents a Eurasian clade of titanosaurs, it is not currently known to have given rise to any latest Cretaceous forms. Moreover, the geodispersal event(s) that would have produced this Eurasian clade predate the Coniacian–Santonian sea-level lowstand highlighted by Upchurch (in press). Therefore, this mid-Cretaceous biogeographical pattern could be part of a more general phenomenon among dinosaurs whereby an Aptian–Albian sea-level lowstand established land connections between Europe and Asia, Europe and Africa, and potentially also Europe and North America, allowing multiple dispersal events (e.g. Upchurch, in press; Upchurch et al., 2002).

Summary. Part of the difficulty in understanding the origins of the Campanian–Maastrichtian European titanosaur faunas stems from placing dispersal from Gondwana in opposition to the idea of Early Cretaceous European/Eurasian relicts persisting into the latest Cretaceous. However, these two concepts can be reconciled by postulating Barremian–Albian dispersals from Africa into Europe (and vice versa), followed by survival of those lineages through the 'sauropod hiatus' into the latest Cretaceous (H2.1). Notwithstanding issues of uneven sampling and a particularly poor Late Cretaceous African terrestrial fossil record, H2.1 is most consistent with our results. This scenario side-steps ongoing controversies over the extent of marine barriers between Europe and Africa, and between the latter and South America, during the latest Cretaceous, and also avoids the necessity of inferring that titanosaurs underwent multiple long-distance transoceanic dispersals. Moreover, H2.1 also matches the growing evidence for continuous occupation of the European region by titanosaurs from at least the Barremian through to the Maastrichtian. Yet, the combination of titanosaur egg chronostratigraphical data, occurrence of several episodes of sea-level lowstands in the Campanian and earliest Maastrichtian, and the phylogenetic relationships of *Mansourasaurus* and *Igai*, mean that it would be premature to fully reject H1. The evidence supporting these different ideas tends to wax or wane depending on which phylogeny is preferred. For example, our phylogenetic results are clearly more consistent with H2.1, and offer only sparse and weak support for H1 and H3. By contrast, phylogenies based on the Gorscak and O'Connor (2016) family of data matrices tend to support a Eurasian clade (H3), although usually in a way that is also compatible with H2.1 (e.g. lineages crossing from Gondwana into Europe during the mid-Cretaceous and then dispersing from Europe into Asia during the Late Cretaceous). Thus, establishing a consensus on the relationships and divergence times of European and Asian titanosaurs, and improved sampling of the critical Cenomanian–Santonian time interval in both Europe and Africa, will be central to resolving these biogeographical debates.

Titanosaur colonization of the latest Cretaceous Hațeg Island

The absence of any close phylogenetic relationship between *Magyarosaurus*, *Paludititan*, *Petrustitan* (Figs. 64, 65), and probably *Uriash*, combined with the absence of any pre-Maastrichtian titanosaur remains on the Transylvanian landmass (e.g. Bălc et al., 2024; Vremir et al., 2014), suggests that representatives of each of these lineages migrated into this insular area after the Campanian/Maastrichtian boundary, via four separate dispersal events. Although the details of these dispersals remain contentious (see the previous section), it is nonetheless clear that the assembly of the Hațeg Island titanosaur fauna was a protracted process involving several different episodes of biotic connection with other areas. Most intriguingly, the near-absence of any particularly close phylogenetic relationships between most latest Cretaceous Transylvanian and Ibero-Armorican titanosaurs also suggests that there may had been little faunal exchange between these two parts of the Late Cretaceous European Archipelago, and that most of the Transylvanian and Ibero-Armorican titanosaurs were derived from different source areas.

This multi-step assembly scenario, fuelled by recurrent faunal exchange events, potentially characterizes the Hațeg Island faunas overall, as was recently hinted at in the description of a new Transylvanian rhabdodontid by Augustin et al. (2022). Thus, despite ample evidence for a high level of endemism in the Hațeg Island assemblages (e.g. Csiki & Grigorescu, 2007; Csiki-Sava et al., 2015; Weishampel et al., 2010), which is reinforced by our results, it appears that this area may not have been as isolated as previously thought (e.g. Weishampel et al., 2010) and that occasional faunal connections were possible throughout the latest Cretaceous. Although this combination of endemism and recurrent episodes of faunal connection might appear counter-intuitive at first glance, similar patterns have been documented in the Cenozoic insular fossil record (see examples in e.g. van der Geer et al., 2021). Such instances usually result from a synergic interaction between repeated episodes of: (1) areal connections being established among previously isolated areas due to short-term eustatic changes and/or tectonic events (which promote range expansion of previously isolated faunal elements); and (2) subsequent rapid evolution of the newly introduced faunal elements (a characteristic of insular evolution; e.g. Cucchi et al., 2014; Keogh et al., 2005; Millien, 2006; van der Geer et al., 2021 and references therein) once connections are severed again and some degree of more stringent biotic isolation is re-established. The relatively large number of eustatic sea-level fall episodes that took place during the first half of the Maastrichtian (four in fewer than 4 million years; Haq, 2014), all of which are documented in Europe, combined with the tectonically active nature of the entire eastern European area, including the surroundings of the Transylvanian landmass (e.g. Csiki-Sava et al., 2016; Schmid et al., 2020; van Hinsbergen et al., 2020), and references therein), would have created the ideal setting for such a palaeobiogeographical evolutionary scenario.

Body size evolution and island dwarfism in Transylvanian titanosaurs

Dwarfism. One of the most striking features of the Transylvanian titanosaurs, excluding *Uriash*, is their small size compared to most other sauropods. Nopcsa (1914; see also Nopcsa, 1923a) noted a similar phenomenon among other sympatric herbivorous dinosaurs (ornithopod and ankylosaur ornithischians) and linked it to an isolated island habitat. He hypothesized that the small titanosaurs were insular dwarfs, Mesozoic correlatives of the Plio-Pleistocene dwarf elephants of the Mediterranean islands. The dwarfed status of the Hațeg titanosaurs was supported by morphometric regression analyses of their humeri by Jianu and Weishampel (1999), who regarded it as a by-product of paedomorphosis. This interpretation was, however, subsequently questioned by Le Loeuff (2005a, fig. 1a), who noted the presence of large skeletal elements (including the humerus of *Uriash*) among the titanosaurian fossils from the Hațeg Basin, demonstrating that not all Transylvanian titanosaur specimens were of small size. Le Loeuff (2005a) proposed that the relatively small specimens were merely juveniles of a larger-bodied taxon, and that the observed abundance of small elements could be explained by taphonomical and/or palaeoecological biases. In order to resolve this issue, Stein et al. (2010; see also Benton et al., 2010) conducted an osteohistological survey of a large sample of Transylvanian titanosaur limb bones, concluding that the most common remains did indeed belong to dwarfed, adult individuals. Nevertheless, the presence of a larger-bodied taxon in this sample was also suggested based on distinctive osteohistological traits shown by one of the sampled elements, reigniting a long-lasting thread of taxonomic discussions concerning these titanosaurs.

A total of 22 appendicular specimens were sampled by Stein et al. (2010, see table 1), and the new referrals presented in the current work provide an opportunity to review and update their data and conclusions. Of the originally sampled elements: 16 are currently regarded as indeterminate/unidentified titanosaurs; five can be referred to *Magyarosaurus dacus* – the humerus SZTFH Ob.3089 and the fibula SZTFH Ob.3086 of Assemblage A (representing the type material of this taxon), and the

humerus LPB (FGGUB) R.1047 and the femora LPB (FGGUB) R.1046 and R.1992 of Individual E; and one belongs to *Uriash kadici* – the humerus SZTFH Ob.3104 (Individual C). Stein et al. (2010) highlighted significant osteohistological differences between SZTFH Ob.3104 and those referred here to *Magyarosaurus dacus*, and indicated that this humerus cannot be placed on the same growth trajectory with those referred to the latter taxon. Indeed, although being markedly larger, the humerus of *Uriash kadici* (SZTFH Ob.3104) displays an earlier histological ontogenetic stage (HOS11) than the elements referred to *Magyarosaurus dacus* (HOS13 for the humerus LPB [FGGUB] R.1047; HOS14 for the femora LPB [FGGUB] R.1046 and R.1992 of Individual E, and the elements sampled from Assemblage A), making *Uriash* an ontogenetically younger titanosaur individual than the sampled material of *M. dacus*.

Magyarosaurus has the best skeletal representation of any Transylvanian titanosaur, allowing robust body size and mass estimates for several individuals using the formulae proposed by Benson et al. (2018), Packard et al., (2009), and Seebacher (2001) (see Table 2). With an estimated total length of less than 3 metres, *Magyarosaurus* is the smallest adult sauropod currently known, smaller than the Brazilian dwarf titanosaur species *Ibirania parva* (5.7 metres, Navarro et al., 2022), and the latest Cretaceous Ibero-Armorican taxa *Lirainosaurus* and *Atsinganosaurus*, which reached body lengths of 4–9 metres (Díez Díaz et al., 2021, table 3). Moreover, the adult body mass estimate for *M. dacus* of under 1 tonne has not been observed for any other titanosaur (Benson et al., 2018). All of this evidence confirms that *Magyarosaurus* was the product of a dramatic dwarfing process. However, it should be noted that the body length value of 2.5–2.7 metres for *Magyarosaurus* would indicate a remarkably gracile, long-limbed body shape for this animal, with an estimated hip height of approximately 1 metre based on the summed lengths of its hind limb elements (Table 2). These could be regarded as unrealistic body proportions for a sauropod, perhaps indicating that the formulae used here for calculating titanosaur body lengths have problematically wide error margins when applied to particularly small taxa. However, comparable changes in overall body shape (relative elongation of limbs, and overall more gracile posture) have also been reported for other Late Cretaceous European island-dwelling dinosaurs (Ősi & Makádi, 2009), suggesting that such body shape modifications might have arisen convergently as a result of adaptation to the demands of island life.

Elements from two other key titanosaur individuals/assemblages discussed in this study were also sampled by Stein et al. (2010), including several limb bones from Assemblage J in the LPB (FGGUB) collection (humerus [R.1246], ulna [R.1598], femora [R.1220, R.1511], and tibia [R.1252]), and both elements referred to Assemblage M (humerus [SZTFH v.13492], and ulna [SZTFH Ob.3099]). In the case of Assemblage J, the osteohistological maturity of the elements varies between HOS12 (tibia) to HOS14 (humerus, ulna), despite all the sampled elements being even smaller than those of *Magyarosaurus*. The same is also true for Assemblage M, where both elements display very advanced osteohistological stages (HOS13–14), for a body size comparable to that of *Magyarosaurus*. Stein et al. (2010) implicitly considered all these elements referable to *Magyarosaurus dacus*, because they could be easily accommodated within the same growth trajectory. However, here we are unable to unequivocally refer these assemblages to *M. dacus* based on shared autapomorphies, and thus they are currently left as indeterminate titanosaurs. Nevertheless, these occurrences show that the advanced degree of dwarfing documented in *Magyarosaurus* was potentially more widespread among Transylvanian titanosaurs.

The specimens referred to *Petrustitan* have dimensions close to those of *Magyarosaurus* (Table S1), although *Petrustitan* may had been somewhat larger, in line with the original proposal of Huene (1932). The largest *Petrustitan* specimen (Individual B, the type material) is estimated to have been approximately 16–20% larger in linear dimensions than the largest specimen referred to *Magyarosaurus* (Individual E), assuming a more or less isometric scaling between the two taxa. This would translate into a body length estimate of *c*. 3.2 metres for *Petrustitan*, a figure that still places it at the lower end of the titanosaur body size spectrum, even when compared to the other generally small-bodied European titanosaurs. However, because no histological analyses have been carried out for any *Petrustitan* specimens, it is currently unknown whether they belong to immature or adult individuals, and thus their attribution to a dwarf species must be treated with caution at present.

The elements of *Paludititan* that overlap anatomically with *Magyarosaurus* (mainly dorsal and caudal vertebrae) similarly indicate a somewhat larger body size for the former taxon (3.5–4 metres in length), albeit still markedly smaller than the largest known specimens of *Lirainosaurus* and *Atsinganosaurus* (4–9 metres in length). Furthermore, the degree of fusion between neural centra and arches in both the dorsal and caudal vertebrae of the only known individual of *Paludititan* suggests that it most probably represents an ontogenetically advanced growth stage. However, in the absence of osteohistological data, its adult status cannot be

confirmed unequivocally at present. To summarize, both *Petrustitan* and *Paludititan* potentially represent further examples of small-sized titanosaurs present on the Transylvanian landmass, although whether they also displayed the extreme degree of dwarfism recognized in *Magyarosaurus* and assemblages J and M cannot currently be ascertained. Nevertheless, the available evidence (e.g. absolute size of the largest skeletal elements belonging to their different referred individuals) suggests only marginally larger adult body sizes for the former two taxa when compared to *Magyarosaurus*.

Nopcsa (1914) proposed that the insular environment of Haţeg Island was the main cause of the dwarfing displayed by the Transylvanian dinosaurs. Subsequently, the nature of this phenomenon has become much better understood with the discovery and interpretation of a large number of Recent and fossil examples of distinctive body size changes occurring on islands. Island dwarfism is part of what is often termed the 'island rule', according to which large-sized animals tend to evolve towards smaller body sizes, and small-sized animals tend to evolve towards larger body sizes, both supposedly converging on a hypothetical 'optimal body size' characteristic for a given clade and ecological type (e.g. Benítez-López et al., 2021; Foster, 1964; Lomolino, 2005). Several different mechanisms have been proposed to account for these patterns (e.g. see the synthesis by van der Geer et al., 2021). These mechanisms are not necessarily mutually exclusive and include: adaptation to resource (area, food) limitations on islands; ecological release (from predators and/or competitors); niche expansion and/or shifts resulting from adaptations to the particulars of the insular environments; and optimization/change of life-history traits (see also Benton et al., 2010). In addition, energetic constraints related to movement across the potentially more rugged habitats of a tectonically active island – such as that reconstructed for the Transylvanian landmass – may have also promoted body size reduction (e.g. Ruxton & Wilkinson, 2014). Although the identification of the precise mechanisms driving dwarfism in Transylvanian titanosaurs remains problematic, the isolated insular environment (e.g. Benton et al., 2010; Csiki-Sava et al., 2015; Nopcsa, 1915, 1923a; Weishampel et al., 1991, 2010; but see dissenting opinions by Jianu & Boekschoten, 1999; Krause et al., 2020) and its unbalanced faunal content (e.g. Csiki-Sava et al., 2015, 2016) almost certainly resulted in both resource limitations and ecological release (see below).

Larger-bodied titanosaurs. *Uriash kadici* is estimated to have had a body mass of between 5 and 8 tonnes, and a body length close to 12 metres (Table 2). This means that *Uriash* is the largest titanosaurian taxon known from the Haţeg Basin, and surpassed the maximum values reached by most other Late Cretaceous European titanosaurs (e.g. Díez Díaz et al., 2021), with the exception of *Abditosaurus* (with estimates of 14 tonnes and 17.5 meters in length) (Vila et al., 2022).

The presence of large-sized titanosaurs such as *Uriash* is noteworthy and requires explanation because it appears to contradict (or at least undermine) the supposed action of the 'island rule' upon these faunas. Several hypotheses have been put forward to account for the presence of these 'outlier' large-bodied titanosaurs within dinosaur assemblages that were otherwise characterized by the dominance of small-sized (and potentially dwarfed) herbivorous taxa (e.g. Benton et al., 2010; Ősi et al., 2014; Stein et al., 2010). In particular, Stein et al. (2010, p. 9261) proposed several scenarios that might account for the presence of larger-bodied titanosaurs in this fauna: S1, sea-level drops and/or tectonic events led to the expansion of the emergent land area, relaxing the potential constraints of insular resource limitation, and allowing newly introduced and large-bodied taxa to retain their body sizes (see also Vila et al., 2022); S2, 'accidental' occurrences of stray individuals of larger-bodied taxa that originated from larger nearby landmasses, either as the result of chance overseas dispersal or as washed-up carcasses; and S3, large-bodied Haţeg taxa represent members of the earliest stages of an immigration wave. Scenario 3 has two variants: S3.1, the large-bodied immigrants eventually gave rise to dwarfed forms because of the operation of island-rule processes; and S3.2, the large-bodied immigrants eventually went extinct because the limitations on resources meant that Haţeg Island could not support them (see also Benton et al., 2010). These scenarios are not mutually exclusive, and all of these processes may have operated to some extent to bring about the presence of larger-body forms on Haţeg Island. Nevertheless, our revised understanding of the taxonomy, geographical distributions, and stratigraphical ranges, of Transylvanian titanosaurs, provides an opportunity to re-evaluate these scenarios.

In our view, beyond the statistically highly improbable discovery of the remains of some accidentally stranded animals (whether arriving alive or as floating carcasses), S2 can be reasonably dismissed, given the continuous (albeit rare) occurrences of large-sized titanosaur individuals throughout the Maastrichtian on the Transylvanian landmass (see the 'Did the "Maastrichtian Dinosaur Turnover" occur in the Haţeg Basin?' section). Rejection of S2 is also consistent with the lack of palaeogeographical data supporting the existence of significantly larger landmasses populated by large-sized titanosaurs in close proximity to the latest Cretaceous

Haţeg Island. Indeed, the only currently documented example of a geographically close titanosaur occurrence that comes from a sizeable emergent area in the western Balkans is both significantly older (dated close to the Santonian/Campanian boundary) and very probably pertains to a small-sized, potentially dwarfed taxon (Nikolov et al., 2020).

Scenario S3 similarly requires the fortuitous (and palaeontologically highly improbable) sampling of the earliest settling stages of a large-bodied immigrant titanosaur population (i.e. *Uriash*). In addition, as with S2, the temporally recurrent occurrence of large-sized titanosaur fossils in different areas of the Transylvanian landmass mitigates against a scenario in which we have obtained a fortuitous glimpse of the potentially stratigraphically very narrow window between the earliest arrival of large body forms and their subsequent dwarfism/extinction. Under S3.1, the original large-bodied taxon is expected to have undergone dwarfing over time according to the 'island rule', leading to subsequent establishment of either a population displaying smaller-body size on average, or a smaller-bodied descendant taxon; for example, van der Geer et al. (2021) presented several instances of such outcomes in Cenozoic island mammals. However, neither of these possible outcomes are supported in the case of the Haţeg Basin titanosaurs because *Uriash* does not seem to be particularly closely related to (i.e. con-specific with or ancestral to) any of the stratigraphically younger and smaller-sized titanosaurs known from Haţeg Island. Scenario S3.2 would require extinction of these immigrant larger-bodied taxa rather shortly after their introduction on Haţeg Island, in order to prevent preservation of any further individuals. Moreover, given the recurrent presence of large titanosaur specimens in the Haţeg fauna, S3.2 would require such local extirpations to occur repeatedly during the Maastrichtian, such that none of these large-sized titanosaurs were able to permanently establish themselves as components of the Haţeg Island palaeofaunas. Again, such a pattern has been documented in Cenozoic placental mammals by van der Geer et al. (2021). However, S3.2 is difficult to test in the case of Transylvanian titanosaurs because we lack the data needed to distinguish between genuine absence resulting from extinction as opposed to pseudo-absence caused by factors such as sampling failures, lack of stratigraphical resolution, and/or taxonomic uncertainty.

Of the scenarios proposed to date, S1 appears to be the palaeobiogeographically, palaeogeographically and palaeoecologically soundest explanation for the presence of large-bodied titanosaurs on the Transylvanian landmass, whereby expansion of the emergent land area would have provided suitable accommodation for large-bodied late-arriving immigrants. This is consistent with palaeogeographical hypotheses for the evolution of the Haţeg Island that propose a progressive enlargement of its land area from the late Campanian through to the Maastrichtian (e.g. Csiki-Sava et al., 2016; Vremir et al., 2014). Enlargement of Haţeg Island is potentially explained by latest Cretaceous mountain-building events in the circum-Transylvanian Basin region that suggest generalized uplift (e.g. Krézsek & Bally, 2006; Willingshofer et al., 2001). Nevertheless, the quasi-continuous coexistence of small and large Transylvanian titanosaurs from the beginning of the Maastrichtian onwards (see the 'Did the "Maastrichtian Dinosaur Turnover" occur in the Haţeg Basin?' section) suggests that increase in land area and corresponding resources may not have been the main driver behind the successful settlement of large-sized titanosaurs.

In short, scenarios S2 and S3.1 are plausible, but rely on chance observations of rare events and therefore appear statistically improbable. Scenarios S1 and 3.2 appear to be more probable and are supported by analogous dwarfing of placental mammals during the Cenozoic, but S3.2 is difficult to test. None of these previously proposed scenarios fully account for the apparent coexistence of both small- and large-bodied titanosaurs in the same Haţeg faunas, and we therefore propose two new scenarios. The first of these, S4, relates to ecological exclusion. Case studies of insular body size evolution in large placental mammals (e.g. proboscideans) suggest that drastic body size reduction is prohibited whenever smaller-sized herbivores are present alongside the invading larger-bodied proboscideans (see examples discussed in van der Geer et al., 2021). This is because dwarfing of originally large megaherbivores results in increased competition from incumbent members of the mesoherbivore guild. These cases suggest that important potential drivers of island dwarfing (e.g. resource limitations, release from predator pressure) may be trumped on occasion by the adverse effects of ensuing ecological competition. Thus, larger-sized titanosaurs that invaded the Haţeg Island region would have been sympatric with several smaller-bodied herbivorous dinosaurs (e.g. ornithopods, dwarfed titanosaurs). According to S4, any attempt by these large-bodied sauropods to reduce their body size might have been evolutionarily counter-productive because smaller bodied herbivorous niches were already occupied, regardless of the concurrent action of other mechanisms that would otherwise have promoted island dwarfing. Ecological exclusion, itself driven in part by effects of the 'island rule' upon other contemporaneous herbivores, was potentially a key factor allowing the quasi-continuous

existence of large-bodied titanosaurs alongside smaller ones on Haţeg Island.

Our final scenario, S5, is that the dwarf titanosaurs are not the product of island dwarfing at all, or at least this dwarfing did not occur on Haţeg Island. Under this scenario, dwarfing occurred stratigraphically earlier among several lineages, and the small-bodied titanosaurs on Haţeg Island are the descendants of existing dwarfed ancestors. This would explain why *Uriash* also lived in the same environment, without reducing its body size. This scenario would be in keeping with the fact that most latest Cretaceous Ibero-Armorican titanosaurs are also small-bodied, and that at least one contemporaneous titanosaurian lineage also shows evidence of a reduction in body size, namely South American saltasaurines (e.g. Navarro et al., 2022; Powell, 2003), demonstrating that dwarfism is relatively widespread amongst Titanosauria (see also D'Emic, 2023). A similar explanation has been proposed recently to explain the presence of at least some of the small-bodied latest Cretaceous hadrosauroids from of Europe, i.e. that these are members of an existing lineage of smaller taxa (Chiarenza et al., 2021). Given that our sampling of pre-late Campanian titanosaurs from Europe (and elsewhere) is scarce (Mannion & Upchurch, 2011), we cannot rule out that unsampled taxa ancestral to the Transylvanian titanosaurs had already undergone body size reductions (e.g. see the material described by Nikolov et al., 2020, of a small-bodied titanosaur from the Santonian/Campanian boundary beds of the western Balkans).

In summary, although we accept that both enlargement of the available land area (S1) and/or episodes of local extinction (S3.2) potentially contributed to controlling the body size evolution of Transylvanian titanosaurs, we contend that S4 (ecological exclusion) and/or S5 (pre-Haţeg Island dwarfing) are the more likely scenarios for explaining the observed body size disparity.

Did the 'Maastrichtian Dinosaur Turnover' occur in the Haţeg Basin?

The Maastrichtian Dinosaur Turnover (MDT) was first proposed as a rather abrupt transition from rhabdodontid- and titanosaur-dominated to hadrosauroid-dominated faunas that took place in the Ibero-Armorican domain around the early/late Maastrichtian boundary (e.g. Le Loeuff et al., 1994). Subsequently, the timing, extent, and impact of the turnover have been further refined, painting a more nuanced picture of this transition (e.g. Fondevilla et al., 2016; Vila et al., 2012, 2016). For example, the faunal replacement is now estimated to have been protracted rather than abrupt, extending over a time interval of 2.5–2.8 million years, from the middle of the early Maastrichtian to the early part of the late Maastrichtian (i.e. the early part of magnetochron C31r to magnetochron C30r; Fondevilla et al., 2019). Moreover, a survey of the Ibero-Armorican latest Cretaceous fossil record by Vila et al. (2012) suggested that both small- and larger-sized titanosaurs were present up until the very end of the Maastrichtian, alongside several hadrosauroid lineages, whereas rhabdodontids and nodosaurids had apparently become extinct by the end of the early Maastrichtian (Fondevilla et al., 2019). Vila et al. (2022) proposed a variant of the MDT in which small-bodied (potentially dwarfed) titanosaurs formed endemic Campanian–early Maastrichtian faunas in Ibero-Armorica and possibly elsewhere in Europe, followed by the invasion of larger-bodied forms such as *Abditosaurus* from outside Europe during the early Maastrichtian. These authors further supported this scenario with evidence from the sauropod egg fossil record, and tentatively extended this MDT scenario to include Transylvania as well as Ibero-Armorica (see above). For example, these authors noted that the larger Transylvanian forms appeared to be stratigraphically younger than smaller-bodied forms such as *Magyarosaurus*, based on the conclusions of Botfalvai et al. (2021).

Our updated review of the Transylvanian (and especially, the Haţeg Basin) titanosaur record provides an opportunity to address the scenario put forward by Vila et al. (2022) in more depth. In particular, our survey does not support Botfalvai et al.'s (2021) suggestion of a somewhat later date for the first occurrence of large-bodied titanosaurs compared to smaller-sized taxa in the Transylvanian area, and specifically in the Haţeg Basin. Botfalvai et al.'s (2021) assertion was based on the presence of large-sized forms (here identified as *Uriash*) recorded at Kadić's locality VI at a marginally higher stratigraphical position compared to those of smaller-sized titanosaurs discovered at Kadic's localities I (Assemblage A, the lectotype of *Magyarosaurus*) and II (Individual K), and at site K2 (Individual V) (see more details in Botfalvai et al., 2021). However, current evidence suggests that unlike Ibero-Armorica, where titanosaurs were already both common and taxonomically diverse by the late Campanian (e.g. Díez Díaz, 2022), members of this clade appeared on the Transylvanian landmass only later, probably after the Campanian/Maastrichtian boundary (e.g. Bălc et al., 2024; Vremir et al., 2014). Furthermore, small- and large-bodied Transylvanian titanosaurs were penecontemporaneous members of the same early Maastrichtian faunas, with *Magyarosaurus* and *Uriash* being approximately sympatric. Admittedly, Vila et al.'s (2022) hypothesis does allow for limited spatiotemporal overlap between the stratigraphically older dwarf and younger invading large-bodied titanosaurs in the Ibero-Armorican area, so

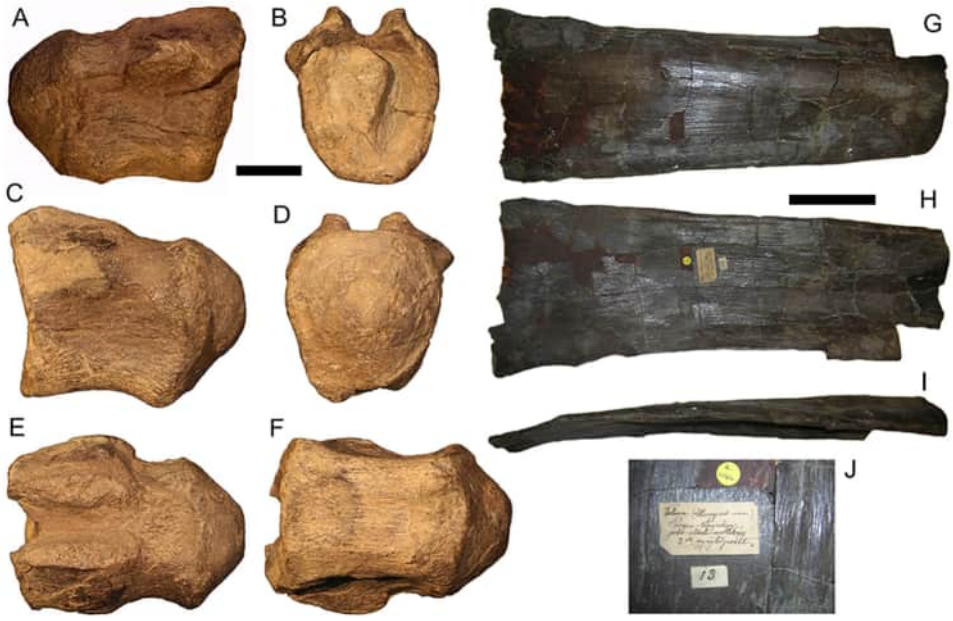

Figure 66. Lithostrotia *incertae sedis*, large titanosaurian remains from the Maastrichtian of the Hațeg Basin. Anterior caudal centrum from Densuș (LPB [FGGUB] R.1787) in **A,** right lateral; **B,** anterior; **C,** left lateral; **D,** posterior; **E,** dorsal; and **F,** ventral views. Left scapular blade NHMUK R.11144 from Assemblage K in **G,** lateral; **H,** medial; and **I,** dorsal views; **J,** detail of the label. Scale bar equals 50 mm in A–F and 100 mm in G–I.

this *Magyarosaurus-Uriash* sympatry by itself does not falsify the replacement scenario for the Hațeg region. However, these taxa appear to be replaced by *Paludititan* during the middle part of the Maastrichtian, so it must be acknowledged that the stratigraphically youngest of the currently known named Transylvanian taxa was relatively small.

More importantly, there seems to be no indication for a clear-cut body size-related taxon replacement in the Transylvanian assemblages when the entire titanosaur fossil record is considered (i.e. irrespective of whether or not specimens have been referred to a named taxon). Indeed, our review of the Hațeg Basin material has revealed the presence of (admittedly, rare) titanosaur remains belonging to large-sized individuals in localities that are penecontemporaneous with those yielding the stratigraphically earliest small-sized titanosaurs. Among these remains is a relatively large anterior caudal centrum from Densuș (LPB [FGGUB] R.1787; Fig. 66).

Unfortunately, there are no precise locality data for this specimen, collected in the first half of the twentieth century (based on the oldest available label associated with it). Nevertheless, continental beds cropping out near Densuș village have been referred either to the lower or to the basal-most part of the middle member of the Densuș-Ciula Formation (Csiki-Sava et al., 2016; Grigorescu, 1992; Laufer, 1925; Nopcsa, 1905), suggesting that its age is earliest Maastrichtian, possibly approximately coeval with *Magyarosaurus dacus*. A second example of a relatively early occurrence of a large-sized titanosaur is the scapular blade NHMUK R.11144 (Fig. 66) that apparently comes from the same locality as the (probably) small-sized Individual K (site II of Kadić, 1916; see the 'Key localities and skeletal associations' section), and from approximately the same place and stratigraphical level as the small-sized Individual V from site K2 reported by Botfalvai et al. (2021). Based on these occurrences, it thus appears that both small taxa (such as the dwarfed *Magyarosaurus*) and large-bodied titanosaurs made their appearance contemporaneously in the Hațeg Basin near the beginning of the early Maastrichtian. Subsequently, as noted by Botfalvai et al. (2021), small- and large-bodied forms continued to coexist until the latest Maastrichtian in the south-western Transylvanian Basin (e.g. Csiki & Vremir, 2011; Csiki-Sava et al., 2012). In conclusion, contrary to previous suggestions (Vila et al., 2022), there is no indication of a body-size related titanosaur turnover, involving replacement of dwarfed taxa with larger-sized ones, in the uppermost Cretaceous of the Transylvanian area.

Moreover, a brief survey of the entire dinosaur fossil record from the Transylvanian landmass fails to identify any significant higher-level faunal turnover similar to that reported in Ibero-Armorica during the Maastrichtian. The Transylvanian faunas were generally dominated by co-occurring titanosaurs and rhabdodontid ornithopods throughout the Maastrichtian, whereas

hadrosauroids, although present, constituted less important components (e.g. Csiki, Grigorescu, et al., 2010; Csiki-Sava et al., 2015, 2016; Vremir et al., 2015), especially when compared to their relative abundance and diversity in post-MDT Ibero-Armorican faunas (e.g. Blanco et al., 2015; Cruzado-Caballero et al., 2014; Fondevilla et al., 2019; Marmi et al., 2016; Pérez-Pueyo et al., 2021). Moreover, rhabdodontids, hadrosauroids and titanosaurs were already members of the same local assemblages by the early part of the early Maastrichtian (e.g. Botfalvai et al., 2021; Csiki-Sava et al., 2016; Nopcsa, 1915), and this clade-level faunal composition seems to have continued largely uninterrupted into the late Maastrichtian (e.g. Csiki-Sava et al., 2016; Smith et al., 2002; Vremir et al., 2015), including the survival of the otherwise rare nodosaurids (e.g. Codrea et al., 2002; Vasile et al., 2011), again in stark contrast with patterns reported from the Ibero-Armorican landmass (e.g. Fondevilla et al., 2019; Pérez-Pueyo et al., 2021; Vila et al., 2016). In fact, in some of the stratigraphically highest-occurring faunal assemblages from the south-western Transylvanian (e.g. Vremir et al., 2015) and Haţeg (Brusatte et al., 2017; Csiki-Sava et al., 2016; Smith et al., 2002) basins, hadrosauroids are either absent or very rare, whereas there are numerous titanosaur remains, often associated with rhabdodontids.

Thus, it is currently unclear whether any dwarf to large-bodied titanosaur transition, and the MDT more generally, occurred either in the Haţeg region or on the Transylvanian landmass overall – in fact, all current evidence points to the contrary. Nevertheless, it is entirely conceivable that lower-level compositional changes did take place during the Maastrichtian, such as the apparent replacement of the early Maastrichtian *Magyarosaurus* by the 'middle' Maastrichtian *Paludititan* (Fig. 8).

Conclusion

Since the first Late Cretaceous titanosaurian sauropod dinosaur remains were found in Transylvania, and especially in the Haţeg Basin, towards the end of the nineteenth century, an extensive number of new sites, isolated specimens and partial skeletons have been found and described, greatly advancing our understanding of these faunas. However, a detailed study of these sites and skeletal remains as a whole has never been carried out, with a number of taxonomic problems preventing any understanding of the diversity and phylogenetic affinities of the Haţeg Basin titanosaurs. Following our systematic revision, we now recognize a minimum of four titanosaurian taxa: *Magyarosaurus dacus*, *Paludititan nalatzensis*, *Petrustitan hungaricus* n. gen. and *Uriash kadici* n. gen. n. sp. This diversity was likely even higher, as evidenced by the substantial amount of associated material that cannot currently be adequately diagnosed as a new taxon, and yet display differences from these four named taxa. Our phylogenetic analyses show that these Transylvanian titanosaurs present particularly close relationships with Gondwanan taxa: *Magyarosaurus* is recovered either as a member or a close relative of Saltasauridae; *Paludititan* has affinities with Lognkosauria, along with the approximately contemporaneous Spanish titanosaur *Lohuecotitan*; *Petrustitan* is most closely related to South American early diverging eutitanosaurian taxa; and *Uriash* shares one feature uniquely with Gondwanan titanosaurs. These analyses also strengthen the palaeobiogeographical hypothesis that the latest Cretaceous European titanosaurs were members of Gondwanan lineages that invaded the former area during the Barremian–Albian. Since its initial discovery, *Magyarosaurus dacus* has been identified as a dwarfed sauropod, with island dwarfism proposed as an explanation for the diminutive size of this species and other dinosaurs on Haţeg Island. Whereas *Paludititan* and *Petrustitan* are also small-bodied sauropods, *Uriash* was an order of magnitude heavier and represents one of the largest titanosaurian taxa found in the Late Cretaceous of Europe. We interpret the presence of this body-size disparity as either evidence that large-bodied taxa were ecologically excluded from body-size reduction by competition from small-bodied titanosaurs, or that dwarfing occurred stratigraphically earlier among several lineages and the small-bodied titanosaurs on Haţeg Island are the descendants of existing dwarfed ancestors. By contrast with some previous studies, we find no indication of a body-size related titanosaur turnover, involving replacement of dwarfed taxa with larger-sized ones, in the uppermost Cretaceous of the Transylvanian area.

Acknowledgements

This project was funded by the Jurassic Foundation (VDD), a Royal Society International Exchange award (IES\R1\180088; PDM and ZCs-S) and a Royal Society University Research Fellowship (UF160216, URF\R\221010; PDM); it was also supported by the Romanian Ministry of Research, Innovation and Digitalization CNCS-UEFISCDI project PN-III-P4-ID-PCE-2020-2570, within PNCDI III and the Hungarian National Research, Development and Innovation Office project NKFIH OTKA FK 146097 (ZCsS). We would like to thank S. Maidment, P. Barrett and S. Chapman (Natural History Museum London, UK), L. Kordos and L. Makádi (Budapest Mining and Geological Survey of Hungary), V. Codrea (Babeş-Bolyai University of Cluj-Napoca, Romania), C.-M. Jianu and S. Burnaz (Muzeul

Civilizatiei Dacice si Romane, Deva, Romania), R. Costa da Silva (Museu de Ciências da Terra, Serviço Geológico do Brasil), L. Filippi (Museo Municipal 'Argentino Urquiza'), and M. Reguero (Museo de la Plata, Argentina) for access to the collections under their care. We are also grateful to B. Vila and A. Sellés for providing information on *Abditosaurus*. We also want to thank Scott Hartman for providing the titanosaur skeletal outline used in figures. We are grateful for the helpful comments provided by the editor Zerina Johanson and the reviewers Alejandro Otero and Julian Silva Junior, which have improved a first version of this manuscript. We acknowledge the Willi Hennig Society, which has sponsored the development and free distribution of TNT.

Disclosure statement

No potential conflict of interest was reported by the author(s).

Supplemental material

Supplemental material for this article can be accessed online here: https://doi.org/10.1080/14772019.2024.2441516.

ORCID

Verónica Díez Díaz http://orcid.org/0000-0002-9840-9829
Philip D. Mannion http://orcid.org/0000-0002-9361-6941
Zoltán Csiki-Sava http://orcid.org/0000-0001-7144-0327
Paul Upchurch http://orcid.org/0000-0002-8823-4164

References

Agnolin, F. L., **González Riga, B. J.**, **Aranciaga Rolando, A. M.**, **Rozadilla, S.**, **Motta, M. J.**, **Chimento, N. R.**, & **Novas, F. E.** (2023). A new giant titanosaur (Dinosauria, Sauropoda) from the Upper Cretaceous of Northwestern Patagonia, Argentina. *Cretaceous Research*, 105487. https://doi.org/10.1016/j.cretres.2023.105487

Antonescu, E., **Lupu, D.**, & **Lupu, M.** (1983). Correlation palinologique du Crétacé terminal du sud-est des Monts Metaliferi et des Depressions de Haţeg et de Rusca Montană. *Anuarul Institutului de Geologie Şi Geofizică*, *59*(3), 71–77.

Apesteguía, S. (2005). Evolution of the titanosaur metacarpus. In V. Tidwell, & K. Carpenter (Eds.), *Thunder lizards: The Sauropodomorph dinosaurs* (pp. 321–345). Indiana University Press.

Astibia, H., **Buffetaut, E.**, **Buscalioni, A. D.**, **Cappetta, H.**, **Corral, C.**, **Estes, R.**, **Garcia-Garmilla, F.**, **Jaeger, J. J.**, **Jimenez-Fuentes, E.**, **Le Loeuff, J.**, **Mazin, J. M.**, **Orue-Etxebarria, X.**, **Pereda-Suberbiola, J.**, **Powell, J. E.**, **Rage, J. C.**, **Rodriguez-Lazaro, J.**, **Sanz, J. L.**, & **Tong, H.** (1990). The fossil vertebrates from Laño (Basque Country, Spain); new evidence on the composition and affinities of the Late Cretaceous continental faunas of Europe. *Terra Nova*, *2*(5), 460–466.

Augustin, F. J., **Bastiaans, D.**, **Dumbravă, M. D.**, & **Csiki-Sava, Z.** (2022). A new ornithopod dinosaur, *Transylvanosaurus platycephalus* gen. et sp. nov. (Ornithischia). from the Upper Cretaceous of the Ha□eg Basin, Romania. *Journal of Vertebrate Paleontology*, *42*(2), e2133610. https://doi.org/10.1080/02724634.2022.2133610

Augustin, F. J., **Matzke, A. T.**, **Csiki-Sava, Z.**, & **Pfretzschner, H.-U.** (2019). Bioerosion on vertebrate remains from the Upper Cretaceous of the Haţeg Basin, Romania and its taphonomic implications. *Palaeogeography, Palaeoclimatology, Palaeoecology*, *534*, 109318.

Averianov, A., & **Efimov, V.** (2018). The oldest titanosaurian sauropod of the Northern Hemisphere. *Biological Communications*, *63*(3), 145–162. https://doi.org/10.21638/spbu03.2018.301

Averianov, A., **Podlesnov, A.**, **Slobodin, D.**, **Skutschas, P.**, **Feofanova, O.**, & **Vladimirova, O.** (2023). First sauropod dinosaur remains from the Early Cretaceous Shestakovo 3 locality, Western Siberia, Russia. *Biological Communications*, *68*(4), Article 4. https://doi.org/10.21638/spbu03.2023.404

Averianov, A. O., **Sizov, A. V.**, & **Skutschas, P. P.** (2021). Gondwanan affinities of *Tengrisaurus*, Early Cretaceous titanosaur from Transbaikalia, Russia (Dinosauria, Sauropoda). *Cretaceous Research*, *122*, 104731.

Bălc, R., **Bindiu-Haitonic, R.**, **Kövecsi, S.-A.**, **Vremir, M.**, **Ducea, M.**, **Csiki-Sava, Z.**, **Ţabără, D.**, & **Vasile, Ş.** (2024). Integrated biostratigraphy of Upper Cretaceous deposits from an exceptional continental vertebrate-bearing marine section (Transylvanian Basin, Romania) provides new constraints on the advent of 'dwarf dinosaur' faunas in Eastern Europe. *Marine Micropaleontology*, *187*, 102328.

Baraboshkin, E. Y., **Alekseev, A. S.**, & **Kopaevich, L. F.** (2003). Cretaceous palaeogeography of the north-eastern Peri-Tethys. *Palaeogeography, Palaeoclimatology, Palaeoecology*, *196*(1–2), 177–208.

Beeston, S., **Poropat, S.**, **Mannion, P.**, **Pentland, A.**, **Enchelmaier, M.**, **Sloan, T.**, & **Elliott, D.** (2024). Reappraisal of sauropod dinosaur diversity in the Upper Cretaceous Winton Formation of Queensland, Australia, through 3D digitisation and description of new specimens. *PeerJ*, *12*, e17180, https://doi.org/10.7717/peerj.17180

Bellardini, F., **Coria, R. A.**, **Pino, D. A.**, **Windholz, G. J.**, **Baiano, M. A.**, & **Martinelli, A. G.** (2022). Osteology and phylogenetic relationships of *Ligabuesaurus leanzai* (Dinosauria: Sauropoda) from the Early Cretaceous of the Neuquén Basin, Patagonia, Argentina. *Zoological Journal*

of the Linnean Society. https://doi.org/10.1093/ZOOLINNEAN/ZLAC003

Benítez-López, A., **Santini, L.**, **Gallego-Zamorano, J.**, **Milá, B.**, **Walkden, P.**, **Huijbregts, M. A. J.**, & **Tobias, J. A.** (2021). The island rule explains consistent patterns of body size evolution in terrestrial vertebrates. *Nature Ecology & Evolution*, *5*(6), 768–786. https://doi.org/10.1038/s41559-021-01426-y

Benson, R. B. J., **Hunt, G.**, **Carrano, M. T.**, & **Campione, N.** (2018). Cope's rule and the adaptive landscape of dinosaur body size evolution. *Palaeontology*, *61*(1), 13–48. https://doi.org/10.1111/pala.12329

Benton, M. J., **Csiki, Z.**, **Grigorescu, D.**, **Redelstorff, R.**, **Sander, P. M.**, **Stein, K.**, & **Weishampel, D. B.** (2010). Dinosaurs and the island rule: The dwarfed dinosaurs from Haţeg Island. *Palaeogeography, Palaeoclimatology, Palaeoecology*, *293*(3), 438–454. https://doi.org/10.1016/j.palaeo.2010.01.026

Benton, M. J., **Forth, J.**, & **Langer, M. C.** (2014). Models for the rise of the dinosaurs. *Current Biology*, 24(2). https://doi.org/10.1016/j.cub.2013.11.063

Blanco, A., **Prieto-Márquez, A.**, & **De Esteban-Trivigno, S.** (2015). Diversity of hadrosauroid dinosaurs from the Late Cretaceous Ibero-Armorican Island (European Archipelago) assessed from dentary morphology. *Cretaceous Research*, *56*, 447–457.

Bojar, A.-V., **Halas, S.**, **Bojar, H.-P.**, **Grigorescu, D.**, & **Vasile, S.** (2011). Upper Cretaceous volcanoclastic deposits from the Haţeg Basin, South Carpathians (Romania): K-Ar ages and intrabasinal correlation. *Geochronometria*, *38*(2), 182–188. https://doi.org/10.2478/s13386-011-0023-8

Bonaparte, J. F., & **Coria, R. A.** (1993). A new and huge titanosaur sauropod from the Rio Limay Formation (Albian-Cenomanian) of Neuquén Province, Argentina. *Ameghiniana*, *30*, 271–282.

Bonaparte, J. F., **González Riga, B. J.**, & **Apesteguia, S.** (2006). *Ligabuesaurus leanzai* gen. et sp. nov. (Dinosauria, Sauropoda), a new titanosaur from the Lohan Cura Formation (Aptian, Lower Cretaceous) of Neuquén, Patagonia, Argentina. *Cretaceous Research*, *27*(3), 364–376. https://doi.org/10.1016/j.cretres.2005.07.004

Borsuk-Białynicka, M. (1977). A new camarasaurid sauropod *Opisthocoelicaudia skarzynskii* gen. n., sp. n. from the Upper Cretaceous of Mongolia. *Palaeontologia Polonica*, *37*(5), 5–64.

Botfalvai, G., **Csiki-Sava, Z.**, **Grigorescu, D.**, & **Vasile, Ş.** (2017). Taphonomical and palaeoecological investigation of the Late Cretaceous (Maastrichtian) Tuştea vertebrate assemblage (Romania; Haţeg Basin)-insights into a unique dinosaur nesting locality. *Palaeogeography, Palaeoclimatology, Palaeoecology*, *468*, 228–262.

Botfalvai, G., **Csiki-Sava, Z.**, **Kocsis, L.**, **Albert, G.**, **Magyar, J.**, **Bodor, E. R.**, **Ţabără, D.**, **Ulyanov, A.**, & **Makádi, L.** (2021). 'X' marks the spot! Sedimentological, geochemical and palaeontological investigations of Upper Cretaceous (Maastrichtian) vertebrate fossil localities from the Vălioara valley (Densuş-Ciula Formation, Haţeg Basin, Romania). *Cretaceous Research*, *123*, 104781. https://doi.org/10.1016/j.cretres.2021.104781

Brusatte, S. L., **Dumbravă, M.**, **Vremir, M.**, **Csiki-Sava, Z.**, **Totoianu, R.**, & **Norell, M. A.** (2017). A catalog of *Zalmoxes* (Dinosauria: Ornithopoda) specimens from the Upper Cretaceous Nălaţ-Vad Locality, Haţeg Basin, Romania. *American Museum Novitates*, *2017*(3884), 1–36.

Buffetaut, E. (1989). Archosaurian reptiles with Gondwanan affinities in the Upper Cretaceous of Europe. *Terra Nova*, *1*(1), 69–74. https://doi.org/10.1111/j.1365-3121.1989.tb00328.x

Buffetaut, E., **Mechin, P.**, & **Mechin-Salessy, A.** (1988). Un dinosaure théropode d'affinités gondwaniennes dans le Crétacé supérieur de Provence. *Comptes Rendus de l'Académie Des Sciences. Série 2, Mécanique, Physique, Chimie, Sciences de l'univers, Sciences de La Terre*, *306*(2), 153–158.

Calvo, J. O. (2014). New fossil remains of *Futalognkosaurus dukei* (Sauropoda, titanosauria) from the Late Cretaceous of Neuquén, Argentina. *4th International Palaeontological Congress, "The History of Life: A View from the Southern Hemisphere"*, Abstract Volume, 325.

Calvo, J. O., & **González Riga, B. J.** (2003). *Rinconsaurus caudamirus* gen. et sp. nov., a new titanosaurid (Dinosauria, Sauropoda) from the Late Cretaceous of Patagonia, Argentina. *Revista Geológica de Chile*, *30*(2), 333–353. https://doi.org/10.4067/S0716-02082003000200011

Calvo, J. O., **González Riga, B. J.**, & **Porfiri, J. D.** (2007). A new titanosaur sauropod from the Late Cretaceous of Neuquén, Patagonia, Argentina. *Arquivos Do Museu Nacional*, *65*(4), 485–504.

Calvo, J. O., **Porfiri, J. D.**, **Riga, B. J. G.**, & **Kellner, A. W. A.** (2007). Anatomy of *Futalognkosaurus dukei* Calvo, Porfiri, González Riga & Kellner, 2007 (Dinosauria, Titanosauridae) from the Neuquén Group (Late Cretaceous), Patagonia, Argentina. *Archivos Do Museu Nacional Do Rio de Janeiro*, *65*(4), 511–526.

Calvo, J. O., & **Salgado, L.** (1995). *Rebbachisaurus tessonei* sp. nov. A new Sauropoda from the Albian-Cenomanian of Argentina; new evidence on the origin of the Diplodocidae. *Gaia*, *11*, 13–33.

Campione, N. E., & **Evans, D. C.** (2012). A universal scaling relationship between body mass and proximal limb bone dimensions in quadrupedal terrestrial tetrapods. *BMC Biology*, *10*, 60. https://doi.org/10.1186/1741-7007-10-60

Campione, N. E., **Evans, D. C.**, **Brown, C. M.**, & **Carrano, M. T.** (2014). Body mass estimation in non-avian bipeds using a theoretical conversion to quadruped stylopodial proportions. *Methods in Ecology and Evolution*, *5*(9), 913–923.

Campos, D., **de A.**, **Kellner, A. W.**, **Bertini, R. J.**, & **Santucci, R. M.** (2005). On a titanosaurid (Dinosauria, Sauropoda) vertebral column from the Bauru group, Late Cretaceous of Brazil. *Arquivos Do Museu Nacional*, *63*(3), 565–593.

Canudo, J. I., **Royo-Torres, R.**, & **Cuenca-Bescós, G.** (2008). A new sauropod: *Tastavinsaurus sanzi* gen. et sp. nov. from the Early Cretaceous (Aptian) of Spain. *Journal of Vertebrate Paleontology*, *28*(3), 712–731. https://doi.org/10.1671/0272-4634(2008)28[712:ANSTSG]2.0.CO;2

Carballido, J. L., **Marpmann, J. S.**, **Schwarz-Wings, D.**, & **Pabst, B.** (2012). New information on a juvenile sauropod specimen from the Morrison Formation and the reassessment of its systematic position. *Palaeontology*, *55*(3), 567–582. https://doi.org/10.1111/j.1475-4983.2012.01139.x

Carballido, J. L., **Otero, A.**, **Mannion, P. D.**, **Salgado, L.**, & **Moreno, A. P.** (2022). Titanosauria: a critical reappraisal

of its systematics and the relevance of the South American record. In A. Otero, J. L. Carballido, & D. Pol (Eds.), *South American Sauropodomorph Dinosaurs: Record, Diversity and Evolution* (pp. 269–298). Springer International Publishing. https://doi.org/10.1007/978-3-030-95959-3_8

Carballido, J. L., **Pol, D.**, **Otero, A.**, **Cerda, I. A.**, **Salgado, L.**, **Garrido, A. C.**, **Ramezani, J.**, **Cúneo, N. R.**, & **Krause, J. M.** (2017). A new giant titanosaur sheds light on body mass evolution among sauropod dinosaurs. *Proceedings of the Royal Society B: Biological Sciences*, *284*(1860), 20171219. https://doi.org/10.1098/rspb.2017.1219

Cerda, I. A., **Paulina Carabajal, A.**, **Salgado, L.**, **Coria, R. A.**, **Reguero, M. A.**, **Tambussi, C. P.**, & **Moly, J. J.** (2011). The first record of a sauropod dinosaur from Antarctica. *Die Naturwissenschaften*, *99*(1), 83–87. https://doi.org/10.1007/s00114-011-0869-x

Cerda, I. A., **Salgado, L.**, & **Powell, J. E.** (2012). Extreme postcranial pneumaticity in sauropod dinosaurs from South America. *Palaontologische Zeitschrift*, *86*(4), 441–449. https://doi.org/10.1007/s12542-012-0140-6

Cerda, I., **Zurriaguz, V. L.**, **Carballido, J. L.**, **González, R.**, & **Salgado, L.** (2021). Osteology, paleohistology and phylogenetic relationships of *Pellegrinisaurus powelli* (Dinosauria: Sauropoda) from the Upper Cretaceous of Argentinean Patagonia. *Cretaceous Research*, *128*, 104957. https://doi.org/10.1016/j.cretres.2021.104957

Chiappe, L. M., **Coria, R. A.**, **Dingus, L.**, **Jackson, F.**, **Chinsamy, A.**, & **Fox, M.** (1998). Sauropod dinosaur embryos from the Late Cretaceous of Patagonia. *Nature*, *396*(6708), 258–261. https://doi.org/10.1038/24370

Chiappe, L. M., **Salgado, L.**, & **Coria, R. A.** (2001). Embryonic skulls of titanosaur sauropod dinosaurs. *Science*, *293*(September), 2444–2446. https://doi.org/10.1126/science.1063723

Chiarenza, A. A., **Fabbri, M.**, **Consorti, L.**, **Muscioni, M.**, **Evans, D. C.**, **Cantalapiedra, J. L.**, & **Fanti, F.** (2021). An Italian dinosaur Lagerstätte reveals the tempo and mode of hadrosauriform body size evolution. *Scientific Reports*, *11*(1), 23295. https://doi.org/10.1038/S41598-021-02490-X

Chure, D., **Britt, B. B.**, **Whitlock, J. A.**, & **Wilson, J. A.** (2010). First complete sauropod dinosaur skull from the Cretaceous of the Americas and the evolution of sauropod dentition. *Die Naturwissenschaften*, *97*(4), 379–391. https://doi.org/10.1007/s00114-010-0650-6

Codrea, V. A., & **Godefroit, P.** (2008). New Late Cretaceous dinosaur findings from northwestern Transylvania (Romania). *Comptes Rendus Palevol*, *7*(5), 289–295.

Codrea, V., **Godefroit, P.**, & **Smith, T.** (2012). First discovery of Maastrichtian (latest Cretaceous) terrestrial vertebrates in Rusca Montană Basin (Romania). In P. Godefroit (Ed.), *Bernissart Dinosaurs and Early Cretaceous Terrestrial Ecosystems* (pp. 570–581). Indiana University Press.

Codrea, V., & **Mărginean, R.** (2007). A catalogue of fossil vertebrates from Aiud Natural Sciences Museum. *Oltenia, Studii Şi Comunicări*, *Ştiinţe Naturale*, *23*, 177–186.

Codrea, V., **Murzea-Jipa, C.**, & **Venczel, M.** (2008). A sauropod vertebra at Râpa Roşie (Alba district). *Acta Palaeontologica Romaniae*, *6*, 43–48.

Codrea, V., **Smith, T.**, **Dica, P.**, **Folie, A.**, **Garcia, G.**, **Godefroit, P.**, & **Van Itterbeeck, J.** (2002). Dinosaur egg nests, mammals and other vertebrates from a new Maastrichtian site of the Haţeg Basin (Romania). *Comptes Rendus Palevol*, *1*(3), 173–180.

Codrea, V. A., & **Solomon, A.** (2012). Peculiar fossilization and taphonomy in Maastrichtian terrestrial deposits of Pui (Haţeg Basin, Romania). *Studii Şi Cercetări (Geologie-Geografie)*, *17*, 51–69.

Codrea, V., **Vremir, M.**, **Jipa, C.**, **Godefroit, P.**, **Csiki, Z.**, **Smith, T.**, & **Fărcaş, C.** (2010). More than just Nopcsa's Transylvanian dinosaurs: A look outside the Haţeg Basin. *Palaeogeography, Palaeoclimatology, Palaeoecology*, *293*(3–4), 391–405.

Coria, R. A., **Filippi, L. S.**, **Chiappe, L. M.**, **García, R.**, & **Arcucci, A. B.** (2013). *Overosaurus paradasorum* gen. et sp. nov., a new sauropod dinosaur (Titanosauria: Lithostrotia) from the Late Cretaceous of Neuquén, Patagonia, Argentina. *Zootaxa*, *3683*(4), 357–376. https://doi.org/10.11646/zootaxa.3683.4.2

Cruzado-Caballero, P., **Ruiz-Omeñaca, J. I.**, **Gaete, R.**, **Riera, V.**, **Oms, O.**, & **Canudo, J. I.** (2014). A new hadrosaurid dentary from the latest Maastrichtian of the Pyrenees (north Spain) and the high diversity of the duck-billed dinosaurs of the Ibero-Armorican Realm at the very end of the Cretaceous. *Historical Biology*, *26*(5), 619–630. https://doi.org/10.1080/08912963.2013.822867

Csiki, Z. (1997). Legături paleobiogeografice ale faunei de vertebrate continentale Maastrichtian superioare din Bazinul Haţeg. *Nimphaea*, *23*, 45–68.

Csiki, Z. (1999). New evidence of armoured titanosaurids in the Late Cretaceous. *Magyarosaurus dacus* from the Haţeg Basin (Romania). *Oryctos*, *2*, 93–99.

Csiki, Z. (2005). *Systematics, taphonomy and paleoecology of the Maastrichtian microvertebrates and saurischian dinosaurs from the Haţeg Basin*. [Unpublished PhD thesis]. University of Bucharest.

Csiki, Z. (2006). Insect borings in dinosaur bones from the Maastrichtian of the Haţeg Basin, Romania – Paleoecological and paleoclimatic implications. In Z. Csiki (Ed.), *Mesozoic and Cenozoic Vertebrates and Paleoenvironments. Tributes to the Career of Dan Grigorescu* (pp. 95–104). Ars Docendi.

Csiki, Z., **Barnes, R. N.**, & **Upchurch, P.** (2011). The revision of the genus *Magyarosaurus*, and titanosaur diversity in the Maastrichtian of the Haţeg Basin, Romania – preliminary results. In R. Forrest (Ed.), *Abstracts of Presentations, 59th Annual Symposium of Vertebrate Palaeontology and Comparative Anatomy* (p. 10), Lyme Regis, UK.

Csiki, Z., **Codrea, V.**, **Jipa-Murzea, C.**, & **Godefroit, P.** (2010). A partial titanosaur (Sauropoda, Dinosauria) skeleton from the Maastrichtian of Nălaţ-Vad, Haţeg Basin, Romania. *Neues Jahrbuch Fur Geologie Und Palaontologie – Abhandlungen*, *258*(3), 297–324. https://doi.org/10.1127/0077-7749/2010/0098

Csiki, Z., & **Grigorescu, D.** (2004). Maastrichtian sauropods of the Haţeg Basin, Romania. *Program of the 2nd Meeting of EAVP* (p. 10), Brno. https://doc.rero.ch/record/16292/files/PAL_E568.pdf#page=10

Csiki, Z., & **Grigorescu, D.** (2006). The revision of "*Magyarosaurus*" *hungaricus* Huene (Dinosauria: Sauropoda) from the Haţeg Basin. *Extended Abstracts, 8th Mining, Metallurgy and Geology Conference, EMT*, *65*, 70.

Csiki, Z., & **Grigorescu, D.** (2007). The "Dinosaur Island" – new interpretation of the Haţeg Basin vertebrate fauna after 110 years. *Sargetia, 20*, 5–26.

Csiki, Z., **Grigorescu, D.**, **Codrea, V.**, & **Therrien, F.** (2010). Taphonomic modes in the Maastrichtian continental deposits of the Haţeg Basin, Romania – Palaeoecological and palaeobiological inferences. *Palaeogeography, Palaeoclimatology, Palaeoecology*, *293*(3–4), 375–390. https://doi.org/10.1016/j.palaeo.2009.10.013

Csiki, Z., **Grigorescu, D.**, & **Weishampel, D. B.** (2007). A new titanosaur sauropod (Dinosauria: Saurischia) from the Upper Cretaceous of the Haţeg Basin (Romania). In J. Le Loeuff (Ed.), *Abstracts Volume, 5th Annual Meeting of the European Association of Vertebrate Palaeontologists (EAVP)* (p. 17), Carcassone, France.

Csiki, Z., **Ionescu, A.**, & **Grigorescu, D.** (2008). The Budurone microvertebrate site from the Maastrichtian of the Haţeg Basin-flora, fauna, taphonomy and paleoenvironment. *Acta Palaeontologica Romaniae*, *6*, 49–66.

Csiki, Z., & **Vremir, M.** (2011). A large-sized (?)Late Maastrichtian titanosaur from Râpa Roşie, Sebeş. In Z. Csiki (Ed.), *Abstract Book, 8th Romanian Symposium of Paleontology, Bucharest (Romania)* (pp. 28–29). Ars Docendi.

Csiki, Z., **Vremir, M.**, **Brusatte, S. L.**, & **Norell, M. A.** (2010). An aberrant island-dwelling theropod dinosaur from the Late Cretaceous of Romania. *Proceedings of the National Academy of Sciences*, *107*(35), 15357–15361. https://doi.org/10.1073/pnas.1006970107

Csiki-Sava, Z., **Buffetaut, E.**, **Ősi, A.**, **Pereda-Suberbiola, X.**, & **Brusatte, S. L.** (2015). Island life in the Cretaceous – Faunal composition, biogeography, evolution, and extinction of land-living vertebrates on the Late Cretaceous European archipelago. *ZooKeys 469*, 1–161. https://doi.org/10.3897/zookeys.469.8439

Csiki-Sava, Z., **Butiseacă, G.**, **Grigorescu, D.**, **Dumbravă, M.**, & **Vasile, Ş.** (2012). "A new piece to the puzzle" – titanosaur skeletal remains from the Tuştea dinosaur nesting site and its surroundings, Haţeg Basin, Romania. In R. Royo-Torres, F. Gascó & L. Alcalá (Coord.), *10th Annual Meeting of the European Association of Vertebrate Palaeontologists. ¡Fundamental! 20*, 49–51.

Csiki-Sava, Z., **Vasile, Ș.**, **Grigorescu, D.**, & **Vremir, M.** (2018). Mind the gap! Significance of a new latest Cretaceous fossiliferous site in the northern Haţeg Basin, Romania. In M. Marzola, O. Mateus, & M. Moreno-Azanza (Eds.), *Abstract Book of the XVI Annual Meeting of the European Association of Vertebrate Palaeontology* (p. 53). Faculdade de Ciências e Tecnologia da Universidade Nova de Lisboa.

Csiki-Sava, Z., **Vremir, M.**, **Vasile, Ş.**, **Brusatte, S. L.**, **Dyke, G.**, **Naish, D.**, **Norell, M. A.**, & **Totoianu, R.** (2016). The East Side Story – The Transylvanian latest Cretaceous continental vertebrate record and its implications for understanding Cretaceous-Paleogene boundary events. *Cretaceous Research*, *57*, 662–698. https://doi.org/10.1016/j.cretres.2015.09.003

Cucchi, T., **Barnett, R.**, **Martínková, N.**, **Renaud, S.**, **Renvoisé, E.**, **Evin, A.**, **Sheridan, A.**, **Mainland, I.**, **Wickham-Jones, C.**, & **Tougard, C.** (2014). The changing pace of insular life: 5000 years of microevolution in the Orkney vole (*Microtus arvalis orcadensis*). *Evolution*, *68*(10), 2804–2820.

Curry Rogers, K. (2009). The postcranial osteology of *Rapetosaurus krausei* (Sauropoda: Titanosauria) from the Late Cretaceous of Madagascar. *Journal of Vertebrate Paleontology*, *29*(4), 1046–1086.

Curry Rogers, K. A. (2005). Titanosauria: a phylogenetic overview. In K. A. Curry Rogers & J. A. Wilson (Eds.), *The sauropods: Evolution and paleobiology* (pp. 50–103), University of California Press.

Curry Rogers, K. A., & **Wilson, J. A.** (2014). *Vahiny depereti*, gen. et sp. nov., a new titanosaur (Dinosauria, Sauropoda) from the Upper Cretaceous Maevarano Formation, Madagascar. *Journal of Vertebrate Paleontology*, *34*(3), 606–617. https://doi.org/10.1080/02724634.2013.822874

Dal Sasso, C., **Pierangelini, G.**, **Famiani, F.**, **Cau, A.**, & **Nicosia, U.** (2016). First sauropod bones from Italy offer new insights on the radiation of Titanosauria between Africa and Europe. *Cretaceous Research*, *64*, 88–109. https://doi.org/10.1016/j.cretres.2016.03.008

D'Emic, M. D. (2012). The early evolution of titanosauriform sauropod dinosaurs. *Zoological Journal of the Linnean Society*, *166*(3), 624–671. https://doi.org/10.1111/j.1096-3642.2012.00853.x

D'Emic, M. D. (2023). The evolution of maximum terrestrial body mass in sauropod dinosaurs. *Current Biology*, *33*(9), R349–R350. https://doi.org/10.1016/j.cub.2023.02.067

D'Emic, M. D., & **Wilson, J. A.** (2011). New remains attributable to the holotype of the sauropod dinosaur *Neuquensaurus australis*, with implications for saltasaurine systematics. *Acta Palaeontologica Polonica*, *56*(1), 61–73. https://doi.org/10.4202/app.2009.0149

D'Emic, M. D., **Wilson, J. A**, & **Chatterjee, S.** (2009). The titanosaur (Dinosauria: Sauropoda) osteoderm record: review and first definitive specimen from India. *Journal of Vertebrate Paleontology*, *29*(1), 165–177. https://doi.org/10.1671/039.029.0131

D'Emic, M. D., **Wilson, J. A.**, & **Thompson, R.** (2010). The end of the sauropod dinosaur hiatus in North America. *Palaeogeography, Palaeoclimatology, Palaeoecology*, *297*(2), 486–490. https://doi.org/10.1016/j.palaeo.2010.08.032

Díez Díaz, V. (2022). Titanosaur boom. *Nature Ecology and Evolution*, *6*(3), 251–252. https://doi.org/10.1038/s41559-022-01677-3

Díez Díaz, V., **Demuth, O. E.**, **Schwarz, D.**, & **Mallison, H.** (2020). The tail of the Late Jurassic sauropod *Giraffatitan brancai*: digital reconstruction of its epaxial and hypaxial musculature, and implications for tail biomechanics. *Frontiers in Earth Science*, *8*, 160. https://doi.org/10.3389/feart.2020.00160

Díez Díaz, V., **Garcia, G.**, **Knoll, F.**, **Pereda Suberbiola, X.**, & **Valentin, X.** (2012). New cranial remains of titanosaurian sauropod dinosaurs from the Late Cretaceous of Fox-Amphoux-Métisson (Var, SE France). *Proceedings of the Geologists' Association*, *123*(4), 626–637. https://doi.org/10.1016/j.pgeola.2012.04.002

Díez Díaz, V., **Garcia, G.**, **Pereda-Suberbiola, X.**, **Jentgen-Ceschino, B.**, **Stein, K.**, **Godefroit, P.**, & **Valentin, X.** (2018). The titanosaurian dinosaur *Atsinganosaurus velauciensis* (Sauropoda) from the Upper Cretaceous of southern France: New material, phylogenetic affinities, and palaeobiogeographical implications. *Cretaceous*

Research, *91*, 429–456. https://doi.org/10.1016/j.cretres.2018.06.015

Díez Díaz, V., **Garcia, G.**, **Pereda Suberbiola, X.**, **Jentgen-Ceschino, B.**, **Stein, K.**, **Godefroit, P.**, & **Valentin, X.** (2021). A new titanosaur (Dinosauria: Sauropoda) from the Upper Cretaceous of Velaux-La-Bastide Neuve (southern France). *Historical Biology*, *33*(11), 2998–3017. https://doi.org/10.1080/08912963.2020.1841184

Díez Díaz, V., **Mocho, P.**, **Páramo, A.**, **Escaso, F.**, **Marcos-Fernández, F.**, **Sanz, J. L.**, & **Ortega, F.** (2016). A new titanosaur (Dinosauria, Sauropoda) from the Upper Cretaceous of Lo Hueco (Cuenca, Spain). *Cretaceous Research*, *68*, 49–60. https://doi.org/10.1016/j.cretres.2016.08.001

Díez Díaz, V., **Ortega, F.**, & **Sanz, J. L.** (2014). Titanosaurian teeth from the Upper Cretaceous of 'Lo Hueco' (Cuenca, Spain). *Cretaceous Research*, *51*, 285–291. https://doi.org/10.1016/j.cretres.2014.07.003

Díez Díaz, V., **Pereda Suberbiola, X.**, & **Company, J.** (2015). Updating titanosaurian diversity (Sauropoda) from the Late Cretaceous of Spain: The fossil sites of Lano and Chera. *Spanish Journal of Paleontology*, *30*(2), 293–306.

Díez Díaz, V., **Pereda Suberbiola, X.**, & **Luis Sanz, J.** (2011). Braincase anatomy of the titanosaurian sauropod *Lirainosaurus astibiae* from the Late Cretaceous of the Iberian Peninsula. *Acta Palaeontologica Polonica*, *56*(3), 521–533. https://doi.org/10.4202/app.2010.0043

Díez Díaz, V., **Pereda-Suberbiola, X.**, & **Sanz, J. L.** (2012). Juvenile and adult teeth of the titanosaurian dinosaur *Lirainosaurus* (Sauropoda) from the Late Cretaceous of Iberia. *1 Geobios*, *45*(3), 265–274. https://doi.org/10.1016/j.geobios.2011.10.002

Díez Díaz, V., **Pereda Suberbiola, X.**, & **Sanz, J. L.** (2013a). Appendicular skeleton and dermal armour of the late cretaceous titanosaur *Lirainosaurus astibiae* (Dinosauria: Sauropoda) from Spain. *Palaeontologia Electronica*, *16*(2), 18.

Díez Díaz, V., **Pereda Suberbiola, X.**, & **Sanz, J. L.** (2013b). The axial skeleton of the titanosaur *Lirainosaurus astibiae* (Dinosauria: Sauropoda) from the latest Cretaceous of Spain. *Cretaceous Research*, *43*, 145–160. https://doi.org/10.1016/j.cretres.2013.03.002

Díez Díaz, V., **Tortosa, T.**, & **Le Loeuff, J.** (2013). Sauropod diversity in the Late Cretaceous of southwestern Europe: The lessons of odontology. *Annales de Paléontologie*, *99*(2), 119–129. https://doi.org/10.1016/j.annpal.2012.12.002

Dincă, A., **Tocorjescu, M.**, & **Stilla, A.** (1972). Despre vîrsta depozitelor continentale cu dinozaurieni din Bazinele Haţeg şi Rusca Montană. *Dări de Seamă Ale Institutului Geologic Român*, *58*, 83–94.

Dunhill, A. M., **Bestwick, J.**, **Narey, H.**, & **Sciberras, J.** (2016). Dinosaur biogeographical structure and Mesozoic continental fragmentation: A network-based approach. *Journal of Biogeography*, *43*(9), 1691–1704. https://doi.org/10.1111/jbi.12766

Ezcurra, M. D., & **Agnolin, F. L.** (2012). An abelisauroid dinosaur from the Middle Jurassic of Laurasia and its implications on theropod palaeobiogeography and evolution. *Proceedings of the Geologists' Association*, *123*(3), 500–507.

Filippi, L. S., **García, R. A.**, & **Garrido, A. C.** (2011). A new titanosaur sauropod dinosaur from the Upper Cretaceous of North Patagonia, Argentina. *Acta Palaeontologica Polonica*, *56*(3), 505–520. https://doi.org/10.4202/app.2010.0019

Filippi, L. S., **Salgado, L.**, & **Garrido, A. C.** (2019). A new giant basal titanosaur sauropod in the Upper Cretaceous (Coniacian) of the Neuquén Basin, Argentina. *Cretaceous Research*, *100*, 61–81. https://doi.org/10.1016/j.cretres.2019.03.008

Fondevilla, V., **Dinarès-Turell, J.**, & **Oms, O.** (2016). The chronostratigraphic framework of the South-Pyrenean Maastrichtian succession reappraised: Implications for basin development and end-Cretaceous dinosaur faunal turnover. *Sedimentary Geology*, *337*, 55–68. https://doi.org/10.1016/j.sedgeo.2016.03.006

Fondevilla, V., **Riera, V.**, **Vila, B.**, **Sellés, A. G.**, **Dinarès-Turell, J.**, **Vicens, E.**, **Gaete, R.**, **Oms, O.**, & **Galobart, À.** (2019). Chronostratigraphic synthesis of the latest Cretaceous dinosaur turnover in south-western Europe. *Earth-Science Reviews*, *191*, 168–189. https://doi.org/10.1016/j.earscirev.2019.01.007

Foster, J. B. (1964). Evolution of mammals on islands. *Nature*, *202*(4929), 234–235.

Franco-Rosas, A. C., **Salgado, L.**, **Rosas, C. F.**, & **de Carvalho, I.S.** (2004). Nuevos materiales de titanosaurios (Sauropoda) en el Cretácico Superior de Mato Grosso, Brasil. *Revista Brasileira de Paleontologia*, *7*(3), 329–336.

Gallina, P. A., & **Apesteguía, S.** (2011). Cranial anatomy and phylogenetic position of the titanosaurian sauropod *Bonitasaura salgadoi*. *Acta Palaeontologica Polonica*, *56*(1), 45–60. https://doi.org/10.4202/app.2010.0011

Gallina, P. A., & **Apesteguía, S.** (2015). Postcranial anatomy of *Bonitasaura salgadoi* (Sauropoda, Titanosauria) from the Late Cretaceous of Patagonia. *Journal of Vertebrate Paleontology*, *35*(3), e924957. https://doi.org/10.1080/02724634.2014.924957

Gallina, P. A., **Canale, J. I.**, & **Carballido, J. L.** (2021). The earliest known titanosaur sauropod dinosaur. *Ameghiniana*, *58*(1), 35–51. https://doi.org/10.5710/AMGH.20.08.2020.3376

Gallina, P. A., **González Riga, B. J.**, & **Ortiz David, L. D.** (2022). Time for giants: Titanosaurs from the Berriasian–Santonian Age. In A. Otero, J. L. Carballido, & D. Pol (Eds.), *South American Sauropodomorph Dinosaurs* (pp. 299–340). Springer International Publishing. https://doi.org/10.1007/978-3-030-95959-3_9

Gallina, P. A., & **Otero, A.** (2015). Reassessment of *Laplatasaurus araukanicus* (Sauropoda: Titanosauria) from the Upper Cretaceous of Patagonia, Argentina. *Ameghiniana*, *52*(5), 487–501. https://doi.org/10.5710/AMGH.08.06.2015.2911

Garcia, G. É., **Amico, S. A.**, **Fournier, F. R.**, **Thouand, E. U.**, & **Valentin, X. A.** (2010). A new Titanosaur genus (Dinosauria, Sauropoda) from the Late Cretaceous of southern France and its paleobiogeographic implications. *Bulletin de La Société Géologique de France*, *181*(3), 269–277. https://doi.org/10.2113/gssgfbull.181.3.269

Gheerbrant, E., & **Rage, J.-C.** (2006). Paleobiogeography of Africa: How distinct from Gondwana and Laurasia? *Palaeogeography, Palaeoclimatology, Palaeoecology*, *241*(2), 224–246.

Gierliński, G. D. (2015). New dinosaur footprints from the Upper Cretaceous of Poland in the light of paleogeographic context. *Ichnos*, *22*(3–4), 220–226. https://doi.org/10.1080/10420940.2015.1063489

Goloboff, P. A. (2014). Extended implied weighting. *Cladistics*, *30*(3), 260–272. https://doi.org/10.1111/cla.12047

Goloboff, P. A., Farris, J. S., & Nixon, K. C. (2008). TNT, a free program for phylogenetic analysis. *Cladistics*, *24*(5), 774–786. https://doi.org/10.1111/j.1096-0031.2008.00217.x

Goloboff, P. A., & Morales, M. E. (2023). TNT version 1.6, with a graphical interface for MacOS and Linux, including new routines in parallel. *Cladistics*, *39*(2), 144–153. https://doi.org/10.1111/cla.12524

Goloboff, P. A., & Szumik, C. A. (2015). Identifying unstable taxa: Efficient implementation of triplet-based measures of stability, and comparison with Phyutility and RogueNaRok. *Molecular Phylogenetics and Evolution*, *88*, 93–104. https://doi.org/10.1016/j.ympev.2015.04.003

Goloboff, P. A., Torres, A., & Arias, J. S. (2018). Weighted parsimony outperforms other methods of phylogenetic inference under models appropriate for morphology. *Cladistics*, *34*(4), 407–437. https://doi.org/10.1111/cla.12205

Gomani, E. M. (2005). Sauropod dinosaurs from the Early Cretaceous of Malawi, Africa. *Palaeontologia Electronica*, *8*(1), 1–37.

González Riga, B. J. (2003). A new titanosaur (Dinosauria, Sauropoda) from the Upper Cretaceous of Mendoza Province, Argentina. *Ameghiniana*, *40*(2), Article 2.

González Riga, B. J., Lamanna, M. C., Ortiz David, L. D., Calvo, J. O., & Coria, J. P. (2016). A gigantic new dinosaur from Argentina and the evolution of the sauropod hind foot. *Scientific Reports*, *6*(1), 19165. https://doi.org/10.1038/srep19165

González Riga, B. J., Lamanna, M. C., Otero, A., Ortiz David, L. D., Kellner, A. W. A., & Ibiricu, L. M. (2019). An overview of the appendicular skeletal anatomy of South American titanosaurian sauropods, with definition of a newly recognized clade. *Anais Da Academia Brasileira de Ciencias*, *91*(suppl 2), e20180374. https://doi.org/10.1590/0001-3765201920180374

González Riga, B. J., Mannion, P. D., Poropat, S. F., Ortiz David, L. D., & Coria, J. P. (2018). Osteology of the Late Cretaceous Argentinean sauropod dinosaur *Mendozasaurus neguyelap*: Implications for basal titanosaur relationships. *Zoological Journal of the Linnean Society*, 1–46. https://doi.org/10.1093/zoolinnean/zlx103/4816851

Gorscak, E., Lamanna, M. C., Schwarz, D., Díez Díaz, V., Salem, B. S., Sallam, H. M., & Wiechmann, M. F. (2023). A new titanosaurian (Dinosauria: Sauropoda) from the Upper Cretaceous (Campanian) Quseir Formation of the Kharga Oasis, Egypt. *Journal of Vertebrate Paleontology*, *42*(6), e2199810. https://doi.org/10.1080/02724634.2023.2199810

Gorscak, E., & O'Connor, P. M. (2016). Time-calibrated models support congruency between Cretaceous continental rifting and titanosaurian evolutionary history. *Biology Letters*, *12*(4). https://doi.org/10.1098/rsbl.2015.1047

Gorscak, E., & O'Connor, P. M. (2019). A new African titanosaurian sauropod dinosaur from the Middle Cretaceous Galula Formation (Mtuka Member), Rukwa Rift Basin, Southwestern Tanzania. *PLoS ONE*, *14*(2), e0211412. https://doi.org/10.1371/JOURNAL.PONE.0211412

Gorscak, E., O'Connor, P. M., Roberts, E. M., & Stevens, N. J. (2017). The second titanosaurian (Dinosauria: Sauropoda) from the middle Cretaceous Galula Formation, southwestern Tanzania, with remarks on African titanosaurian diversity. *Journal of Vertebrate Paleontology*, *37*(4), e1343250. https://doi.org/10.1080/02724634.2017.1343250

Gorscak, E., O'Connor, P. M., Stevens, N. J., & Roberts, E. M. (2014). The basal titanosaurian *Rukwatitan bisepultus* (Dinosauria, Sauropoda) from the middle Cretaceous Galula Formation, Rukwa Rift Basin, southwestern Tanzania. *Journal of Vertebrate Paleontology*, *34*(5), 1133–1154. https://doi.org/10.1080/02724634.2014.845568

Grellet-Tinner, G., Codrea, V., Folie, A., Higa, A., & Smith, T. (2012). First evidence of reproductive adaptation to 'island effect' of a dwarf Cretaceous Romanian titanosaur, with embryonic integument in ovo. *PloS One*, *7*(3), e32051. https://doi.org/10.1371/journal.pone.0032051

Grigorescu, D. (1983). A stratigraphic, taphonomic and paleoecologic approach to a 'forgotten land': The dinosaur-bearing deposits from the Haţeg Basin (Transylvania-Romania). *Acta Palaeontologica Polonica*, *28*(1–2), 103–121. https://bibliotekanauki.pl/articles/22306.pdf

Grigorescu, D. (1987). Considerations on the age of the "Red Beds" continental formations in SW Transylvanian Depression. *The Eocene from the Transylvanian Basin. Cluj-Napoca*, 189–196.

Grigorescu, D. (1992). Nonmarine Cretaceous formations of Romania. In N. J. Matter & P.-J. Chen (Eds.), *Aspects of Nonmarine Cretaceous Geology* (pp. 142–164). China Ocean Press.

Grigorescu, D. (2010). The "Tustea puzzle": Hadrosaurid (Dinosauria, Ornithopoda) hatchlings associated with Megaloolithidae eggs in the Maastrichtian of the Haţeg Basin (Romania). *Ameghiniana*, *47*(1), 89–97.

Grigorescu, D. (2017). The 'Tuştea puzzle' revisited: Late Cretaceous (Maastrichtian) *Megaloolithus* eggs associated with *Telmatosaurus* hatchlings in the Haţeg Basin. *Historical Biology*, *29*(5), 627–640. https://doi.org/10.1080/08912963.2016.1227327

Grigorescu, D., & Csiki, Z. (2008). A new site with megaloolithid egg remains in the Maastrichtian of the Haţeg Basin. *Acta Palaeontologica Romaniae*, *6*, 115–121.

Grigorescu, D., Garcia, G., Csiki, Z., Codrea, V., & Bojar, A.-V. (2010). Uppermost Cretaceous megaloolithid eggs from the Haţeg Basin, Romania, associated with hadrosaur hatchlings: Search for explanation. *Palaeogeography, Palaeoclimatology, Palaeoecology*, *293*(3–4), 360–374.

Grigorescu, D., Hartenberger, J.-L., Radulescu, C., Samson, P., & Sudre, J. (1985). Découverte de mammifères et dinosaures dans le Crétacé supérieur de Pui (Roumanie). *Comptes Rendus de l'Académie Des Sciences. Série 2, Mécanique, Physique, Chimie, Sciences de l'univers, Sciences de La Terre*, *301*(19), 1365–1368.

Grigorescu, D., Şeclăman, M., Norman, D. B., & Weishampel, D. B. (1990). Dinosaur eggs from Romania. *Nature*, *346*(6283), 417.

Grigorescu, D., Weishampel, D. B., Norman, D. B., Seclamen, M., Rusu, M., Baltres, A., & Teodorescu, V. (1994). Late Maastrichtian dinosaur eggs from the Haţeg Basin (Romania). In K. Carpenter, K. F. Hirsch, & J. R.

Horner (Eds.), *Dinosaur eggs and babies* (pp. 75–87). Cambridge University Press.

Groza, I. (1983). Rezultatele preliminare ale cercetărilor întreprinse de către Muzeul Judeţean Hunedoara-Deva în stratele cu dinosauri de la Sînpetru-Haţeg. *Sargetia*, *13*, 49–66.

Halaváts, G. (1897). Adatok a Hátszegi medence földtani viszonyainak ismeretéhez. *Magyar Királyi Földtani Intézet Évi Jelentései*, *1896-ról*, 90–95.

Haq, B. U. (2014). Cretaceous eustasy revisited. *Global and Planetary Change*, *113*, 44–58.

Hechenleitner, E. M., **Leuzinger, L.**, **Martinelli, A. G.**, **Rocher, S.**, **Fiorelli, L. E.**, **Taborda, J. R. A.**, & **Salgado, L.** (2020). Two Late Cretaceous sauropods reveal titanosaurian dispersal across South America. *Communications Biology*, *3*(1), 622. https://doi.org/10.1038/s42003-020-01338-w

Hocknull, S. A., **White, M. A.**, **Tischler, T. R.**, **Cook, A. G.**, **Calleja, N. D.**, **Sloan, T.**, & **Elliott, D. A.** (2009). New Mid-Cretaceous (Latest Albian) dinosaurs from Winton, Queensland, Australia. *PLoS ONE*, *4*(7), e6190. https://doi.org/10.1371/journal.pone.0006190

Hocknull, S. A., **Wilkinson, M.**, **Lawrence, R. A.**, **Konstantinov, V.**, **Mackenzie, S.**, & **Mackenzie, R.** (2021). A new giant sauropod, *Australotitan cooperensis* gen. et sp. nov., from the mid-Cretaceous of Australia. *PeerJ*, *9*, e11317. https://doi.org/10.7717/peerj.11317

Holwerda, F. M., **Díez Díaz, V.**, **Blanco, A.**, **Montie, R.**, & **Reumer, J. W. F.** (2018). Late Cretaceous sauropod tooth morphotypes may provide supporting evidence for faunal connections between North Africa and Southern Europe. *PeerJ*, 2018(11), e5925. https://doi.org/10.7717/peerj.5925

Horner, J. R. (2000). Dinosaur reproduction and parenting. *Annual Review of Earth and Planetary Sciences*, *28*(1), 19–45. https://doi.org/10.1146/annurev.earth.28.1.19

Huene, F. von. (1929). Short review of the Saurischia and their natural interrelationships. *Palaeontologische Zeitschrift, 11*, 269–273.

Huene, F. von. (1932). Die fossile Reptilordnung Saurischia: Ihre Entwicklung und Geschichte. *Monographien Zur Geologie Und Palaeontologie*, *1*(4), 1–361.

Ibiricu, L. M., **Lamanna, M. C.**, & **Lacovara, K. J.** (2013). The influence of caudofemoral musculature on the titanosaurian (Saurischia: Sauropoda) tail skeleton: Morphological and phylogenetic implications. *Historical Biology*, *26*(April 2013), 454–471. https://doi.org/10.1080/08912963.2013.787069

Jain, S. L., & **Bandyopadhyay, S.** (1997). New titanosaurid (Dinosauria: Sauropoda) from the Late Cretaceous of central India. *Journal of Vertebrate Paleontology*, *17*(1), 114–136. https://doi.org/10.1080/02724634.1997.10010958

Jianu, C.-M., & **Boekschoten, G. J.** (1999). The Haţeg area-island or outpost? *Deinsea*, *7*(1), 195–198.

Jianu, C.-M., **Mészáros, N.**, & **Codrea, V.** (1997). A new collection of Haţeg and Râpa Roşie material (Dinosauria, Crocodilia, Chelonia) in the Cluj-Napoca University. *Sargetia, Series Scientia Naturae*, *17*, 219–232.

Jianu, C.-M., & **Weishampel, D. B.** (1999). The smallest of the largest: A new look at possible dwarfing in sauropod dinosaurs. *Geologie En Mijnbouw*, *78*(3), 335–343.

Kadić, O. (1911). A Runki völgy földtani viszonyai Hunyadmegyében. *A Magyar Királyi Földtani Intézet Évi Jelentése*, *1909-ről*, 77–80.

Kadić, O. (1916). Jelentés az 1915, évben végzett ásatásaimról: II A valiorai dinosaurusok gyujtése. *A Magyar Királyi Földtani Intézet Évi Jelentések*, *1915-ről*, 573–576.

Kellner, A. W., & **Azevedo, S. D.** (1999). A new sauropod dinosaur (Titanosauria) from the Late Cretaceous of Brazil. *National Science Museum Monographs*, *15*(111), e142.

Kellner, A. W., **Campos, D. D. A.**, & **Trotta, M. N. F. M.** (2005). Description of a titanosaurid caudal series from the Bauru Group, Late Cretaceous of Brazil. *Arquivos Do Museu Nacional, Rio de Janeiro*, *63*, 529–564.

Keogh, J. S., **Scott, I. A.**, & **Hayes, C.** (2005). Rapid and repeated origin of insular gigantism and dwarfism in Australian tiger snakes. *Evolution*, *59*(1), 226–233.

Koch, A. (1894). Die Tertiärbildungen des Beckens der Siebenbürgischen Landesteile. I. Paläogen Abtheilung. *Mitteilungen Aus Den Jahrbuch Der Königlishes Ungarische Geologischen Anstalt*, *10*, 177–399.

Krause, D. W., **Hoffmann, S.**, **Hu, Y.**, **Wible, J. R.**, **Rougier, G. W.**, **Kirk, E. C.**, **Groenke, J. R.**, **Rogers, R. R.**, **Rossie, J. B.**, & **Schultz, J. A.** (2020). Skeleton of a Cretaceous mammal from Madagascar reflects long-term insularity. *Nature*, *581*(7809), 421–427.

Krause, D. W., **Sertich, J. J. W.**, **O'Connor, P. M.**, **Curry Rogers, K.**, & **Rogers, R. R.** (2019). The Mesozoic biogeographic history of Gondwanan terrestrial vertebrates: Insights from Madagascar's fossil record. *Annual Review of Earth and Planetary Sciences*, *47*(1), 519–553. https://doi.org/10.1146/annurev-earth-053018-060051

Krézsek, C., & **Bally, A. W.** (2006). The Transylvanian Basin (Romania) and its relation to the Carpathian fold and thrust belt: Insights in gravitational salt tectonics. *Marine and Petroleum Geology*, *23*(4), 405–442.

Lacovara, K. J., **Lamanna, M. C.**, **Ibiricu, L. M.**, **Poole, J. C.**, **Schroeter, E. R.**, **Ullmann, P. V.**, **Voegele, K. K.**, **Boles, Z. M.**, **Carter, A. M.**, **Fowler, E. K.**, **Egerton, V. M.**, **Moyer, A. E.**, **Coughenour, C. L.**, **Schein, J. P.**, **Harris, J. D.**, **Martínez, R. D.**, & **Novas, F. E.** (2014). A gigantic, exceptionally complete titanosaurian sauropod dinosaur from southern Patagonia, Argentina. *Scientific Reports*, *4*(1), 6196. https://doi.org/10.1038/srep06196

Laufer, F. (1925). Contribuţiuni la studiul geologic al împrejurimilor oraşului Haţeg. *Anuarul Institutului Geologic al României*, *10*, 301–333.

Le Loeuff, J. (1991). The Campano-Maastrichtian vertebrate faunas from southern Europe and their relationships with other faunas in the world; palaeobiogeographical implications. *Cretaceous Research*, *12*(2), 93–114.

Le Loeuff, J. (1993). European titanosaurids. *Revue de Paléobiologie*, *7*, 105–117.

Le Loeuff, J. (1995). *Ampelosaurus atacis* (nov. gen., nov. sp.), a new titanosaurid (Dinosauria, Sauropoda) from the Late Cretaceous of the Upper Aude Valley (France). *Comptes Rendus de l'Academie Des Sciences-Serie II-Sciences de La Terre et Des Planetes*, *321*, 693–700.

Le Loeuff, J. (1997). Biogeography. In P. J. Currie & K. Padian (Eds.), *Encyclopedia of Dinosaurs* (pp. 51–56). Academic Press.

Le Loeuff, J. (2005a). Romanian late cretaceous dinosaurs: Big dwarfs or small giants? *Historical Biology*, *17*(1–4), 15–17. https://doi.org/10.1080/08912960500376210

Le Loeuff, J. (2005b). Osteology of *Ampelosaurus atacis* (Titanosauria) from southern France. In V. Tidwell, & K. Carpenter (Eds.), *Thunder-lizards: The sauropodomorph dinosaurs* (pp. 115–137). Indiana University Press.

Le Loeuff, J., & **Buffetaut, E.** (1995). The evolution of Late Cretaceous non-marine vertebrate fauna in Europe. In A.-L. Sun & Y.-Q. Wang (Eds.), *Sixth Symposium on Mesozoic Terrestrial Ecosystems and Biota, Short Papers* (pp. 181–184). China Ocean Press.

Le Loeuff, J., **Buffetaut, E.**, & **Martin, M.** (1994). The last stages of dinosaur faunal history in Europe: A succession of Maastrichtian dinosaur assemblages from the Corbières (southern France). *Geological Magazine*, *131*(5), 625–630. https://doi.org/10.1017/S0016756800012413

Le Loeuff, J., **Suteethorn, S.**, & **Buffetaut, E.** (2013). A new sauropod dinosaur from the Albian of Le Havre (Normandy, France). *Oryctos*, *10*, 23–30.

Lerzo, L. N., **Carballido, J. L.**, & **Gallina, P. A.** (2021). Rebbachisaurid sauropods in Asia? A re-evaluation of the phylogenetic position of *Dzharatitanis kingi* from the Late Cretaceous of Uzbekistan. *Publicación Electrónica de La Asociación Paleontológica Argentina*, *21*(1), 18–27.

Li, L. G., **Li, D. Q.**, **You, H. L.**, & **Dodson, P.** (2014). A new titanosaurian sauropod from the Hekou Group (Lower Cretaceous) of the Lanzhou-Minhe Basin, Gansu Province, China. *PLoS ONE*, *9*(1), e85979. https://doi.org/10.1371/journal.pone.0085979

Lomolino, M. V. (2005). Body size evolution in insular vertebrates: Generality of the island rule. *Journal of Biogeography*, *32*(10), 1683–1699. https://doi.org/10.1111/j.1365-2699.2005.01314.x

Longrich, N. R., **Pereda-Suberbiola, X.**, **Bardet, N.**, & **Jalil, N.-E.** (2024). A new small duckbilled dinosaur (Hadrosauridae: Lambeosaurinae) from Morocco and dinosaur diversity in the late Maastrichtian of North Africa. *Scientific Reports*, *14*(1), 3665. https://doi.org/10.1038/s41598-024-53447-9

Longrich, N. R., **Pereda Suberbiola, X.**, **Pyron, R. A.**, & **Jalil, N.-E.** (2021). The first duckbill dinosaur (Hadrosauridae: Lambeosaurinae) from Africa and the role of oceanic dispersal in dinosaur biogeography. *Cretaceous Research*, *120*, 104678. https://doi.org/10.1016/j.cretres.2020.104678

Lucas, S. G., & **Hunt, A. P.** (1989). *Alamosaurus* and the sauropod hiatus in the Cretaceous. *Geological Society of America Special Papers*, *238*, 75.

Lydekker, R. (1877). Notices of new and other Vertebrata from Indian Tertiary and Secondary rocks. *Records of the Geological Survey of India*, *10*(1), 30–43.

Magyar, J., **Csiki-Sava, Z.**, **Ősi, A.**, **Augustin, F. J.**, & **Botfalvai, G.** (2024). Rhabdodontid (Dinosauria, Ornithopoda) diversity suggested by the first documented occurrence of associated cranial and postcranial material at Vălioara (uppermost Cretaceous Densuș-Ciula Formation, Hațeg Basin, Romania). *Cretaceous Research*, *156*, 105810.

Mamulea, M. A. (1953a). Cercetări geologice în partea de Vest a Bazinului Hațeg (Regiunea Sarmisegetuza-Răchitova). *Dări de Seamă Ale Comitetului Geologic Român*, *37*, 142–148.

Mamulea, M. A. (1953b). Studii geologice în regiunea Sânpetru-Pui (Bazinul Hațegului). *Anuarul Comitetului Geologic Român*, *25*, 211–274.

Mannion, P. D., & **Barrett, P. M.** (2013). Additions to the sauropod dinosaur fauna of the Cenomanian (early Late Cretaceous) Kem Kem beds of Morocco: Palaeobiogeographical implications of the mid-Cretaceous African sauropod fossil record. *Cretaceous Research*, *45*, 49–59. https://doi.org/10.1016/j.cretres.2013.07.007

Mannion, P. D., & **Calvo, J. O.** (2011). Anatomy of the basal titanosaur (Dinosauria, Sauropoda) *Andesaurus delgadoi* from the mid-Cretaceous (Albian-early Cenomanian) Río Limay Formation, Neuquén Province, Argentina: Implications for titanosaur systematics. *Zoological Journal of the Linnean Society*, *163*(1), 155–181. https://doi.org/10.1111/j.1096-3642.2011.00699.x

Mannion, P. D., & **Otero, A.** (2012). A reappraisal of the Late Cretaceous Argentinean sauropod dinosaur *Argyrosaurus superbus*, with a description of a new titanosaur genus. *Journal of Vertebrate Paleontology*, *32*(3), 614–638. https://doi.org/10.1080/02724634.2012.660898

Mannion, P., & **Upchurch, P.** (2011). A re-evaluation of the 'mid-Cretaceous sauropod hiatus' and the impact of uneven sampling of the fossil record on patterns of regional dinosaur extinction. *Palaeogeography, Palaeoclimatology, Palaeoecology*, *299*(3–4), 529–540. https://doi.org/10.1016/j.palaeo.2010.12.003

Mannion, P. D., **Upchurch, P.**, **Barnes, R. N.**, & **Mateus, O.** (2013). Osteology of the Late Jurassic Portuguese sauropod dinosaur *Lusotitan atalaiensis* (Macronaria) and the evolutionary history of basal titanosauriforms: *Lusotitan* and Titanosauriform Evolution. *Zoological Journal of the Linnean Society*, *168*(1), 98–206. https://doi.org/10.1111/zoj.12029

Mannion, P. D., **Upchurch, P.**, **Jin, X.**, & **Zheng, W.** (2019). New information on the Cretaceous sauropod dinosaurs of Zhejiang Province, China: Impact on Laurasian titanosauriform phylogeny and biogeography. *Royal Society Open Science*, *6*(8). https://doi.org/10.1098/rsos.191057

Mannion, P. D., **Upchurch, P.**, **Schwarz, D.**, & **Wings, O.** (2019). Taxonomic affinities of the putative titanosaurs from the Late Jurassic Tendaguru Formation of Tanzania: Phylogenetic and biogeographic implications for eusauropod dinosaur evolution. *Zoological Journal of the Linnean Society*, *185*, 784–909. https://doi.org/10.1093/zoolinnean/zly068/5300162

Marmi, J., **Blanco, A.**, **Fondevilla, V.**, **Dalla Vecchia, F. M.**, **Sellés, A. G.**, **Vicente, A.**, **Martín-Closas, C.**, **Oms, O.**, & **Galobart, A.** (2016). The Molí del Baró-1 site, a diverse fossil assemblage from the uppermost Maastrichtian of the southern Pyrenees (north-eastern Iberia). *Cretaceous Research*, *57*, 519–539.

Marsh, O. C. (1878). Principal characters of American Jurassic dinosaurs. *American Journal of Science*, *3*(95), 411–416.

Marshall, C. R. (1990). Confidence intervals on stratigraphic ranges. *Paleobiology*, *16*(1), 1–10.

Martinelli, A., & **Forasiepi, A.** (2004). Late Cretaceous vertebrates from Bajo de Santa Rosa (Allen Formation), Río Negro province, Argentina, with the description of a new sauropod dinosaur (Titanosauridae). *Revista del Museo Argentino de Ciencias Naturales*, *6*(2), 257–265. https://doi.org/10.22179/REVMACN.6.88

Martínez, R. D., **Giménez, O.**, **Rodríguez, J.**, **Luna, M.**, & **Lamanna, M. C.** (2004). An articulated specimen of the

basal titanosaurian (Dinosauria: Sauropoda) *Epachthosaurus sciuttoi* from the early Late Cretaceous Bajo Barreal Formation of Chubut Province, Argentina. *Journal of Vertebrate Paleontology*, *24*(1), 107–120. https://doi.org/10.1671/9.1

Mateus, O., **Jacobs, L. L.**, **Schulp, A. S.**, **Polcyn, M. J.**, **Tavares, T. S.**, **Buta Neto, A.**, **Morais, M. L.**, & **Antunes, M. T.** (2011). *Angolatitan adamastor*, a new sauropod dinosaur and the first record from Angola. *Anais Da Academia Brasileira De Ciencias*, *83*(1), 221–233.

Matzke, N. J. (2013). BioGeoBEARS: BioGeography with Bayesian (and likelihood) evolutionary analysis in R Scripts. *R Package, Version 0.2*, 1, 2013

Matzke, N. J. (2014). Model selection in historical biogeography reveals that founder-event speciation is a crucial process in island clades. *Systematic Biology, 63*(6), 951–970.

May Lindfors, S., **Csiki, Z.**, **Grigorescu, D.**, & **Friis, E. M.** (2010). Preliminary account of plant mesofossils from the Maastrichtian Budurone microvertebrate site of the Haţeg Basin, Romania. *Palaeogeography, Palaeoclimatology, Palaeoecology*, *293*(3–4), 353–359.

McIntosh, J. S. (1990). Sauropoda. In D. B. Weishampel, P. Dodson, & H. Osmólska (Eds.), *The Dinosauria* (pp. 345–401). University of California Press.

Melinte-Dobrinescu, M. C. (2010). Lithology and biostratigraphy of Upper Cretaceous marine deposits from the Haţeg region (Romania): Palaeoenvironmental implications. *Palaeogeography, Palaeoclimatology, Palaeoecology*, *293*(3–4), 283–294.

Mezga, A., **Meyer, C. A.**, **Tešović, B. C.**, **Bajraktarević, Z.**, & **Gušić, I.** (2006). The first record of dinosaurs in the Dalmatian part (Croatia) of the Adriatic-Dinaric carbonate platform (ADCP). *Cretaceous Research*, *27*(6), 735–742.

Millien, V. (2006). Morphological evolution is accelerated among island mammals. *PLoS Biology*, *4*(10), e321.

Mocho, P., **Pérez-García, A.**, & **Codrea, V. A.** (2023). New titanosaurian caudal remains provide insights on the sauropod diversity of the Haţeg Island (Romania) during the Late Cretaceous. *Historical Biology*, *35*(10), 1881–1916. https://doi.org/10.1080/08912963.2022.2125807

Mocho, P., **Pérez-García, A.**, **Martín Jiménez, M.**, & **Ortega, F.** (2019). New remains from the Spanish Cenomanian shed light on the Gondwanan origin of European Early Cretaceous titanosaurs. *Cretaceous Research*, *95*, 164–190. https://doi.org/10.1016/j.cretres.2018.09.016

Navarro, B. A., **Ghilardi, A. M.**, **Aureliano, T.**, **Díez Díaz, V.**, **Bandeira, K. L. N.**, **Cattaruzzi, A. G. S.**, **Iori, F. V.**, **Martine, A. M.**, **Carvalho, A. B.**, **Anelli, L. E.**, **Fernandes, M. A.**, & **Zaher, H.** (2022). A new nanoid titanosaur (Dinosauria: Sauropoda) from the Upper Cretaceous of Brazil. *Ameghiniana*, *59*(5), 317–354. https://doi.org/10.5710/AMGH.25.08.2022.3477

Nicosia, U., **Petti, F. M.**, **Perugini, G.**, **Porchetti, S. D.**, **Sacchi, E.**, **Conti, M. A.**, **Mariotti, N.**, & **Zarattini, A.** (2007). Dinosaur tracks as paleogeographic constraints: New scenarios for the Cretaceous geography of the Periadriatic Region. *Ichnos*, *14*(1–2), 69–90. https://doi.org/10.1080/10420940601006859

Nikolov, V., **Yaneva, M.**, **Dochev, D.**, **Konyovska, R.**, **Sergeeva, I.**, & **Hristova, L.** (2020). Bone histology reveals the first record of titanosaur (Dinosauria: Sauropoda) from the Late Cretaceous of Bulgaria. *Palaeontologia Electronica*, *23*(1), 1–38.

Nopcsa, F. (1897). Vorläufiger Bericht über das Auftreten von oberer Kreide im Hátszeger Thale in Siebenbürgen. *Verhandlungen der Kaiserlich-Königlichen Geologischen Reichsanstalt, 14*, 273–274.

Nopcsa, F. (1900). Dinosaurierreste aus Siebenbürgen I. Schädel von *Limnosaurus transsylvanicus* nov. gen. et nov. spec. *Denkschriften der Kaiserlichen Akademie der Wissenschaften. Mathematisch-Naturwissenschaftliche Classe, 68*, 555–591.

Nopcsa, F. (1902a). Dinosaurierreste aus Siebenbürgen II. (Schädelreste von *Mochlodon*). Mit einem Anhange: zur Phylogenie der Ornithopodiden. *Denkschriften der Kaiserlichen Akademie der Wissenschaften. Mathematisch-Naturwissenschaftliche Classe, 72*, 149–175.

Nopcsa, F. (1902b). Über das Vorkommen der Dinosaurier bei Szentpéterfalva. *Zeitschrift Der Deutschen Geologischen Gesellschaft*, *72*, 34–39.

Nopcsa, F. (1904). Dinosaurierreste aus Siebenbürgen III. Weitere Schädelreste von *Mochlodon*. *Denkschriften der Kaiserlichen Akademie der Wissenschaften. Mathematisch-Naturwissenschaftliche Classe*, *74*, 229–263.

Nopcsa, F. (1905). Zur Geologie der gegend zwischen Gyulafehérvár: Déva, Ruszkabánya und der rumänischen Landesgrenze. *Mitteilungen Aus Dem Jahrbuche Der Königlisch Ungarischen Geologische Reichsanstalt*, *14*, 93–279.

Nopcsa, F. (1910). IV. – On the systematic position of the Upper Cretaceous Dinosaur Titanosaurus. *Geological Magazine*, *7*(6), 261–261. https://doi.org/10.1017/s0016756800134429

Nopcsa, F. (1914). Die Lebensbedingungen der obercretacischen Dinosaurier Siebenbürgens. *Centralblatt fur Mineralogie, Geologie und Paläontologie*, *1914*, 564–574.

Nopcsa, F. (1915). Die Dinosaurier der siebenbürgischen Landesteile Ungarns. *Mitteilungen Aus Dem Jahrbuche Der Königlisch Ungarischen Geologischen Reichsanstalt*, *23*, 1–24.

Nopcsa, F. (1923a). *Kallokibotium*: A primitive amphichelydean tortoise from the uppermost Cretaceous of Hungary. *Palaeontologica Hungarica*, *79*, 100–116.

Nopcsa, F. (1923b). On the geological importance of the primitive reptilian fauna in the uppermost Cretaceous of Hungary; With a description of a new tortoise (*Kallokibotion*). *Quarterly Journal of the Geological Society*, *79*(1–4), 100–116. https://doi.org/10.1144/GSL.JGS.1923.079.01-04.08

Nopcsa, F. (1929). Dinosaurierreste aus Siebenbürgen. V. *Struthiosaurus transylvanicus. Geologica Hungarica, Ser. Palaeontologica*, *4*, 1–76.

Novas, F. E., **Agnolín, F. L.**, **Ezcurra, M. D.**, **Porfiri, J.**, & **Canale, J. I.** (2013). Evolution of the carnivorous dinosaurs during the Cretaceous: The evidence from Patagonia. *Cretaceous Research*, *45*, 174–215.

Ősi, A., **Apesteguía, S.**, & **Kowalewski, M.** (2010a). Non-avian theropod dinosaurs from the early Late Cretaceous of Central Europe. *Cretaceous Research*, *31*(3), 304–320.

Ősi, A., **Butler, R. J.**, & **Weishampel, D. B.** (2010b). A Late Cretaceous ceratopsian dinosaur from Europe with Asian affinities. *Nature*, *465*(7297), 466–468.

Ősi, A., **Codrea, V.**, **Prondvai, E.**, & **Csiki-Sava, Z.** (2014). New ankylosaurian material from the Upper Cretaceous of

Transylvania. *Annales de Paléontologie*, *100*(3), 257–271. https://www.sciencedirect.com/science/article/pii/S0753396914000202

Ősi, A., Csiki-Sava, Z., & Prondvai, E. (2017a). A sauropod tooth from the Santonian of Hungary and the European Late Cretaceous sauropod hiatus. *Scientific Reports*, *7*(1), 3261. https://doi.org/10.1038/s41598-017-03602-2

Ősi, A., Csiki-Sava, Z., & Prondvai, E. (2017b). Needles in the haystack – Sauropod teeth from the uppermost Cretaceous of Iharkút (Santonian, Hungary) and Haţeg (Maastrichtian, Romania), and latest Cretaceous sauropod diversity in central-eastern Europe. In I. Lazăr, M. Grădinaru, & Ş. Vasile (Eds.), *Abstract Book, 11th Romanian Symposium of Palaeontology* (pp. 83–84). University of Bucharest Press.

Ősi, A., & Makádi, L. (2009). New remains of *Hungarosaurus tormai* (Ankylosauria, Dinosauria) from the Upper Cretaceous of Hungary: Skeletal reconstruction and body mass estimation. *Paläontologische Zeitschrift*, *83*(2), 227–245. https://doi.org/10.1007/s12542-009-0017-5

Otero, A. (2010). The appendicular skeleton of *Neuquensaurus*, a Late Cretaceous saltasaurine sauropod from Patagonia, Argentina. *Acta Palaeontologica Polonica*, *55*(3), 399–426. https://doi.org/10.4202/app.2009.0099

Otero, A. (2018). Forelimb musculature and osteological correlates in Sauropodomorpha (Dinosauria, Saurischia). *PLOS ONE*, *13*(7), e0198988. https://doi.org/10.1371/JOURNAL.PONE.0198988

Otero, A., Carballido, J. L., & Moreno, A. P. (2020). The appendicular osteology of *Patagotitan mayorum* (Dinosauria, Sauropoda). *Journal of Vertebrate Paleontology*, *40*(4), e1793158. https://doi.org/10.1080/02724634.2020.1793158

Otero, A., Gallina, P. A., Canale, J. I., & Haluza, A. (2012). Sauropod haemal arches: morphotypes, new classification and phylogenetic aspects. *Historical Biology*, *24*(3), 243–256.

Otero, A., & Vizcaíno, S. F. (2008). Hindlimb musculature and function of *Neuquensaurus australis* (Sauropoda: Titanosauria). *Ameghiniana*, *45*(2), 333–348.

Packard, G. C., Boardman, T. J., & Birchard, G. F. (2009). Allometric equations for predicting body mass of dinosaurs. *Journal of Zoology*, *279*(1), 355–361. https://doi.org/10.1111/j.1469-7998.2009.00594.x

Páll-Gergely, B., Magyar, J., Csiki-Sava, Z., & Botfalvai, G. (2023). *Ferussina petofiana* sp. n. (Gastropoda, Caenogastropoda, Cyclophoridae), the oldest representative of its subfamily from the Late Cretaceous of Romania. *Acta Zoologica Academiae Scientiarum Hungaricae*, *69*(4), 337–352.

Pană, I., Grigorescu, D., Csiki, Z., & Costea, C. (2002). Paleo-ecological significance of the continental gastropod assemblages from the Maastrichtian dinosaur beds of the Haţeg Basin. *Acta Palaeontologica Romaniae*, *3*, 337–343.

Panaiotu, A. G., Ciobănete, D., Panaiotu, C. G., & Panaiotu, C. E. (2011). New palaeomagnetic data from the Haţeg Basin, Romania. In Z. Csiki (Ed.), *Abstract Book, 8th Romanian Symposium of Paleontology* (pp. 84–85). Ars Docendi.

Panaiotu, C. G., & Panaiotu, C. E. (2010). Palaeomagnetism of the Upper Cretaceous Sânpetru Formation (Haţeg Basin, South Carpathians). *Palaeogeography, Palaeoclimatology, Palaeoecology*, *293*(3–4), 343–352.

Paulina Carabajal, A., Filippi, L., & Knoll, F. (2020). Neuroanatomy of the titanosaurian sauropod *Narambuenatitan palomoi* from the Upper Cretaceous of Patagonia. *Argentina. Publicación Electrónica de la Asociación Paleontológica Argentina*, *20*(2), 1–9. https://doi.org/10.5710/PEAPA.21.05.2020.298

Pereda-Suberbiola, X. (2009). Biogeographical affinities of Late Cretaceous continental tetrapods of Europe: A review. *Bulletin de La Société Géologique de France*, *180*(1), 57–71. https://doi.org/10.2113/gssgfbull.180.1.57

Pérez Moreno, A., Carballido, J. L., Otero, A., Salgado, L., & Calvo, J. O. (2022). The axial skeleton of *Rinconsaurus caudamirus* (Sauropoda: Titanosauria) from the Late Cretaceous of Patagonia, Argentina. *Ameghiniana*, *59*(1), 1–46. https://doi.org/10.5710/AMGH.13.09.2021.3427

Pérez Moreno, A., Otero, A., Carballido, J. L., Salgado, L., & Calvo, J. O. (2023). The appendicular skeleton of *Rinconsaurus caudamirus* (Sauropoda: Titanosauria) from the Upper Cretaceous of Patagonia, Argentina. *Cretaceous Research*, *142*, 105389. https://doi.org/10.1016/j.cretres.2022.105389

Pérez-Pueyo, M., Cruzado-Caballero, P., Moreno-Azanza, M., Vila, B., Castanera, D., Gasca, J. M., Puértolas-Pascual, E., Bádenas, B., & Canudo, J. I. (2021). The tetrapod fossil record from the uppermost Maastrichtian of the Ibero-Armorican Island: An integrative review based on the outcrops of the western Tremp Syncline (Aragón, Huesca Province, NE Spain). *Geosciences*, *11*(4), 162.

Pol, D., & Escapa, I. H. (2009). Unstable taxa in cladistic analysis: Identification and the assessment of relevant characters. *Cladistics*, *25*(5), 515–527. https://doi.org/10.1111/j.1096-0031.2009.00258.x

Popa, M. E., Kvaček, J., Vasile, Ş., & Csiki-Sava, Z. (2014). Maastrichtian monocotyledons of the Rusca Montană and Haţeg basins, South Carpathians, Romania. *Review of Palaeobotany and Palynology*, *210*, 89–101.

Popa, M. E., Kvaček, J., Vasile, Ş., & Csiki-Sava, Z. (2016). Maastrichtian dicotyledons of the Rusca Montană and Haţeg basins, South Carpathians, Romania. *Cretaceous Research*, *57*, 699–712.

Poropat, S. F., Frauenfelder, T. G., Mannion, P. D., Rigby, S. L., Pentland, A. H., Sloan, T., & Elliott, D. A. (2022). Sauropod dinosaur teeth from the lower Upper Cretaceous Winton Formation of Queensland, Australia and the global record of early titanosauriforms. *Royal Society Open Science*, *9*(7), 220381. https://doi.org/10.1098/RSOS.220381

Poropat, S. F., Kundrát, M., Mannion, P. D., Upchurch, P., Tischler, T. R., & Elliott, D. A. (2021). Second specimen of the Late Cretaceous Australian sauropod dinosaur *Diamantinasaurus matildae* provides new anatomical information on the skull and neck of early titanosaurs. *Zoological Journal of the Linnean Society*, *192*(2), 610–674. https://doi.org/10.1093/zoolinnean/zlaa173

Poropat, S. F., Mannion, P. D., Rigby, S. L., Duncan, R. J., Pentland, A. H., Bevitt, J. J., Sloan, T., & Elliott, D. A. (2023). A nearly complete skull of the sauropod dinosaur *Diamantinasaurus matildae* from the Upper Cretaceous Winton Formation of Australia and implications for the early evolution of titanosaurs. *Royal Society Open Science*, *10*(4), 221618. https://doi.org/10.1098/rsos.221618

Poropat, S. F., Mannion, P. D., Upchurch, P., Hocknull, S. A., Kear, B. P., & Elliott, D. A. (2015). Reassessment

of the non-titanosaurian somphospondylan *Wintonotitan wattsi* (Dinosauria: Sauropoda: Titanosauriformes) from the mid-Cretaceous Winton Formation, Queensland, Australia. *Papers in Palaeontology*, *1*(1), 59–106. https://doi.org/10.1002/spp2.1004

Poropat, S. F., **Mannion, P. D.**, **Upchurch, P.**, **Hocknull, S. A.**, **Kear, B. P.**, **Kundrát, M.**, **Tischler, T. R.**, **Sloan, T.**, **Sinapius, G. H. K.**, **Elliott, J. A.**, & **Elliott, D. A.** (2016). New Australian sauropods shed light on Cretaceous dinosaur palaeobiogeography. *Scientific Reports*, *6*(1), 34467. https://doi.org/10.1038/srep34467

Poropat, S. F., **Mannion, P. D.**, **Upchurch, P.**, **Tischler, T. R.**, **Sloan, T.**, **Sinapius, G. H. K.**, **Elliott, J. A.**, & **Elliott, D. A.** (2020). Osteology of the wide-hipped Titanosaurian sauropod dinosaur *Savannasaurus elliottorum* from the Upper Cretaceous Winton Formation of Queensland, Australia. *Journal of Vertebrate Paleontology*, *40*(3), e1786836. https://doi.org/10.1080/02724634.2020.1786836

Poropat, S. F., **Upchurch, P.**, **Mannion, P. D.**, **Hocknull, S. A.**, **Kear, B. P.**, **Sloan, T.**, **Sinapius, G. H. K.**, & **Elliott, D. A.** (2015). Revision of the sauropod dinosaur *Diamantinasaurus matildae* Hocknull et al. 2009 from the mid-Cretaceous of Australia: Implications for Gondwanan titanosauriform dispersal. *Gondwana Research*, *27*(3), 995–1033. https://doi.org/10.1016/j.gr.2014.03.014

Powell, J. E. (1992). Osteología de *Saltasaurus loricatus* (Sauropoda-Titanosauridae) del Cretácico Superior argentino. In J. L. Sanz, & A. D. Buscalioni (Eds.), *Los dinosaurios y su entorno biótico: II Curso de Paleontologia, 10 a 12 de julio de 1990, Actas* (pp. 165–230). Instituto "Juan de Valdes". https://dialnet.unirioja.es/servlet/articulo?codigo=4737616

Powell, J. E. (2003). Revision of South American titanosaurid dinosaurs: Palaeobiological, palaeobiogeographical and phylogenetic aspects. *Records of the Queen Victoria Museum and Art Gallery*, *111*, 1–173.

Prieto-Márquez, A., **Dalla Vecchia, F. M.**, **Gaete, R.**, & **Galobart, À.** (2013). Diversity, relationships, and biogeography of the lambeosaurine dinosaurs from the European Archipelago, with Description of the New Aralosaurin *Canardia garonnensis*. *PLoS ONE*, *8*(7), e69835. https://doi.org/10.1371/journal.pone.0069835

Prieto-Marquez, A., & **Wagner, J. R.** (2009). *Pararhabdodon isonensis* and *Tsintaosaurus spinorhinus*: A new clade of lambeosaurine hadrosaurids from Eurasia. *Cretaceous Research*, *30*(5), 1238–1246.

Rage, J.-C. (1996). Les Madtsoiidae (Reptilia, Serpentes) du Crétacé supérieur d'Europe: Témoins gondwaniens d'une dispersion transtéthysienne. *Comptes Rendus de l'Académie Des Sciences Paris*, *322*, 603–608.

Rage, J.-C. (2002). The continental Late Cretaceous of Europe: Toward a better understanding. *Comptes Rendus Palevol*, *1*(5), 257–258.

Remes, K., **Ortega, F.**, **Fierro, I.**, **Joger, U.**, **Kosma, R.**, **Ferrer, J. M. M.**, **Chiappe, L. M.**, **Dantas, P.**, **Escaso, F.**, **Gasulla, J. M.**, **López, E.**, **Pomares, A.**, **Ribeiro, B.**, **Sanz, J. L.**, **Tent-Manclús, J. E.**, **Faust, J.**, **Joger, H.**, **Joger, J.**, **Krüger, F. J.**, … **Maga, A.** (2009). A new basal sauropod dinosaur from the Middle Jurassic of Niger and the early evolution of sauropoda. *PLoS ONE*, *4*(9), e6924. https://doi.org/10.1371/journal.pone.0006924

Rigby, S. L., **Poropat, S. F.**, **Mannion, P. D.**, **Pentland, A. H.**, **Sloan, T.**, **Rumbold, S. J.**, **Webster, C. B.**, & **Elliott, D. A.** (2022). A juvenile *Diamantinasaurus matildae* (Dinosauria: Titanosauria) from the Upper Cretaceous Winton Formation of Queensland, Australia, with implications for sauropod ontogeny. *Journal of Vertebrate Paleontology*, *41*(6), e2047991. https://doi.org/10.1080/02724634.2021.2047991

Russell, D. A., & **Zheng, Z.** (1993). A large mamenchisaurid from the Junggar Basin, Xinjiang, People's Republic of China. *Canadian Journal of Earth Sciences*, *30*(10), 2082–2095. https://doi.org/10.1139/e93-180

Ruxton, G. D., & **Wilkinson, D. M.** (2014). Energetic arguments predict larger-bodied animals will be increasingly confined to flat environments. *Journal of Theoretical Biology*, *355*, 236–238.

Salgado, L., **Apesteguía, S.**, & **Heredia, S. E.** (2005). A new specimen of *Neuquensaurus australis*, a Late Cretaceous saltasaurine titanosaur from north Patagonia. *Journal of Vertebrate Paleontology*, *25*(3), 623–634. https://doi.org/10.1671/0272-4634(2005)025[0623:ANSONA]2.0.CO;2

Salgado, L., & **Azpilicueta, C.** (2000). Un nuevo saltasaurino (Sauropoda, Titanosauridae) de la provincia de Río Negro (Formación Allen, Cretácico Superior), Patagonia, Argentina. *Ameghiniana*, *37*(3), 259–264.

Salgado, L., & **Carvalho, I. D. E. S.** (2008). *Uberabatitan ribeiroi*, a new titanosaur from The Marília Formation (Bauru Group, Upper Cretaceous), Minas Gerais, Brazil. *Palaeontology*, *51*(4), 881–901. https://doi.org/10.1111/j.1475-4983.2008.00781.x

Salgado, L., **Coria, R. A.**, & **Calvo, J. O.** (1997). Evolution of titanosaurid sauropods I: Phylogenetic analysis based on the postcranial evidence. *Ameghiniana*, *34*, 3–32.

Salgado, L., **Gallina, P. A.**, & **Paulina Carabajal, A.** (2015). Redescription of *Bonatitan reigi* (Sauropoda: Titanosauria), from the Campanian–Maastrichtian of the Río Negro Province (Argentina). *Historical Biology*, *27*(5), 525–548. https://doi.org/10.1080/08912963.2014.894038

Salgado, L., & **García, R.** (2002). Variación morfológica en la secuencia de vertebras caudales de algunos seudópodos titanosaurios. *Spanish Journal of Palaeontology*, *17*(2), 211–216.

Sallam, H. M., **Gorscak, E.**, **O'Connor, P. M.**, **El-Dawoudi, I. A.**, **El-Sayed, S.**, **Saber, S.**, **Kora, M. A.**, **Sertich, J. J. W.**, **Seiffert, E. R.**, & **Lamanna, M. C.** (2018). New Egyptian sauropod reveals Late Cretaceous dinosaur dispersal between Europe and Africa. *Nature Ecology and Evolution*, *2*(3), 445–451. https://doi.org/10.1038/s41559-017-0455-5

Sander, P. M. (2008). Upper Cretaceous titanosaur nesting sites and their implications for sauropod dinosaur reproductive biology. *Palaeontographica Abteilung A*, *284*(4–6), 69–107.

Sander, P. M., **Christian, A.**, **Clauss, M.**, **Fechner, R.**, **Gee, C. T.**, **Griebeler, E.-M.**, **Gunga, H.-C.**, **Hummel, J.**, **Mallison, H.**, **Perry, S. F.**, **Preuschoft, H.**, **Rauhut, O. W. M.**, **Remes, K.**, **Tütken, T.**, **Wings, O.**, & **Witzel, U.** (2011). Biology of the sauropod dinosaurs: The evolution of gigantism. *Biological Reviews of the Cambridge Philosophical Society*, *86*(1), 117–155. https://doi.org/10.1111/j.1469-185X.2010.00137.x

Santucci, R. M., & **Arruda-Campos, A. C.** (2011). A new sauropod (Macronaria, Titanosauria) from the Adamantina Formation, Bauru Group, Upper Cretaceous of Brazil and the phylogenetic relationships of Aeolosaurini. *Zootaxa*, *3085*(1), 1. https://doi.org/10.11646/zootaxa.3085.1.1

Santucci, R. M., & **Filippi, L. S.** (2022). Last Titans: Titanosaurs from the Campanian–Maastrichtian Age. In A. Otero, J. L. Carballido, & D. Pol (Eds.), *South American Sauropodomorph Dinosaurs* (pp. 341–391). Springer International Publishing. https://doi.org/10.1007/978-3-030-95959-3_10

Sanz, J. L., **Powell, J. E.**, **Le Loeuff, J. L. E.**, **Martinez, R.**, & **Pereda Suberbiola, X.** (1999). Sauropod remains from the Upper Cretaceous of Laño (northcentral Spain). Titanosaur phylogenetic relationships. *Estudios del Museo de Ciencias Naturales de Álava*, *14*(Núm. Espec. 1), 235–255.

Schafarzik, F. (1909). Nyíresfalva és Vaspatak környékének geológiai viszonyai Hunyad vármegyében. *Magyar Királyi Földtani Intézet Évi jelentése, 1907-ről*, 69–80.

Schafarzik, F. (1910). Gyalár környékének földtani viszonyai (1908. évi felvételi jelentés.). *Magyar Királyi Földtani Intézet Évi Jelentése, 1908-ról*, 58–66.

Schmid, S. M., **Fügenschuh, B.**, **Kounov, A.**, **Maţenco, L.**, **Nievergelt, P.**, **Oberhänsli, R.**, **Pleuger, J.**, **Schefer, S.**, **Schuster, R.**, & **Tomljenović, B.** (2020). Tectonic units of the Alpine collision zone between Eastern Alps and western Turkey. *Gondwana Research*, *78*, 308–374.

Schwarz, D., **Ikejiri, T.**, **Breithaupt, B. H.**, **Sander, P. M.**, & **Klein, N.** (2007). A nearly complete skeleton of an early juvenile diplodocid (Dinosauria: Sauropoda) from the Lower Morrison Formation (Late Jurassic) of north central Wyoming and its implications for early ontogeny and pneumaticity in sauropods. *Historical Biology*, *19*(3), 225–253. https://doi.org/10.1080/08912960601118651

Scotese, C. (2016). PALEOMAP PaleoAtlas for GPlates and the PaleoDataPlotter program. https://www.earthbyte.org/paleomap-paleoatlas-for-gplates/

Seebacher, F. (2001). A new method to calculate allometric length-mass relationships of dinosaurs. *Journal of Vertebrate Paleontology*, *21*(1), 51–60.

Sekiya, T. (2011). Re-examination of *Chuanjiesaurus anaensis* (Dinosauria: Sauropoda) from the Middle Jurassic Chuanjie Formation, Lufeng County, Yunnan Province, southwest China. *Memoir of the Fukui Prefectural Dinosaur Museum*, *10*, 1–54.

Sellés, A. G., **Vila, B.**, **Brusatte, S. L.**, **Currie, P. J.**, & **Galobart, À.** (2021). A fast-growing basal troodontid (Dinosauria: Theropoda) from the latest Cretaceous of Europe. *Scientific Reports*, *11*(1), 4855.

Sereno, P. C., & **Brusatte, S. L.** (2008). Basal abelisaurid and carcharodontosaurid theropods from the Lower Cretaceous Elrhaz Formation of Niger. *Acta Palaeontologica Polonica*, *53*(1), 15–46.

Sereno, P. C., **Wilson, J. A**, & **Conrad, J. L.** (2004). New dinosaurs link southern landmasses in the Mid-Cretaceous. *Proceedings of the Royal Society B: Biological Sciences*, *271*(1546), 1325–1330. https://doi.org/10.1098/rspb.2004.2692

Silva Junior, J. C. G., **Marinho, T. S.**, **Martinelli, A. G.**, & **Langer, M. C.** (2019). Osteology and systematics of *Uberabatitan ribeiroi* (Dinosauria; Sauropoda): A Late Cretaceous titanosaur from Minas Gerais, Brazil. *Zootaxa*, *4577*(3), 401–438. https://doi.org/10.11646/zootaxa.4577.3.1

Silva Junior, J. C. G., **Martinelli, A. G.**, **Iori, F. V.**, **Marinho, T. S.**, **Hechenleitner, E. M.**, & **Langer, M. C.** (2022). Reassessment of *Aeolosaurus maximus*, a titanosaur dinosaur from the Late Cretaceous of Southeastern Brazil. *Historical Biology*, *34*(3), 403–411. https://doi.org/10.1080/08912963.2021.1920016

Silva Junior, J. C. G., **Martinelli, A. G.**, **Marinho, T. S.**, **da Silva, J. I.**, & **Langer, M. C.** (2022). New specimens of *Baurutitan britoi* and a taxonomic reassessment of the titanosaur dinosaur fauna (Sauropoda) from the Serra da Galga Formation (Late Cretaceous) of Brazil. *PeerJ*, *10*, e14333. https://doi.org/10.7717/peerj.14333

Silye, L., **Colin, J.-P.**, & **Codrea, V.** (2014). *Globotalicypridea mirabilis* sp. nov. – the first non-marine ostracod taxon from the Upper Cretaceous of the Haţeg Basin, Romania. *Annales de Paléontologie*, *100*(3), 273–280. https://www.sciencedirect.com/science/article/pii/S0753396914000421

Smith, J. B., **Lamanna, M. C.**, **Lacovara, K. J.**, **Dodson, P.**, **Smith, J. R.**, **Poole, J. C.**, **Giegengack, R.**, & **Attia, Y.** (2001). A giant sauropod dinosaur from an Upper Cretaceous mangrove deposit in Egypt. *Science*, *292*(5522), 1704–1706. https://doi.org/10.1126/science.1060561

Smith, T., **Codrea, V.**, **Săsăran, E.**, **van Itterbeeck, J.**, **Bultynck, P.**, **Csiki, Z.**, **Dica, P.**, **Fărcaş, C.**, **Folie, A.**, **Garcia, G.**, & **Godefroit, P.** (2002). A new exceptional vertebrate site from the Late Cretaceous of the Haţeg Basin (Romania). *Studia Universitatis Babeş-Bolyai, Geologia*, *Special Issue 1*, 321–330.

Solt, P., **Szuromi-Korecz, A.**, & **Ősi, A.** (2020). New Late Cretaceous (Coniacian) sauropod tracks from Hvar Island, Croatia. *Central European Geology*, *63*(1), 19–26.

Steel, R. (1970). *Handbuch Der Paläoherpetologie: Saurischia* (Vol. **14**). Gustav Fischer Verlag.

Stein, K., **Csiki, Z.**, **Curry, K.**, **Weishampel, D. B.**, **Redelstorff, R.**, & **Carballido, J. L.** (2010). Small body size and extreme cortical bone remodeling indicate phyletic dwarfism in *Magyarosaurus dacus* (Sauropoda: Titanosauria). *Proceedings of the National Academy of Sciences of the United States of America*, *107*(20), 9258–9263. https://doi.org/10.1073/pnas.1000781107

Stilla, A. (1985). Geologie de la region de Hateg–Cioclovina–Pui–Banita (Carpathes Meridionales). *Anuarul Institutului de Geologie Si Geofizica, Bucuresti*, *66*, 91–179.

Ştiucă, E. (1983). *Studiul geologic complex al regiunii Baru-Pui (jud. Hunedoara) cu privire specială asupra depozitelor de vârstă Cretacic superioară* [BSc thesis]. University of Bucharest, Bucharest.

Ştiucă, E., **Panaitescu, C.**, & **Simionescu, D.** (1982). Depozitele continentale cu dinosaurieni din Bazinul Haţeg. In *Monumentele Geologice ale Naturii* (pp. 29–35). Universitatea Bucureşti.

Sues, H. D., **Averianov, A.**, **Ridgely, R. C.**, & **Witmer, L. M.** (2015). Titanosauria (Dinosauria, Sauropoda) from the Upper Cretaceous (Turonian) Bissekty Formation of Uzbekistan. *Journal of Vertebrate Paleontology*, *35*(1), e889145. https://doi.org/10.1080/02724634.2014.889145

Ţabără, D., & **Csiki-Sava, Z.** (2024). Palynostratigraphic and palaeoenvironmental investigations of the Maastrichtian from Oarda de Jos (southwestern Transylvanian Basin). *Acta Palaeontologica Romaniae*, *20*(1), 87–107.

Ţabără, D., **Vasile, Ş.**, **Csiki-Sava, Z.**, **Bălc, R.**, **Vremir, M.**, & **Chelariu, M.** (2022). Palynological and organic geochemical analyses of the Upper Cretaceous Bozeș Formation at Petrești (southwestern Transylvanian Basin)–biostratigraphic and palaeoenvironmental implications. *Cretaceous Research*, *134*, 105148.

Therrien, F. (2005). Palaeoenvironments of the latest Cretaceous (Maastrichtian) dinosaurs of Romania: Insights from fluvial deposits and paleosols of the Transylvanian and Haţeg basins. *Palaeogeography, Palaeoclimatology, Palaeoecology*, *218*(1–2), 15–56.

Therrien, F., **Zelenitsky, D.**, & **Weishampel, D.** (2009). Palaeoenvironmental reconstruction of the Late Cretaceous Sânpetru Formation (Haţeg Basin, Romania) using paleosols and implications for the "disappearance" of dinosaurs. *Palaeogeography, Palaeoclimatology, Palaeoecology*, *272*(1–2), 37–52. https://doi.org/10.1016/j.palaeo.2008.10.023

Tortosa, T., **Buffetaut, E.**, **Vialle, N.**, **Dutour, Y.**, **Turini, E.**, & **Cheylan, G.** (2014). A new abelisaurid dinosaur from the Late Cretaceous of southern France: Palaeobiogeographical implications. *Annales de Paleontologie*, *100*(1), 63–86. https://doi.org/10.1016/j.annpal.2013.10.003

Tschopp, E., & **Mateus, O.** (2013). Clavicles, interclavicles, gastralia, and sternal ribs in sauropod dinosaurs: New reports from Diplodocidae and their morphological, functional and evolutionary implications. *Journal of Anatomy*, *222*(3), 321–340. https://doi.org/10.1111/joa.12012

Tschopp, E., **Mateus, O.**, & **Benson, R. B. J.** (2015). A specimen-level phylogenetic analysis and taxonomic revision of Diplodocidae (Dinosauria, Sauropoda). *PeerJ*, *2015*(4), e857. https://doi.org/10.7717/peerj.857

Tschopp, E., & **Upchurch, P.** (2018). The challenges and potential utility of phenotypic specimen-level phylogeny based on maximum parsimony. *Earth and Environmental Science Transactions of the Royal Society of Edinburgh*, *109*(1–2), 301–323.

Tykoski, R. S., & **Fiorillo, A. R.** (2017). An articulated cervical series of *Alamosaurus sanjuanensis* Gilmore, 1922 (Dinosauria, Sauropoda) from Texas: New perspective on the relationships of North America's last giant sauropod. *Journal of Systematic Palaeontology*, *15*(5), 339–364. https://doi.org/10.1080/14772019.2016.1183150

Ullmann, P. V., & **Lacovara, K. J.** (2016). Appendicular osteology of *Dreadnoughtus schrani*, a giant titanosaurian (Sauropoda, Titanosauria) from the Upper Cretaceous of Patagonia, Argentina. *Journal of Vertebrate Paleontology*, *36*(6). https://doi.org/10.1080/02724634.2016.1225303

Ungureanu, C. (1979). *Studiul geologic complex al depozitelor Cretacic superioare din bazinul Haţeg*. University of Bucharest.

Upchurch, P. (1995). The evolutionary history of sauropod dinosaurs. *Philosophical Transactions of the Royal Society of London. Series B: Biological Sciences*, *349*(1330), 365–390. https://doi.org/10.1098/rstb.1995.0125

Upchurch, P. (1998). The phylogenetic relationships of sauropod dinosaurs. *Zoological Journal of the Linnean Society*, *124*(1), 43–103.

Upchurch, P. (in press). The biogeographic history of Mesozoic dinosaurs. In D. B. Weishampel, P. M. Barrett, P. J. Makovicky, & M. T. Carrano (Eds.), *The Dinosauria III*. Cambridge University Press.

Upchurch, P., **Barrett, P. M.**, & **Dodson, P.** (2004). Sauropoda. In D. B. Weishampel, P. Dodson, & H. Osmólska (Eds.), *The Dinosauria* (2nd ed., pp. 259–324). University of California Press. https://cir.nii.ac.jp/crid/1360855570923012608

Upchurch, P., **Hunn, C. A.**, & Norman, D. B. (2002). An analysis of dinosaurian biogeography: Evidence for the existence of vicariance and dispersal patterns caused by geological events. *Proceedings of the Royal Society of London. Series B: Biological Sciences*, *269*(1491), 613–621. https://doi.org/10.1098/rspb.2001.1921

Upchurch, P., **Mannion, P. D.**, **Benson, R. B. J.**, **Butler, R. J.**, & **Carrano, M. T.** (2011). Geological and anthropogenic controls on the sampling of the terrestrial fossil record: A case study from the Dinosauria. *Geological Society, London, Special Publications*, *358*(1), 209–240. https://doi.org/10.1144/SP358.14

Upchurch, P., **Mannion, P. D.**, & **Taylor, M. P.** (2015). The anatomy and phylogenetic relationships of *Pelorosaurus becklesii* (Neosauropoda, Macronaria) from the Early Cretaceous of England. *PLOS ONE*, *10*(6), e0125819. https://doi.org/10.1371/journal.pone.0125819

van der Geer, A., **Lyras, G.**, & **de. Vos, J.** (2021). *Evolution of Island Mammals: Adaptation and Extinction of Placental Mammals on Islands* (2nd ed.). Wiley-Blackwell.

van Hinsbergen, D. J., **Torsvik, T. H.**, **Schmid, S. M.**, **Maţenco, L. C.**, **Maffione, M.**, **Vissers, R. L.**, **Gürer, D.**, & **Spakman, W.** (2020). Orogenic architecture of the Mediterranean region and kinematic reconstruction of its tectonic evolution since the Triassic. *Gondwana Research*, *81*, 79–229.

van Itterbeeck, J., **Markevich, V. S.**, & **Codrea, V.** (2005). Palynostratigraphy of the Maastrichtian dinosaur and mammal sites of the Râul Mare and Bărbat valleys (Haţeg Basin, Romania). *Geologica Carpathica*, *56*(2), 137–147.

van Itterbeeck, J., **Sasaran, E.**, **Codrea, V.**, **Sasaran, L.**, & **Bultynck, P.** (2004). Sedimentology of the Upper Cretaceous mammal-and dinosaur-bearing sites along the Râul Mare and Barbat rivers, Haţeg Basin, Romania. *Cretaceous Research*, *25*(4), 517–530.

Vasile, Ş., & **Csiki, Z.** (2011). New Maastrichtian microvertebrates from the Rusca Montană Basin (Romania). *Oltenia. Studii Şi Comunicări. Ştiinţele Naturii*, *27*(1), 221–230.

Vasile, Ş., **Zaharia, A.**, **Csiki, Z.**, & **Grigorescu, D.** (2011). The first report of continental fossil remains from Crăguiș (Haţeg Basin, Romania), and their stratigraphical significance. In Z. Csiki (Ed.), *Abstract Book, 8th Romanian Symposium on Paleontology* (pp. 127–128). Ars Docendi.

Vila, B., **Galobart, À.**, **Canudo, J. I.**, **Le Loeuff, J.**, **Dinarès-Turell, J.**, **Riera, V.**, **Oms, O.**, **Tortosa, T.**, & **Gaete, R.** (2012). The diversity of sauropod dinosaurs and their first taxonomic succession from the latest Cretaceous of southwestern Europe: Clues to demise and extinction. *Palaeogeography, Palaeoclimatology, Palaeoecology*, *350–352*, 19–38. https://doi.org/10.1016/j.palaeo.2012.06.008

Vila, B., **Jackson, F. D.**, & **Galobart, À.** (2010). First data on dinosaur eggs and clutches from Pinyes locality (Upper Cretaceous, Southern Pyrenees). *Ameghiniana*, *47*(1), 79–87. https://doi.org/10.5710/AMGH.v47i1.3

Vila, B., **Sellés, A. G.**, & **Brusatte, S. L.** (2016). Diversity and faunal changes in the latest Cretaceous dinosaur communities of southwestern Europe. *Cretaceous Research*, *57*, 552–564. https://doi.org/10.1016/j.cretres.2015.07.003

Vila, B., **Sellés, A.**, **Moreno-Azanza, M.**, **Razzolini, N. L.**, **Gil-Delgado, A.**, **Canudo, J. I.**, & **Galobart, À.** (2022). A titanosaurian sauropod with Gondwanan affinities in the latest Cretaceous of Europe. *Nature Ecology and Evolution*, *6*(3), 288–296. https://doi.org/10.1038/s41559-021-01651-5

Voegele, K., **Lamanna, M.**, & **Lacovara, K.** (2017). Osteology of the dorsal vertebrae of the giant titanosaurian sauropod dinosaur *Dreadnoughtus schrani* from the Late Cretaceous of Argentina. *Acta Palaeontologica Polonica*, *62*(4), 667–681. https://doi.org/10.4202/app.00391.2017

Voegele, K. K., **Ullmann, P. V.**, **Lamanna, M. C.**, & **Lacovara, K. J.** (2020). Appendicular myological reconstruction of the forelimb of the giant titanosaurian sauropod dinosaur *Dreadnoughtus schrani*. *Journal of Anatomy*, *237*(1), 133–154. https://doi.org/10.1111/joa.13176

Voegele, K. K., **Ullmann, P. V.**, **Lamanna, M. C.**, & **Lacovara, K. J.** (2021). Myological reconstruction of the pelvic girdle and hind limb of the giant titanosaurian sauropod dinosaur *Dreadnoughtus schrani*. *Journal of Anatomy*, *238*(3), 576–597. https://doi.org/10.1111/joa.13334

Vremir, M. (2009). Insect-related traces associated to the Maastrichtian vertebrate assemblages of Alba-Iulia and Haţeg areas (Romania). In I. I. Bucur, E. Săsăran, & D. Pop (Eds.), *Abstract Book, 7th Romanian Symposium on Palaeontology, Cluj-Napoca* (pp. 119–121), Cluj University Press.

Vremir, M. (2010). New faunal elements from the late Cretaceous (Maastrichtian) continental deposits of Sebeş area (Transylvania). *Terra Sebus*, *Acta Musei Sabesiensis*, *2*, 635–684.

Vremir, M., **Bălc, R.**, **Csiki-Sava, Z.**, **Brusatte, S. L.**, **Dyke, G.**, **Naish, D.**, & **Norell, M. A.** (2014). Petreşti-Arini – An important but ephemeral Upper Cretaceous continental vertebrate site in the southwestern Transylvanian Basin, Romania. *Cretaceous Research*, *49*, 13–38. https://doi.org/10.1016/j.cretres.2014.02.002

Vremir, M., **Dyke, G.**, & **Totoianu, R.** (2015). Repertoire of the Late Cretaceous vertebrate localities from Sebeş Area, Alba County (Romania). *Terra Sebus*, *Acta Musei Sabesiensis*, *7*, 695–724.

Waskow, K., & **Sander, P. M.** (2014). Growth record and histological variation in the dorsal ribs of *Camarasaurus* sp. (Sauropoda). *Journal of Vertebrate Paleontology*, *34*(4), 852–869. https://doi.org/10.1080/02724634.2014.840645

Weishampel, D. B., **Csiki, Z.**, **Benton, M. J.**, **Grigorescu, D.**, & **Codrea, V.** (2010). Palaeobiogeographic relationships of the Haţeg biota – Between isolation and innovation. *Palaeogeography, Palaeoclimatology, Palaeoecology*, *293*(3–4), 419–437. https://doi.org/10.1016/j.palaeo.2010.03.024

Weishampel, D. B., **Grigorescu, D.**, & **Norman, D. B.** (1991). The dinosaurs of Transylvania. *National Geographic Research & Exploration*, *7*(2), 196–215.

Weishampel, D. B., & **Jianu, C.-M.** (2011). *Transylvanian Dinosaurs*. JHU Press.

Weishampel, D. B., & **Kerscher, O.** (2013). Franz Baron Nopcsa. *Historical Biology*, *25*(4), 391–544.

Whitlock, J. A. (2011). A phylogenetic analysis of Diplodocoidea (Saurischia: Sauropoda). *Zoological Journal of the Linnean Society*, *161*(4), 872–915. https://doi.org/10.1111/j.1096-3642.2010.00665.x

Widlansky, S. J., **Clyde, W. C.**, **O'Connor, P. M.**, **Roberts, E. M.**, & **Stevens, N. J.** (2018). Paleomagnetism of the Cretaceous Galula Formation and implications for vertebrate evolution. *Journal of African Earth Sciences*, *139*, 403–420. https://doi.org/10.1016/j.jafrearsci.2017.11.029

Wilhite, D. R. (2003). *Biomechanical reconstruction of the appendicular skeleton in three North American Jurassic sauropods*. Louisiana State University and Agricultural & Mechanical College.

Willingshofer, E., **Andriessen, P.**, **Cloetingh, S.**, & **Neubauer, F.** (2001). Detrital fission track thermochronology of Upper Cretaceous syn-orogenic sediments in the South Carpathians (Romania): Inferences on the tectonic evolution of a collisional hinterland. *Basin Research*, *13*(4), 379–395. https://doi.org/10.1046/j.0950-091x.2001.00156.x

Wilson, J. (2002). Sauropod dinosaur phylogeny: Critique and cladistic analysis. *Zoological Journal of the Linnean Society*, *136*(2), 215–275. https://doi.org/10.1046/j.1096-3642.2002.00029.x

Wilson, J. A. (1999). A nomenclature for vertebral laminae in sauropods and other saurischian dinosaurs. *Journal of Vertebrate Paleontology*, *19*(4), 639–653.

Wilson, J. A. (2006). Anatomical nomenclature of fossil vertebrates: Standardized terms or 'lingua franca'? *Journal of Vertebrate Paleontology*, *26*(3), 511–518. https://doi.org/10.1671/0272-4634(2006)26[511:ANOFVS]2.0.CO;2

Wilson, J. A., & **Carrano, M. T.** (1999). Titanosaurs and the origin of 'wide-gauge' trackways: A biomechanical and systematic perspective on sauropod locomotion. *Paleobiology*, **25**(2), 252–267.

Wilson, J. A., **D'Emic, M. D.**, **Curry Rogers, K. A.**, **Mohabey, D. M.**, & **Sen, S.** (2009). Reassessment of the sauropod dinosaur *Jainosaurus* (="*Antarctosaurus*") *septentrionalis* from the Upper Cretaceous of India. *Museum of Paleontology, The University of Michigan*, *32*(2), 17–40.

Wilson, J. A., **D'Emic, M. D.**, **Ikejiri, T.**, **Moacdieh, E. M.**, & **Whitlock, J. A.** (2011). A nomenclature for vertebral fossae in sauropods and other saurischian dinosaurs. *PLoS ONE*, *6*(2). https://doi.org/10.1371/journal.pone.0017114

Wilson, J. A., **Pol, D.**, **Carvalho, A. B.**, & **Zaher, H.** (2016). The skull of the titanosaur *Tapuiasaurus macedoi* (Dinosauria: Sauropoda), a basal titanosaur from the Lower Cretaceous of Brazil. *Zoological Journal of the Linnean Society*, *178*(3), 611–662. https://doi.org/10.1111/zoj.12420

Wilson, J. A., & **Sereno, P. C.** (1998). Early evolution and higher-level phylogeny of sauropod dinosaurs. *Journal of Vertebrate Paleontology*, *18*(2), 1–68.

Wilson, J. A., & **Upchurch, P.** (2003). A revision of *Titanosaurus* Lydekker (Dinosauria – Sauropoda), the first dinosaur genus with a 'Gondwanan' distribution. *Journal of Systematic Palaeontology*, *1*(November), 125–160. https://doi.org/10.1017/S1477201903001044

Wilson, J., & **Upchurch, P.** (2009). Redescription and reassessment of the phylogenetic affinities of *Euhelopus zdanskyi* (Dinosauria: Sauropoda) from the Early Cretaceous of China. *Journal of Systematic Palaeontology*, *7*(2), 199–239. https://doi.org/10.1017/S1477201908002691

Xu, X., **Upchurch, P.**, **Mannion, P. D.**, **Barrett, P. M.**, **Regalado-Fernandez, O. R.**, **Mo, J.**, **Ma, J.**, & **Liu, H.** (2018). A new Middle Jurassic diplodocoid suggests an earlier dispersal and diversification of sauropod dinosaurs. *Nature Communications*, *9*(1), 2700.

Zurriaguz, V. (2016). Morphological diversity of *Neuquensaurus* Powell, 1992 (Sauropoda; Titanosauria): Insights from geometric morphometrics applied to the vertebral centrum shape. *Historical Biology*, *28*(7), 972–977. https://doi.org/10.1080/08912963.2015.1079630

Associate Editor: Kimberley Chapelle